On The Causation and Timing of Mutations During Cancer Evolution

Daniel Peter Harry Temko

Doctoral Thesis submitted for the degree of PhD

University College London.

Department of Computer Science

UCL

April 25, 2018

I, Daniel Peter Harry Temko, confirm that the work presented in this thesis is my own. Where information has been derived from other sources, I confirm that this has been indicated in the thesis.

Abstract

Mutations are the proximal causes of cancer and of drug resistance. Better understanding the causation of mutations before and during cancer can open up avenues for improved cancer prevention and treatment. Early mutations may be of particular interest for therapeutic targeting and early detection.

In Chapter 2, I use a mathematical model of breast cancer development to assess the hypothesis that varying numbers of progenitor cells causes a slow-down in mutation accumulation. In Chapter 3, I present an adapted method to time the accumulation of copy number changes using sequencing data, and an application of this method in colorectal cancer. This application supports the hypothesis of a catastrophic process where multiple copy number alterations develop at the same time in colorectal cancer.

In Chapter 4, I present evidence that a mutational process linked to defects in the *POLE* gene causes key driver mutations in colorectal and endometrial cancer. Based on this evidence and other analyses I argue that *POLE* mutations are very early events in colorectal and endometrial cancer.

In Chapter 5, I build on the ideas presented in Chapter 4 to assess the causation of driver mutations by mutational processes in a pan-cancer analysis. These results suggest causal explanations for key driver mutations in terms of mutational processes, and shed light on the important underlying biology of selection of driver mutations.

In whole my work expands our knowledge of the effects of mutational processes on cancer mutations and the timing of these mutations, indicates research strategies for novel approaches to cancer prevention and treatment, and informs our

understanding of the biological context of cancer evolution.

Impact Statement

In this thesis I present several mathematical modelling-based analyses that investigate the causation and timing of mutations, and the cellular dynamics of tumours. The key findings of the research include:

(i) Evidence that copy number alterations (CNAs) often occur in a punctuated fashion, close in time to the last common ancestor of all tumour cells, in colorectal cancers.
(ii) Evidence that pathogenic mutations in the *POLE* gene are early events in the colorectal and endometrial cancers in which these mutations occur.
(iii) Suggestive evidence of causal relationships between mutational processes and driver mutations.
(iv) Evidence for differences in selection between different mutations (amino acid changes) in the same driver gene and related driver genes.

There are several ways in which the work presented in this thesis could have a beneficial impact:

My findings on mutation timing have potential implications for tumour surveillance. I argue that *POLE* mutations are early events in colorectal and endometrial cancers in which they occur somatically. CNAs, by contrast, appear to often occur in a cluster of late events (close to the last common ancestor of cancer cells) in colorectal cancer. The early occurrence of *POLE* mutations make them good candidates for surveillance programs, albeit the relatively small proportion of tumours in which these mutations are found must be taken into account. In terms of CNA

mutations, my results suggest that there may be limited scope to assess progression towards colorectal cancer in terms of CNA accumulation, since the window of time before the last clonal expansion during which these changes are detectable is relatively narrow.

The results presented here also point to possible mechanisms of mutation causation that could be of relevance for cancer prevention. The results in Chapters 4 and 5 identify a key role for potentially modifiable alterations to the mutation rate in accumulation of driver mutations. Whereas, the results of Chapter 3 support the hypothesis that WGD events play an important role in the aetiology of colorectal cancer, and motivate further research into the mechanisms of this type of change.

The differential selection results presented here are of interest for our wider understanding of cancer evolution. These results challenge the prevailing thinking on driver mutations and passenger mutations by demonstrating a spectrum of selective effects between driver mutations. Many previous studies have assumed a fixed selective impact among drivers [Beerenwinkel et al., 2007, Waclaw et al., 2015, McFarland et al., 2014]. Some studies have allowed for a distribution of effects, but have relied on indirect estimates for parameter estimation [Foo et al., 2015]. My results argue in favour of incorporating such distributions in future studies, and also point to possible parameterisations. Thus, these findings have the potential to impact discourse and thinking in the cancer research field, to promote future discoveries.

In summary, the results presented in this thesis have the potential to impact tumour surveillance and prevention, and could also impact our wider understanding of cancer evolution. In total, the work provides a contribution to the growing body of work on the forces that govern the course of tumour evolution.

Publications

Work from the following manuscripts forms an important part of this thesis:

* Equal contribution

1. Temko D.*, Cheng Y.K.*, Polyak K., and Michor F. (2017). Mathematical modeling links pregnancy-associated changes and breast cancer risk. *Cancer Res*, 77(11):2800-2809

2. Temko D., Van Gool I.C., Rayner E., Glaire M., Makino S., Brown M., Chegwidden L., Palles C., Depreeuw J., Beggs A., Stathopoulou C., Mason M, Baker A., Williams M., Cerundolo V., Rei M., Taylor J.C., Schuh A., Ahmed A., Amant F., Lambrechts D., Smit V.T.H.B.M., Bosse T., Graham T.A., Church D.N., Tomlinson I. Somatic *POLE* exonuclease domain mutations are early events in sporadic endometrial and colorectal carcinogenesis, determining driver mutation landscape, clonal neo-antigen burden and immune response. *in press*, *The Journal of Pathology*, 2018

3. Temko D., Tomlinson I., Severini S., Schuster-Bckler B., Graham T.A. The effects of mutational processes and selection on driver mutations across cancer types, *in press*, *Nature Communications*, 2018

4. Cross W., Kovac M., Mustonen V., Temko D., Davis H., Baker A., Biswas S., Arnold R., Chegwidden L., Gatenbee C., Anderson A.R., Koelzer V.H., Martinez P., Jiang X., Domingo E., Woodcock D., Feng Y., Kovacova M., Jansen M., Rodriguez-Justo M., Ashraf S., Guy R., Cunningham C., East J.E., Wedge D., Wang L.M., Palles C., Heinimann K., Sottoriva A., Leedham S.J., Graham T.A. and Tomlinson I. The evolutionary landscape of colorectal tumorigenesis, *in preparation*, 2018

I have also contributed to the following manuscripts which do not feature prominently in the thesis:

1. Baker A.*, Cross W.*, Curtius K.*, Al-Bakir I.*, Choi C.R.*, Davis H., Temko D., Biswas S., Martinez P., Williams M., Lindsay J.O., Feakins R., Vega R., Hayes S., Tomlinson I., McDonald S.A.C., Moorghen M., Silver A., East J.E., Wright N.A., Wang L.M., Rodriguez-Justo M., Jansen M., Hart A.L., Leedham S.J. and Graham T.A. The evolutionary history of human colitis-associated colorectal cancer, *submitted*, 2018

2. Werner B., Case J., Williams M., Chkhaidze K., Temko D., Cross W., Spiteri I., Huang W., Tomlinson I., Barnes C., Graham T. and Sottoriva A. Measuring single cell divisions in human cancers from multi-region sequencing data, *in preparation*, 2018

Acknowledgements

I would like to thank my supervisors Simone Severini, Trevor Graham and Ian Tomlinson. Through your expertise and insights you have helped me to turn vague ideas into research of relevance to the terrible disease that is the topic of this thesis. Through your passion for your work and love of life, you have demonstrated to me that on top of the grit and grind, the best science involves an essential ingredient of fun (and occasionally beer too). In your different leadership styles you have also each been role models to me, providing an example of fair, and effective leadership, which I hope one day to emulate. Finally, thank you for both the support you have provided on a personal level, which has been a great help throughout the process, and for trusting me to make my own mistakes and come to my own conclusions, which undoubtedly has helped make me a better scientist. Also, thank you for teaching me statistics.

In addition, I would like to thank my collaborators: Benjamin Schuster-Boeckler, David Church, Franziska Michor, Nelly Polyak, Marc Williams, Anne-Marie Baker, William Cross, Laura Gay, Kit Curtius, Ibrahim Al-Bakir, Viola Walther, Jacob Househam, Pierre Martinez, Weini Huang, and Philipp Altrock form a necessarily incomplete list.

I must also thank my funders, the Engineering and Physical Sciences Research Council (EPSRC) and the Yule Bogue bequest, without the support of whom this work would not have have been possible.

Lastly, I wish to thank my family (current and future). To my parents Ned and Astra, thank you for your ever-willingness to lend an ear and provide me with good food throughout this journey. And to Gaby, my fiancée, thank you for your

endless patience and willingness to discuss cancer evolution, long after the novelty had presumably warn off.

Contents

List of Tables

Chapter 1

Introduction

1.1 Précis

Mutations play a causal role in cancer initiation and progression. Mutations arise due to mutation-causing processes (mutation processes or mutational processes) in somatic tissues and change in frequency in the population due to natural selection and drift. Improved understanding of these mutation processes is therefore of interest for prevention, early detection, and treatment of cancer. In addition, refined understanding of mutation causation is important to define a null model against which it is possible to identify those mutations that are more frequent than expected in cancer genomes, and are subject to selection; a task of central importance to cancer research. The lack of data following the evolution of individual patients over time presents a major challenge for identification of mutation processes. Mathematical modelling can be a useful toolset to recover information on the causes of mutation in data that comes from a single point in time. Here, I present several analyses that aim to infer mutation-causing processes from molecular data that represents a snapshot in time. In the final chapter, I will present an application of a model of mutation-causing processes that aims to infer the strength of selection experienced by individual mutations. Overall, I aim to contribute to the expanding literature on the operation of mutation-causing processes in cancer and the selective impact of individual mutations.

1.2 Motivation

Genetic mutations are proximal causes of cancer inititiation [Lawrence et al., 2014, Vogelstein et al., 2013], and play an important role in resistance to targeted therapy [Chong and Janne, 2013, Weisberg et al., 2007]. In addition, somatic mutations can lead to the recognition of tumours by the immune system [Brown et al., 2014], and this recognition can be harnessed for therapy [McGranahan et al., 2016]. Albeit, the identity of the mutations that play a causal role in disease is a matter of long-standing research and the subject of ongoing debate [Cooper, 1982, Lawrence et al., 2014, Martincorena et al., 2017]. Mutations arise in human tissues at varying rates, their survival and expansion depends on natural selection and drift, both of which relate to population structure.

As a result, understanding the causation and timing of mutations during cancer evolution is important for several reasons. First, due to the causal role of mutation in disease progression, in a straightforward sense this understanding is important for cancer prevention and treatment. Indeed, many existing cancer prevention strategies are based on removal of mutation-causing processes that have already been identified, including strategies to reduce ultra-violet, and tobacco exposure. By the same token understanding of mutation-causing processes and how they impact the accumulation of mutations in the evolving tumour population could enable better prognostication. In many cases the mutation processes present in cancer genomes are measurable [Alexandrov et al., 2013a], so in theory it may be possible to predict evolutionary trajectories.

Secondly, there is a particular rationale for identifying early mutation-causing processes and mutations [Loeb, 2011]: In a straightforward sense early mutations have the most relevance for early detection. In addition, mutations that occur before the last common ancestor of all tumour cells (LCA) are expected to be present in every tumour cell (clonal) and can consequently be targeted in every tumour cell by a therapy. Finally, some researchers have argued that oncogene addiction is most likely for early mutations [Cristea et al., 2017]. Oncogene addiction is a phenomenon where tumour cells, but not healthy cells, become dependent on the

presence of a mutation for survival [Weinstein, 2002].

In addition, accurate understanding of muation-causing processes is key to determining the selective impacts of individual mutations. Multiple studies (reviewed below) have aimed to identify genes under selection by finding genes that are mutated more (or less) frequently in tumours than would be expected based on underlying mutation rates [Greenman et al., 2007, Kan et al., 2010, Martincorena et al., 2017]. The conclusions of these studies have been shown to be sensitive to the underlying model of mutation rate [Lawrence et al., 2013], and have generally developed in step with improved understanding of mutation-causing processes (see below). Further improvements in the understanding of mutation-causing processes could continue to drive these efforts forward.

Identifying the role played by individual mutations in disease can help to design treatments. The *EGFR* gene is a case in point. Multiple lines of evidence, including frequent mutations, supported a causal role for this gene in disease [Dowell and Minna, 2006]. This lead to the development of treatments targeting the protein encoded by this gene, including Erlotinib, which interferes with the capacity of the *EGFR*-coded protein to propagate signalling cascades via phosphorylation [Dowell and Minna, 2006, Schettino et al., 2008]. Although resistance remains a major problem, such therapies have improved survival time in non-small cell lung cancer [Dowell and Minna, 2006]. Treatments targeting a fusion mutation involving the genes *BCR* and *ABL* provide another example in chronic myeloid leukemia [Mitelman et al., 2007, Quintas-Cardama et al., 2009]. Thus, mutations that play a causal role in disease can provide good treatment targets.

A major challenge for the identification of mutation processes, and indeed in cancer research more broadly, is that the process of cancer development in humans cannot usually be directly observed. By necessity, the molecular data that is available to cancer researchers represents a single snapshot in time at the point when the tumour was removed. There are some exceptions in the case of blood cancers [da Silva-Coelho et al., 2017], and promising technological advances suggest that this may not always be the case for solid tumours; recent research has demonstrated

that tumour DNA is detectable in the blood from the earliest stages of tumorigenesis and tumour relapse [Abbosh et al., 2017, Cohen et al., 2018]. At present, though, single time-point data remains a major challenge for most tumour types.

At that single timepoint, there has recently been a rapid expansion in the amount of data available. Of note, since 2005 the Cancer Genome Atlas (TCGA) study generated publicly available whole exome sequencing (WXS) data for over 11,000 patients across 21 primary cancer sites (https://portal.gdc.cancer.gov). The PanCancer Analysis of Whole Genome (PCAWG) study that is currently in progress promises to generate a similarly rich public resource of tumour whole genome sequencing (WGS) data.

There is a precedent for mathematical modelling approaches to these questions (which I discuss). However, there are two, informative, reasons why they are not more common. First, the complexity of the process of mutation accumulation and subsequent DNA sequencing means that mathematical models of mutation accumulation often have multiple free parameters. This has historically been the case for mathematical models of cancer development. A case in point is the seminal 1954 study by Armitage and Doll [Armitage and Doll, 1954] that provided key evidence that cancer initiation is a multi-step process. While the study is rightly regarded as one of the key contributions of mathematical modelling to cancer research, the conclusions on the specific number of mutations required for cancer have been questioned by later research – it has become clear that changes to the model to take into account the impact of clonal expansions can greatly effect the estimation of the number of steps required for cancer [Moolgavkar, 2004]. This exemplifies the fact that the findings from mathematical modelling studies are typically subject to caveats, and progress can be incremental.

Secondly, this approach is mutli-disciplinary. My approach requires applications of mathematical techniques to biological content (including formalisation of biological concepts and synthesis of diverse areas of biological theory). This requires some appreciation of both the mathematics and the biology in the researcher, in addition to close collaboration between genuine subject area experts. As a result,

the pool of researchers and groups with appropriate interests and backgrounds is relatively limited.

Below, I review the literature on causes and timing of mutations in cancer. I first review the literature on mutation-causing processes. I then turn to the literature on the inference of selection, which often relies on modelling of mutation processes. Finally, I review the literature on the impact of varying mutation rates on outcomes in cancer.

1.3 Identification and timing of mutator processes: Theory

The question of whether mutator phenotypes (defined as an increased cell-intrinsic mutation rates compared to non-cancerous cells) are common in cancer is a matter of longstanding debate. Two types of argument have been made in favour of prevalent mutator phenotypes, by Lawrence Loeb and others. First, it has been argued that increased mutation rates are necessary to explain disordered genomes found in cancer cells, and the high incidence levels of cancer [Loeb, 2001] (necessity arguments). The second argument is based on two observations. First, that there are numerous genetically-encoded cellular processes involved in the faithful replication of DNA and the repair of insults to DNA [Loeb, 2011]. Secondly, that cancer initiation requires the accumulation of multiple genetic mutations that occur slowly in the absence of a mutator phenotype. The argument claims that, as a result, mutator mutations and likely to be common during the process of carcinogenesis, leading to mutator phenotypes in the resulting cancers [Christians et al., 1995, Loeb, 2011] (efficiency arguments).

Historically necessity arguments for a mutator phenotype by Loeb and colleagues have relied on the need for more than two rate-limiting steps in carcinogenesis [Loeb, 1991], and the possibility that even six or 12 mutations are required for carcinogenesis. [Loeb, 2001, Armitage and Doll, 1954].

Theoretical models [Moolgavkar and Knudson, 1981] and novel data-driven approaches [Tomasetti et al., 2015] have challenged traditional views that a large

number of mutations are required for cancer development – the latter study suggested that only three driver mutations are required for the development of lung cancer and colon cancer. In addition, studies that consider the effects of clonal expansion have predicted faster rates of mutation accumulation under normal mutation rates, and concluded that mutator phenotypes are unlikely to be necessary to explain mutation and incidence rates [Beerenwinkel et al., 2007, Tomlinson et al., 1996].

However, none of these considerations are definitive. The Tomasetti study was restricted to colon cancer and lung cancer, and the length of routes to cancer across all cancer types is not known. Regarding the effects of clonal expansions - [Beerenwinkel et al., 2007] finds that cancers can develop within a human lifespan under a normal mutation rate assuming that drivers confer a selective advantage of 1%. However, the study assumes a well-mixed population in which the effects of selection could be overstated.

It is likely that the necessity or not of a mutator will depend on the balance between the length of routes to cancer (i.e. the number of causal mutations required and the probability of these mutations), and the efficacy of selection to accelerate mutagenesis, and there is still a long way to go to understand that balance.

There is a related body of literature evaluating efficiency arguments, describing whether faithful DNA replication should be expected to fail en route to cancer, given its complexity, and in light of the number of mutations required for cancer, and at what time during carcinogenesis we should expect these failures to occur. An important paper in the field investigated the required effect size of a mutator phenotype that would lead to the expectation of seeing mutator phenotypes in over half of cancers [Beckman and Loeb, 2006]. The study found that the required effect size varied over 1,000-fold depending on the number of mutations required for cancer, the number of mutator loci and the mutation rate. The same study found that if mutator phenotypes emerge, then they are more likely to be early events.

A model that took into account both clonal expansion and the effects of deleterious mutations [Datta et al., 2013] also found a wide range of predictions regarding the likelihood of a mutator phenotype emerging, with the probability of mutator

phenotypes varying between zero and one depending on the probability of mutator mutations. Interestingly this study predicted that mutator phenotypes were more likely to occur under intermediate selection for drivers, than under strong or weak selection regimes.

Ian Tomlinson made the intriguing prediction, that although mutator phenotypes were predicted to be early events if they occurred, that they are more likely to occur in later onset cancers [Tomlinson et al., 1996], due to the extra steps required for these cancers to develop. In a model that allows for back-mutation Komarova et al. recently predicted that when the selective effects of drivers mutations are in balance with the potential effects of deleterious mutations, then mutator phenotypes can emerge early in cancer development and later revert to stability [Asatryan and Komarova, 2016]

The impact of 'tumour suppressor genes' (TSGs) which may require two hits before conferring a selective advantage has been studied in detail by Franziska Michor and colleagues. These studies generally focus on chromosomal instability (CIN) as opposed to instability at the level of point mutations, since classical TSGs are thought to be inactivated by chromosomal mutations. A study by Franziska Michor found that the requirement to inactivate a tumour suppressor gene en route to cancer meant that CIN is likely to occur early even if only one or a few CIN-conferring mutations are possible, given a fixed cell population size [Michor, 2005]. The same study found that the requirement for two TSGs to be inactivated implies CIN is likely to occur early even if the mutations that lead to CIN come at a selective cost. A later study, which included a growing population of cells found that the tendency of clones with CIN to accumulate deleterious mutations that could slow their growth had little effect on the prediction that these mutations would be early in the context of tumour suppressor genes [Nowak et al., 2006]. These results suggest that tumour suppressor genes increases the likelihood of early instability during the develop of cancer. However, it is unclear how these results are affected by the complicating factors of multiple possible mutational paths to cancer, some of which may not involve tumour suppressor genes.

These modelling results illustrate the complexity of the evolutionary setting in which cancer develops, often confounding firm predictions from theory. However, on a more optimistic note, they also illustrate the unexpected dynamics that can arise in this complex setting, motivating further research, and potential therapeutic targets.

1.4 Identification and timing of mutation processes: Data

To discuss the literature on mutation-causing processes (mutation processes) it is useful to distinguish two major classes of mutation. Single nucleotide alterations (SNAs) describe substitution of one DNA base (A,C,G or T) for another in the linear DNA sequence, as well as insertions and deletions on the same length scale. Copy number alterations (CNAs) describe changes at the level of megabases. CNAs include duplications (copies of a large section of DNA), and deletions; duplications that are re-inserted adjacent to the copied sequence are known as tandem duplications. CNAs also include rearrangements of the continuous DNA sequence. Here, I have included rearrangements in the definition of CNAs, even though they do not alter copy number (in the sense of the number of genomic copies of a stretch of sequence), for ease of exposition; since my focus here is on mutation-causing processes and many processes that cause CNAs (more narrowly defined) also cause rearrangements. Thus, the term CNA used here, may be thought of as a short-hand for CNA and rearrangement as used elsewhere in the literature.

Although there is a broad literature on mutation processes in cancer, these studies generally share some commonalities in approach. In general, mutations with common genomic features are inferred to be caused by a similar mutation process, often backed up by evidence from experimental systems. It is possible to partially reconstruct the dynamics in several ways. First, temporal information can be accessed by harnessing the idea that different individuals represent different time-points of a common process. Thus types of mutation that correlate across individuals can identify the influence of a common process realised across different

time-points. Similarly, evidence from putative pre-malignant lesions can be compared to frank carcinomas to approximate temporal data. Further evidence is provided by studies of the clonal status of mutations attributed to different processes; mutations that are present in every cell probably occurred before the last common ancestor of all tumour cells. In addition, for copy number change in particular, the final state records some information on the order of events. This is the case for two reasons. First, since copy number changes effect large regions of the genome they often overlap and the order of events influences the final pattern. Secondly, the SNAs within CNA mutations can be used as a molecular clock to time their occurrence. This research has cast light on multiple mutation processes involving different types of mutation that are active in cancer (reviewed presently).

1.4.1 SNA mutation processes

There are a number of well-described mutation processes at the level of SNAs, two of these processes merit special mention given their relevance to the content of the thesis. The first is microsatellite instability (MSI). Microsatellites are segments of DNA consisting of multiple repeats of the same short sequence of one to several bases. In microsatellite instability frequent indels increase or decrease the number of repeats in the segment. MSI was described in 1993 in colorectal cancer [Thibodeau et al., 1993]. It has since been shown to occur in around 15% of colorectal cancers [Vilar and Gruber, 2010]. In this setting it is most commonly caused by methylation of the *MLH1* gene, which is one of those genes involved in the mismatch repair (MMR) process that repairs microsatellite indels, in addition to other types of mutation [Vilar and Gruber, 2010]. While MSI is traditionally recognised as playing a role in colorectal, endometrial and gastric cancers, a recent support suggested that that MSI may occur at low levels in most tumour types [Hause et al., 2016].

The second is a mutation process linked with mutations in the *POLE* gene (discussed in detail in Chapter 4). The *POLE* gene encodes a subunit of the DNA replicase (Polε) [Rayner et al., 2016]. A subset of mutations in the gene cause a mutation process involving a very high rate of C>A changes that occur at TCT trin-

ucleotides due to disrupted DNA repair [Rayner et al., 2016]. These mutations are found in 7-12% of endometrial cancers and 1-2% of colorectal cancers, as well as a range of other tumour types [Rayner et al., 2016], referred to as 'ultramutator' cancers. Endometrial cancers with *POLE* mutations are associated with high immune infiltration and improved prognosis [Hussein et al., 2015, Church et al., 2015].

In 2013 Ludmil Alexandrov and colleagues published a landmark paper introducing a mutational signature framework in cancer that provides a way of estimating the SNA mutation-causing processes involved in the history of a tumour sample and ascribing mutations probabilistically to individual processes [Alexandrov et al., 2013b, Alexandrov et al., 2013a]. The framework classifies SNAs into 96 types defined by the base change (such as C>T), and the genomic context including the two flanking bases of the mutated base (such as TCT). Under the assumption that each mutation process creates a characteristic distribution of mutations across the types (or a mutational signature), the study used the mutational catalogues from multiple tumours to identify 21 inferred processes and their associated mutational signatures. The signatures framework has since been extended to over 30 processes and associated signatures [Petljak and Alexandrov, 2016]. Many, but not all, of the signatures have a biological interpretation. Signatures 6, 15, 20 and 26 are linked to MMR defects, and signature 10 is linked to *POLE* mutation. Other signatures are linked to a range of processes including tobacco-induced damage (signature 4), mutation by APOBEC (apolipoprotein B mRNA editing enzyme, catalytic polypeptide-like) deaminases (signatures 2 and 13) and ultraviolet radiation (UV) (signature 7) (cancer.sanger.ac.uk/cosmic/signatures).

Studies have indicated diverse patterns with respect to SNA mutation process timing. A study that analysed mutation accumulation in individuals spanning a large age range suggests that some SNA mutation processes may occur gradually over the course of a lifetime, showing a clock-like relationship with age, in both tumour tissue [Alexandrov et al., 2015] and normal tissue [Blokzijl et al., 2016]. These include a mutation process thought to be caused by deamination of methylated cytosines, which causes C>T mutations where the C base is followed by a G base in

the normal sequence (signature 1), and a process of unknown etiology which causes a broad spectrum of SNAs (signature 5) [Helleday et al., 2014].

Studies of the clonal status of SNA mutations can also reveal information on the timing of SNA mutational processes. One of the key discoveries of cancer research of recent years has been the widespread presence of intra-tumour heterogeneity at the level of SNAs [Gerlinger et al., 2012, Andor et al., 2016]. This discovery tends to suggest that SNA processes are ongoing in tumours. However, variation in the rate of SNA processes over time has been identified. Mcgranahan et al. [McGranahan et al., 2015] analysed whether mutations associated with a range of SNA mutation processes were clonal (present in all cancer cells), or sublconal, in a range of cancer types. Notably, mutations likely to be caused by APOBEC were enriched for subconal mutations, consistent with a later onset in carcinogenesis of this mutation process. In a multi-region sequencing study of lung cancer, de Bruin et al. also found that mutations likely to be caused by APOBEC were enriched for subclonal mutations, whereas mutations likely to be caused by smoking were depleted among these later mutations [de Bruin et al., 2014]. As against this, a very recent report found heterogoneous timing with respect to the timing of APOBEC signatures, with heterogeneity between patients, including some where the signature was predominantly early and clonal [Yates et al., 2017]. This suggests that APOBEC-linked mutations can also occur in the earlier stages of tumorigenesis.

1.4.2 CNA mutation processes

Copy number alterations were the first type of mutations to be recognised in cancer. In 1914 Theodor Boveri theorised that cancer involves the disruption of cellular chromosomes [Harris, 2008, Jeggo et al., 2016]. Around twenty years later the observation was made that human cancer cells are frequently found with abnormal chromosome numbers [Harris, 2008, Jeggo et al., 2016]. The advent of next generation sequencing has confirmed that over half of breast cancers, colorectal cancers and non-small cell lung cancers have non-diploid chromosome complement [Sansregret et al., 2018]. In 1997, Bert Vogelstein demonstrated ongoing chromosomal instability (CIN) in human colorectal cancer cell

lines [Lengauer et al., 1997]; this provided the first evidence that some cancers have genuinely unstable genomes, as opposed to a stably aneuploid genome. In the literature the presence of aneuploidy is often, confusingly, reported as CIN [Sansregret et al., 2018]. However, determining the extent of ongoing CIN across human cancers remains a major challenge due to the lack of temporally-resolved mutation data.

In 2011 a study identified a mutation process which was labelled *chromothripsis*, involving multiple localised CNAs [Stephens et al., 2011]. In this study, Stephens and colleagues identified complex genomic rearrangements in cancer samples rewiring the linear DNA sequence localised to one or a few chromosomes [Stephens et al., 2011]. They found this pattern in 2-3% of all cancers and 25% of bone cancers. In the same year, Kloosterman et al. found evidence for widespread chromothripsis events in primary and metastatic colorectal cancer [Kloosterman et al., 2011]. In 2016 Notta et al. found evidence for at least one chromothripsis event in 65% (70/107) of pancreatic cancers subjected to whole genome sequencing [Notta et al., 2016].

In the original study that identified chromothripsis, the authors put forward several arguments to suggest that these changes are likely to occur in a single catastrophic event, as opposed to gradually over many cell divisions. The main line of argument observes that the copy number states alternate between just one and sometimes two values. They argue that this is consistent with a single shattering event followed by stitching together of the fragments by DNA repair processes. By contrast, they use an intuitive argument, backed up with Monte Carlo simulations, to argue that this pattern is very unlikely based on a gradual model involving the successive accumulation of multiple types of CNA over multiple cell divisions. However, in my view, the assumed model of what gradual change would look like is rather artificially restricted, and there are plausible scenarios of gradual change that may explain the data, that are not considered in their model. In particular, the model seems to assume gradual change would consist of the random accumulation of CNAs of many types, including duplications, and deletions, and they do not seem

to consider the plausible scenario of multiple small-scale events of shattering and repair. In my view their secondary argument, that it is difficult to explain the highly clustered nature of the CNA breakpoints under a gradual scenario may be more convincing.

More recent experimental evidence has clarified some of these issues. In 2015 another group used a combination of live-cell imaging and DNA sequencing to show that the hallmarks of chromothripsis can indeed result from changes that take place in a single cell division [Zhang et al., 2015]. Specifically, they observed individual cells with a structure called a micronucleus, which is presumed to contain a lagging chromosome that was incorrectly segregated during cell division (micronucleated cells). Single-cell sequencing revealed an asymmetric pattern of copy number change in daughter cells of micronucleated cells, with DNA damage in some daughter cells that recapitulated the hallmarks of chromothripsis. The authors also showed that DNA in micro-nuclei is under-replicated. Therefore one explanation for the data is that under-replicated chromosome fragments in micro-nuclei are stitched together by the cells DNA repair machinery during cell division, leading to chromothripsis.

In 2013, Baca et al. identified complex chains of rearrangements in 88% (50/57) of prostate cancers sequenced by whole genome sequencing, which they labelled *chromoplexy* [Baca et al., 2013]. 63% of tumours had two or more of these chains. Some of these chains involved five or more chromosomes, in contrast to chromothripsis which typically occurs over a few chromosomes (but can involve more in some cases) [Stephens et al., 2011]. However, the authors note that some of the instances of chromoplexy resembled chromothripsis, and it seems plausible that the underlying mechanism may be related.

Another CNA mutation process involving multiple contemporaneous CNA events which may be widespread in cancer is whole genome doubling (WGD). In normal tissue WGD events (tetraploidisations) play a role in the development of a range of cell types [Sansregret et al., 2018]. Carter et al considered the number of copies of the two alleles of each chromosome across samples in a pan-cancer anal-

ysis [Carter et al., 2012]. They found that in high ploidy samples the allele with the higher copy number tended to have an even copy number. They show that this is consistent with a model where gains occur by whole-genome doublings (after which both alleles with have the same even copy number), followed by individual copy losses (which leave two copy states for each allele, with the highest state being even). Based on their analysis they argue that WGD events occurred in the history of over 40% of oesophageal adenocarcinomas and in high proportions of lung adenocarcinomas and several other cancer types. However, arguably, there are other explanations for this pattern of copy number change that are plausible, such as common duplications of individual chromosomes, and this method may be prone to over or under-call WGD events in individual samples. A later pan-cancer study by the same group found a multimodal distribution of copy number states across cancer types which is suggestive of frequent past WGD events [Zack et al., 2013]. One report argues that genome doubling events occurred in the majority of colorectal cancers [Dewhurst et al., 2014]. However, the parsimony-type method for identifying historic WGD used in this study cannot distinguish genuine WGD cases from those cases that have reached high ploidy through other routes. Together, the cumulative evidence supports an important role for WGD events in cancer, but other explanations for the data appear to be possible.

At the molecular level, a variety of mechanisms can lead to whole genome doubling and may underlie WGD events in cancer. Cells may undergo a process called *endoreplication* where DNA duplication proceeds without cell division [Sansregret et al., 2018]. Relatedly, defects in cellular processes including DNA replication and the functioning of the mitotic spindle can cause cells to abort cell division, producing a tetraploid cell [Storchova and Pellman, 2004]. Additionally, *entosis*, engulfment by another cell, may lead to tetraploidisation by blocking cell division [Sansregret et al., 2018]. Cell fusions are known to play a role in development and disease, and could also play a role in tetraploidisation in cancer [Storchova and Pellman, 2004].

Multiple other molecular mechanisms of CNA accumulation are thought to

play a role in cancer, suggesting possible causal sequences of events among the observed CNAs in tumour samples. Merotelic chromosomal attachments are one well-described mechanism of CNA accumulation in cancer [Sansregret et al., 2018, Gordon et al., 2012]. This phenomenon arises when a single chromosomal kinetochore becomes attached to mircotubules from both poles of the mitotic spindle [Gordon et al., 2012] and has been linked with lagging chromosomes during cell division [Sansregret et al., 2018]. Experimentally, a study using long-term live-cell imaging showed that the presence of extra copies of nuclear bodies called centrosomes leads to merotelic attachments and chromosome mis-segregation in cell lines [Ganem et al., 2009]. Thus, given the link between lagging chromosomes and chromothripsis, one possible sequence of events is that WGD due to failed division leads to supernumerary centrosomes and ongoing instability including chromothripsis via frequent merotely.

Another mechanism that is likely to play a role in CNA formation is a phenomenon known as 'telomere crisis', reviewed in [Maciejowski and de Lange, 2017]. Telomeres are composed of long tracts of repetitive double-stranded DNA. They function to protect the ends of chromosomes from recognition as sites of DNA damage by the cell. In most human somatic cells telomeres are depleted by around 50bps in each cell division. Loss of telomeres can trigger apoptosis or senescence. However, cells lacking the capacity for cell cycle arrest may undergo what is known as 'telomere crisis', a process involving multiple DNA aberrations, including fused dicentric chromosomes. Exit from telomere crisis may be acheived by activation of telomerase enzymes by the cell [Maciejowski and de Lange, 2017].

Two recent studies have demonstrated intriguing links between telomere shorting and mutations observed in cancer. The first study showed that human cells in telomere crisis underwent tetraploidisation [Davoli and de Lange, 2012]. The second study used live-cell imaging to show that cells with dicentric chromosomes induce rupture of the nuclear envelope and that cell clones that have undergone telomere crisis show chromothripsis [Maciejowski et al., 2015]. Additionally, the breakage of dicentric chromosomes found in telomere crisis can lead to what is known

as *breakage-fusion-bridge cycle* (BFB cycle) [Maciejowski and de Lange, 2017]. BFB cycles can result in a range of CNAs, including gene amplification and rearrangements. These results suggest another possible chain of events in some human cancers whereby cells undergo telomere crisis, resulting in WGD and chromothripsis, followed by ongoing stability as telomerase activity is restored.

Various other mechanisms of CNA accumulation in cancer have been described, with both cell-intrinsic and cell-extrinsic origins [Sansregret et al., 2018]. Defects in the spindle assembly checkpoint (SAC), and in chromosome cohesion are two cell-intrinsic mechanisms that are of uncertain significance in human cancer [Gordon et al., 2012]. In normal functioning the SAC monitors the correct attachment of kinetochores to the mitotic spindle [Gordon et al., 2012]. SAC defects promote cancer in mice, and predispose to cancer in the rare condition mosaic variegated aneuploidy, albeit the pathway is rarely mutated in humans [Gordon et al., 2012]. Chromosome cohesion is one of the processes involved in ensuring correct chromosome segregation. Mutations in genes related to chromosome cohesion have been found in colorectal cancer, suggesting a potential role for disruption of cohesion in disease [Gordon et al., 2012]. External to the cell, aspects of the tumour micro-environment including hypoxia and glucose deprivation can induce CNAs [Sansregret et al., 2018], and cell migration may lead to karyotypic abnormalities due to nuclear envelope rupture [Sansregret et al., 2018].

There are also interesting links between CNA mutation processes and SNA mutation processes. Nuclear envelope rupture, which is implicated in chromothripsis [Zhang et al., 2015, Maciejowski et al., 2015], exposes DNA to a nuclease present in the cytosol, which can create the single-stranded substrate for SNAs caused by APOBEC [Sansregret et al., 2018]. This may explain clusters of localised mutations, termed *kataegis*, that have been found near chromothripsis breakpoints [Maciejowski et al., 2015]. Thus, mechanisms that cause CIN may be responsible for SNAs caused by APOBEC found in cancer.

There is increasing evidence to suggest that WGD events frequently occur early in cancer. Abou-Elhamd et al. carried out an analysis of premalignant

(n=41) and malignant (n=79) Head and Neck Squamous Cell Carcinoma (HNSCC) lesions using image cytomtery [Abou-Elhamd and Habib, 2007]. They found that 37% of premalignant lesions were tetraploid (appeared genome doubled) and 17% were aneuploid. By contrast, 90% of malignant lesions were aneuploid, and none were tetraploid. This data is consistent with early WGD events giving way to ongoing instability in HNSCC. Supporting this, Jamal-Hanjani et al. reported a high level of clonal WGD events and a significant correlation between WGD and sub-clonal copy number diversity in a large multi-region sequencing study of lung cancer [Jamal-Hanjani et al., 2017]. Studies of pre-cancerous lesions [Stachler et al., 2015, Li et al., 2014] support an early role for WGD events in esophageal adenocarcinoma and colorectal cancer. Finally, a study in pancreatic cancer provides additional temporal resolution by using SNAs within the CNA regions as a molecular clock. This study made three observations. First, polyploidisation events were predominantly clonal. Secondly, most SNA mutations attributed to a mutational signature linked with ageing occurred before polyploidisation. Finally, most CNAs occurred after polyploidisation. These observations support the impression that WGD events can occur early and give rise to ongoing instability, and the first two observations additionally suggest that early WGD events may occur shortly before the last common ancestor of all tumour cells.

Adding to this picture, emerging data suggests heterogeneity in the rate of CNA accumulation across tumours. A recent single-cell sequencing study in triple negative breast cancer by Gao et al. found high inter-tumour copy number profile heterogeneity but high within-tumour copy-number homogeneity among single cells within each of 13 cancers [Gao et al., 2016]. They argue that, precluding a recent clonal expansion, these profiles suggest historic chromosomal instability that has given way to regained stability, representing a historic punctuated burst of evolution (Figure 1.1 A). These data are consistent with earlier longitudinal studies in breast cancer that found similar CNA profiles between (1/2) paired pre-cancerous 'DCIS' lesions invasive carcinomas [Kuukasjarvi et al., 1997b] and between some paired carcinomas and metastases [Kuukasjarvi et al., 1997a]. Very recently similar results

Figure 1.1: Cartoon illustrating punctuated evolution of the genome. The cartoon in A) shows a more punctuated pattern of mutation accumulation than that in B), which shows a more gradual pattern of evolution. Emerging evidence suggests that some (but not all) tumours follow a punctuated pattern of CNA accumulation

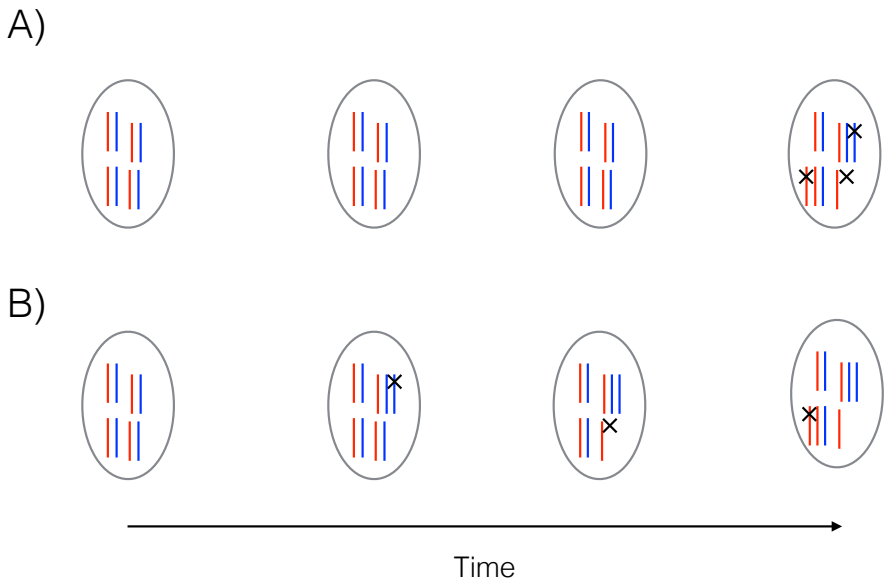

have been found in a follow-up study in breast cancer [Casasent et al., 2018], and using single-cell sequencing in three patients with HBV-related hepatocellular carcinoma [Duan et al., 2018]. Analyses of 21 breast cancer [Nik-Zainal et al., 2012a] and 5 ovarian cancer [Purdom et al., 2013] using SNAs within CNAs as molecular clocks, have found evidence that some tumours accrued CNAs in a punctuated manner, while others followed an approximately constant rate of accumulation (Figure 1.1 B). In summary, these data suggest that both punctuated and gradual patterns of CNA accumulation occur in cancer. Further studies in additional tumour types and with larger sample sizes will be important to assess how widespread these different modes of CNA accumulation are across cancers.

1.5 Selection

As alluded to above, the identification of mutations that are subject to selection during cancer evolution has been one of the most fervently pursued projects in cancer

research in the genomic era. While these studies (reviewed below) have become increasingly sophisticated as new knowledge has emerged on the mechanisms of mutation, they generally follow a common structure: They define a background mutation rate at which non-selected mutations are expected to occur in a cohort of cancer samples. They identify mutations that are found at a higher frequency than expected under neutrality, significantly recurrent mutations (SRMs). These mutations are then classified as driver mutations, typically defined as mutations that have been selected at some point during tumour growth, and the genes that contain them are deemed driver genes. Often these mutations are considered good targets for potential treatment. The implicit rationale for considering these mutations for targeting is that reverting the mutation to wild type could arrest tumour growth.

Before reviewing the findings, it is useful to highlight three points about this argument that are rarely spelled out explicitly. First, the claim that SRMs are driver mutations, in the sense of conferring a selective growth advantage at some point during tumour growth, is not straightforward. Consider a classical tumour suppressor gene, which requires a mutation, or 'hit', to both alleles before providing a growth advantage. Conceivably, a particular mutation that provided the first hit could be recurrent in a set of tumour samples but not have ever provided a selective growth advantage (although the combined mutation consisting of the two hits would provide an advantage). Secondly, consider a mutator mutation, that is neutral or deleterious on whatever background it occurs but increases the rate of future positively selected mutations. Again, this mutation may be recurrent but never have provided a growth advantage. Finally, the argument that an SRM was selected also relies on the assumption that individual mutations occur independently. As a result of these considerations a more appropriate definition of driver gene (that deals with the first two considerations) would perhaps be a mutation that increases the likely number of future progeny of a cell.

Secondly, the rationale that reverting a driver mutation could arrest tumour growth may often be very weak as it depends on biological parameters that are difficult to estimate. The effects of epistasis i.e. the way in which fitness of a mutation

at one genomic sites depends on fitness at others, influence the extent to which the effects of a mutation on one genetic background can predict the effects of reverting the mutation on a likely different genetic background at the time of treatment. Similarly, to the extent that the selective effects of mutations are context-dependent, the reversion of a mutation that was selected early in tumour growth could have unpredictable effects. Consider a hypothetical mutation that is highly immunogenic but is selected in early tumour growth due to an immune-privileged environment. Targeting such a mutation in a later immune-exposed tumour could actually be deleterious. A 2010 study that found that restoration of p53 activity failed to shrink tumours in some mice due to context-specific effects of the gene, illustrates the relevance of this point [Junttila et al., 2010] – Although, the effectiveness of targeting *APC* in colorectal cancer models provides a counterpoint [Dow et al., 2015]. It is important to bear these considerations in mind when interpreting conclusions about SRMs, including those presented here.

The analysis of selection in cancer genomes has developed in step with improved understanding of background mutation rates. Early studies to identify selection from cancer genomes compared numbers of nonsynonymous mutations in genes to a simple cohort-level background mutation rate model inferred from nonsynonymous mutations [Greenman et al., 2007, Kan et al., 2010]. The MutSigCV method represented a major step forward when it was introduced in 2013. This method takes into account patient-specific and gene-specific mutation rates to refine the background mutation model [Lawrence et al., 2013, Lawrence et al., 2014]. Gene-specific mutation rates are determined based on the replication timing and transcription level of the gene, which are known to covary with mutation rate across the genome [Makova and Hardison, 2015]. The method also took into account different rates for several different classes of SNA mutation (such as C>T). The authors demonstrate that these changes can reduce the false positive rate for detecting driver genes. A recent study by the same group that developed MutSigCV identifies suspected indel driver mutations using a model of background indel mutation rates [Maruvka et al., 2017]. It is worth noting that these methods focus on distinguish-

ing genes that are subject to positive selection from those that are not, and do not attempt to quantify the selection experienced by individual genes beyond this binary distinction.

A very recent study by Martincorena and colleagues represented another major advance [Martincorena et al., 2017]. The mutation rate model used in this study takes into account all 96 SNA mutation classes considered by [Alexandrov et al., 2013b] as well as information on the transcribed versus the non-transcribed strand of genes, and other epigenetic mutation rate covariates. More importantly, this study models a distribution of per-gene mutation rates rather than assuming a point mutation rate per gene, and thereby takes into account remaining uncertainty surrounding per-gene mutation rates. This innovation is particularly important given the history of previous refinements to mutation rate models that may suggest further discoveries are likely. Both this study, and another very recent study [Weghorn and Sunyaev, 2017] quantify the effects of selection on individual genes by estimating the ratio of non-synonymous changes to synonymous changes in the gene (dN/dS). Albeit, this dN/dS measure is difficult to interpret.

Another strand of work has focused on identifying the effects of selection based on the frequencies of sub-clonal SNAs. The effects of selection are intertwined with the pattern of cancer growth, and selection may be harder to detect that is usually assumed. A study by Sottoriva et al. indicated that sub-clonal diversity diversity that arose early in colorectal tumour development was maintained during tumour growth, suggesting weak selection at the level of subclones [Sottoriva et al., 2015]. Previous work showed that in c. 30% of tumours the distribution of sub-clonal mutations is consistent with the expectation under neutrality [Williams et al., 2016]. The authors have since gone on to develop techniques to directly quantify the effects of selection, and measure individual fitness effects from samples that deviate from this expected mutation distribution (Williams et al., *in press*).

Inference of selection for CNAs is much less developed, probably due to challenges in determining mutation rates in the absence of selection. A 2013 study by

Zach et al. using TCGA data reported recurrent CNA mutations with the caveat that the recurrence could represent increased mutation rates rather than selection. Of note, the single study that has developed a mutational signature framework for CNAs in breast cancer attempted to use these background mutation rates to infer selected changes, although they do not appear to have used the rearrangement signatures in their inference directly.

In addition to these studies there is a related body of literature on experimental measurement of somatic selection in model systems. These results are important because they circumvent some of the problems of interpretation mentioned above, and it is also generally possible to make more accurate quantitative measurements in these controlled experimental systems. One important study measured the colonisation of mouse colonic crypts by genetically induced mutations over time. The authors observed colonisation by cells with *Kras G12D* mutations and single-allelic *Apc* and bi-allelic *Apc* mutations, which are related to common mutations found in human cancers. The results suggested that the probability of a *Kras G12D*-mutant cell replacing a neighbouring wild-type cell is greater than half (0.75 to 0.81). Single-allelic *Apc* mutations replaced wild-type cells with probability between 0.58 and 0.66, wherease bi-allelic *Apc* mutants replaced wild-type cells with probabilities between 0.75 and 0.82. In yeast, high-throughput experimentation combined with novel cell barcoding techniques have enabled the measurement of the distribution of fitness effects across all genomic mutations [Venkataram et al., 2016]. Important differences between both these model systems and human cancer place a limit on the relevance of these results to human cancer, both in terms of the differences in mutation effects compared to humans and in the micro-environment in which these mutations are selected. Illustrating this, an extensive study that applied the type of selection inference model described above to mutation data from mouse models found marked differences in the genes that were selected compared to human cancers [Ben-David et al., 2017]. However, while results for individual genes and mutations may not be translatable across systems, it seems plausible that general properties in terms of the distribution of selective effects may be less variable.

1.6 Prognostic implications of mutation processes

Here I review the relationship between mutation processes and outcomes in cancer. These relationships provide further motivation for the thesis, by showing in more detail the importance of mutation rates in terms of clinical outcome.

There is a complex relationship between mutation rates and outcome in cancer. Genetically unstable colorectal cancer cells show multidrug resistance in culture [Lee et al., 2011]. In mice, chromosomal instability confers tumours with the ability to survive the removal of an oncogene [Sansregret et al., 2018]. However, in breast cancer, very high levels of chromosomal instability portend a better prognosis, compared to more genetically stable cancers [Birkbak et al., 2011, Roylance et al., 2011]. As mentioned above, in some tissue types at least, ultramutator cancers with *POLE* mutations, also have a better prognosis [Church et al., 2015]. And colon cancers with MSI show high immune cell infiltration and improved prognosis compared to other colon cancers [Vilar and Gruber, 2010].

There is a related complex relationship between mutation diversity and outcomes, which is also informative on the role of mutation processes influencing outcomes, given the close relationship between mutation diversity and the mutation rates that generate this diversity. In Barrett's Oesophagus, higher copy number diversity predicts progression to cancer [Maley et al., 2006, Martinez et al., 2016]. In lung cancer, copy number diversity is an independent factor associated with increased risk of recurrence or death [Jamal-Hanjani et al., 2017]. However, in a pan-cancer analysis tumours in the highest (or lowest) quartile of copy number diversity had reduced mortality risk [Andor et al., 2016]. And in the lung cancer study above, SNA diversity does not predict worse outcome, despite a large sample size (n=100) [Jamal-Hanjani et al., 2017].

One possible explanation for these observations is that raised mutation rates, as well as increasing the likelihood of mutations leading to disease progression, cause mutations that form novel cell-surface proteins, which are recognised by the immune system or neo-antigens. In support of this view, MSI

colon cancers upregulate the ligand PD-1, which suppresses anti-tumour immune response [Llosa et al., 2015], suggesting possible coevolution of cancer and immune cells in the MSI context, with a higher immune response creating a selection pressure for immunosuppressive mutations in the cancer - a phenomenon called immunoediting. More generally, there is a pan-cancer association between the predicted number of neo-antigens, inferred tumour cytotoxic T cell content and prognosis [Brown et al., 2014]. In addition, novel checkpoint inhibitor immunotherapies that inhibit the effects of PD-1, are more effective in lung cancers with more neoantigens, and, in particular, cancers with more clonal neoantigens [McGranahan et al., 2016]. A recent report showed that the clonal status and likelihood of immune recognition of neoantigens predicted response to immunotherapy in cohorts of lung cancer and melanoma patients [Luksza et al., 2017].

A fascinating strand of theory work accompanies these findings. A study by McFarland predicts that mutator cancers will accumulate deleterious mutations, which could include neo-antigens. In particular the authors predict that many moderately deleterious mutations accumulate in mutator tumours, whereas strongly deleterious mutations are filtered out by selection [McFarland et al., 2013]. A followup study shows that these predictions explain certain features of incidence data [McFarland et al., 2014]. Relating these findings to prognosis, a study in HIV viruses has found evidence for a mutational meltdown, caused by a mutation rate beyond which the viruses cannot adapt [Loeb and Mullins, 2000]. There is an indication that a limit of around 20,000 somatic SNAs exists in some cancers with *POLE* mutations [Shlien et al., 2015], which could support the existence of mutational meltdown in tumours. Albeit issues related to the detection limit of sequencing confound the latter observation.

In conclusion, although difficulties in accurately measuring mutation rates in human tumours have limited the amount of data available, there is data to suggest a paradoxical relationship between mutation rates and outcomes in cancer, with highest mutation rates portending a better prognosis. Build-up of deleterious mutations, especially at higher mutation rates, may underlie this data. Improved understand-

ing of the dynamics that relate underlying mutation rates to the accumulation of mutations in the tumour population as a whole, are needed to fully understand the influence of mutation processes on tumour evolution.

1.7 Aims and objectives

In this chapter I have provided a motivation for attempting to better understand the mutation processes that are operative in cancer. I surveyed the literature on mutation processes active in human cancer, the inference of selection in cancer and the prognostic impliations of mutation processes.

Although major progress has been made in the understanding of mutation processes operative in cancer, important questions remain. In particular, questions remain around the timing of SNAs and CNAs during cancer evolution, as well as around identifying the links between mutation causing processes and individual mutations. While improvements in the identification of selection from tumour genomes have been made in step with improvements in understanding mutation rate, there is a need for research that can quantify the effects of selection in a meaningful manner.

At the start of the thesis, in Chapter 2, I present a study of the factors influencing mutation accumulation in breast cancer. I aim to shed light on the influence of population size variation on mutation accumulation during early cancer development, as well as to give a more detailed motivation of the mathematical modelling approach to cancer research.

In the following Chapters (Chapters 3 and 4) I aim to address specific questions about the timing of SNA and CNA mutations during cancer evolution. In chapter 3, I aim to assess the timing of CNA accumulation during colorectal cancer evolution. In chapter 4, I aim to shed light on the timing of *POLE* mutations during the evolution of colorectal and endometrial cancers.

I then turn to analyse the the causal relationships between mutation-causing processes and individual SNA driver mutations in chapter 5.

Finally, also in chapter 5, I aim to infer the selective differences between driver mutations through application of a recent model of mutation causation.

My broader aim in the thesis, in addition to answering the specific points mentioned above, is to make progress towards understanding the complex web of interactions that link the causation of mutations (via population dynamics and selection) to the occurrence and timing of these mutations in patient tumours.

Chapter 2

Mathematical modeling links pregnancy-associated changes and breast cancer risk

The work in this chapter is now published in Cancer Research [Temko et al., 2017].

2.1 Précis

Recent debate has concentrated on the contribution of unavoidable mutations, that may occur on cell division, to cancer development. The tight correlation between the number of tissue-specific stem cell divisions and cancer risk of the same tissue suggests that bad luck has an important role to play in tumor development, but the full extent of this contribution remains an open question. Improved understanding of the interplay between extrinsic (external to the population of cells at risk of cancer) and intrinsic (internal to the population of cells at risk of cancer) factors at molecular scales is one promising route to identifying the limits on extrinsic control of tumor initiation, which is highly relevant to cancer prevention. Here we use a simple mathematical model to show that recent data on the variation in numbers of breast epithelial cells with progenitor features due to pregnancy are sufficient to explain the known protective effect of full-term pregnancy in early adulthood for estrogen receptor positive (ER+) breast cancer later in life. Our work provides a mechanism for this previously ill-understood effect and illuminates the complex in-

fluence of extrinsic factors at the molecular level in breast cancer. These findings represent an important contribution to the ongoing research into the role of bad luck in human tumorigenesis.

2.2 Contribution

Work on this project had already begun when I joined the project; the mathematical model was already largely in place and coded in C++. My main contributions were: (i) To broaden the aims of the analysis to include a more detailed analysis of the model predictions and compare the model predictions to epidemiological data. (ii) To adapt the model outputs for these purposes. (iii) To make some changes to the model, including to accommodate changes in cell proliferation after menopause. (iv) To run the model simulations and analyse the results. (v) To implement a sensitivity analysis, including necessary adaptations to the model code. (vi) To write the manuscript sections other than 'Mathematical Framework', with input from my co-authors (vii) To produce the figures, other than figure 2.2, with input from my co-authors.

2.3 Introduction

A recent study [Tomasetti and Vogelstein, 2015] by Tomasetti and Vogelstein analysed the relationship between the number of stem cell divisions and cancer risk across tissues to investigate the role of "bad luck" in carcinogenesis. The authors demonstrated that the logarithm of lifetime cancer incidence in a tissue is closely correlated with the logarithm of the cumulative number of stem cell divisions in the same tissue ($R^2 = 0.64$; Figure 2.1 A). One possible interpretation of these results runs as follows. The correlation suggests that random mutations that occur when stem cells divide explain most of the differences in cancer risk between tissues. Consequently, exposure to exogeneous mutagens make only a limited contribution to the risk differences between tissues, despite large presumed variation in exposures between anatomic sites. As a result of the correlation the authors claimed that the majority of the variance in cancer risk among tissues is due to bad luck.

In the reporting of the study and ensuing debate some commentators drew

Figure 2.1: Multiple factors can affect cancer risk in a complex setting. **A**, An analysis by Tomassetti and Vogelstein demonstrated a close correlation between the log of lifetime cancer incidence in a tissue and the cumulative number of stem cell divisions in the same tissue. Plot shown is a schematic showing randomly generated data, illustrating the linear relationship that was found by the study. **B**, Variation in multiple molecular factors may affect cancer risk when they change from the homeostatic state (top left), including the number of progenitor cells (top right), the mutation rate (bottom left), and the fitness effect conferred by mutations (bottom right). Blue circles represent wild-type cells, red circles represent mutated cells.

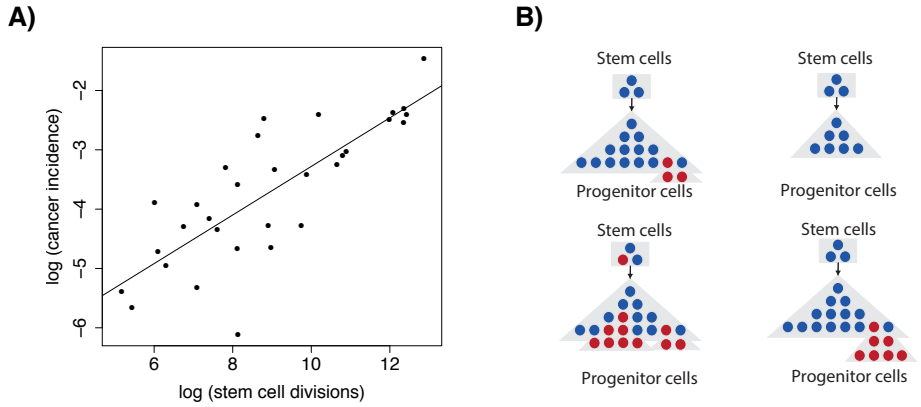

broader conclusions from the correlation found by Tomasetti and Vogelstein. While the initial study claimed that two thirds of the variation in cancer risk between tissues is due to bad luck, an accompanying commentary suggested that two thirds of all cancers, rather than two thirds of the variation, are due to random mutations in healthy cells [Couzin-Frankel, 2015]. Subsequent analyses have shown that the initial correlation is not sufficient to imply a lower bound on the proportion of all cancers that are due to bad luck at 64%. To draw this conclusion from the study would require strong assumptions about the effects of controllable factors in the data set considered. To adapt an example given by Weinberg and Zaykin [Weinberg and Zaykin, 2015]: suppose that all cancers were made four times as likely by a carcinogen; then the correlation between log incidence and log stem cell divisions would remain the same at 0.64. However, cancer risk could be reduced by 75% by removing the carcinogen. So clearly we cannot conclude from the data as it stands that at least 64% of all cancers are due to bad luck.

Importantly, the regression analysis used by Tomassetti and Vogelstein cannot quantify the possible effects of extrinsic factors that do not already vary within the data set used, which notably did not include breast cancer [Potter and Prentice, 2015]. Therefore, the regression cannot be used to draw conclusions about unavoidable bad luck, taking into account the variation of all possible extrinsic factors. To illustrate this point, consider the (perhaps unlikely) possibility that it is possible to safely alter the fitness advantage of mutations that can lead to cancer. The correlation analysis presented in the study cannot tell us about the impact such variation could have on cancer risk.

The insufficiency of the current evidence to draw conclusions about the contribution of unavoidable bad luck to cancer demonstrates the important potential role of mechanistic models in determining the contribution of controllable factors to different cancer types, and whether these factors can be harnessed for cancer prevention. The changes that lead to cancer are thought to develop in a complex molecular setting, which defies simple characterization. In this setting variation of any number of parameters may affect lifetime risk of cancer; these include but are not limited to the number of cells susceptible to transformation, the mutation rate of cells, and the fitness advantage conferred by those mutations when they occur (Fig. 2.1 B).

Full-term pregnancy in young adulthood is a well-documented natural protective factor for breast cancer [MacMahon et al., 1970, Albrektsen et al., 2005]. Estimates suggest that risk increases by 5% for every five-year increase in the age at first birth for women with one birth [Albrektsen et al., 2005]. The specific effects of parity vary by hormone-receptor status of the resulting tumors [Colditz et al., 2004]. Analysis of the Nurses Health Study (NHS) cohort showed that the risk for ER+ breast cancer decreases with the number of pre-menopausal years accumulated since first birth [Colditz et al., 2004]. Hence, early first birth confers the greatest protective effect; a woman with four births at age 20, 23, 26 and 29 years old has an estimated 29% reduced risk of ER+/PR+ breast cancer between the ages of 30 and 70, compared to a nulliparous woman during the same time period. The same study

found that first birth causes a one-off increase in risk for PR- cancer compared to nulliparous women, with an effect size that increases with age at first birth. As a result, women with a first birth over the age of 35 can be at an increased risk of breast cancer.

Mathematical models, informed by data, have demonstrated the plausibility of general molecular explanations for the protective effects of pregnancy. An important study by Moolgavkar et al. explored a framework where breast cancer is caused by two cellular transitions occurring in normal cells [Moolgavkar et al., 1980]. In this model, pregnancy decreases the numbers of normal and partially transformed cells at risk of progression. The study leads to a good fit to the data of MacMahon and colleagues [MacMahon et al., 1970]. Another study [Pike et al., 1983] uses a concept of breast tissue age: breast cancer incidence is modeled as a linear function of the logarithm of breast tissue age, and risk factors for breast cancer alter the rate of breast tissue aging. First full-term pregnancy causes a one-off increase in breast tissue age, but decreases its subsequent rate of increase. This study also demonstrated a good fit to the Moolgavkar et al. data. Rosner and Colditz then adapted and extended the model developed by Pike et al., including changes to further improve the fit and accommodate multiple births, and applied the adapted model to data from the NHS cohort [Colditz et al., 2004, Rosner et al., 1994, Rosner and Colditz, 1996]. The fit of these models to epidemiological data provide support for the theory that pregnancy alters the number of cells that are at risk for accumulating changes leading to breast cancer. However, they do not identify the molecular mechanisms responsible, nor do they accommodate the effects of a cellular hierarchy of stem and progenitor cells.

Recently, single cell technology has made it possible to collect quantitative data on changes in individual mammary sub-populations, presenting the possibility to quantitatively assess the molecular-level changes, as well as the epidemiological incidence curves, associated with pregnancy. Studies in mice and humans provide evidence that p27+ mammary epithelial cells decrease in number with pregnancy, and are present in high numbers in *BRCA1* and *BRCA2* germline mutation carriers

[Choudhury et al., 2013, Huh et al., 2015]. Evidence was presented that a subset of p27+ cells with progenitor features are hormone-responsive quiescent luminal progenitors with proliferative potential, and that their variation could relate to breast cancer risk [Choudhury et al., 2013]. Briefly, p27 cells were found to express estrogen receptor (ER), indicating they may be hormone responsive. The fraction of p27+ cells correlated inversely with the fraction of cells expressing the proliferation marker Ki67, and the two proteins were mutually exclusively expressed, suggesting that the p27+ and Ki67+ cells could represent quiescent and proliferative hormone-responsive cells respectively. Finally, a subset of p27+ cells also express the progenitor cell marker CD44, and the expression of p27 in CD44+ cells decreases significantly with pregnancy. These data, raise the possibility that a subset of p27 cells represent quiescent-hormone responsive progenitors and their number decreases with pregnancy. Here, we use a simple mathematical model to test whether, given a role for p27+ progenitor cells as proliferative progenitors which can accumulate changes leading to breast cancer, the observed reduction in the populations of p27+ progenitor cells with pregnancy is sufficient to explain the protective effect of pregnancy.

2.4 Mathematical Framework

2.4.1 Mathematical model

We aimed to test the hypothesis that a decreasing cell number and proliferative capacity of luminal progenitor cells after pregnancy can result in a protective effect against breast cancer and that the effect decreases with increasing age of pregnancy. To this end, we designed a mathematical model of the dynamics of proliferating cells in the breast tissue that can accumulate the changes leading to cancer initiation. We considered two types of cells: a self-renewing population of stem cells, and a population of proliferating luminal progenitor cells that result from differentiation of these stem cells and respond to hormonal stimuli. We first tested whether we could identify a biologically plausible parameter setting in our model under which the variation in progenitor cell numbers results in a risk decrease that fits the

quantitative risk decreases observed with pregnancy (Section 2.5.1). We then tested the robustness of the fit of our model in the surrounding parameter space (Section 2.5.2).

We first studied the dynamics of stem cells in the breast ductal system. Given the population structure inherent to breast ducts, we considered the stem cells in each duct to act independently. As such, we investigated the dynamics of a single duct within the breast since the total probability of cancer initiation is given by the probability per niche times the number of niches; thus, the relative likelihood of cancer initiation is not altered by considering only one niche. The overall number of stem cells in the breast is estimated to be on the order of 5 to 10 cells per duct [Eirew et al., 2008, Villadsen et al., 2007], and we denoted this number by N (Fig. 2.2), although there is some uncertainty in these estimates. We defined a fundamental time unit of our system to be dictated by the division time of stem cells, t_{cycle}, which varies during pregnancy. In *in vivo* experiments, the mean cell cycle length of benign breast cancer cells was approximately 162 hours per cell [Schiffer et al., 1979]. We assumed that even pre-cancerous cells divide faster than stem cells; thus, using $t_{cycle} = 162$ hours as the average pre-menopausal stem cell cycle length when not pregnant may be an overestimation of the number of stem cell divisions that occur in the normal breast, and we verified that our results were unaffected at higher stem cell cell cycle lengths (shown below). Further, previous data [Choudhury et al., 2013, Popnikolov et al., 2001, Taylor et al., 2009, Chung et al., 2012, Olsson et al., 1996, Going et al., 1988, Anderson et al., 1989] suggests that the percentage of cells in normal breast that stain positive for Ki67 are approximately 3% and 12% in the follicular and luteal phases of the menstrual cycle, respectively. Assuming that the duration of these two menstrual cycle phases is roughly the same, at two weeks per cycle, leads to an average Ki67 value of 7.5%. Considering that Ki67 is detectable for 24 hours during the active phases of the cell cycle [Scholzen and Gerdes, 2000, Cooper, 2000], this translates to an estimate of 320 hours (24 / 0.075) for the average cell cycle length, which is also within the range tested (162 hours to 324 hours). Other studies have shown a broadly consis-

tent range of results [Olsson et al., 1996] or results consistent with still longer cell cycle times [Taylor et al., 2009, Chung et al., 2012].

Experimental data suggests that proliferation decreases 4-5 fold after menopause, irrespective of parity [Choudhury et al., 2013, Huh et al., 2016]. To take this effect into account, we assumed that the cell cycle length increases by a factor of $\alpha_{menopause} = 4$ after menopause. In our model, a single stem cell in each duct is randomly chosen to divide during each time step, proportional to the fitness of the cell, following a stochastic process known as the Moran model [Moran, 1962]. According to this model, the divided cell is replaced by one of the daughter cells of the division, while the other daughter replaces another stem cell that was randomly selected from the population to die. The use of this model ensures preservation of homeostasis in the normal breast epithelial cell population. Since the specific dynamics of stem cells in the breast are not known, we chose the Moran model as it has been used to model stem cell populations in other tissues [Hambardzumyan et al., 2011, Traulsen et al., 2013, Foo et al., 2015]. For each cell division, we allowed for a single mutation to arise in one of the two daughter cells of the division with a certain probability.

In the mature breast, stem cells divide primarily to maintain cellular integrity. However, differentiating events do occur, although rarely [Bresciani, 1968, Daniel and Young, 1971, Faulkin and Deome, 1960]. In our model, with probability p, we allowed the cell division in the current time step to be asymmetric, producing one daughter stem cell to maintain the stem cell population and one progenitor daughter to arise (Fig. 2.2). Since the exact rate of differentiation is unknown, we tested $p = 10^{-1}$ to 10^{-3}. With the remaining $1 - p$ probability, the stem cell division is symmetric and follows the usual Moran division dynamics. In each time step thereafter, all cells resulting from the progenitor daughter divide and differentiate further until a total of z cell divisions are accumulated. The number of luminal epithelial progenitors in humans is unknown. As a result, we set $z = 10$ to fit data from mouse mammary fat pad transplantation experiments [Kordon and Smith, 1998], and tested a wide range of alternate values for this parameter. After z_{pre} divisions,

we considered the cells differentiated and at this point, they are no longer considered in our mathematical model. Thus, in the wild-type system, there are N stem cells per duct and $2^{z+1}-1$ progenitor cells per differentiation cascade. Since the dynamics of progenitor cells in the human breast are not known, we have adopted the assumption that progenitor cells undergo a limited number of divisions, similar to what has been observed for transit-amplifying cells in the colon and other tissues. Figure 2.2 A describes the temporal dynamics of the system.

During each cell division, genetic alterations contributing to cancer initiation may arise with a small probability. We considered a number n_{mut} of mutations that, when combined, result in a single cell leading to cancer initiation. These mutations could each be any of the many mutations commonly found in breast cancer with initiation potential. As a simplifying assumption we considered a mutation rate on the order of 10^{-5} mutations per oncogenic mutation per cell division to limit the required number of simulations for detection to a reasonable number.

The baseline mutation rate is roughly 5×10^{-9} per base pair per cell division [Jones et al., 2008, Salk et al., 2010]. It is estimated that there are roughly 34,000 possible driver base pairs in the genome [Bozic et al., 2010], thus it may be reasonable to assume that there are on the order of 10,000 possible ways to achieve each oncogenic mutation, which would lead to the above rates on the order of 10^{-5} mutations per oncogenic mutation. However, it is important to note that not all driver loci are relevant in breast cancer, and in particular the exact combinations of driver loci that could cause breast cancer are unknown, thus the 10^{-5} figure can only be a broad approximation. For this reason, we also tested our model at other mutation rates, and found that our main conclusions were also consistent at lower mutation rates (shown below).

We studied the following mutational effects for each mutation: under the default assumptions in stem cells, mutant cells had a relative fitness of $f_{mut} = 1.1$, i.e. a fitness increase of 10%, resulting in an increased probability of dividing, while mutant progenitor cells divided an additional $z_{mut} = 1$ times (Fig. 2.2 B). In general a stem cell with n mutations was assumed to have a relative fitness of 1.1^n,

Figure 2.2: Schematic representation of the mathematical model. **A**, Initially, there are N wild-type stem cells (blue), which give rise to a differentiation cascade of $2^{z+1} - 1$ wild-type luminal progenitor cells (purple). At each time step, all progenitor cells as well as one randomly selected stem cell divide. With probability $1 - p$, the stem cell divides symmetrically and one daughter cell replaces another randomly chosen stem cell. With probability p, the stem cell divides asymmetrically and one daughter cell remains a stem cell while the other daughter cell becomes committed to the progenitor population (light pink). Regardless of the dividing stem cell's fate, all existing progenitor cells divide symmetrically for a total of z times to give rise to successively more differentiated cells (progressively darker shades of purple) before becoming terminally differentiated. In the figure, the darkening purple gradations refer to successively more differentiated cells and serve to clarify a single time step of the stochastic process. **B**, The acquisition of mutations leading to breast cancer initiation all result in an increased relative fitness (i.e. growth rate) f_{mut} in stem cells (red) as compared to wild-type cells (blue) and an additional number of divisions z_{mut} progenitor cells can undergo before terminally differentiating. **C**, During pregnancy, progenitor cells experience an expansion in proliferative capacity through an additional number of divisions z_{preg} in order to form terminally differentiated milk-producing cells (dotted triangle) and a decrease in cell cycle length.

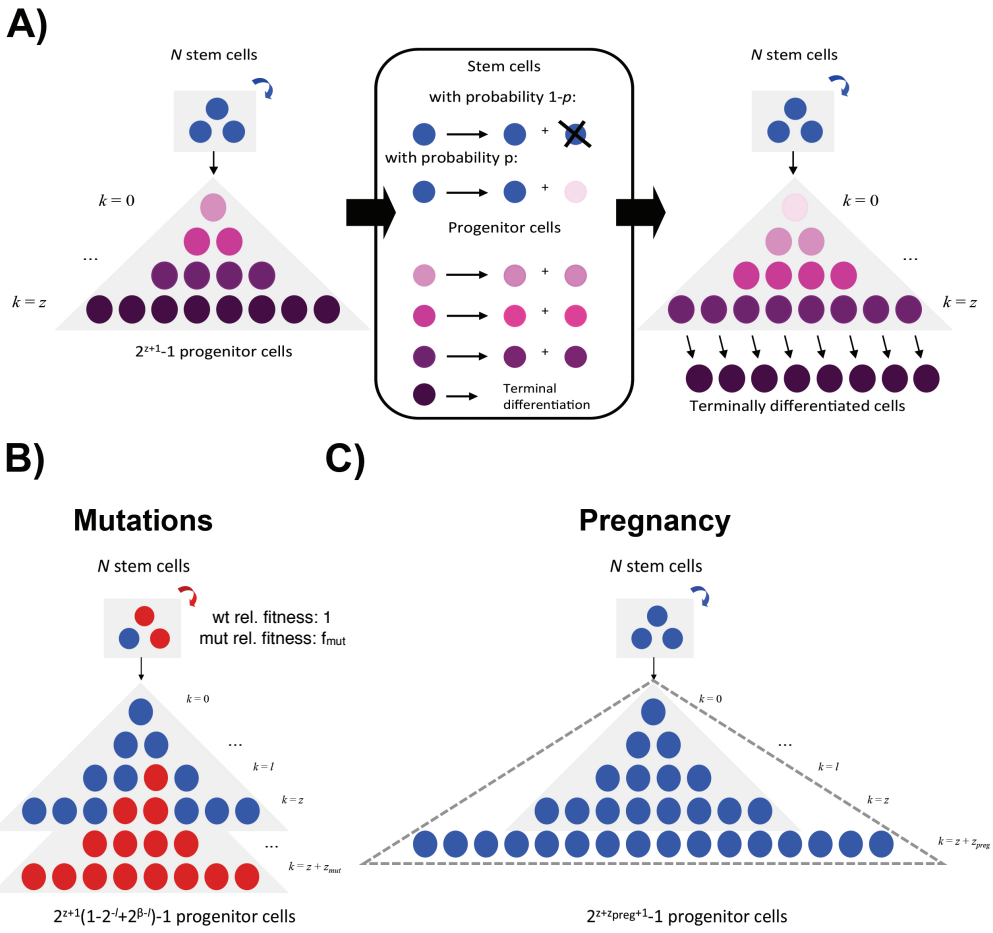

whereas a progenitor cell with n mutations could divide an additional n times before terminal differentiation. Since the number of stem cells per duct is small, the fitness of mutant alleles has little effect on cancer initiation probabilities, as the fixation time of mutations is much smaller than the mutation accumulation time [Hambardzumyan et al., 2011]; we also tested our results at other values of f_{mut} and z_{mut}. Additionally, progenitor cells must accumulate some propensity towards self-renewal: we defined a parameter $\gamma = \gamma_{base} - (i\gamma_{base})/(2 * z)$ as the probability of a progenitor cell at differentiation level $0 \leq i \leq z + nz_{mut}$ to acquire self-renewal. Here n is the number of mutations borne by the progenitor cell. Therefore we assumed that cells closer to the stem cell apex have higher self-renewal propensity, and we explored different values of γ_{base} within this framework. We defined cancer initiation as a single cell that accumulated all required mutations and either retained or acquired the ability to self-renew, either through being a stem cell or through acquiring a genetic or epigenetic self-renewal event.

As we were interested in the effects of the timing of pregnancy, we considered the phenotypic alterations that occur in the breast during pregnancy and as a result of pregnancy. For the purposes of this simulation, we considered the 280 day period of time for the pregnancy itself as the time period during which parameters are altered by pregnancy. Evidence suggests that pregnancy results in the differentiation of mammary epithelial cells [Russo et al., 2005, Russo et al., 1992] as well as their increased proliferation [Chung et al., 2012, Suzuki et al., 2000]. To model these effects, we allowed further differentiation of progenitor cells during pregnancy by an additional z_{preg} differentiation levels, and a decrease in the cell cycle length of stem cells (Figure 2.2 C). There is a 4.5 to 8.5-fold increase in the number of Ki67+ cells during pregnancy [Chung et al., 2012, Suzuki et al., 2000]. Thus, we allowed a 4-fold to 8-fold increase in progenitor cells during pregnancy, corresponding to $z_{preg} = 2$ to 3. The remaining ~ 1.1 fold increase in proliferation was modeled as a decrease in stem cell cycle length, specifically a change by a factor of $\alpha_{preg} = (1/1.1)$. Importantly, we considered that pregnancy reduces the progenitor population in our model. We simulated this change in population

structure by decreasing the rate of asymmetric division of stem cells giving rise to progenitor cells by a factor of $p_{post,init}$ after an initial pregnancy. Our experiments suggested a 2-3 fold drop in p27+ expressing progenitor cells, which suggests a value of $p_{post,init} = 0.5$ [Choudhury et al., 2013].

We also modeled the effects of more than one pregnancy. In runs of the model with more than one birth, we considered the effect of the period of subsequent pregnancies to be the same as for the first birth. That is, the number of levels in the differentiation hierarchy of progenitor cells increases by z_{preg} levels, and the cell cycle length of stem cells decreases to $t_{cycle,preg} = 147$ hours. Regarding the lasting effects of pregnancy on the structure of the breast epithelium, we allowed for the possibility of a smaller decrease in the probability of asymmetric stem cell division after later births compared to the decrease after the first birth, and defined a separate parameter, $p_{post,subs}$, for the decrease in asymmetric divisions after subsequent births.

Our simulation spanned from menarche to death or initiation of cancer within the duct. Our total simulation time was calculated from the average woman's life expectancy in the US, which was 81.2 years in 2014 [NCHS, 2016], and the average age of menarche, which ranged between 12.2 and 12.8 years of age for different ethnic groups in 2007 [Cabrera et al., 2014]. We used the mean age of menarche between the groups, which was 12.5 years and thus resulted in a total of 68.7 years of simulation time.

The parameters in Table 2.1 were set at fixed values from the literature. The parameters in Table 2.2 were set at values that fit to epidemiological data, as described below (Section 2.5.1). We tested the robustness of the fit by varying each of these parameters individually (Section 2.5.2).

Table 2.1: Fixed parameter values. Parameters that remained unchanged throughout all simulations. t_{total}: Simulation time (years), α_{preg}: Proportional reduction of cell cycle time of stem cells during pregnancy, $\alpha_{menopuase}$: Proportional increase of cell cycle time of stem cells after menopause, p_{post}: Proportional reduction in number of progenitor cells after initial pregnancy.

t_{total}	α_{preg}	$\alpha_{menopause}$	p_{post}
68.7	1/1.1	4	0.5

Table 2.2: Range of parameter values investigated. For each parameter of interest, we tested multiple values. Values defaulted to the numbers in bold. t_{cycle}: Cell cycle time of stem cells (hours), N: Stem cell number, z: Progenitor cells divisions, p: Asymmetric division rate, μ: Mutation rate (per cell division), γ_{base}: Self-renewal event rate, f_{mut}: Mutant stem cell relative fitness, z_{mut}: Mutant progenitor expansion, n_{mut}: Mutations required, z_{preg}: Pregnancy progenitor expansion, $p_{post,subs}$: Proportional reduction in number of progenitor cells after subsequent pregnancies.

t_{cycle}	N	z	p	μ	γ_{base}	f_{mut}	z_{mut}	n_{mut}	z_{preg}	$p_{post,subs}$
162	5	6	10^{-3}	2×10^{-6}	3.2×10^{-4}	1.01	**1**	1	**2**	**0.5**
324	**8**	**10**	$\mathbf{10^{-2}}$	$\mathbf{2\times10^{-5}}$	$\mathbf{3.2\times10^{-3}}$	**1.1**	2	**2**	3	0.8
	10	14	10^{-1}	2×10^{-4}	3.2×10^{-2}			3		

2.4.2 Model summary

2.4.2.1 Cellular dynamics of the stem cell and proliferative progenitor cell populations

There are N stem cells per terminal end duct. The stem cells follow a stochastic process known as the Moran model. One cell division occurs during each time step of length t_{cycle}/N. In each time step a single stem cell is randomly chosen to divide proportional to the fitness of the cell, with the two daughter cells replacing the divided cell and another randomly chosen cell.

With probability p, stem cell divisions are asymmetric, giving rise to one stem cell that replaces the divided cell and one progenitor cell that forms the founder in a new cascade of progenitors. All cells in a progenitor cascade divide during every time step. In non-pregnant women, wild-type progenitor cells can divide a total of z times before becoming terminally differentiated (see below for the effects of mutations and effects of pregnancy). Cells that are terminally differentiated exit the simulation.

2.4.2.2 Cancer initiation

During each cell division, one of the two daughter cells in a division attains a new (epi)genetic mutation with probability μ. In stem cells, mutations increase the relative fitness of the cell by a factor of f_{mut}. In progenitor cells mutations increase the number of levels in the differentiation hierarchy by z_{mut} levels. Thus a stem cell with n mutations has relative fitness in the Moran model given by equation 2.1 and a progenitor cell with n mutations is able to divide a total number of times given by equation 2.2 before terminal differentiation:

$$(f_{mut})^n \tag{2.1}$$

$$nz_{mut} \tag{2.2}$$

Additionally, progenitor cells must acquire the ability to self-renew. We assumed that the probability of a progenitor cell at differentiation level $0 \leq i \leq z + nz_{mut}$ attaining self-renewal is given by equation 2.3:

$$\gamma = \gamma_{base} - \frac{i\gamma_{base}}{2z} \tag{2.3}$$

We assumed that cancer initiation occurs when a cell has accumulated a total of n_{mut} mutations and either retained (through being a stem cell) or attained (through a self-renewal event) the ability to self-renew.

2.4.2.3 Effect of pregnancy

Our model simulates an entire life-course over t_{total} years. The model takes into account possible changes to cellular dynamics during pregnancy, after pregnancy, and after menopause. During pregnancy we assumed that the stem cell cycle length decreases to $t_{cycle,preg}$, whereas the number of levels in the differentiation hierarchy of progenitor cells increases by z_{preg} levels. After menopause, the stem cell cycle length increases to $t_{cycle,menopause}$.

In parous scenarios, after the first birth the probability of asymmetric stem cell division changes by a multiplicative factor $p_{post,init}$ ($0 < p_{post,init} < 1$). After the

second birth and subsequent births, the probability of asymmetric stem cell division changes by a factor of $p_{post,subs}$ ($p_{post,init} < p_{post,subs} < 1$).

2.5 Model Exploration

2.5.1 Model fitting procedure

We first investigated whether our model could quantitatively match the epidemiological data available on the protective effect of early pregnancy on breast cancer risk, within the space of biologically plausible parameters. From the literature, a woman with one birth at age 20 has a cumulative relative risk of ER+/PR+ breast cancer of 0.88 (C.I = 0.81 to 0.96) between the ages of 30 and 70, compared to a nulliparous woman, while a woman with four births at ages 20, 23, 26 and 29 has a cumulative relative risk of 0.71 (C.I. = 0.60 to 0.84) over the same age range [Colditz et al., 2004]. To match these rates, we varied the probability that a progenitor cell acquires the ability to self-renew, γ_{base}, and the reduction of the size of the p27+ progenitor cell population after the second pregnancy and later pregnancies, $p_{post,subs}$.

Specifically we tested all 42 combinations of values of γ_{base} and $p_{post,subs}$ with γ_{base} chosen among the seven values evenly spaced in geometric progression between 1e-4 and 1e-1 and $p_{post,subs}$ chosen among the six values evenly spaced in arithmetic progression between 0.5 and 1. All other parameters were set at the default values given in tables 2.1 and 2.2. Under each parameter combination we ran one million model iterations under a nulliparous scenario and under each of two birth scenarios: (i) One birth at age 20, (ii) four births at ages 20, 23, 26 and 29. For comparison to the epidemiological data we then calculated a relative risk for each birth scenario according to the formula (cancer incidence in the scenario between ages 30.5 and 70.5 / cancer incidence in nulliparous scenario between ages 30.5 and 70.5). We considered risk during the 40-year period from age 30.5 to 70.5, rather than 30 to 70, due to binning of modeled incidence into annual groups. We found that with $\gamma_{base} = 3.2x10^{-3}$ and $p_{post,subs} = p_{post,init} = 0.5$, the modeled relative risk were within the confidence intervals reported in the literature for these two data

Figure 2.3: Behaviour of the model under the default parameter settings. Evolution of initiation-free ducts with age under the default parameter settings for three birth scenarios (nulliparous, a single birth at age 20, and four births at ages 20, 23, 26 and 29).

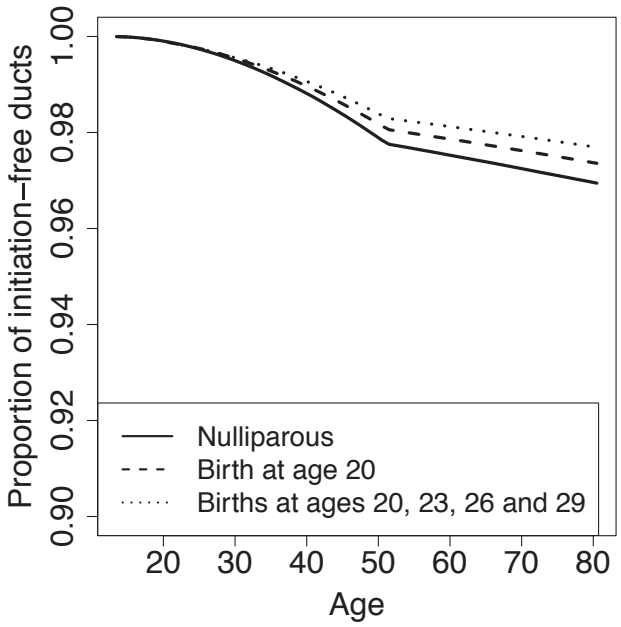

points, at 0.86 and 0.73, respectively (Fig. 2.3). We note that there are likely other parameter settings that could fit the data, in addition to those that we used. Therefore the parameterisation presented here serves as an example of how our model can explain the data, rather than as an exact parameter estimation approach. Similarly, the possibility that multiple parameter settings could explain is one reason for the relatively cautious conclusion of our study, which we see as providing support for, but not proof of, our mechanistic hypotheses.

2.5.2 Analysis of model fit

Using the fitted model, we first tested the effects of varying model parameters in the nulliparous simulations to test the behavior of the model. As expected, we found that the rate of cancer initiation per duct was increased by increasing the number of stem and progenitor cells per duct, the rate of asymmetric stem cell division, the mutation rate, the probability of progenitor cells attaining self-renewal capacity,

Figure 2.4: Effect of parameter variation on cancer initiation in nulliparous simulations. Effects of varying individual parameters of the model on nulliparous cancer initiation. Bars show log fold change of cancer incidence relative to that under default parameter settings.

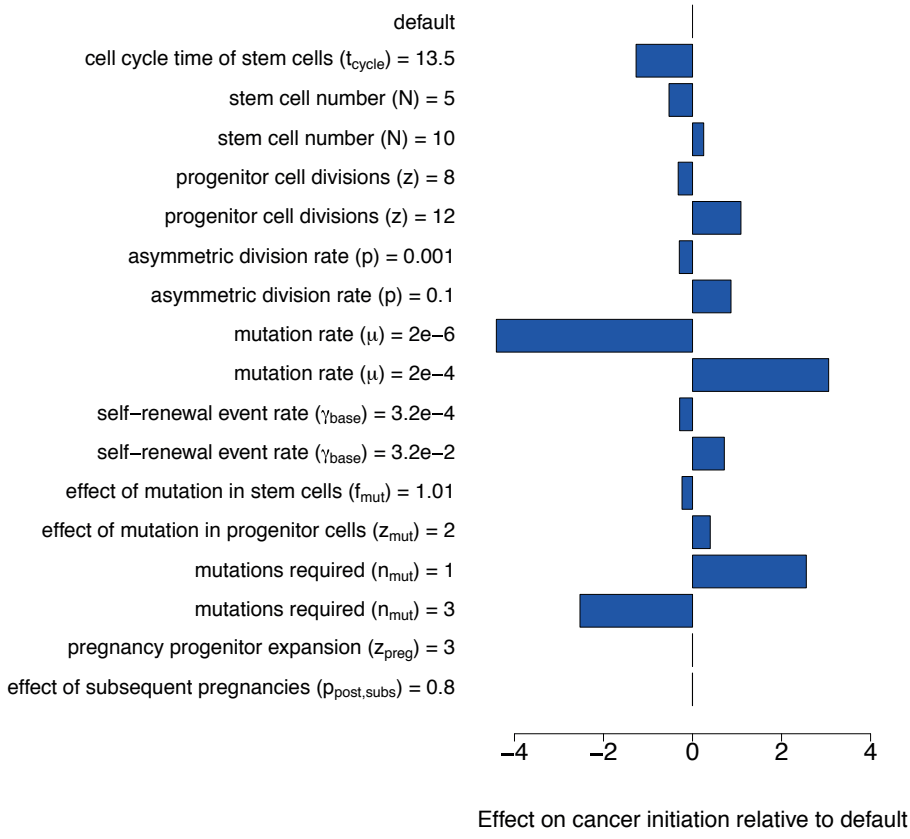

and the fitness advantage of mutated progenitor cells compared to wild type cells. By contrast, the rate of cancer initiation per duct was increased by decreasing the number of mutations required for cancer initiation. Also, as expected, changes in the proliferative capacity of progenitor cells during pregnancy, and the effects of subsequent pregnancies, have no effect in the nulliparous state (Figs. 2.4 2.5).

We then tested the robustness of the fit of our model to the result that early pregnancy protects against breast cancer in the surrounding parameter space. We compared the relative likelihood of cancer initiation with pregnancy occurring at five year intervals during a woman's childbearing years as compared to the nulli-

Figure 2.5: Effect of parameter variation on cancer initiation in nulliparous simulations (continued). Evolution of intiation-free ducts with age under the nulliparous scenario for different settings of the probability of asymmetric division (top), the mutation rate (right), and the number of mutations required for cancer (bottom).

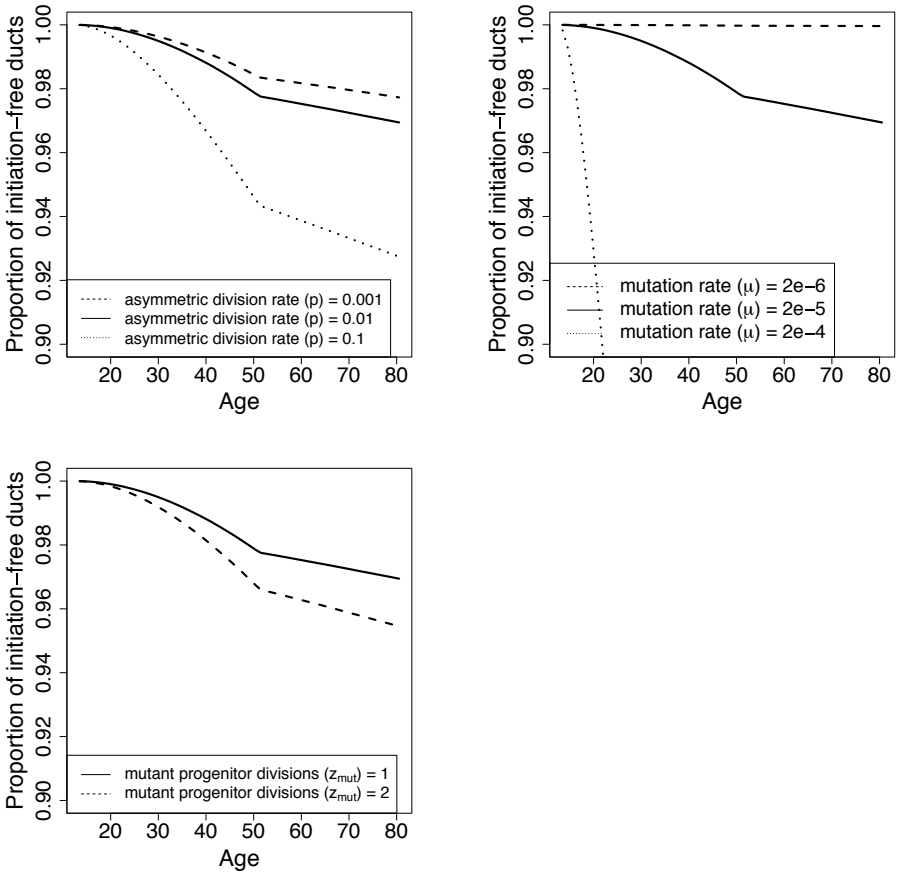

parous simulations. We tested for the effects of pregnancy occurring from the age of menarche until immediately before menopause at the average age of 51.3 in 1998 [Kato et al., 1998]. We tested the effects of varying the simulation parameters independently for each pregnancy age t_{preg}. All fixed value parameters are listed in Table 2.1, while Table 2.2 lists the values of all other parameters. We found that the probability of cancer initiation in a duct increases as the age of first pregnancy increases within the range of all simulated parameters (Fig. 2.6). Additionally, the average probability of cancer initiation across birth ages was lower than the nulliparous risk for all parameter settings. Both of these effects were less marked under

Figure 2.6: Relative probability of cancer initiation per duct as compared to nulliparous simulations. Variation in cancer initiation relative to nulliparous for different ages at first birth under default parameter settings (green lines), and when varying individual model parameters upwards (red lines) or downwards (blue lines). Left to right from top left, effects of varying stem cell cell cyle time, number of stem cells, number of progenitors, probabilities of stem cell differentiation, mutation rate, probability of progenitor cells attaining ability to self-renew, fitness effects of mutations, number of mutations required for cancer initiation, and additional pregnancy divisions, are shown.

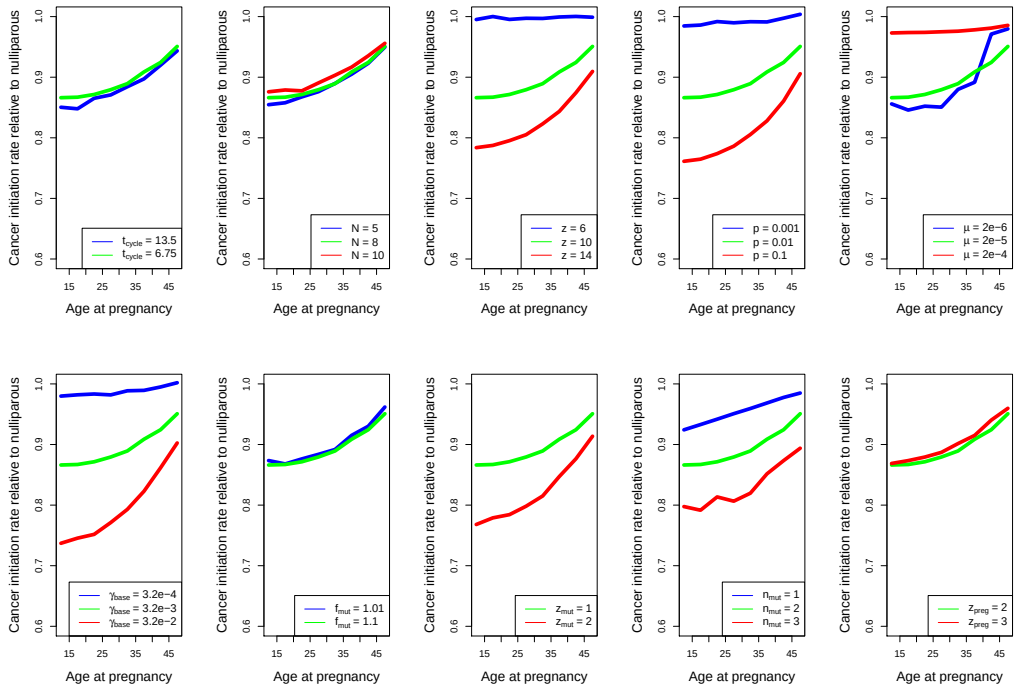

parameter settings in which most of the cancers resulted from the stem cells under the nulliparous scenario ($P < 4 \times 10^{-4}$ Spearman's rank correlation coefficient, in both cases). Indeed, the $z = 6$ setting had the highest proportion of stem cell cancers under the nulliparous setting.

We also investigated the effects of multiple births on cancer risk. We tested model runs with one, two, three, and four total births. For each of these cases, we investigated varying the age at first birth in five year intervals as above from the age of menarche to the age of menopause, assuming that all subsequent births were distributed evenly across the intervening years between the first birth and the age of menopause. For all numbers of total births, risk increased with increasing age at first birth. Additionally, as expected, scenarios with a larger total number of births

Figure 2.7: Relative probability of cancer initiation per duct as compared to nulliparous simulations (continued). Variation in cancer initiation relative to nulliparous for different ages at first birth and different numbers of total births.

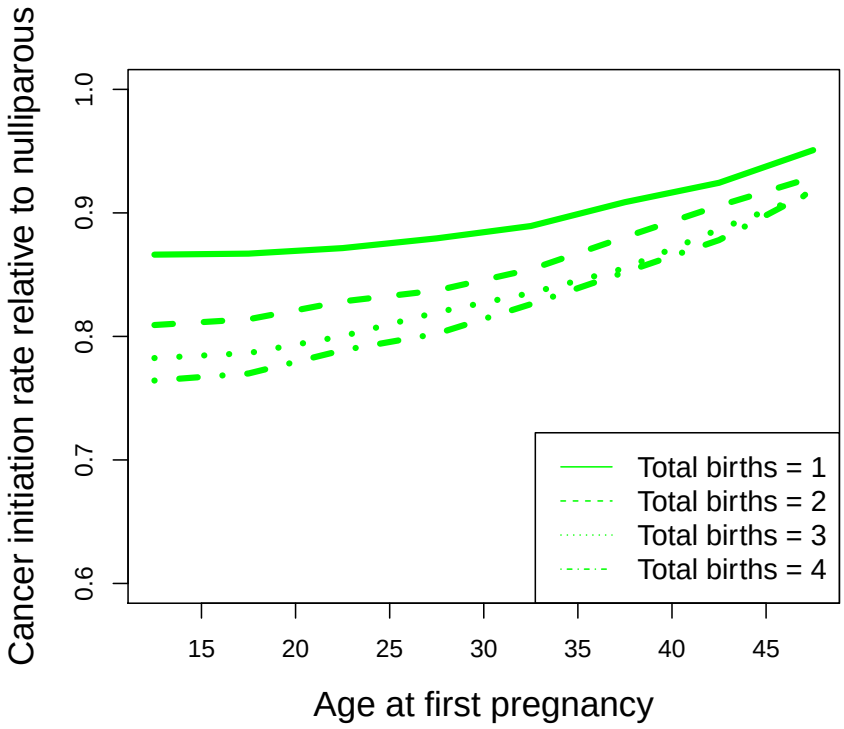

were at a lower risk compared to scenarios with fewer births (Figure 2.7).

We also tested for robustness of the quantitative fit to the two data points considered. As expected, we found that for some parameters the decrease in risk in the two modeled scenarios remained within the bounds of the confidence intervals for all settings tested, whereas for other parameters, there were some settings where the risk decrease did not match the literature values (Fig. 2.8, 2.9, 2.10). In particular the quantitative fit to both data points was robust to changes in the cell cycle time of stem cells, the number of stem cells per duct, the fitness effects of mutations in stem cells, the number of additional progenitor cell divisions during pregnancy and the reduction in numbers of progenitors with subsequent births, within the range of values tested. The quantitative fit was also robust to decrease in the mutation rate in the range of values tested. Thus, our analysis demonstrates that the hypothesis can explain these two observed quantitative decreases in breast cancer risk, under

Figure 2.8: Reduced risk of breast cancer between the ages of 30 and 70 in the scenarios indicated. Dotted and solid lines represent literature estimate and confidence intervals from [Colditz et al., 2004]. '+' Represents base case setting

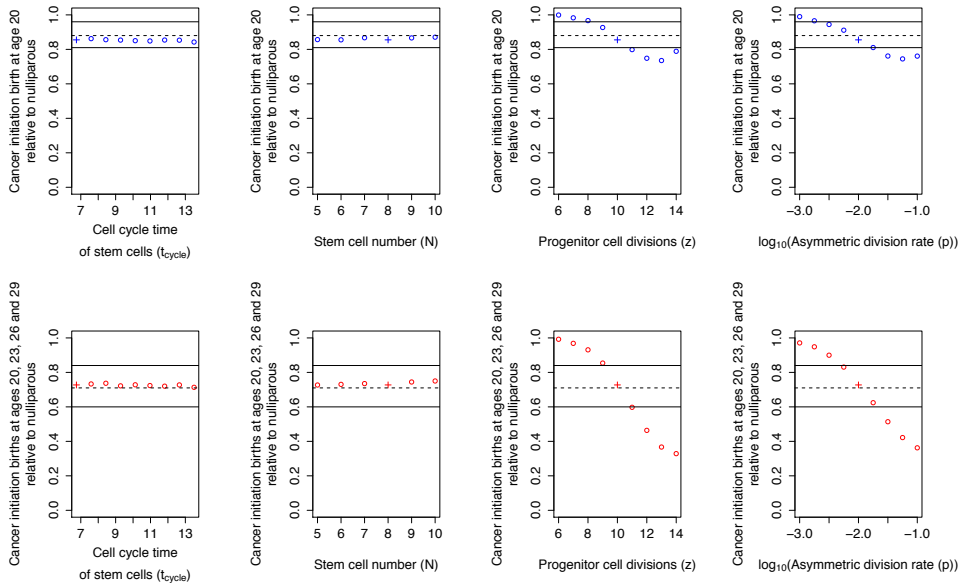

some, but not all, plausible biological settings. Our hypothesis is thus one possible explanation for the observed protective effect of parity. However, we cannot rule out other possible explanations for the relatively limited amount of available data on the quantitative risk reduction.

Another interesting result is the specificity of the effect of the decrease in the progenitor pool with pregnancy to decrease the risk of cancers initiating from the progenitor compartment. We noted that the risk of cancers initiating from the progenitor cell compartment increased with age at first birth, while the risk of cancers where the final mutation occurs in the stem cell compartment showed a (smaller) decrease ($P < 4 \times 10^{-5}$ in both cases under linear regression). Similarly, under the default parameter settings, whereas the risk of cancers initiated from the progenitor compartment was lower under all parous scenarios compared to the nulliparous scenarios, the risk of cancers initiated from the stem compartment was slightly higher under all parous scenarios.

This result raises one possible explanation for the specificity of the protective effect of early pregnancy to ER+/PR+ cancer [Colditz et al., 2004]. Mounting ex-

Figure 2.9: Reduced risk of breast cancer between the ages of 30 and 70 in the scenarios indicated. Dotted and solid lines represent literature estimate and confidence intervals from [Colditz et al., 2004]. '+' Represents base case setting (continued)

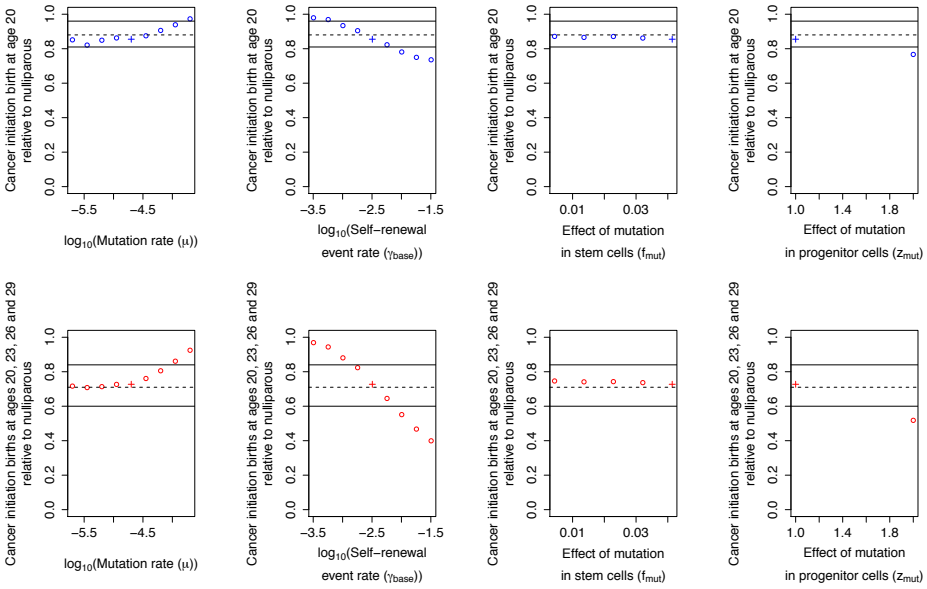

Figure 2.10: Reduced risk of breast cancer between the ages of 30 and 70 in the scenarios indicated. Dotted and solid lines represent literature estimate and confidence intervals from [Colditz et al., 2004]. '+' Represents base case setting (continued)

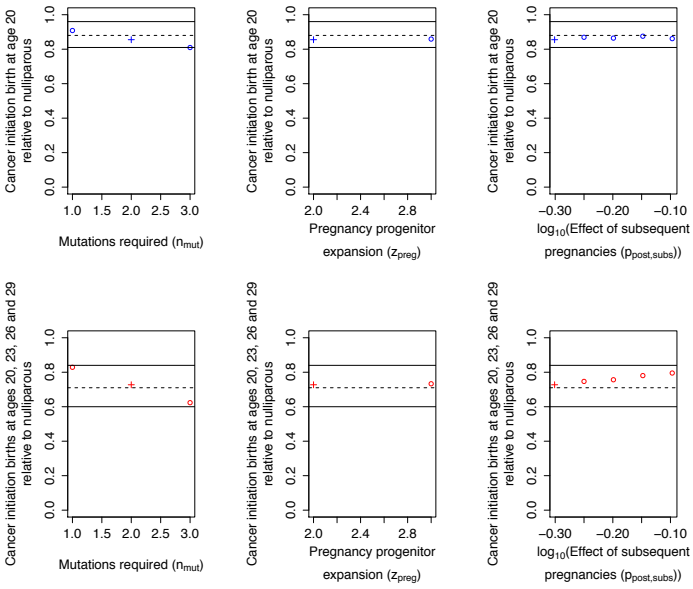

perimental evidence suggests that the typical cell of origin of breast carcinomas is a stem or progenitor cell [Visvader, 2011]. The specificity of the protective effects in our model to a single cellular compartment poses the question of whether other breast cancer molecular subtypes may have a different cell of origin as a possible explanation for the observed specificity of protective effects. Relatedly it is also possible that changes during carcinogenesis render other breast cancer subtypes insensitive to hormone-driven growth or that some of the molecular parameters considered differ between breast cancer subtypes. By the same token, our model is agnostic on whether the pregnancy should protect against other histological breast cancer types, such as lobular cancers. Whether or not protective effects would be expected for these subtypes depend on the extent to which the etiology of these cancer types, in terms of cell of origin and other molecular parameters, corresponds to ER+ cancers. The possibility of a luminal progenitor cell of origin for ER+ breast cancer has been proposed previously [Polyak, 2007]. Explaining the distinct aetiologies of different breast cancer molecular subtypes is a long-standing area of breast cancer research.

As a further test of our framework, we investigated whether our model reproduced the known effect that breast cancer risk is increased for a short period immediately following pregnancy [Albrektsen et al., 2005]. For these purposes we investigated an extended model including a variable delay between initiation of cancer within the duct and clinical presentation. We investigated two scenarios, first birth at age 20, and first birth at age 40, and calculated the relative risk compared to nulliparous women of matched age in the years following pregnancy for varying average waiting times to clinical presentation between 0 and 5 years. We found that with an average waiting time of one year, relative risk in both parous scenarios was greater than one during the two years following the pregnancy (Fig. 2.11).

2.6 Conclusion

Here, we investigated whether variation in the size of the progenitor cell population is sufficient to explain the protective effects of pregnancy against breast cancer. We

Figure 2.11: Evolution of cancer initiation relative to nulliparous with age in a sub-model which includes a delay between initiation of cancer in a duct and clinical presentation. Left panels show cancer initiation relative to nulliparous for a single birth at age 20, right hand panels show cancer initiation relative to nulliparous for a single birth at age 40. Differences in cancer initiation before the age of the birth result arise due to low incidence levels at younger ages.

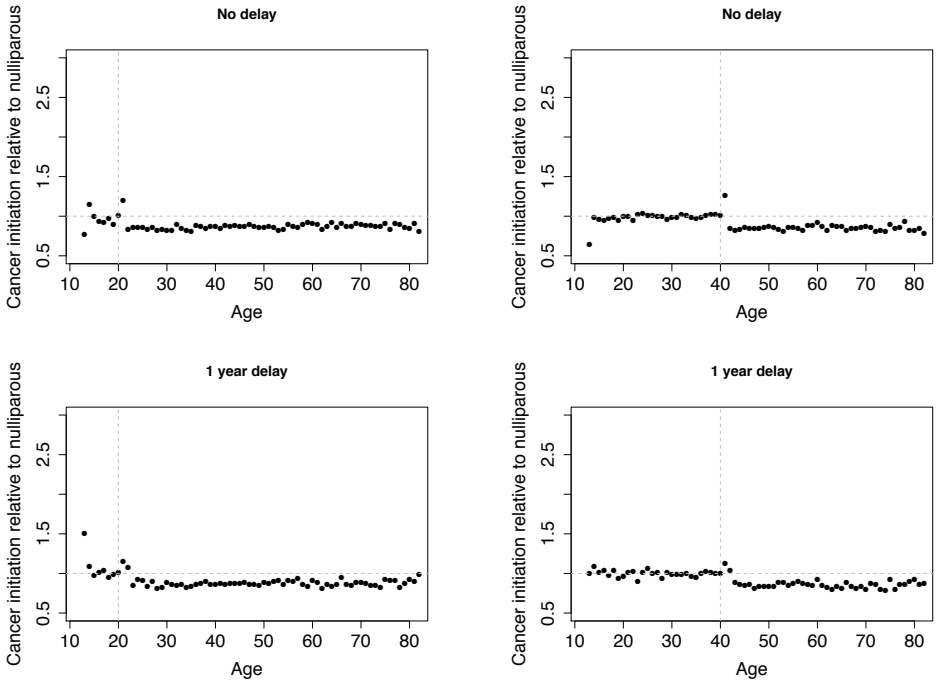

used a simple mathematical model of the steps leading to cancer initiation, which included both stem cells and progenitor cells. We analysed the fit of our model to data from the Nurses' Health Study, a prospective study of breast cancer that followed 66,145 US women over 1,029,414 person years [Colditz et al., 2004]. We found that within the range of biologically plausible parameters, our model matches the observed decrease in ER+/PR+ cancer risk for a woman with a birth at age 20 and a woman with four births in her 20's compared to a nulliparous woman. Using these parameter settings, we found that the risk of cancer in our model decreased with increasing age of first birth in scenarios with one birth. Moreover, the risk of cancer was lower in all scenarios with one birth compared to the nulliparous case. This behavior was robust to variation in key model parameters. The ability of our model to robustly recreate the effect on cancer risk when varying the progen-

itor population size with pregnancy is striking given the modeled assumption that progenitor cells terminally differentiate after a finite number of divisions, so that mutations arising in progenitor cells are liable to leave the population without any functional impact. Taken together, these results support the hypothesis that a subset of p27+ cells represents quiescent hormone-responsive luminal progenitor cells with proliferative potential.

Our mathematical modeling approach for breast cancer can be useful in understanding the contribution of unavoidable bad luck to cancer risk. We have presented evidence that, in the setting of breast cancer, the size of a sub-population of progenitor cells may vary safely over the course of a life to alter breast cancer risk, independent of the probability of mutations. While it is possible that the mechanisms explored here are specific to the breast cancer setting, our results highlight the possibility that extrinsic factors can interact with molecular parameters to affect cancer risk in ways that are not yet fully mapped out. These results therefore further motivate the use of complementary approaches to assess the contribution of bad luck to cancer risk that do not rely on strong assumptions about the effects of extrinsic factors, which may still be subject to revision. The modeling approach developed here is one such possible complementary approach. Therefore, the main implications of our study are support for a mechanism in the breast cancer setting, with potential implications for other cancers with an important role for hormone-driven growth, including endometrial and ovarian cancers. And, in addition, the current approach may be usefully applied in a range of cancer types.

In conclusion, our results demonstrate that variation in the size of the pool of progenitor cells with proliferative potential is capable of explaining the protective effect of early pregnancy against breast cancer. We obtained good agreement between our simple model's predictions and specific epidemiological data points within the range of plausible parameters. Intense recent debate, prompted by the work of Tomasetti and Vogelstein [Tomasetti and Vogelstein, 2015], has indicated the limits of regression techniques for determining the ultimate contribution of bad luck to cancer incidence. Continuing improvements in our mechanistic understand-

ing of the etiology of different cancers can help elucidate the contribution of bad luck to cancer risk and the limits of cancer prevention strategies. Given the complexity of the molecular setting in which cancer develops, mathematical models can be a useful tool in developing such a mechanistic understanding. Our work has developed this approach for the case of breast cancer to provide evidence for a possible mechanism for the protective effect of early pregnancy against the disease.

Chapter 3

Evidence for punctuated accumulation of copy number alterations in colorectal cancer

The work is in preparation for submission

Cross W., Kovac M., Mustonen V., Temko D., Davis H., Baker A., Biswas S., Arnold R., Chegwidden L., Gatenbee C., Anderson A.R., Koelzer V.H., Martinez P., Jiang X., Domingo E., Woodcock D., Feng Y., Kovacova M., Jansen M., Rodriguez-Justo M., Ashraf S., Guy R., Cunningham C., East J.E., Wedge D., Wang L.M., Palles C., Heinimann K., Sottoriva A., Leedham S.J., Graham T.A. and Tomlinson I. The evolutionary landscape of colorectal tumorigenesis, *in preparation*, 2018

3.1 Precis

Emerging evidence from breast cancer and other tumour types suggests that some tumours accumulate (CNAs) in a punctuated fashion, consistent with the occurrence of a 'chromosomal catastrophe' in an ancestral tumour cell, whereas others follow a more gradual pattern of CNA accumulation. The extent to which these patterns exist across cancer types is currently unknown. Here, I present a method that uses SNAs in the region of CNAs as a molecular clock to time the occurrence of CNAs. The method uses information from across the genome to jointly time CNAs, building on previous methods which timed CNAs singly. I also present a method to test for

punctuated CNA evolution using whole exome data (WXS). In the latter part of the chapter I describe applications of the methods to whole genome and exome data from a study of colorectal cancers, and to exome data from a study of inflammatory bowel disease (IBD)-associated colorectal cancers. The results provide support for the occurrence of punctuated CNA accumulation in a subset of colorectal cancers. Although it appears that the whole exome data method often suffers from a lack of power, the whole genome method represents a potentially useful complement to existing methods.

3.2 Contribution

I developed the adapted timing methods in the first part of the chapter. Application of the methods to colorectal cancer WGS data was performed in collaboration with Dr William Cross. I performed the application to WXS data alone. As indicated below, some of the figures presented in this section were generated by Dr William Cross.

3.3 Introduction

The timing, mechanistic cause, and functional consequence of the CNAs observed in cancer samples is still largely unknown and is an active area of research (see Introduction, Chapter 1). Mounting evidence suggests that episodes of punctuated CNA accumulation, where multiple CNA events accrue in a short period of time, are common across cancer types. In particular chromothripsis appears to be common across cancer types [Stephens et al., 2011, Kloosterman et al., 2011, Notta et al., 2016], and several studies have suggested that whole genome duplications are also common [Carter et al., 2012, Zack et al., 2013]. However, accurate identification of WGD events from sequencing data relies on strong assumptions that the most parsimonious explanation for a set of CNAs is the correct explanation.

Recently, several studies in individual cancer types have shed light on some of these questions using a variety of techniques that enable the temporal phasing of CNAs in individual tumour samples (see Chapter 1). Evidence for a punctuated model of CNA accumulation has been presented in breast can-

cer [Nik-Zainal et al., 2012a, Gao et al., 2016, Casasent et al., 2018], lung cancer [Jamal-Hanjani et al., 2017], ovarian cancer [Purdom et al., 2013], and HBV-related hepatocellular carcinoma [Duan et al., 2018]. Studies have indicated that a more gradual model of CNA accumulation, where the CNA accumulation rate appears to be relatively constant in time, is also possible, in breast cancer [Nik-Zainal et al., 2012a] and ovarian cancer [Purdom et al., 2013].

In theory, gradual accumulation of CNAs in small isolated cell populations that occasionally rise to prominence quickly could underlie punctuated changes at the level of the population - a situation known as 'punctuated equilibrium'. By contrast, similar population patterns could result from punctuated CNA accumulation at the level of individual cells that creates highly mutated cells (termed 'hopeful monsters') [Graham and Sottoriva, 2017]. The foregoing studies suggest that hopeful monsters may be a common feature of somatic cell populations en route to cancer.

The methods presented here build on a number of previous methods that use single nucleotide alterations (SNAs) within CNAs as a molcular clock to time CNAs in tumour samples. Steffen Durinck proposed the idea that SNAs that occurred before a duplication in a genomic region were distinguishable from SNAs occurring afterwards, since they are duplicated with the rest of the region [Durinck et al., 2011], suggesting a natural method to time CNA events in the history of tumour samples (see Figure 3.1). This method was adapted and applied to data in the context of breast cancer [Greenman et al., 2012, Nik-Zainal et al., 2012a, Nik-Zainal et al., 2012b]. A later study expanded on the original method, and made adjustments to correct for problems caused by low-depth samples [Purdom et al., 2013].

Whereas previous methods have timed each CNA singly, using the local SNAs, here I present a method to time each of the CNAs in a tumour using a joint likelihood maximisation; I use the information that the total age of every CNA is the same to make use of information from across the genome to time each CNA. The method presented here is agnostic to the causative mutational process; i.e. it can be used to time CNAs that arise due to any mutational process, and uses SNAs in the region of

Figure 3.1: A) Diagram representing a cell genome with an ancestral duplication on one allele of chromosome 1p, and an ancestral duplication on both alleles on chromosome 2q, crosses represent SNAs. In the gained region on 1p, 4 SNAs on the gained allele occured prior to the duplication and so are present on 2 out of 3 copies of the region. B) and C), hypothetical sequencing data from the two gained regions. In B) the SNAs that occurred prior to the gain are distinguishable since a greater proportion of reads from the locus show evidence of the SNA (higher Variant Allele Frequency).

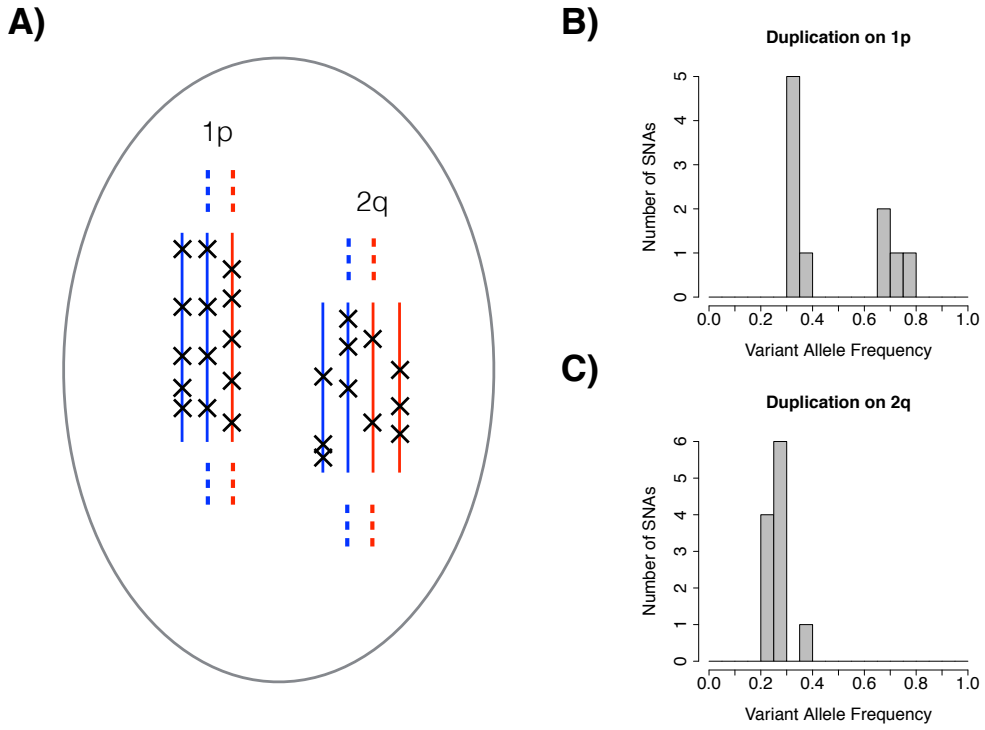

the CNAs as the only indicator of timing. As a result, the inferred timings can point to possible causative mutational processes.

3.4 Mathematical Framework

3.4.1 Growth model

The modelling makes the assumption that the average SNA mutation rate was equal in all of the regions considered, in addition to those assumptions mentioned explicitly below (see 3.6).

Suppose that during the growth of cell lineage L, an ancestral cell, c, gained an extra copy of region r of the A-allele of chromosome j. We note that any SNAs that occurred in an ancestor of c in region r on the A-allele of j will be present on 2 of the 3 copies of this region. However, SNAs that occurred in an ancestor of the cell in region r on the B-allele, and SNAs that occurred in a descendent on the A-allele or B-allele will be present in only 1 of the 3 copies of the region. In general, SNAs in region r will fall into two groups in terms of allele frequency, with SNAs that occurred before the gain, on the gained allele, falling into the higher frequency group [Durinck et al., 2011].

Formalising this reasoning, α, the number of high frequency SNAs in region r, and β, the number of low frequency SNAs in region r, are Poisson distributed random variables with means $\lambda_\alpha = \mu l \theta$ and $\lambda_\beta = 2\mu l(\mathrm{T} - \theta) + \mu l \mathrm{T}$. Here μ is the average SNA mutation rate per base pair per year, l is the length of region r in base pairs, θ is the time in years between the start of the cell lineage and the copy gain of r, and T is the time in years between the start of the lineage and the end of the lineage.

We can consider three types of copy number alteration that result in A copies of the A-allele (the more numerous allele) and B copies of the B-allele (the less numerous allele), ordered for ease of exposition:

Case I: $A \geq 2, B = 0$ (LOH and amplification)

Case II: $A = B \geq 2$ (balanced amplification)

Case III: $A \geq 2, B = 1$ (unbalanced amplification)

leading to Poisson distributions for α and β with mean parameters:

Case I: $\lambda_\alpha = \mu l \theta$, $\lambda_\beta = A\mu l(\mathrm{T} - \theta)$

Case II: $\lambda_\alpha = 2\mu l \theta$, $\lambda_\beta = 2A\mu l(\mathrm{T} - \theta)$

Case III: $\lambda_\alpha = \mu l\theta$, $\lambda_\beta = A\mu l(\mathrm{T}-\theta) + \mu l\mathrm{T}$

3.4.2 Joint estimation procedure

Suppose that sequencing data reveals N CNA events as described above, in a single cell lineage, of lengths l_i, resulting in A_i copies of the major allele and B_i copies of the minor allele, and harbouring α_i high frequency SNAs and β_i low frequency SNAs, for $i \in \{1,...,N\}$. Suppose that these events occurred at unknown times $0 \leq \theta_i \leq \mathrm{T}$ for $i \in \{1,...,N\}$. Finally, suppose that the length of the genome that is diploid is l_d and that there are γ_d SNAs in these regions. The derivation below, relies on the α_i and the β_i being strictly greater than 0. This is the case for all the applications of the test presented here, and is generally expected given the high resolution of whole genome sequencing data.

Scaling the time parameters by the mutation rate we define $t_i = \mu\theta_i$, and define $T = \mu\mathrm{T}$. Further we define the index sets $C_i := \{i : \text{CNA } i \text{ falls under Case } i\}$.

Now consider the joint-likelihood $\mathscr{L}(\boldsymbol{\alpha},\boldsymbol{\beta},\mathbf{t},T)$ of the data, as a function of the data $\boldsymbol{\alpha} = (\alpha_1,\alpha_2,...,\alpha_N)$, $\boldsymbol{\beta} = (\beta_1,\beta_2,...,\beta_N)$ and the parameters of interest $\mathbf{t} = (t_1,t_2,...,t_N)$, T. This likelihood is given by a multiple of Poisson probabilities (since the number of SNAs at each frequency in each region is independent):

$$\begin{aligned}\mathscr{L}(\boldsymbol{\alpha},\boldsymbol{\beta},\mathbf{t},T) = &\prod_{i\in C_1} e^{-l_i t_i}\frac{(l_i t_i)^{\alpha_i}}{\alpha_i!}e^{-A_i l_i(T-t_i)}\frac{(A_i l_i(T-t_i))^{\beta_i}}{\beta_i!}\\ &\times\prod_{i\in C_2} e^{-2l_i t_i}\frac{(2l_i t_i)^{\alpha_i}}{\alpha_i!}e^{-2A_i l_i(T-t_i)}\frac{(2A_i l_i(T-t_i))^{\beta_i}}{\beta_i!}\\ &\times\prod_{i\in C_3} e^{-l_i t_i}\frac{(l_i t_i)^{\alpha_i}}{\alpha_i!}e^{-(A_i l_i(T-t_i)+l_i T)}\frac{(A_i l_i(T-t_i)+l_i T)^{\beta_i}}{\beta_i!}\\ &\times e^{-2l_d T}\frac{(2l_d T)^{\gamma_d}}{\gamma_d!}\end{aligned} \tag{3.1}$$

In the next section we seek to maximise this likelihood subject to the constraints $0 \leq \mathbf{t} \leq T$

3.4.3 Likelihood Maximisation

We seek to solve the constrained optimisation $\max_{0\leq \mathbf{t}\leq T} \mathscr{L}$

For this type of problem we can find a set of conditions on the Lagrangian, known as the Kuhn-Tucker conditions, satisfied by any feasible local maximum, and, *a fortiori*, by a global maximum (Theorem 2.1 in [Luptacik, 2010])

Thus, defining $I = \{1,2,...,N\}$, we have the Lagrangian:

$$L(\boldsymbol{\alpha},\boldsymbol{\beta},\mathbf{t},T) = \mathscr{L}(\boldsymbol{\alpha},\boldsymbol{\beta},\mathbf{t},T) + \sum_{i\in I}\lambda_i t_i + \sum_{i\in I}\lambda_{N+i}(T-t_i) \tag{3.2}$$

and Kuhn-Tucker conditions:

$$\begin{aligned}
&\forall i \in I, \quad \frac{\partial L}{\partial t_i} = 0, \quad \frac{\partial L}{\partial T} = 0,\\
&\forall i \in I, \quad t_i \geq 0, \quad T - t_i \geq 0,\\
&\forall i \in I, \quad \lambda_i t_i = 0, \quad \lambda_{N+i}(T-t_i) = 0,\\
&\forall i \in I, \quad \lambda_i \geq 0, \quad \lambda_{N+i} \geq 0
\end{aligned}$$

We will now find expressions for $(\mathbf{t},T)$ that must hold at a global maximum, and show that there is at most one solution.

For all $i \in I$, since $\alpha_i > 0$, $t_i = 0 \implies \mathscr{L} = 0$. There are at least some admissible points where $\mathscr{L} > 0$, so at a global maximum, $0 < t_i$ and therefore $\lambda_i = 0$.

Similarly, for all $i \in C_1 \cup C_2$, since $\beta_i > 0$, $t_i = T \implies \mathscr{L} = 0$. So in these cases $t_i < T$ and therefore $\lambda_{N+i} = 0$.

So we can simplify 3.2

$$L = \mathscr{L}(\boldsymbol{\alpha},\boldsymbol{\beta},\mathbf{t},T) + \sum_{i\in C_3}\lambda_{N+i}(T-t_i) \tag{3.3}$$

Our strategy will now be to express each t_i in terms of T and then solve for T.

Consider $i \in C_1$:

$$\frac{\partial L}{\partial t_i} = 0$$
$$\implies \frac{\partial \mathscr{L}}{\partial t_i} = 0$$
$$\implies \frac{\partial \log(\mathscr{L})}{\partial t_i} = 0$$

Since $\log(\mathscr{L}) = (A_i - 1) l_i t_i + \alpha_i \log(t_i) + \beta_i \log(T - t_i) + C$, where C does not depend on t_i

$$\implies (A_i - 1) l_i + \frac{\alpha_i}{t_i} - \frac{\beta_i}{(T - t_i)} = 0$$
$$\implies (A_i - 1) l_i (T - t_i) t_i + \alpha_i (T - t_i) - \beta_i t_i = 0$$
$$\implies (1 - A_i) l_i t_i^2 + ((A_i - 1) l_i T - \alpha_i - \beta_i) t_i + T \alpha_i = 0$$
$$\implies t_i = \frac{((1 - A_i) l_i T + \alpha_i + \beta_i) \pm \sqrt{((1 - A_i) l_i T + \alpha_i + \beta_i)^2 - 4(1 - A_i) l_i T \alpha_i}}{2(1 - A_i) l_i}$$

Since $-4(1 - A_i) l_i T \alpha_i > 0$, $2(1 - A_i) l_i < 0$ and $t_i > 0$

$$\implies t_i = \frac{((1 - A_i) l_i T + \alpha_i + \beta_i) - \sqrt{((1 - A_i) l_i T + \alpha_i + \beta_i)^2 - 4(1 - A_i) l_i T \alpha_i}}{2(1 - A_i) l_i} \tag{3.4}$$

Consider $i \in C_2$:

$$\begin{aligned}
&\frac{\partial L}{\partial t_i} = 0 \\
\implies &\frac{\partial \mathscr{L}}{\partial t_i} = 0 \\
\implies &\frac{\partial \log(\mathscr{L})}{\partial t_i} = 0
\end{aligned}$$

Similar to the above

$$\implies 2(A_i - 1)l_i + \frac{\alpha_i}{t_i} - \frac{\beta_i}{(T - t_i)} = 0$$

By a similar argument to the above

$$\implies t_i = \frac{(2(1-A_i)l_iT + \alpha_i + \beta_i) - \sqrt{(2(1-A_i)l_iT + \alpha_i + \beta_i)^2 - 8(1-A_i)l_iT\,\alpha_i}}{4(1-A_i)l_i} \tag{3.5}$$

Consider $i \in C_3$:

$$\begin{aligned}
&\frac{\partial L}{\partial t_i} = 0 \\
\implies &\mathscr{L}((A_i - 1)l_i + \frac{\alpha_i}{t_i} - \frac{A_i\beta_i}{(A_i+1)T - A_it_i}) - \lambda_{N+i} = 0
\end{aligned}$$

Since $\mathscr{L} > 0$

$$\implies (A_i - 1)l_i + \frac{\alpha_i}{t_i} - \frac{A_i\beta_i}{(A_i+1)T - A_it_i} = \frac{\lambda_{N+i}}{\mathscr{L}}$$

If $t_i < T$, since $\lambda_{N+i}(T - t_i) = 0$, we have $\lambda_{N+i} = 0$. So

$$(A_i - 1)l_i + \frac{\alpha_i}{t_i} - \frac{A_i\beta_i}{(A_i+1)T - A_it_i} = 0$$

and similar to Cases 1 and 2

$$t_i = \frac{((1-A_i)(A_i+1)l_iT + A_i(\alpha_i+\beta_i))}{2(1-A_i)A_il_i} - \frac{\sqrt{((1-A_i)(1+A_i)l_iT + A_i(\alpha_i+\beta_i))^2 - 4(1-A_i)A_i(A_i+1)l_iT\alpha_i}}{2(1-A_i)A_il_i} \quad (3.6)$$

Moreover

$$0 = \frac{\lambda_{N+i}}{\mathscr{L}} = (A_i-1)l_i + \frac{\alpha_i}{t_i} - \frac{A_i\beta_i}{(A_i+1)T - A_it_i} > (A_i-1)l_i + \frac{\alpha_i - A_i\beta_i}{T}$$
$$\implies T < \frac{A_i\beta_i - \alpha_i}{(A_i-1)l_i}$$

Whereas if $t_i - T = 0$, then

$$t_i = T \quad (3.7)$$

$$\frac{\lambda_{N+i}}{\mathscr{L}} = (A_i-1)l_i + \frac{\alpha_i}{t_i} - \frac{A_i\beta_i}{(A_i+1)T - A_it_i} = (A_i-1)l_i + \frac{\alpha_i - A_i\beta_i}{T} \quad (3.8)$$

Moreover, since $\lambda_{N+i} \geq 0$

$$0 \leq \frac{\lambda_{N+i}}{\mathscr{L}} = (A_i-1)l_i + \frac{\alpha_i}{t_i} - \frac{A_i\beta_i}{(A_i+1)T - A_it_i} = (A_i-1)l_i + \frac{\alpha_i - A_i\beta_i}{T}$$
$$\implies T \geq \frac{A_i\beta_i - \alpha_i}{(A_i-1)l_i}$$

So defining $T_{crit_i} := \frac{A_i\beta_i - \alpha_i}{(A_i-1)l_i}$; if $T < T_{crit_i}$ then 3.6 holds, and if $T \geq T_{crit_i}$ then 3.7 and 3.8 hold.

Defining $C_{3_1}(T) := \{i \in C_3 : T < T_{crit_i}\}$ and $C_{3_2}(T) := \{i \in C_3 : T \geq T_{crit_i}\}$, we can now give a piecewise determination of $\frac{\partial \mathscr{L}}{\partial T}$ in terms of T only, with the determination depending on which of the possible $|C_3|+2$ intervals, defined by the

$|C_3|$ values of T_{crit} , contains T

$$\frac{\partial \mathscr{L}}{\partial T} = \mathscr{L}(-(\sum_{i\in C_1} A_i l_i + \sum_{i\in C_2} 2A_i l_i + \sum_{i\in C_3} (A_i+1)l_i + 2l_d) + (\sum_{i\in C_1} \frac{\beta_i}{T-t_i} + \sum_{i\in C_2} \frac{\beta_i}{T-t_i} + \sum_{i\in C_3} \frac{(A_i+1)\beta_i}{(A_i+1)T - A_i t_i} + \frac{\gamma_d}{T})) + \sum_{i\in C_{3_2}} \lambda_{N+i} \quad (3.9)$$

So we have

$$0 = \frac{\partial \mathscr{L}}{\partial T}$$

$$\implies 0 = \sum_{i\in C_1} \frac{\beta_i}{T-t_i} + \sum_{i\in C_2} \frac{\beta_i}{T-t_i} + \sum_{i\in C_3} \frac{(A_i+1)\beta_i}{(A_i+1)T - a_i t_i} + \frac{\gamma_d}{T} - \Big(\sum_{i\in C_1} A_i l_i + \sum_{i\in C_2} 2A_i l_i + \sum_{i\in C_3} (A_i+1)l_i + 2l_d\Big) + \sum_{i\in C_{3_2}} \frac{\lambda_{N+i}}{\mathscr{L}}$$

Substituting from 3.7 and 3.8

$$\implies 0 = \sum_{i\in C_1} \frac{\beta_i}{T-t_i} + \sum_{i\in C_2} \frac{\beta_i}{T-t_i} + \sum_{i\in C_3} \frac{(A_i+1)\beta_i}{(A_i+1)T - A_i t_i} + \frac{\gamma_d}{T} - \Big(\sum_{i\in C_1} A_i l_i + \sum_{i\in C_2} 2A_i l_i + \sum_{i\in C_3} (A_i+1)l_i + 2l_d\Big) + \sum_{i\in C_{3_2}} ((A_i-1)l_i + \frac{\alpha_i - A_i\beta_i}{T})$$

$$\implies 0 = \sum_{i\in C_1\cup C_2} \frac{\beta_i}{T-t_i} + \sum_{i\in C_{3_1}} \frac{(A_i+1)\beta_i}{(A_i+1)T - A_i t_i} + \sum_{i\in C_{3_2}} \frac{\alpha_i+\beta_i}{T} + \frac{\gamma_d}{T} - \Big(\sum_{i\in C_1} A_i l_i + \sum_{i\in C_2} 2A_i l_i + \sum_{i\in C_{3_1}} (A_i+1)l_i + \sum_{i\in C_{3_2}} 2l_i + 2l_d\Big) \quad (3.10)$$

It is easily shown that this function is continuous by showing it is continuous at the piecewise breakpoints. Moreover we now show it is decreasing in T so that it has at most one solution.

The right summand is a negative constant. The left summand is a sum of fractions with constant numerators. Therefore it suffices to show that denominators of the fractions in the left summand are all increasing.

Consider $i \in C_1$

From 3.4

$$T - t_i = \frac{((1-A_i)l_iT - \alpha_i - \beta_i) + \sqrt{((1-A_i)l_iT + \alpha_i + \beta_i)^2 - 4(1-A_i)l_iT\alpha_i}}{2(1-A_i)l_i}$$

Let $x = (1-A_i)l_i$, then

$$T - t_i = \frac{(xT - \alpha_i - \beta_i) + \sqrt{(xT + \alpha_i + \beta_i)^2 - 4xT\alpha_i}}{2x}$$

Suppose for a contradiction that $\frac{\partial(T-t_i)}{\partial T} < 0$

$$\begin{aligned}
&\implies \frac{1}{2} + \frac{(2x(xT + \alpha_i + \beta_i) - 4x\alpha_i)}{4x\sqrt{(xT + \alpha_i + \beta_i)^2 - 4xT\alpha_i}} < 0 \\
&\implies \frac{(xT + \alpha_i + \beta_i) - 2\alpha_i}{\sqrt{(xT + \alpha_i + \beta_i)^2 - 4xT\alpha_i}} < -1 \\
&\implies \sqrt{(xT + \alpha_i + \beta_i)^2 - 4xT\alpha_i} < -(xT - \alpha_i + \beta_i) \\
&\implies x^2T^2 + (\beta_i + \alpha_i)^2 + 2xT(\beta_i - \alpha_i) < x^2T^2 + (\beta_i - \alpha_i)^2 + 2xT(\beta_i - \alpha_i) \\
&\implies 4\alpha_i\beta_i < 0
\end{aligned}$$

Which contradicts the fact that in all cases α_i and β_i are greater than 0

The other denominators can all be shown to be increasing by similar reasoning.

In all cases presented here we are able to find a root of 3.10, numerically, and can thus be confident that it is the only root.

3.4.4 Confidence intervals

We use bootstrapping to calculate mean square errors for each of the estimated parameters $(\mathbf{t}, T)$. Using the generative mathematical model described above parameterised by the estimates for $(\mathbf{t}, T)$, we generate 100 simulated mutation data-sets. In each case the numbers of high and low frequency SNAs α_i and β_i are simulated as Poisson random numbers with mean values depending on the $(\mathbf{t}, T)$ estimates.

In each case we then use the pipeline to re-estimate $(\mathbf{t}, T)$ from the simulated data. We then calculate the mean square error of these results compared to the original estimates used for the simulation.

3.4.5 Testing for punctuated CNA evolution in exome data

Mounting evidence suggests that multiple CNA events may occur at the same time, as described above. However, the majority of sequencing studies to date do not have whole genome resolution, so there may be insufficient mutations to time individual CNAs with high resolution. As such I developed a method to test the null hypothesis that all CNAs occurred in a single event ($H_0 : \forall i,j(t_i = t_j)$), which can be applied to whole exome sequencing data. As an indication, among the samples where I applied the test, there were an average of 32 (range: 2-96) usable SNAs, within on average 48 separate CNAs (range: 25-96).

Taking the parameters and concepts as defined above; for each CNA i, we estimate the number of SNAs that occurred per allele before the CNA n_{early_i} and the number of SNAs that occurred per allele after the CNA n_{late_i} according to the heuristic calculations below:

Case I: $n_{early} = \alpha$, $n_{late} = \frac{\beta}{A}$

Case II: $n_{early} = \frac{\alpha}{2}$, $n_{late} = \frac{\beta}{2A}$

Case III: $n_{early} = \alpha$, $n_{late} = \frac{\beta - n_{early}}{A}$

We generate a $2 \times N$ table of the early and late SNA rate per allele for each of the N CNAs. We then use Fisher's exact test to test against the null hypothesis that the distribution of SNAs between late and early groups is independent of which CNA is under consideration.

3.5 Application to data

This section describes the application of the methods to whole genome and exome data from a study of colorectal cancers, and to exome data from a study of inflammatory bowel disease (IBD)-associated colorectal cancers.

Table 3.1: Colorectal cancer whole genome sequencing data considered for timing analysis

Sample	Sequencing Strategy	Regions Sequenced
Adenoma 4	WGS	3
Carcinoma 3	WGS	6
Carcinoma 5	WGS	6
Carcinoma 9 Distal	WGS	5
Carcinoma 9 Proximal	WGS	5
Carcinoma 10	WGS	5

3.5.1 Application of timing model to whole genome sequencing data in a study of colorectal cancer

The method was applied to 6 tumours, each with multiregion whole genome sequencing data (see Table 3.1).

The timing model requires as input the number of high and low frequency SNAs in regions of specific copy number changes at the endpoint of the evolution of a lineage of cells. We used the availability of multi-region sequencing data to determine this information for a subset of genomic regions in the last common ancestor of all tumour samples as described below.

We identified regions of the genome with a clonal copy number state of either 2:0, 2:1 or 2:2 across samples within a tumour. Since these states were common across samples, we reasoned that these states represented the state in the last common ancestor in these genomic regions. Similarly, within these regions we considered SNAs that were present in all samples as these SNAs were likely to have already been present in the last common ancestor of all tumour samples. We also identified regions that were diploid in all samples, and identified clonal SNAs within these regions to input into the model (see Figure 3.2).

Within each region we clustered the SNAs into a high frequency and a low frequency group using the R package MClust [Fraley et al., 2012, Fraley and Raftery, 2002]. CNAs where the clustering of SNAs violated expectations based on the inferred cancer cell fraction (cellularity) and copy number states were discarded, as were CNAs with genomic length below a threshold (see Figure 3.3).

Figure 3.2: Schematic illustration of a tumour used for multi-region sequencing. The cartoon cells within tumour samples represent the average states inferred by sequencing each bulk sample. Here, the duplication pictured on the bottom right chromosome would be correctly assumed to have been present in the LCA of tumours samples as evidence survives in all samples. Similarly the 3/4 SNAs on this chromosome present in alls samples would be correctly assumed to have been present in the LCA. The CNA on the top left chromosome which was present in the LCA, would be missed, as it has been lost in sample 2.

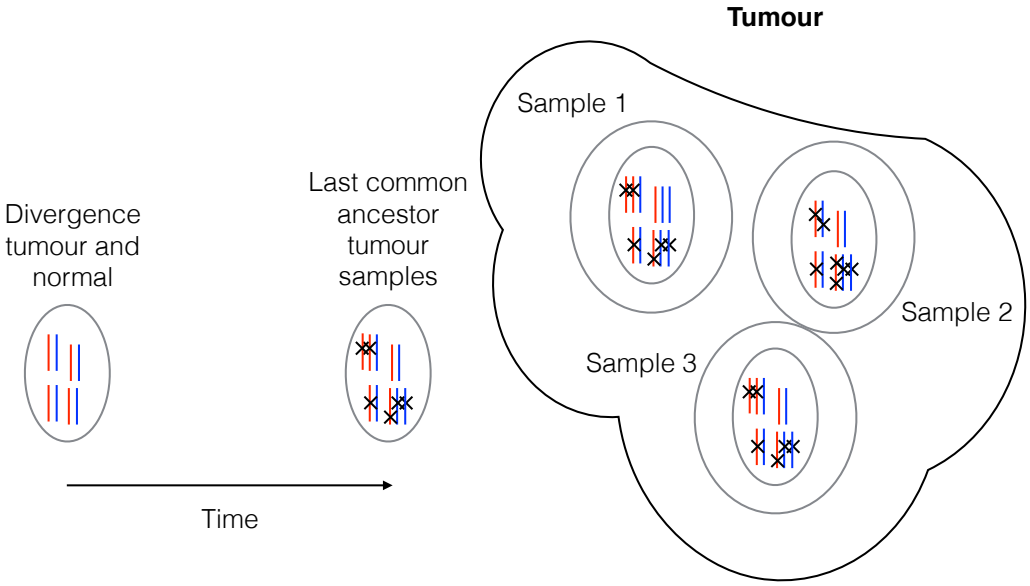

The results of the model application (See Figure 3.4) indicate a rapid accumulation of CNAs in the time period before the last common ancestor of all tumour samples in four of the five tumours where the model was applied - the exception being Carcinoma 5, which appears to show a more even distribution of the CNAs in time between the tumour divergence from the normal and the last common ancestor. The rapid accumulation of CNAs is in keeping with a model of punctuated copy number evolution, as opposed to gradual evolution, during colorectal cancer development, similar to observations in breast cancer and pancreatic cancer. Furthermore, the presence of a cluster of CNAs close in time to the last common ancestor of tumour samples in four cases, is consistent with a potential causal role

Figure 3.3: Figure created by Dr William Cross showing two examples of clustering of SNAs within CNAs into high and low allele frequency groups. The region shown in A) was used for the timing model. The region shown in B) was not used, as the SNAs did not show the clustering expected given the assumed presence of a CNA.

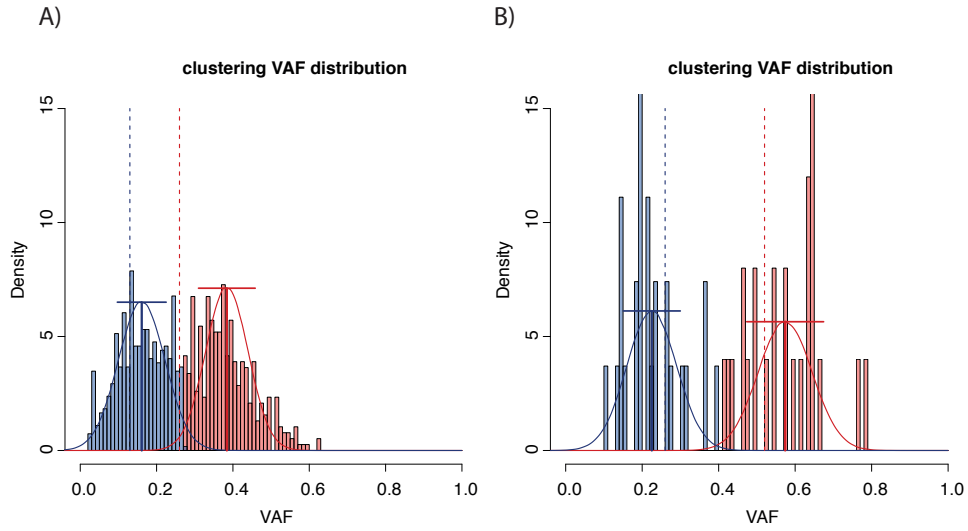

for a punctuated CNA event in driving the last clonal expansion. However, more evidence is needed to draw a firm conclusion.

3.5.2 Exome test power analysis

The detection power of the exome data punctuated evolution test was investigated using simulations. I investigated the power to reject the null hypothesis that all CNAs occurred simultaneously under different scenarios of the numbers of detected CNAs and the number of SNAs within them. For each scenario I simulated 1,000 mutation data sets with random CNA timings chosen from a uniform distribution. The CNAs in each simulation were chosen with random lengths and types (among the three possibilities of types of copy number alteration considered), and the SNA mutation rate in each scenario was set so that the expected number of SNAs, given the CNA lengths, timings and states was equal to the number of SNAs for the scenario. In each scenario the test was applied to the number of early and late SNAs in the region of each CNA, sampled using a Poisson distribution. These simulations

Figure 3.4: Figure created by Dr William Cross showing CNA timings in colorectal cancer data. The timing model was applied to 1 adenoma and 5 carcinomas. The bottom left figure of each panel shows the accumulation of CNAs over time (x-axis), with horizontal lines representing the confidence interval for the timing of each CNA (y-axis). The top figures show the cumulative proportion of CNAs that have occurred at each point in time. Cumulative line is plotted relative to inferred time of 5q LOH (measured in a few cases, then assumed to the same proportion in the other cases).

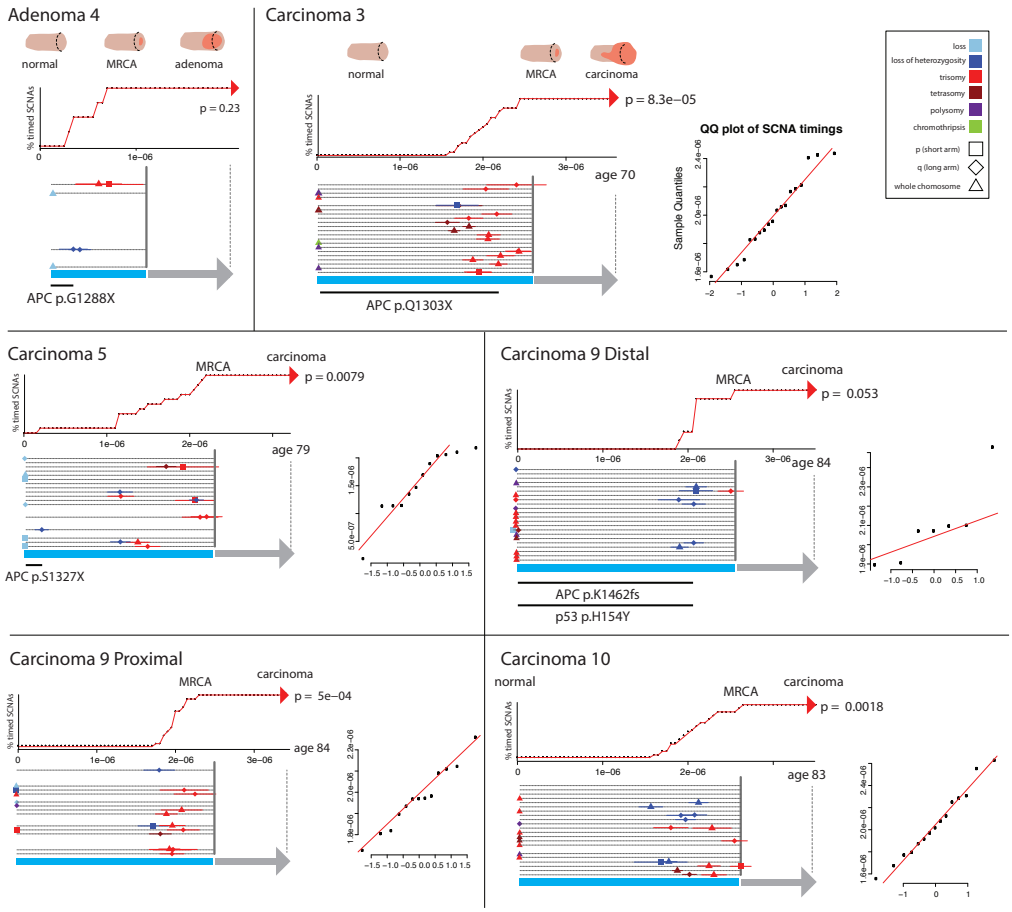

Figure 3.5: Power to detect heterogeneous (non-catastrophic) timing of CNAs in WXS data. Proportion of tests with significant P values (<0.05) based on testing 1,000 simulated data sets assuming a uniform distribution of CNA mutations over time. Dotted line indicates 80% power. Among the combinations tested detection power was highest for the largest number of informative SNAs (100) distributed across the smallest number of CNAs (10).

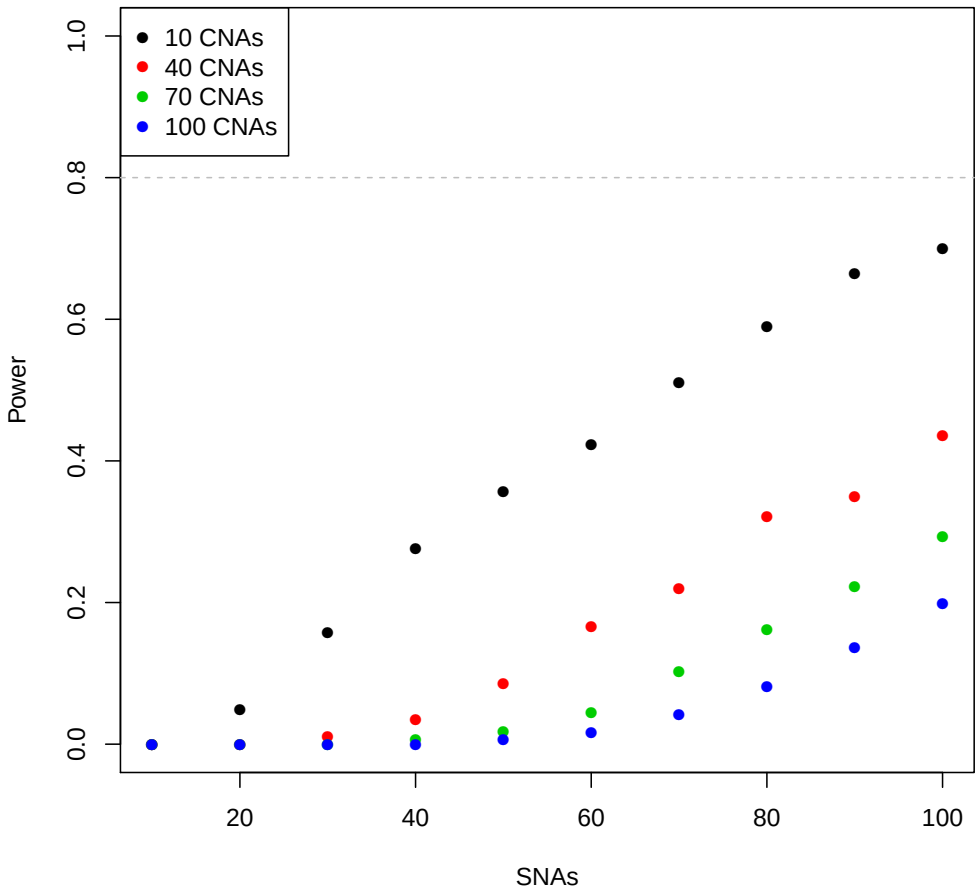

showed that, as expected, the power to detect non-catastrophic CNA accumulation increased with the number of informative SNAs, and decreased with the number of CNAs across which these SNAs were distributed (Figure 3.5).

3.5.3 Application of timing model to whole exome sequencing data in a study of colorectal cancer

I applied the exome data punctuated evolution test to 8 tumours (4 adenomas and 4 cancers) from the same study where multi-region whole exome sequencing data

Table 3.2: Colorectal cancer whole exome sequencing data considered for CNA catastrophe test

Sample	Sequencing Strategy	Regions Sequenced
Adenoma 1	WES	6
Adenoma 2	WES	4
Adenoma 3	WES	5
Adenoma 9	WES	6
Carcinoma 1	WES	5
Carcinoma 6	WES	13
Carcinoma 7	WES	8
Carcinoma 8	WES	5

was available (see Table 3.2).

As above, I attempted to identify a subset of the regions of the genome that were subject to specific types of CNAs in the last common ancestor of all tumour samples, and to identify low and high frequency SNAs present at the time in those regions. Due to noise associated with calling CNAs from exome data, which can lead to incorrect copy number assignments due to the low numbers of mutations providing information about the copy number state in each region (see Figure 3.2), I relaxed the assumption for CNAs to be clonal in every sample. Instead I considered regions where the most common copy number state across samples was one of the states described in Cases I,II and III in Section 3.4, inferring that this was the state in the last common ancestor of all tumour cells in these regions and that differences in the inferred copy number were false.

For each ancestral CNA event, I found the SNAs that were clonal across regions with the common copy state. For each such SNA, considering each tumour sample with surviving evidence of the CNA, I tested the number of variant reads of the clonal SNA for consistency with occurence before the CNA, and for consistency with occurence after the CNA. Fisher's method was used to combine tests of the same hypothesis across tumour samples. I considered SNAs to be present early, if the early hypothesis was not rejected, and the late hypothesis was rejected, and vice-versa. I did not consider SNAs that were inconsistent with both the early and late hypotheses (see Figure 3.6).

One adenoma could not be used for the test since there were no late SNAs

Figure 3.6: For each SNA in a CNA region I tested the hypotheses that the SNA was early (before the CNA), and the hypothesis that the SNA was late (after the CNA). P-values generated for the same hypothesis across samples were combined using Fisher's method. SNAs which were consistent with earliness and inconsistent with lateness were classed as early – illustrative example shown in (A). SNAs inconsistent with both the early and late hypotheses were not considered for the test – illustrative example shown in (B).

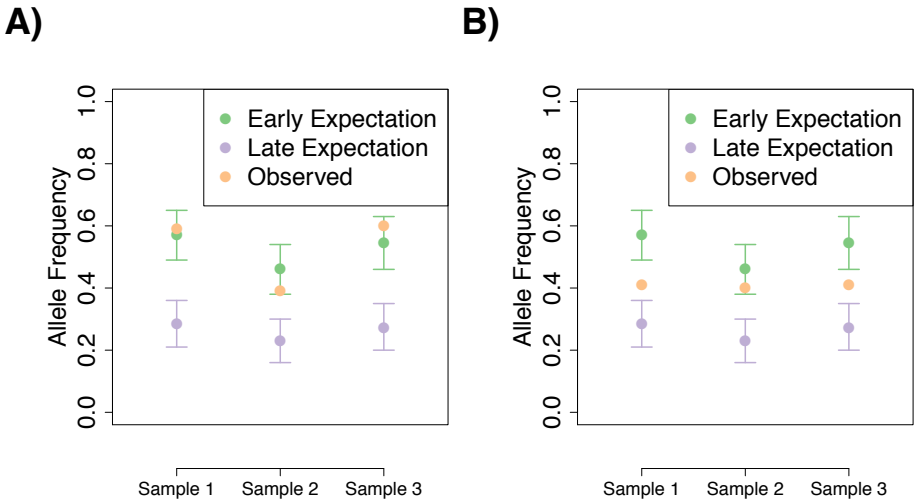

found. The null hypothesis of chromosomal catastrophe was rejected in 1/3 adenomas tested (P = 0.001, Table 3.3). The null hypothesis was not rejected in the other two cases, albeit based on my simulations the test appeared underpowered, with only 2-3 SNAs used for the test in these cases. One cancer could not be used as there were no early SNAs found. The null hypothesis of catastrophe was rejected in 2/3 cancers (min (P) = 0.002), and not rejected in the other cancer (P = 0.772). This cancer had a higher number of informative SNAs (51), albeit the power still appears low based on my simulations. Additionally in this cancer 89% of SNAs occured before the CNAs, consistent with late occurence of many CNAs recently before the last clonal expansion. Notwithstanding the low power, the failure of 1/3 cancers to reject the null hypothesis of punctuated evolution is consistent with the hypothesis

Table 3.3: Application of test for punctuated CNA evolution to colorectal cancer exomes

Sample	Number CNAs	Number SNAs	P
Adenoma 2	37	2	1.00
Adenoma 3	61	54	0.001
Adenoma 5	32	3	1.00
Adenoma 9	18	1	NA
Carcinoma 1	96	51	0.772
Carcinoma 6	77	1	NA
Carcinoma 7	51	17	0.048
Carcinoma 8	71	48	0.002

Table 3.4: IBD-associated-colorectal cancer whole exome sequencing data considered for CNA catastrophe test

Sample	Sequencing Strategy	Regions Sequenced
H1195	WES	2
H1331	WES	2
Oxford IBD1	WES	4
Oxford IBD2	WES	5
STM003	WES	2
STM005	WES	2
STM006	WES	2
STM007	WES	2
STM008	WES	2
UCL001	WES	2

that some colorectal cancers show evidence of punctuated bursts of copy number change.

3.5.4 Application of timing model to whole exome sequencing data in a study of IBD-associated-colorectal cancer

I applied the catastophe test to 10 tumours (10 cancers) with multi-region whole exome sequencing data from a study of IBD-associated colorectal cancer, (see Table 3.4). The data was processed as described above in section 3.5.3

Four tumours were not considered due to having no early SNAs or no late SNAs. The null hypothesis of a chromosomal catastrophe was not rejected in any of the six cases where the test was applied (min (P) = 0.176, Table 3.5). These data suggest that chromosomal catastrophes may be commmon in IBD-associated colorectal cancer, in as much as the test is powered to reject the null hypothesis.

Table 3.5: Application of test for punctuated CNA evolution to IBD-associated colorectal cancer exomes

Sample	Number CNAs	Number SNAs	P
H1195	41	34	0.176
H1331	39	96	0.275
Oxford IBD1	56	37	0.448
Oxford IBD2	25	12	1.00
STM003	38	14	0.714
STM005	38	0	NA
STM006	34	17	1.00
STM007	4	0	NA
STM008	44	1	NA
UCL001	36	37	NA

3.6 Conclusion

Here, I developed an adapted method to time the accumulation of CNAs in tumour samples. I also developed a test to assess the hypothesis that all CNAs occurred simultaneously in a tumour sample, designed to be applied to WXS data. I applied these models to data from multi-region sequencing studies of sporadic colorectal cancer and IBD-associated colorectal cancer that are ongoing in our laboratory. The results suggest that punctuated evolution is a common feature of sporadic colorectal cancer, and that a model of more gradual CNA accumulation also occurs in some samples. Punctuated evolution may also be a feature of IBD-associated colorectal cancer. Interestingly, our analysis of WGS data found catastrophic CNA accumulation shortly before the last common ancestor of all tumour cells, suggesting a potential role for these catastrophic events in cancer causation. As to the causative mechanism of these punctuated copy number events, the large number of chromosomes affected indicates that WGD events are a likely explanation for many of the punctuated events described in the whole-genome sequenced samples. However, the causative mechanism cannot be definitively determined from our data alone. Taken together the results support the hypothesis that catastrophic genome-disruption events can occur in the colon during the progression to cancer and play an important role in disease, but do not explain all CNAs that occur during the progression to cancer.

The joint timing method developed represents a potentially useful complement to existing methods; albeit the advantage over other methods appears to be more limited than I had hoped. The method combines information from across the genome to jointly estimate the timing of multiple CNAs. Initially I was under the impression that this approach could lead to more accurate timing of CNAs (narrower confidence intervals) than existing methods that time CNAs individually. Based on a recent re-evalution of the literature it appears that the method of Purdom and colleagues [Purdom et al., 2013] is as accurate as my method in terms of estimation of the relative time of CNAs as a fraction of the total age of the cell lineage. However, to the extent that the parameters estimated here, ($\mathbf{t}$,T), which give a sense of the absolute timing of CNAs, are of interest, then my approach will give more accurate estimates than other methods. Although, often the relative timing of CNAs is likely to be of most interest, the estimated total mutation time $\mathbf{t}$ of CNAs may be of interest in linking chromosomal instablity to choronological age. In this regard, recent studies giving accurate estimates of SNA mutation rates in non-dysplastic tissue would be of use [Alexandrov et al., 2015].

The whole exome data timing test, although of interest, appears to suffer from a lack of power in most contexts. The applications presented of the WXS timing test provide interesting complementary information to the joint timing method. However, the low power of the test due to the relatively few SNAs within CNAs in WXS data, combined with the difficulty in accurately assigning copy number states to WXS samples, means that the extra information provided by this test is limited. As a result, we decided not to focus on further development and applications of this test.

While methods that use SNAs as a molecular clock to time CNAs can provide important insight into CNA accumulation, it is worth noting that these methods make several important assumptions. First, I have assumed that the SNA mutation rate is constant over time (as well as across genomic regions). To the extent that this assumption is violated then the timing estimations here are expected to be skewed. To illustrate this, suppose that SNAs occur at an accelerating rate

during tumorigenesis (the SNA clock starts to run faster). It is likely that this will lead to overestimation of the times between later events. Secondly, since the SNA mutation rate is assumed to be constant, I assume *a fortiori* that the per base pair SNA mutation rates are independent of CNA accumulation. There is some evidence to support this, in the case of whole genome doublings, where the per chromosome point mutation rate appears to be unchanged before and after doubling events *in vitro* [Dewhurst et al., 2014]. However, there is also evidence to suggest that rupture of the nuclear envelope which has been associated with chromothripsis [Zhang et al., 2015], can also lead to point mutations due to APOBEC [Sansregret et al., 2018]. Thirdly, I have assumed that mutation rates are constant across regions considered. This assumption is likely to be incorrect; multiple studies have found variation in mutation rates across the genome [Lawrence et al., 2013, Makova and Hardison, 2015]. The issue is likely to be partially mitigated by considering only large CNAs (above a length threshold). However, we cannot rule out possible biases to our results due to this assumption. Finally, and relatedly, I make the assumption that SNA mutations are neutral (i.e. their rates of accumulation are not affected by selection).

The assumption that the majority of SNAs in cancer genomes are effectively neutral is well supported by data [Williams et al., 2016] and is a common assumption in the literature [Tomasetti et al., 2013]. Concerns stemming from the first two assumptions could be partially mitigated in future work by considering restricted classes of SNA mutations for which there is stronger evidence of clock-like accumulation. C>T mutations where the C base is followed by a G base in genomic sequence are good candidates to consider based on current data due to their prominence in signature 1 which is clock-like with age in normal tissue [Blokzijl et al., 2016] and their relative rarity in the APOBEC-associated signatures 2 and 13. Overall, the assumption of constant SNA mutation rates is important to bear in mind for applications of this model, but adjustments might be possible to limit their impact in future work.

In all, the results of this chapter provide novel information on CNA mutation

accumulation in colorectal cancer, and develop methods that may be of use in future research into the biology of CNA accumulation.

Chapter 4

POLE mutations are early events in colorectal cancer and endometrial cancer

The work in this chapter is now published in the Journal of Pathology [Temko et al., 2018].

4.1 Précis

Mutations in the *POLE* gene affecting the polymerase epsilon proofreading domain (*POLE* proofreading mutations) predispose to a range of cancer types, including colorectal and endometrial cancer. *POLE* proofreading mutations also occur somatically in several tumour types. Tumours with *POLE* mutations are ultra-mutated (with a distinctive mutational signature). In addition, *POLE* proofreading mutations are associated with an improved prognosis and a high immune infiltrate, features which are probably related to high neo-antigen burden. The timing of *POLE* mutations is currently unknown, but may cast light on tumour-immune dynamics, and is of clinical interest. Here, I first present a model that relates the complement of driver mutations found in a tumour to the timing of mutation processes during tumour growth. Secondly I analyse the timing of somatic *POLE* proofreading mutations in a combined cohort of colorectal and endometrial cancers, including six tumours subjected to whole genome sequencing and public mutation data from 32

tumours analysed with a combination of whole genome and whole exome sequencing. I first provide evidence that *POLE* mutations are often clonal, in all tumour cells. I then apply the model developed earlier in the chapter to driver mutations in these samples. The results suggest that *POLE* mutation often occurs early relative to key driver mutations. These results provide an insight into the temporal acquisition of genetic instability in *POLE*-mutant tumours and the influence of mutation and selection on cancer genomes.

4.2 Contribution

I conducted the analyses in this chapter and developed the mathematical model. DNA sequencing library preparation was carried out by Dr Ann-Marie Baker. I wrote the text in this chapter, with the following exceptions: (i) I did not write the sections of the Methods on DNA sequencing, ethics and definition of driver genes. (ii) Dr David Church provided input to the parts of the Methods sections "POLE consensus mutational signature scores in driver genes" and "Clonality of *POLE* mutations"

4.3 Introduction

In 2013, Ian Tomlinson's group and collaborators identified two mutations in the genes *POLE* and *POLD1*, namely *POLE L424V* and *POLD1 S478N*, that predispose to colorectal cancer [Palles et al., 2013]. *POLE* and *POLD1* encode subunits of the DNA replicases polymerase epsilon (Polε) and polymerase delta (Polδ), respectively [Rayner et al., 2016]. The mutations identified are within the proofreading, or exonuclease, domains of the respective genes, which encode the ability to remove mis-incorporated bases from the newly synthesised DNA strands [Briggs and Tomlinson, 2013]. Since this initial publication, multiple other pathogenic germline mutations have been identified in the *POLE* and *POLD1* proofreading domains, predisposing to a range of tumour types including pancreatic cancer, as well as colorectal cancer and endometrial cancer [Rayner et al., 2016].

Somatic *POLE* exonuclease domain mutations (EDMs) are also found in a range of tumour types, with distinct molecular features. Whereas somatic *POLD1*

Figure 4.1: Mutations in the *POLE* gene are associated with a mutational signature, whereby C>A mutations in the TCT context (referred to as TCT>TAT mutations) and C>T mutations in the TCG context (referred to as TCG>TTG mutations) each account for more 20% of SNAs. Data from http://cancer.sanger.ac.uk/cosmic/signatures

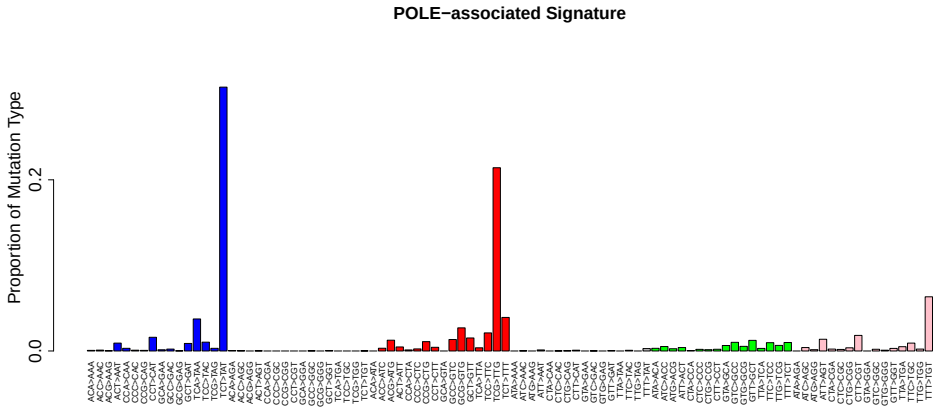

EDMs are rare, somatic *POLE* EDMs are found in 7-12% of endometrial cancers and 1-2% of colorectal cancers, and are also reported in cancers of the brain, breast stomach and pancreas, reviewed in [Rayner et al., 2016]. *POLE* EDMs are associated with a distinctive mutator phenotype, occuring in tumours with very high mutation burden and an excess of C>A mutations; the most common somatic mutation, *POLE P286R* occurs in tumours with a median of 5,147 exonic mutations, in 93% of which over one fifth of mutations are C>A changes [Rayner et al., 2016]. Some of these mutator mutations have been shown to disrupt polymerase activity in model systems or occur in a conserved region of DNA sequence. In these cases there is good evidence that the mutation is pathogenic, i.e. disrupts polymerase function leading to a strong mutator phenotype. *POLE* mutation is associated with Alexandrov Signature 10 [Alexandrov et al., 2013a] (Figure 4.1).

A number of studies suggest that tumours with *POLE* somatic EDMs (EDMs hereinafter) have relatively good outcomes. Church et al. investigated survival in a large endometrial cancer cohort of 788 patients, 48 of which had *POLE* EDMs, and all of which underwent some form of radiation therapy [Church et al., 2015]. The authors found that among grade 3 tumours (109/788 tumours analysed) *POLE*-mutant tumours had significantly greater recurrence free survival compared to

POLE-wild type tumours of matched grade in a multivariate analysis. Several other studies have found an association between *POLE*-mutation and improved outcome in endometrial cancer [Kandoth et al., 2013, Meng et al., 2014, Talhouk et al., 2015]; with one study finding no association, likely due to being underpowered [Billingsley et al., 2015]. However, at present there are insufficient data to assess whether the independent association of *POLE* mutation status and positive prognosis extends beyond grade 3 tumours to lower-grade tumours, or importantly, holds in the absence of adjuvant treatment. Early data from a study with six *POLE*-mutant tumours suggests a similar trend may hold in glioma [Erson-Omay et al., 2015]. Further data will be important to back up these promising findings.

Relatedly, several studies have shown *POLE*-mutant tumours have a high level of immune infiltration, which may be related to ultramutation. High levels of infiltrating immune cells have been observed in *POLE*-mutant endometrial cancers [Hussein et al., 2015, van Gool et al., 2015] and glioma [Erson-Omay et al., 2015] et al. In their study Van Gool et al also presented evidence that CD8+ T-Cells are enriched in *POLE*-mutant endometrial cancer compared to MSS comparators, and (in the central tumour region) compared to MSI comparators. As explained in Chapter 1, there is a correlation between predicted neo-antigen burden, inferred cytotoxic T cell response, and prognosis, across tumour types [Brown et al., 2014]. Therefore increased neo-antigen load, due to raised mutation rates, is one possible explanation for the immune infiltrate, and indeed for the good prognosis.

The timing of *POLE* EDMs during tumour evolution is therefore of key interest. As explained in the Introduction, the dynamics of mutation accumulation – the mutation rate – appears to be an important determinant of tumour evolutionary trajectory, including immune response. The timing of *POLE* mutation could cast light on this important relationship. In addition, to the extent that *POLE* mutations occur early and drive tumorigenesis, they are of potential interest for targeting and early intervention (see Introduction).

Theoretical considerations support a hypothesis that *POLE* EDMs occur early.

The implication of germline proofreading domain mutations in cancer predisposition makes it plausible that somatic EDMs could be found as the first event in a sequence of somatic mutations leading to cancer [Rayner et al., 2016]. In addition, although identifying selected genes in samples with high mutation rates is particularly difficult [Martincorena et al., 2017], the recurrence of certain 'hotspot' mutations, such as *POLE* P286R, suggests these mutations are under positive selection. Indeed, the Cancer Genome Atlas (TCGA) study of endometrial cancer found *POLE* to be a 'significantly mutated gene' [Kandoth et al., 2013]. Mutations under positive selection may play a role in the earliest stages of disease, and indeed driver mutations have been found to be predominantly clonal in a pan-cancer analysis [McGranahan et al., 2015]. Finally, tumours with *POLE* EDMs have a distinctive pattern of mutations in driver genes [Church et al., 2013, Palles et al., 2013]. And links have been drawn between the distinctive spectrum of mutations in driver genes and the *POLE* mutational signature [Shinbrot et al., 2014]. In endometrial cancer, among other differences, cancers with *POLE* EDMs have a higher frequency of *PTEN* codon 130 mutations than those cancers without *POLE* or *POLD1* mutations [Church et al., 2013]. In colorectal cancer, *POLE*-mutant cancers have an increased frequency of *APC R1114X* mutations [Briggs and Tomlinson, 2013]. Since the genes *PTEN* and *APC* are thought to be mutated early in endometrial and colorectal cancer respectively, these differences could suggest that *POLE* mutations occur as early events. However, it may also be possible that initial pathogenic mutations to these genes that occur before *POLE* mutation are drowned out by later, frequent, mutations bearing the *POLE* mutational signature.

There is currently limited data on the timing of *POLE* EDMs during cancer evolution. Shlien et al. analysed variant allele frequencies of seven *POLE* mutations in brain tumours that developed on a genetic background of inherited defects in mismatch repair genes. The results suggest that *POLE* mutations were clonal in these tumours, occurring before the last ancestor of all tumour cells. Erson-Omay et al. found evidnece that *POLE* mutations were clonal in five out of six gliomas, two of which, similarly, developed on a genetic background of mismatch repair de-

fects [Erson-Omay et al., 2015]. A recent large-scale targeted sequencing study of cancers with mutator phenotypes used mutation variant allele frequencies to argue that *POLE* mutations were early events in a subset of cases [Campbell et al., 2017]. However, this study did not have matched normal samples and was unable to distinguish somatic and germline mutations. Very recently, a single example of a *POLE* EDM shared between an endometrial cancer and a likely precursor lesion was found [Miyamoto et al., 2018]. Overall, limited data suggests that *POLE* mutations may often occur before the last common ancestor of all tumour cells, but the timing of *POLE* mutations relative to other clonal mutations has not been systematically analysed.

The mathematical model presented in this chapter represents a formalisation of long-standing ideas. The mutational signatures framework presented by Alexandrov et al. [Alexandrov et al., 2013a] is based on the notion that mutations in cancer genomes bear the signatures of mutational processes. By the same reasoning, the specific cancer-causing mutations in individual samples are also influenced by mutational processes. In fact, both of these ideas long predate the mutational signatures study of Alexndrov et al. [Greenblatt et al., 1994]. Early studies to identify mutational signatures in cancer were based on sequencing the driver gene *TP53* [Greenblatt et al., 1994]. Multiple studies, summarised in [Greenblatt et al., 1994] took advantage of the high frequency of mutations in this gene, using comparatively low-throughput Sanger sequencing, to gain early indications of the signatures of Ultraviolet (UV) radiation and the mutagen aflatoxin. Based on similar ideas, Homfray et al. [Homfray et al., 1998] and Sarebo et al. [Sarebo et al., 2006] carried out an informal analysis of the spectrum of mutation in driver genes to assess the likelihood that certain mutation processes were operative at the time when these driver genes were mutated. Alexandrov and colleagues formalised the dependence of the spectrum of neutral mutations in cancer samples on mutational processes, but did not consider the effects of selection. Here, we make progress towards formalising the alternate contributions of mutation and selection to determining the specific cancer-causing mutations found in individual tumour samples.

4.4 Methods

4.4.1 Mutational signature framework

Below, I introduce the model that is relied upon in [Alexandrov et al., 2013b] and used in both this chapter and chapter 5. Here, I develop the model using the 96 mutation classes described in Chapter 1. However, any mutation classification can be used.

We assume that mutations in cancer genomes are generated by a finite number of muational processes Π_i, $1 \leq i \leq n$. Let $\mu_j(\Pi_i, t, G)$, $1 \leq j \leq 96$ be the rate of mutation type j under process Π_i in a given tumour at time t, considering genomic sequence G. Now define $p_j(\Pi_i, G) = \mu_j(\Pi_i, t, G) / \sum_{k=1}^{96}(\mu_k(\Pi_i, t, G))$. For a given process and genomic sequence, the $p_j(\Pi_i, G)$ are assumed to be invariant over time and across tumours, and the 96-element vector $p(\Pi_i, G) = (p_1(\Pi_i, G), p_2(\Pi_i, G), ..., p_{96}(\Pi_i, G))$ is referred to as the mutational signature of process Π_i for the genomic sequence G. Additionally, for a given tumour we define the activity of Π_i between times t_1 and t_2 for genomic sequence G, $\alpha_i(t_1, t_2, G) = \int_{t_1}^{t_2} \sum_{k=1}^{96}(\mu_k(\Pi_i, t, G))dt$. And the exposure to Π_i between t_1 and t_2 for genomic sequence G is then defined as, $e_i(t_1, t_2, G) = \alpha_i(t_1, t_2, G) / \sum_{k=1}^{n}(\alpha_k(t_1, t_2, G))$.

The relevant sequence G is not always stated explicitly when referring to a mutational signature, or to the activity or exposure of a mutational signature in a tumour sample. Unless otherwise stated, or clear from the context, mutational signatures and their activities and exposures given here are stated based on equal trinucleotide frequencies (i.e. a genomic sequence G with sites at which each mutation type can occur present in equal proportions). On another definitional point, I will sometimes refer to the activity, or exposure, of a mutational signature as a convenient shorthand for the activity or exposure of the mutational process associated with that signature.

Mutational signatures have been reported for 30 mutational processes in the human genome (http://cancer.sanger.ac.uk/cosmic/signatures). Under the assumption that these signatures represent the complete set of mutational processes, the spectrum of mutations across the 96 types in a cancer genome can be viewed as being generated by a linear combination of of these signatures. Specifically, defining

M_j as the random variable describing the number of mutations of type j accumulated in a tumour genomic sequence G between times t_1 and t_2, then the expectation of this variable is given by

$$E(M_j) = \sum_{k=1}^{n} \alpha_k(t_1, t_2, G) p_j(\Pi_k, G)$$

Therefore the reported signatures can be used in conjunction with the spectrum of mutations in a tumour sample to estimate the activities of individual processes in individual tumour samples.

Finally, we note that a mutational signature of a process Π_i quoted in terms of a genomic sequence G can be transformed to the mutational signature of the same process, with respect to another genome H, in the following way. Let g_j be the number of sites in sequence G where a mutation of type j is possible, and, similarly, let h_j be the number of sites in sequence H at which a mutation of type j is possible $1 \leq j \leq 96$. Then the mutational signature of Π_i in terms of H is given by $S(\Pi_i, H) = (p_1(\Pi_i, H), p_2(\Pi_i, H), ..., p_{96}(\Pi_i, H))$, where

$$p_j(\Pi_i, H) = \frac{p_j(\Pi_i, G)(h_j/g_j)}{\sum_{k=1}^{96} p_k(\Pi_i, G)(h_k/g_k)}$$

And similarly, the activity of process Π_i between t_1 and t_2 for genome G can be transformed to the activity of the same process between t_1 and t_2 with respect to genome H, using the formula

$$\alpha_i(t_1, t_2, H) = \alpha_i(t_1, t_2, G) \sum_{k=1}^{96} p_k(\Pi_i, G)(h_k/g_k)$$

4.4.2 Tumour growth model

Following Tomassetti [Tomasetti and Vogelstein, 2015] we make the simplifying assumption that a given mutation M_i occurs at a constant low rate μ_i per year, $\mu_i \ll 1$. Suppose that after the occurrence of the mutation sequence $R = \langle M_1, M_2, ..., M_n \rangle$, cancer occurs with constant rate $\lambda \ll 1$. Then, by well-known results [Tomasetti and Vogelstein, 2015, Armitage and Doll, 1954], the probability of cancer incidence at time t is given by:

$$I(t) = \frac{\mu_1 \mu_2 ... \mu_n t^n \lambda}{n!}$$

Extending this framework to take into account cancer causation by multiple sequences of mutations $S_j =< M_1(j), ..., M_n(j) >$, with rate λ_j. Cancer incidence at time t is given by

$$I(t) = \sum_j \frac{\mu_1(j)\mu_2(j)...\mu_n(j)\lambda_j t^n}{n!}$$

The above closely follows [Tomasetti and Vogelstein, 2015].

Definition: - Mutations M_1 and M_2 are *similar* with relative risk r_{12} if they satisfy the following property: A mutation sequence S_j containing M_2 causes cancer with rate λ_j, just if the mutation sequence S_k, that results from substituting M_1 for M_2 in S_j, causes cancer with rate $\lambda_k = r_{12}\lambda_j$. Mutations are said to be *equivalent* if they are similar with relative risk 1.

We note that by this definition all cancer-causing mutations are trivially equivalent to themselves.

Now consider a set of similar mutations $A = \{M_i : 1 \leq i \leq n\}$. Let r_{ij} be the relative risk of mutation M_i compared to mutation M_j. Then the probability that M_i occurs in a cancer sample, given that one of these mutations occurs is given by:

$$P(M_i|A) = \frac{\mu_i}{\sum_{j=1}^{n} \mu_j r_{ji}} \tag{4.1}$$

4.4.3 Likelihood of a cancer mutation on the background of a mutational signature

Let $B = \{M_i, M_2, ..., M_j\}$ be the full set of cancer-causing mutations in a single gene. Define $c(M)$ as the type of mutation M among the 96 possibilities, referred to as the 'causal channel' of M . Let $S = (p_1, ..., p_{96})$ be the mutational signature active in a tumour sample rescaled to a genome with equal trinucleotide frequencies (i.e. a genome where the number of sites where each mutation type can occur is equal). We make the following two simplifying assumptions, the appropriateness of which

are discussed in Section 4.6:

Assumption 1: The mutations in B are uniformly distributed across the 96 mutation channels (irrespective of the frequency of the channels in the genome)

Assumption 2: All mutations in B are equivalent, in the sense defined above

Then based on Equation 4.1 we can give the probability of the tumour sample harbouring a mutation from B with a given causal channel, c, given that it harbours a mutation from B.

$$P(M \in B, c(M) = c|B) = p_c$$

Put another way, we can express the likelihood of observing a mutation in B with causal channel c (the data), given that there is some mutation in B, in terms of the mutational signature of the sample

$$\mathscr{L}(c,S) = p_c \tag{4.2}$$

A concrete example can help to illustrate the approach. Suppose that a colorectal cancer sample includes a *KRAS* mutation with causal channel (ACC>ATC) (*KRAS G12D*, is one possible such *KRAS* mutation). Under the assumptions above, the likelihood of observing a mutation in *KRAS* with this causal channel on the background of the *POLE*-associated mutational signature, given that there is a cancer-causing *KRAS* mutation, is equal to the probability of the (ACC>ATC) channel in the signature.

4.4.4 POLE heuristic mutational signature score

We were interested in using the causal channels of mutations in driver genes to assess the likelihood that all the mutations in the gene occurred on the background of the *POLE* mutational signature. To this effect we devised a score for each driver gene with at least one mutation in a sample. We assume that at any time during the development of *POLE*-mutant samples there are three possible mutational signatures active:

(i) $S_0 = (p_{0,1}, p_{0,2}, ..., p_{0,96})$ (*POLE*-mut signature) is active on a background

of *POLE* mutation

(ii) $S_1 = (p_{1,1}, p_{1,2}, ..., p_{1,96})$ (MSI signature) is active on a *POLE*-wild type and microsatellite unstable background

(iii) $S_2 = (p_{2,1}, p_{2,2}, ..., p_{2,96})$ (MSS) is active on a *POLE*-wild type and microsatellite stable background

Thus we assume that, when present, the signal of mismatch repair defects dominates; except when there is a pathogenic *POLE* mutation, in which case the *POLE* mutational signature dominates. We assume that there is a single MSS signature for convenience. However, in reality, this group is likely to contain considerable variation among samples. This is especially relevant in endometrial cancer, where APOBEC-linked mutational processes are reported (https://cancer.sanger.ac.uk/signatures/matrix.png). This heterogeneity is not expected to greatly influence the modeling conclusions - albeit refining of the three mutational signature framework would be a potential area for future development.

Given a putative driver gene, D, with n mutations, U=$\{M_1, M_2, ..., M_n\}$, in a sample, we define the *POLE* mutational signature score of the gene, $s(D)$, as

$$s(D) = \log\Big(\min_{i\in\{1,...,n\}}\Big(\min\Big(\frac{\mathscr{L}(c_i, S_0)}{\mathscr{L}(c_i, S_1)}, \frac{\mathscr{L}(c_i, S_0)}{\mathscr{L}(c_i, S_2)}\Big)\Big)\Big) \tag{4.3}$$

where c_i is the causal channel of mutation M_i

Note that this heuristic score is similar to a likelihood ratio. However, since there are two possible background signatures (other than *POLE*-mut) and may be more than one possible causal mutation ($n > 1$), the minimum (most conservative) likelihood ratio out of all the possible comparisons is used for the score. It is useful in terms of interpretation to note that the heuristic score has the property that if $s(D) > 0$ then for all mutations in D the most probable background for the mutation is the *POLE*-mut signature.

Under the assumptions above and using 4.2, we can calculate 4.3 using

$$s(G) = \log\Big(\min_{i\in\{1,...,n\}}\Big(\min\Big(\frac{p_{0,c_i}}{p_{1,c_i}}, \frac{p_{0,c_i}}{p_{2,c_i}}\Big)\Big)\Big)$$

Table 4.1: POLE-mutant tumours

Sample	Sequencing Strategy
OXF_001	WGS
POLE_040	WGS
POLE_049	WGS
POLE_072	WGS
POLE_147	WGS
BIR_001	WGS

4.4.5 Ethical approval

Patient consent for research on tumour tissue was obtained at the recruiting centres under local ethical approval. Molecular analysis of anonymised tissue was performed under Oxford Research Ethics Committee A approval (05/Q1605/66).

4.4.6 Patients and tumour samples

Six fresh frozen tumours with pathogenic somatic *POLE* mutations (five endometrial, one colorectal) were identified from a Leuven endometrial cancer cohort used in a previous study [Church et al., 2015], a prospective clinical sequencing programme (HICF2) at the University of Oxford, or the University of Birmingham tissue bank (Table 4.1). TCGA colorectal (COADREAD) [TCG, 2012] and endometrial (uterine corpus endometrial carcinoma - UCEC) [Kandoth et al., 2013] cancer data were downloaded from the Genomic Data Commons (GDC) Data Portal (https://portal.gdc.cancer.gov; June 2017). Molecular analyses were performed on a single tumour region in each case.

4.4.7 DNA extraction

After review to confirm adequate tumour cellularity, DNA was extracted from fresh frozen or microdissected FFPE tumours and precursors using standard methods (Roche FFPE-T DNA kit, Machery Nagel Nucleospin DNA FFPE XS / FFPE DNA kit or Qiagen Blood and Tissue kit) and resuspended in buffer or water.

4.4.8 DNA sequencing

DNA from fresh frozen endometrial tumours and paired normal samples for whole genome sequencing (WGS) was quantified using the Qubit 2.0 fluorometer (Life

Technologies, Paisley, UK), and fragmented using the Covaris M220 ultrasonicator (Covaris, Inc., Woburn, MA) to an average fragment size of 250-300bp. Approximately 50ng was used as input for the NEBNext Ultra DNA Library Prep Kit for Illumina (New England Biolabs, Hitchin, UK). Libraries were prepared as per the manufacturer's guidelines, with size selection for a 250bp insert size, dual indexing and 9 cycles of library amplification. Libraries were sequenced to a median depth of 50x on Illumina's HiSeq X Ten (150bp paired end reads) at BGI Tech Solutions Ltd, Hong Kong. Sequenced reads were aligned to the 'hg19' human genome assembly using bwa-mem [Heng and Durbin, 2009] (see Methods, Chapter 7). Somatic mutations were called from DNA sequencing data using Mutect2 [Cibulskis et al., 2013]. Variants flagged as 'PASS' or 'clustered_events' were accepted as somatic. Variants were annotated using Annovar [6]. Copy number profiles were derived using Sequenza [Favero et al., 2015] for a subset of samples, and manually curated to remove probable model artefacts. DNA from the colorectal cancer was prepared for WGS using the Truseq PCR-free library preparation kit (Illumina) as per manufacturer's guidelines and sequenced on an Illumina HiSeq 2500. Sequenced reads were aligned to the GrCh37 reference genome using the Isaac aligner [Raczy et al., 2013], and variant calling performed using Strelka [Saunders et al., 2012].

Somatic mutations in TCGA cancers were called from BAMs using Mutect2 [5]. Additional cases from the TCGA COADREAD and UCEC data sets were downloaded as Mutect Mutation Annotation Format (MAF) files from the GDC Data Portal. Variant annotation and model curation was performed as for the WGS cases.

4.4.9 Definition of driver genes

Driver genes were defined using the IntOGen driver gene repository (https://-www.intogen.org/search) and included both PanCancer (Pooled_driver) and tumour type-specific (perProject_driver) variants [Gonzalez-Perez et al., 2013]. High confidence driver mutations (defined as either truncating mutation in genes likely to be tumour suppressors or recurrent missense mutations in any endometrial or colorec-

tal cancer-specific or pan-cancer gene from the IntOGen set), were determined for a subset of driver genes by manual curation, blinded to tumour molecular characteristics.

4.4.10 Clonality of POLE mutations

36 of 38 endometrial and colorectal cancers with pathogenic *POLE* mutations were disomic at the *POLE* locus (chr12q24) and were informative for clonality analysis. Of these, 20 of 22 endometrial cancers, and 12 or 14 colorectal cancers had available copy number annotation. As all 32 of these showed near-diploid genomes ($> 80\%$ of the genome), we assumed diploid genomes for the four remaining cases.

Mutations were filtered to include only autosomal variants in diploid regions of the genome, with depth of at least 20x. Mutation allele frequency distributions were generated using the R 'histogram' function, and tumour cellularity inferred as twice the mid-point of the allele frequency bin with highest mutation density, excluding bins with a lower bound below allele frequency 0.1. These values were then subjected to manual curation. The hypothesis that the mutation was present in every tumour cell was tested by a one-sided binomial test, based on the numbers of reference and variant reads at the *POLE* mutation site and the inferred tumour cellularity. Specifically, for a mutation with coverage R, in a tumour with cellularity C, the number of variant reads was modelled as a random variable X, with distribution:

$$X \sim Bin(R, C/2).$$

In each case we calculated the probability, p, of finding the observed number of variant reads, v, or fewer, $P(X \leq v)$. Mutations were considered subclonal for $p \leq 0.05$.

4.4.11 Classification of SNAs to a mutational processes

Previously reported mutational signatures based on the trinucleotide frequencies of the human genome were obtained from http://cancer.sanger.ac.uk-/cosmic/signatures/ on 1st June 2017. In each tumour mutations were classified into 96 categories following Alexandrov [Alexandrov et al., 2013a] (Cosmic Signa-

tures). Non-negative least squares regression, implemented in the R package 'nnls' [Katharine M. Mullen, 2012], was used to model the counts of mutations across categories in each tumour as a linear combination of the Cosmic Signatures. For cases analysed by whole exome sequencing, mutational signatures were rescaled to exonic trinucleotide frequencies before conducting the regression. For this analysis, only mutational signatures previously reported as active in that cancer type (endometrial signatures 1, 2, 5, 6, 10, 13, 14 and 26; colorectal signatures 1, 5, 6, and 10) were used for the regression. A mutational process was deemed to have been active in the life-history of a tumour if the associated mutational signature had a coefficient of at least 2 per cent of the total coefficients in the best-fitting model. Mutations likely to be due to *POLE* exonuclease domain mutation (POLE), APOBEC upregulation (APOBEC) or deficient DNA mismatch repair (dMMR) were identified by considering mutational signatures as multinomial probability distributions. The probability of the causal channel of each mutation under all mutational processes active in that tumour was calculated, and mutations were assigned to a particular mutational process in cases where the probability of the mutation causal channel under that process was at least twice the probability under any other process.

4.4.12 POLE consensus mutational signature scores in driver genes

Tumour mutations were obtained from calling based on tumour/normal .bam files (*POLE* mutant cases) or TCGA MAF files (MMR-P, MMR-D cases), and classified into 96 categories following Alexandrov [Alexandrov et al., 2013a]. For each tumour, the distribution of mutations across the 96 types was found (i.e. the proportion of mutations in the sample falling into each category) as an estimate of the sample-specific active mutational signature. The signatures for each sample were then rescaled to equal trinucleotide frequencies. Tumours were categorised into three groups according to *POLE* mutation and mismatch repair status (i.e. *POLE*-mutant, MMR-P and MMR-D), and a consensus mutational signature was calculated for each group as the average of the rescaled sample-specific signatures among

samples in the group, weighted by the number of mutations in each sample. The probability of all non-silent mutations ('nonsynonymous SNV', or 'stopgain') in driver genes (as defined above) under each of the three consensus mutational signatures was then calculated, and the ratio of the probability of each mutation under the *POLE* consensus mutational signature compared to that under each of the other two consensus mutational signatures was obtained. For each individual gene, a '*POLE* score' was then calculated as the base two logarithm of the minimum value of these ratios across all the non-silent mutations within that gene.

4.5 Results

4.5.1 Whole genome sequencing

As expected, all tumours were highly mutated (122 mutations per megabase (Mb) to 731 mutations per Mb). All samples showed a preponderance of TCT>TAT mutations (Figure 4.2), as expected based on the *POLE*-associated mutational signature.

4.5.2 *POLE* mutations often occur before the last common ancestor of all tumour cells

In all six cases the number of reads supporting the *POLE* mutation was consistent with the mutation being clonal (present in every tumour cell) (Figure 4.3, Table 4.2). I also analysed the allele frequencies of mutations that could be probabilistically assigned to a single generating mutational process (Figure 4.3). Mutations likely to be due to the *POLE*-associated mutational process (e.g. TCT>TAT mutations), were present across the allele frequency distribution. These data support the hypothesis that *POLE* mutations occurred prior to the last common ancestor of all tumour cells (Figure 4.3).

I carried out a similar analysis for 17 endometrial cancers and 13 colorectal cancers from the TCGA series with pathogenic *POLE* mutations. The allele frequency of the *POLE* mutation was consistent with clonality in 17/17 endometrial cancers and 12/13 colorectal cancers (Figures 4.4, 4.5, Table 4.2); one colorectal cancer had an apparently subclonal *POLE* P286R mutation (TCGA-CA-6717),

Figure 4.2: Whole genome sequencing of five endometrial cancers and one colorectal cancer with the *POLE P286R* mutation. Plots show distribution of mutations across 96 mutation channels in each of the six tumour samples

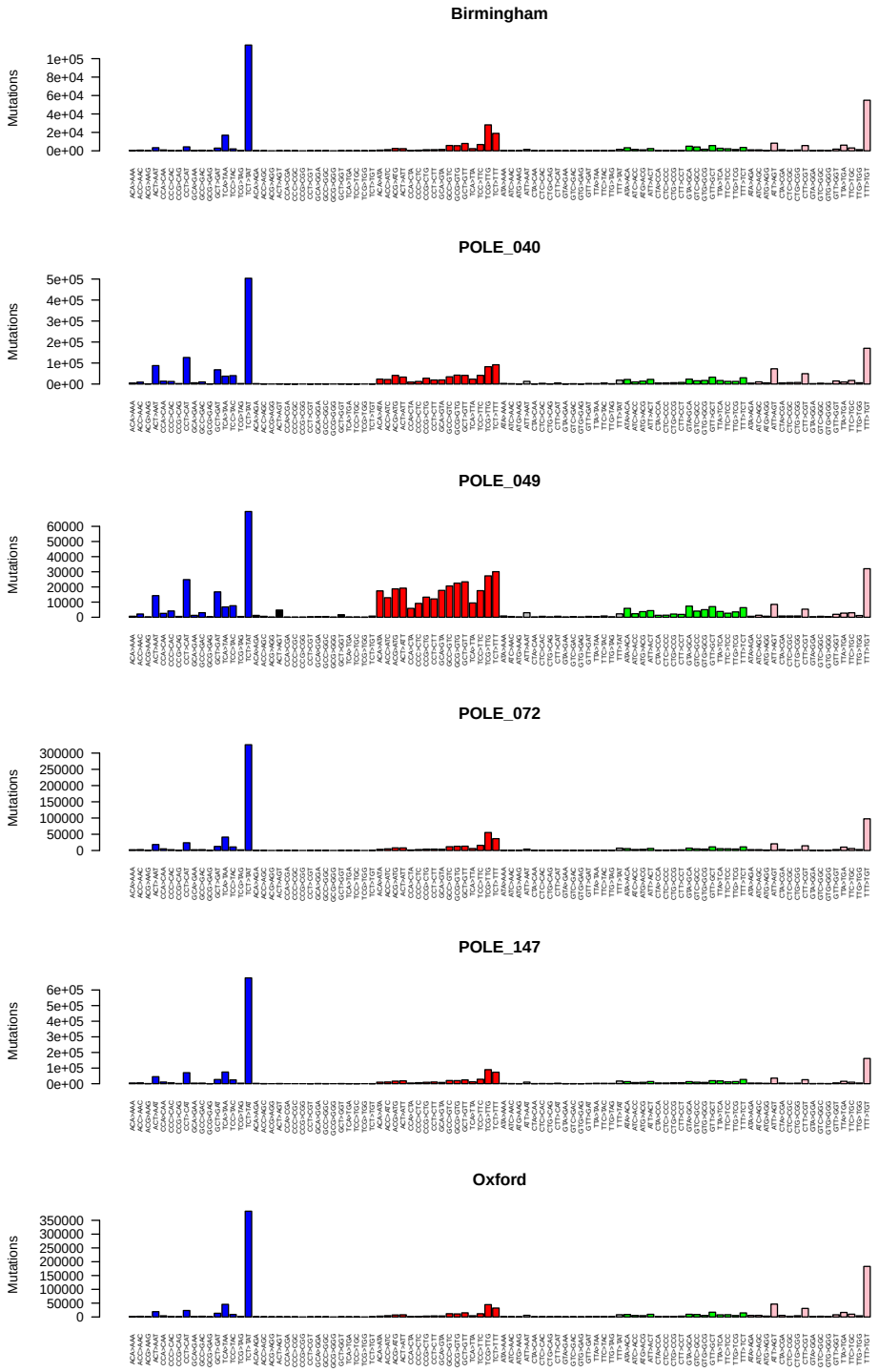

Figure 4.3: Clonality of *POLE* mutations and mutational processes in six samples subjected to whole genome sequencing. Frequency histograms and kernel density plots showing variant allele frequency (VAF) of all SNA mutations, and SNAs likely due to *POLE* exonuclease domain mutation (POLE) and APOBEC mutagenesis (APOBEC). Only mutations in diploid regions of autosomes, and with coverage $>$ 20x are shown. The relatively low proportion of SNAs categorised as being due to *POLE* mutation reflects the stringency of the classification used (see Methods, Classification of SNAs to a mutational process). Vertical red line indicates clonal peak used to calculate cellularity. Arrow indicates VAF of pathogenic *POLE* mutation.

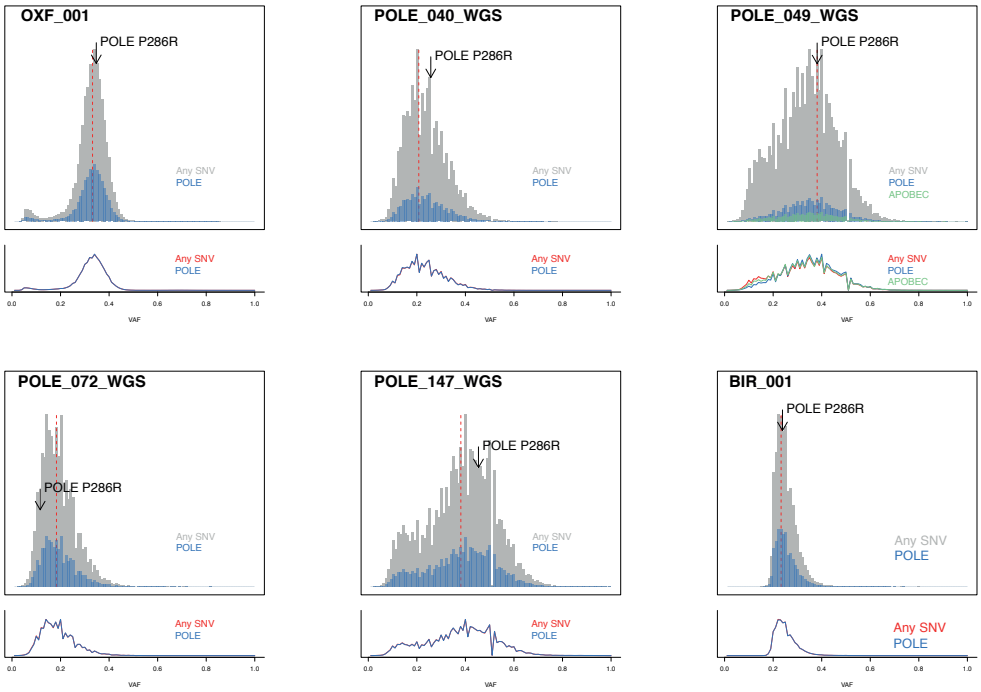

(Figure 4.5, Table 4.2). Again mutations attributed to the *POLE* mutator phenotype were present across the allele frequency spectrum in all cases (Figures 4.4, 4.5). Taken together, these data suggest that pathogenic *POLE* mutations are often early events (prior to the last common ancestor of tumour cells) in endometrial and colorectal cancers.

4.5.3 POLE signature scores of driver mutations

I next sought to investigate the timing of *POLE* mutation relative to driver mutations. Since driver mutations are often clonal in tumour samples [McGranahan et al., 2015], the fact that *POLE* mutations are often clonal provides little information about their

Figure 4.4: Clonality of *POLE* mutations and mutational processes in TCGA endometrial cancers. Frequency histograms and kernel density plots showing variant allele frequency (VAF) of all SNA mutations, and SNAs likely due to *POLE* exonuclease domain mutation (POLE), APOBEC upregulation (APOBEC) and deficient DNA mismatch repair (dMMR). Only mutations in diploid regions of autosomes, and with coverage $>$ 20x are shown. The relatively low proportion of SNAs categorised as being due to *POLE* mutation reflects the stringency of the classification used (see Methods, Classification of SNAs to a mutational process). VAF of *POLE* mutations are highlighted. Vertical red line indicates clonal peak used to calculate cellularity. Arrow indicates VAF of pathogenic *POLE* mutation.

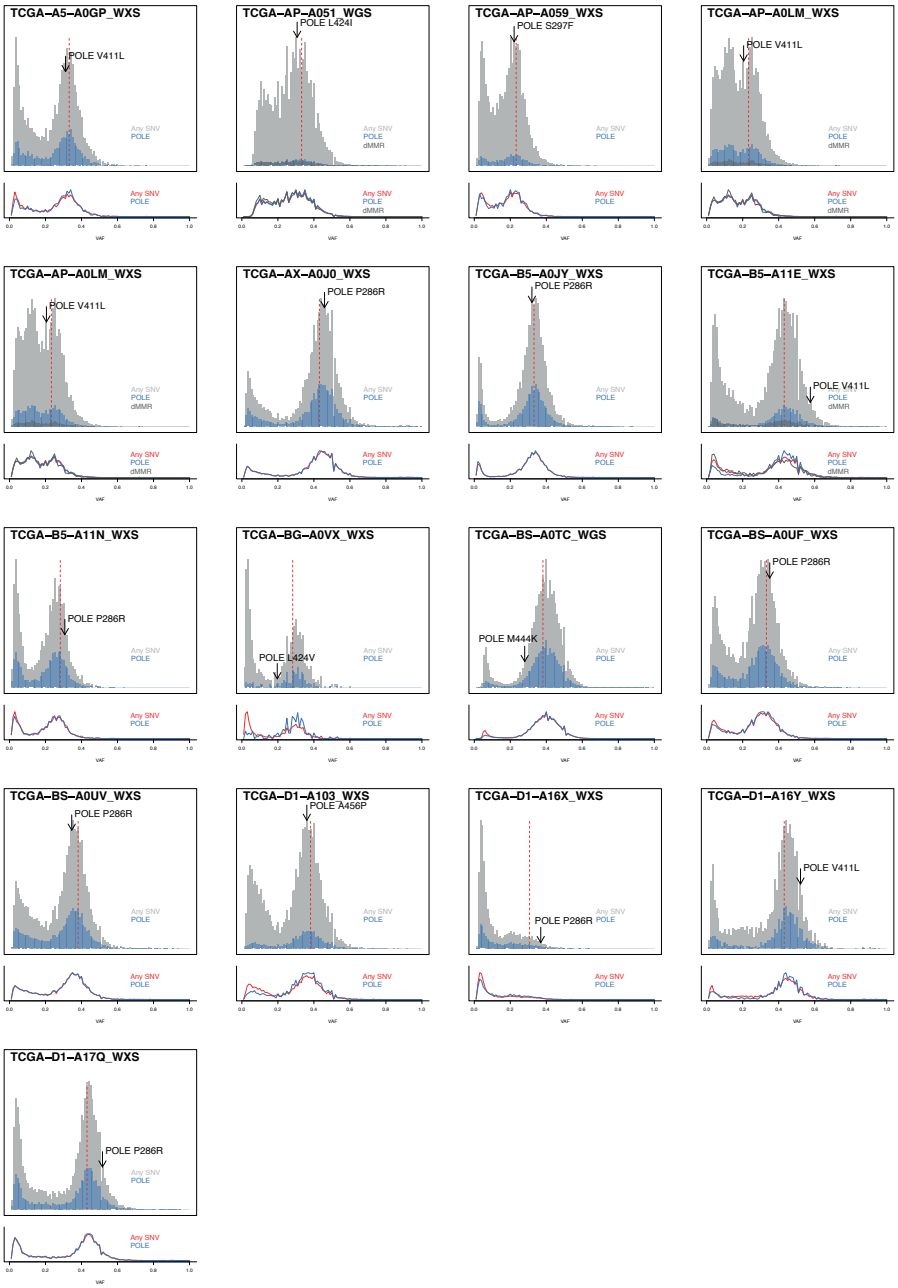

Figure 4.5: Clonality of *POLE* mutations and mutational processes in TCGA colorectal cancers. Frequency histograms and kernel density plots showing variant allele frequency (VAF) of all SNA mutations, and SNAs likely due to *POLE* exonuclease domain mutation (POLE) and deficient DNA mismatch repair (dMMR). Only mutations in diploid regions of autosomes, and with coverage $>$ 20x are shown. The relatively low proportion of SNAs categorised as being due to *POLE* mutation reflects the stringency of the classification used (see Methods, Classification of SNAs to a mutational process). VAF of *POLE* mutations are highlighted. Vertical red line indicates clonal peak used to calculate cellularity. Arrow indicates VAF of pathogenic *POLE* mutation.

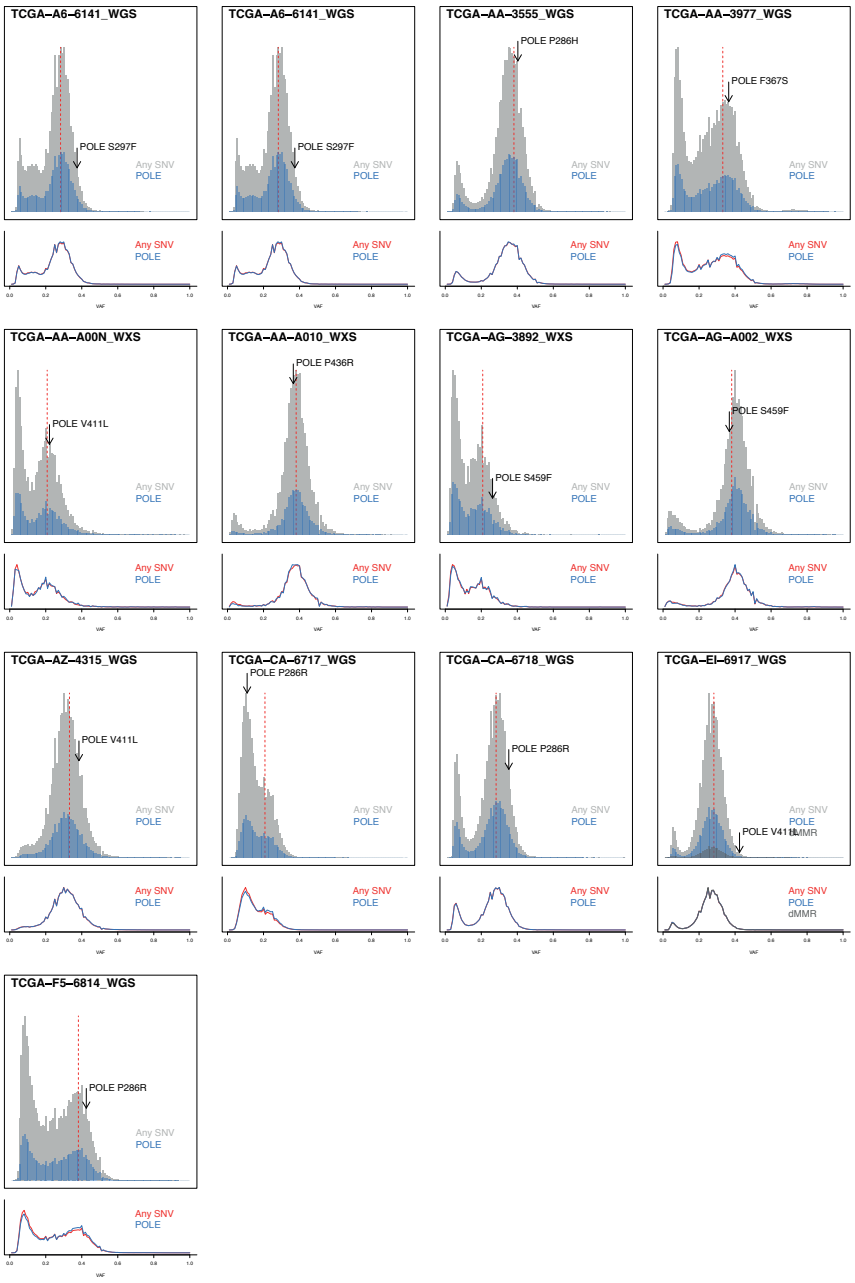

Table 4.2: Clonality of *POLE* mutations in endometrial cancer and colorectal cancer samples. p-value's shown are for one-sided binomial tests of the null hypothesis that the mutation was present in every tumour cell.

	Sample	Tumour type	*POLE* mutation	VAF	p-value
1	POLE_040	Endometrial	P286R	7/28	0.82
2	POLE_049	Endometrial	P286R	15/40	0.57
3	POLE_072	Endometrial	P286R	6/56	0.12
4	POLE_147	Endometrial	P286R	13/29	0.84
5	Oxford	Endometrial	P286R	31/91	0.67
6	TCGA-A5-A0GP	Endometrial	V411L	81/266	0.26
7	TCGA-AP-A051	Endometrial	L424I	6/20	0.51
10	TCGA-AP-A059	Endometrial	S297F	35/164	0.40
11	TCGA-AP-A0LM	Endometrial	V411L	14/71	0.35
12	TCGA-AX-A05Z	Endometrial	P286R	9/41	0.27
13	TCGA-AX-A0J0	Endometrial	P286R	44/97	0.75
14	TCGA-B5-A0JY	Endometrial	P286R	52/166	0.41
15	TCGA-B5-A11E	Endometrial	V411L	12/21	0.94
16	TCGA-B5-A11N	Endometrial	P286R	67/223	0.82
17	TCGA-BG-A0VX	Endometrial	L424V	13/69	0.07
18	TCGA-BS-A0TC	Endometrial	M444K	15/55	0.07
20	TCGA-BS-A0UF	Endometrial	P286R	56/163	0.72
21	TCGA-BS-A0UV	Endometrial	P286R	39/115	0.24
22	TCGA-D1-A103	Endometrial	A456P	62/175	0.31
23	TCGA-D1-A16X	Endometrial	P286R	41/113	0.94
24	TCGA-D1-A16Y	Endometrial	V411L	16/31	0.89
25	TCGA-D1-A17Q	Endometrial	P286R	88/172	0.99
26	Birmingham	Colorectal	P286R	15/65	0.61
27	TCGA-A6-6141	Colorectal	S297F	25/68	0.96
28	TCGA-AA-3510	Colorectal	A456P	21/55	0.85
29	TCGA-AA-3555	Colorectal	P286H	27/68	0.69
30	TCGA-AA-3977	Colorectal	F367S	24/67	0.76
32	TCGA-AA-A00N	Colorectal	V411L	20/94	0.68
33	TCGA-AA-A010	Colorectal	P436R	42/117	0.40
34	TCGA-AG-3892	Colorectal	S459F	25/98	0.93
36	TCGA-AG-A002	Colorectal	S459F	34/94	0.44
37	TCGA-AZ-4315	Colorectal	V411L	45/119	0.91
39	TCGA-CA-6717	Colorectal	P286R	7/70	0.02
41	TCGA-CA-6718	Colorectal	P286R	36/104	0.96
44	TCGA-EI-6917	Colorectal	V411L	31/74	1.00
47	TCGA-F5-6814	Colorectal	P286R	39/93	0.84

timing compared to drivers. I therefore applied the *POLE* mutational signature score method, described above, to analyse whether the genomic context of muta-

tions in driver genes could provide information about the mutational processes that were present at the time of these mutations.

For this analysis, in addition to the 38 *POLE*-mutant samples, mutation data was downloaded for 802 MMR-proficient (MMR-P) tumours and 194 MMR-deficient (MMR-D) tumours from the TCGA series (450 endometrial cancers and 546 colorectal tumours). *POLE* signature scores (*POLE* scores) were calculated for each driver gene with at least one non-silent mutation in a sample (scores were calculated for mutated genes in MMR-D and MMR-P samples as a comparison for scores in genes in *POLE*-mutant samples).

In total, among 206 endometrial and/or colorectal cancer driver genes examined in the cases from the combined endometrial and colorectal cancer cohorts, 50% (1,065/2,118) of those in *POLE*-mutant samples had a *POLE* signature score > 0, compared to 14% (628/4,427) in MMR-D and MMR-P cancers ($P < 1 \times 10^{-26}$) (Figure 4.6, 4.7). This suggests that many mutations in driver genes in *POLE*-mutant samples occurred on a background of *POLE* mutations.

To minimise the possibility of confounding by non-pathogenic mutations in the complete set of driver genes, I repeated these analyses considering only manually curated, high-confidence pathogenic mutations. High confidence driver mutations (defined as either truncating mutation in genes likely to be tumour suppressors or recurrent missense mutations in any endometrial or colorectal cancer-specific or pan-cancer gene from the IntOGen set), were determined for a subset of driver genes by manual curation, blinded to tumour molecular characteristics. Again, the propotion of genes in *POLE*-mutant samples that had a score above zero, was significantly greater than among MMR-P and MMR-D samples ($P < 1 \times 10^{-26}$, Figures 4.8, 4.9).

As mutation of the tumour suppressors *PTEN* and *APC* are well recognised as early, if not initiating, events in the pathogenesis of endometrial and colorectal cancers respectively, I specifically examined whether somatic variants in these genes varied according to tumour *POLE* mutation status. Among high-confidence pathogenic *PTEN* mutations in endometrial cancers, the proportion with *POLE* con-

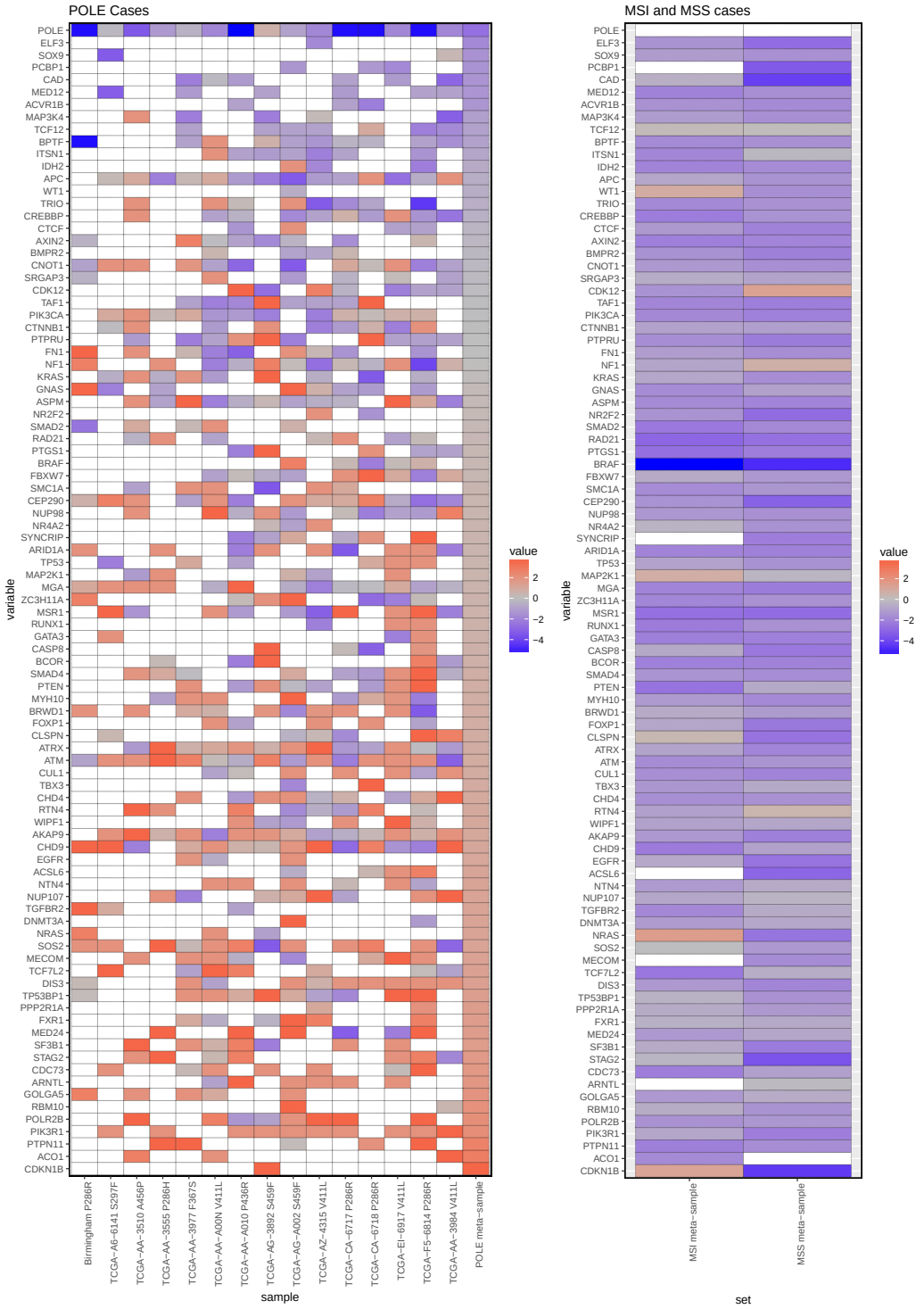

Figure 4.6: "*POLE* scores" in driver genes in endometrial cancer samples. Scores are shown for individual genes (rows) in individual *POLE*-mutant samples (columns left-hand raster), averaged across MMR-D samples (first column right-hand raster) and averaged across MMR-P samples (second column right-hand raster). Most genes had a *POLE*-score greater than zero in at least one *POLE*-mutant sample, indicating that all mutations in the gene in that sample were more likely to have occurred on a *POLE*-mutant background than on a MMR-D or MMR-P backround.

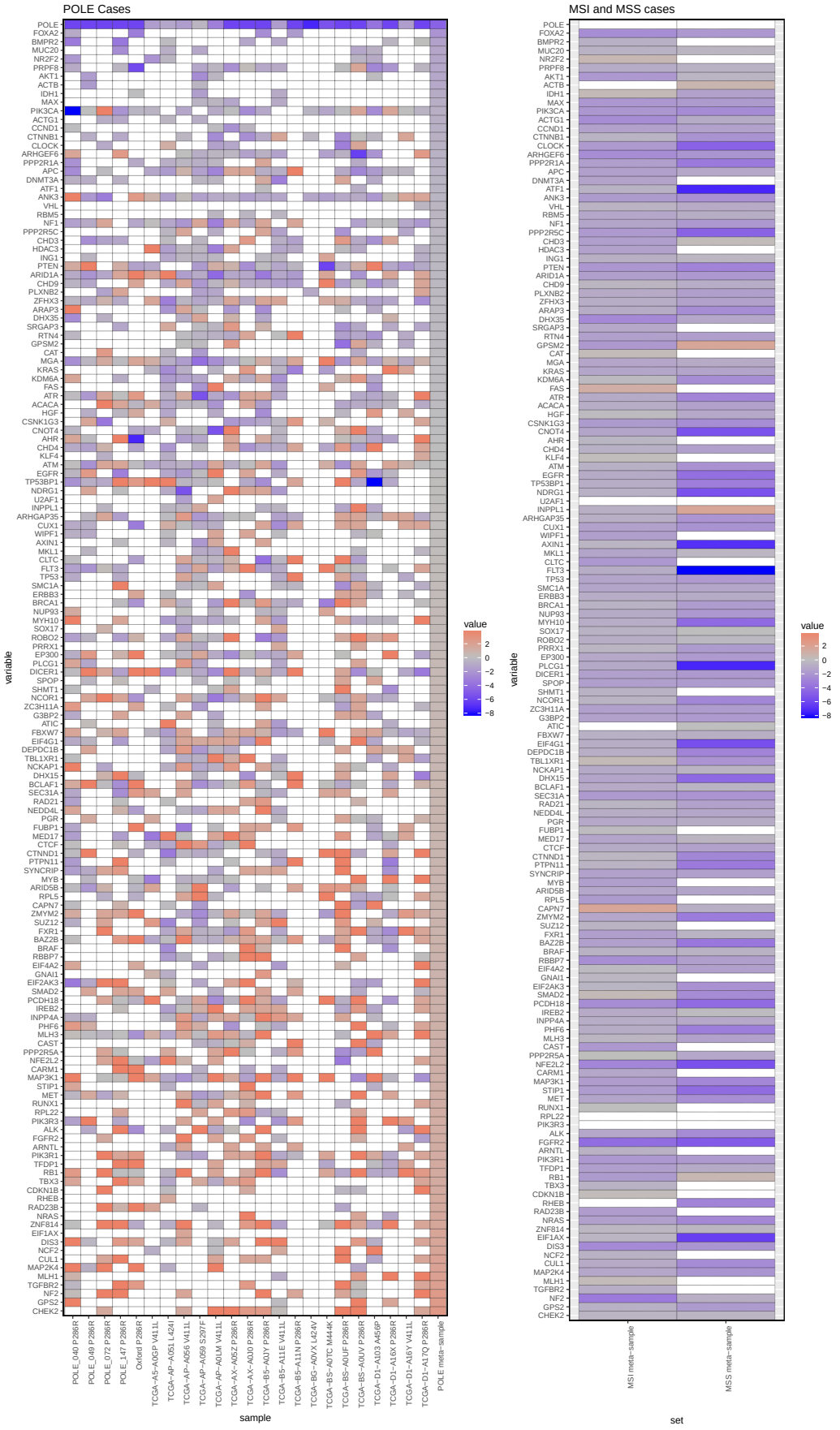

Figure 4.7: "*POLE* scores" in driver genes in colorectal cancer samples. Rows and columns as for Figure 4.6. Most genes had a *POLE*-score greater than zero in at least one *POLE*-mutant sample, indicating that all mutations in the gene in that sample were more likely to have occurred on a *POLE*-mutant background than on a MMR-D or MMR-P backround.

Figure 4.8: "*POLE* scores" in driver genes in endometrial cancer samples - high confidence pathogenic mutations only. Rows and columns as for Figure 4.6. Most genes had a *POLE*-score greater than zero in at least one *POLE*-mutant sample, indicating that all pathogenic mutations in the gene in that sample were more likely to have occurred on a *POLE*-mutant background than on a MMR-D or MMR-P backround.

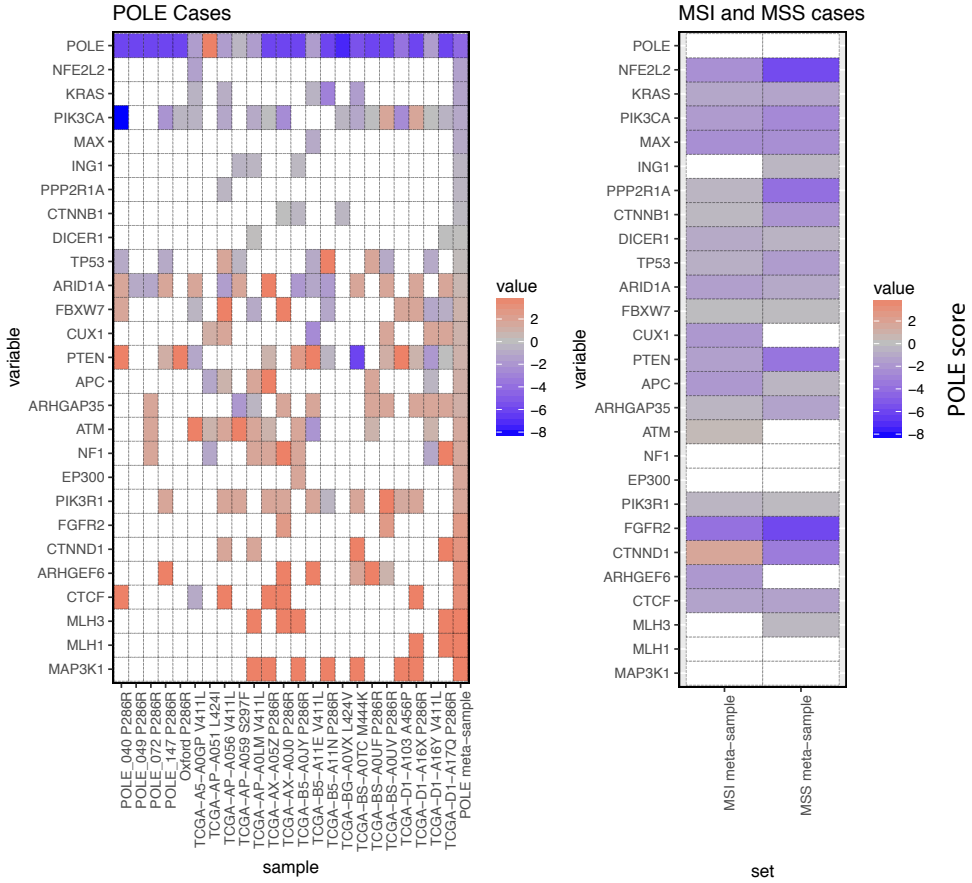

sensus mutational signature scores > 0 was substantially and significantly greater among *POLE*-mutant cases than among MMR-P and MMR-D tumours (10 of 14 [71.4%] vs. 14 of 82 [17.1%] mutations respectively; $P = 7.8 \times 10^{-3}$, Fisher's Exact Test). Analysis of high-confidence pathogenic *APC* mutations in colorectal cancers revealed similar results (corresponding proportions 9 of 14 [64.3%] vs. 10 of 69 [14.5%] mutations; $P = 0.012$, Fisher's Exact Test).

Figure 4.9: "*POLE*" in driver genes in colorectal cancer samples - high confidence pathogenic mutations only. Rows and columns as for Figure 4.6. Most genes had a *POLE*-score greater than zero in at least one *POLE*-mutant sample, indicating that all pathogenic mutations in the gene in that sample were more likely to have occurred on a *POLE*-mutant background than on a MMR-D or MMR-P backround.

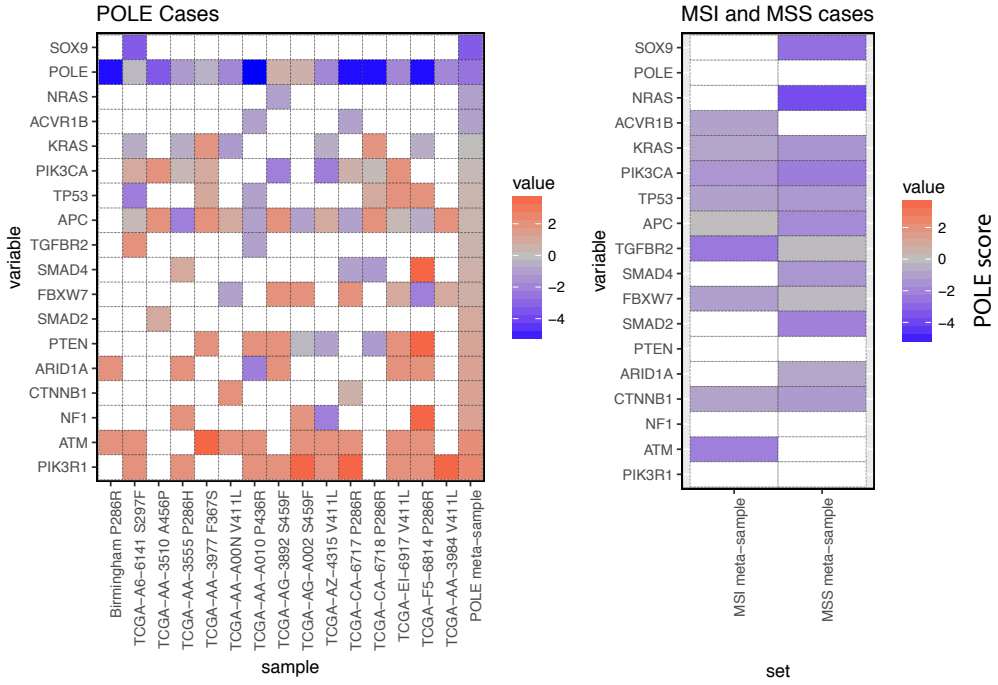

4.6 Conclusion

Here, I have analysed the timing of *POLE* mutations using a combination of whole genome sequencing and re-analysis of publicly available mutation data sets. My clonality analysis suggest that pathogenic *POLE* mutations often occured prior to the last common ancestor of all tumour cells. Analysis of the genomic contexts of driver mutations suggests that *POLE* mutations can precede mutations in key driver genes. In particular, it appears likely that *POLE* mutation preceded pathogenic *APC* mutations in some colorectal cancer samples and preceded pathogenic *PTEN* mutations in some endometrial cancer samples.

Previous studies have commented on a distinctive spectrum of mutation in driver genes in *POLE*-mutant tumours [Church et al., 2013, Rayner et al., 2016]. Our study makes progress towards placeing these observations in a theoretical

framework and assesses, to our knowledge for the first time, the extent to which all the potentially pathogenic mutations in putative driver genes are likely to have occurred on the background of the *POLE* mutational signature.

Further analysis by co-authors that is included in the manuscript supports the conclusions that *POLE* mutations are early events. Dr David Church and colleagues analysed four cases where a *POLE*-mutant endometrial cancer was resected together with what is likely to be a remnant of the precursor lesion. In all four cases, the same *POLE* mutation that was present in the cancer portion of the sample was also identified in the precursor lesion. These results are consistent with *POLE* mutations occuring in the very earliest stages of tumour evolution.

Our findings provide an important contribution to the growing understanding of the relationship between mutation rates and tumour immune response. Early *POLE* mutations are expected to generate large numbers of clonal neo-antigens [McGranahan et al., 2016]. Given the important role that is hypothesised for clonal neo-antigens in immunotherapy response (see Chapter 1), the early timing of *POLE* mutations is relevant to the (very limited) data showing these tumours may respond well to immunotherapy [Santin et al., 2016]. The findings motivate further research into the potential for immunotherapy in these tumours. More broadly these results suggest that early ongoing instability may be associated with immune recognition and good prognosis. This is an important data point in terms of understanding the dynamic relationship between mutation and immune response. Further studies to clarify the relationship between immune response and other types of instability will be important in this regard.

There are some limitations to the application of the model presented in this chapter. In particular, the application assumes that the cancer-causing mutations in a driver gene are uniformly distributed across the 96 mutation channels, and that similar mutations are equivalent in terms of selection. The first assumption represents a fair estimate in the absence of information. Arguably it is more likely to be correct for tumour suppressor genes (TSGs), where there may be a large number of alternative mutations for any given cancer-causing mutation, than in oncogenes.

In theory this would make the effects of mutational process more easily discernible from mutations in TSGs than oncogenes, and this is one potential reason that mutational signatures were first recognised in TP53, which has many characteristics of a TSG. The second assumption is unlikely to be true. It is testable in large cohorts with known (or assumed) timing of mutational processes and is analysed directly in the next chapter. Potential error due to these assumptions is partially mitigated by the use of multiple cancer genes and comparison with MMR-D and MMR-P tumours. However, I accept that some uncertainty remains due to these assumptions.

The model I have presented here goes some way to formalising the dependence of driver mutations in a sequenced tumour on the mutational processes present in the history of the tumour and selection. Developing these ideas more fully is of potential interest to dissect the causes of driver mutations in other tumours and tumour types. Some of this development is done in the next chapter. In the next chapter, I present a pan-cancer analysis of the differential contributions of mutation processes and selection in determining driver mutation complement. In addition, some development is left for future work. In particular, the *POLE* signature score presented here is a heuristic measure designed to capture the probability that cancer mutations developed on a background of *POLE* mutation. Developing this further into an exact Bayesian posterior probability is of potential interest for future work.

In conclusion, I have presented evidence that suggests *POLE* EDMs are early events in colorectal and endometrial cancer in two, largely orthogonal senses; with respect to the last common ancestor of the all tumour cells and with respect to driver mutations. These findings suggest cautious further research into whether immunotherapy could benefit patients with *POLE*-mutant tumours. I have also presented a model of the effects of mutation and selection on cancer mutations. Notwithstanding certain limitations of the model, these findings represent an important contribution to our understanding of *POLE*-mutant tumours and, more broadly, the relationship between mutation and selection in tumour development.

Chapter 5

The effects of mutation and selection on driver mutations across cancer types

The work presented in this chapter has been accepted at Nature Communications

3. Temko D., Tomlinson I., Severini S., Schuster-Bckler B., Graham T.A. The effects of mutational processes and selection on driver mutations across cancer types, *in press*, *Nature Communications*, 2018

5.1 Précis

Epidemiological evidence has long associated environmental mutagens with increased cancer risk. However, links between specific mutation-causing processes and the acquisition of individual driver mutations have remained obscure. Here I have used public cancer sequencing data from 11,336 cancers of various types to infer the independent effects of mutation and selection on the set of driver mutations in a cancer type. First, I detect associations between a range of mutational processes, including those linked to smoking, ageing, APOBEC and DNA mismatch repair (MMR) and the presence of key driver mutations across cancer types. Second, I quantify differential selection between well-known alternative driver mutations, including differences in selection between distinct mutant residues in the same gene. These results show that while mutational processes play a large role in determin-

ing which driver mutations are present in a cancer, the role of selection frequently dominates.

5.2 Contribution

I designed and carried out all the analysis in this chapter. The text in this chapter closely mirrors the paper, which was written by TG and myself with input from the other authors.

5.3 Summary

Mutational likelihood and evolutionary selection together determine which driver mutations a cancer will accrue. In a pan-cancer analysis, here I show that the occurrence of a particular driver mutation is strongly correlated with the activity of underlying mutational processes, suggesting a potentially causative role for the mutational process in determining which driver mutations are found in a cancer. Then, by using these relationships to normalise differences in mutational likelihood, I infer large differences in the selective advantage of mutually exclusive driver mutations. Overall, the study provides a quantitative understanding of the evolutionary forces governing driver mutation acquisition across cancer types.

5.4 Introduction

Environmental mutagens have long been associated with cancer risk [Weinberg, 2014, Parkin et al., 2011, Hanahan and Weinberg, 2011], but links between mutagens and the generation of specific pathological mutations have remained obscure. A landmark study by Alexandrov et al. [Alexandrov et al., 2013a, Alexandrov et al., 2013b] identified distinct "mutational signatures", each the outcome of distinct mutagenic processes, many of which are attributable to environmental mutagens (see Chapter 1). The study described 21 different mutational signatures, each characterised by different proportions of the 96 mutation types. Subsequently more than 30 signatures, many with tumour type-specificity, have been reported [Wagener et al., 2015, Mouw et al., 2016, Nik-Zainal et al., 2016, Hong et al., 2015, Schulze et al., 2015, Petljak and Alexandrov, 2016].

In the previous chapter I investigated the dependence of the likelihood of acquisition of specific cancer-causing mutations [Sieber et al., 2005] on the underlying mutational processes and selection. Under this model analysis of the genomic context of driver mutations in *POLE*-mutant tumours suggested that the *POLE*-associated mutational signature was implicated in causing many of the driver mutations, consistent with early *POLE* mutation in these tumours. In the first part of this chapter I use a related analysis (measuring the covariation between mutational signatures and driver mutations across tumour types) to investigate causation between a broad range of mutational processes and driver mutations. Specifically, I provide a comprehensive statistical assessment of the relationship between relative mutational process activity and driver mutation acquisition across cancer types (methodology summarised in Figure 5.1 A).

The strength of selection experienced by a mutation is also expected to influence the frequency at which the mutation is detected in the patient population. If two mutations are equally likely to occur, I reason that the more strongly selected mutation will be found more frequently across cancers. Traditionally, it has been convenient to classify mutations found in cancer as drivers or passengers [Bozic et al., 2010], but it is likely that the effects of driver mutations actually lie on a continuum, including both "mini-drivers" and major drivers [Castro-Giner et al., 2015, Vogelstein et al., 2013]. However, the relative selective advantages of individual driver mutations have not yet been quantified. Here, I present evidence for differential selection between frequently mutated amino acids within a driver gene by controlling for differences in the sequence-specific mutation rate, in cases where the mutational signatures alone cannot fully explain the spectra of mutations in driver genes. I also explore differential selection between sets of related genes that show patterns of mutational exclusivity (methodology summarised in Figure 5.1 B).

Together, my analysis quantifies the contributions of both mutation and selection in shaping the spectrum of driver mutations across cancer types.

Figure 5.1: Schematic representation of the approach. A) In the first part of the chapter, the effects of mutational process activity on driver mutation frequencies are investigated. For a driver mutation, the change was assigned to one of the 96 trinucleotide mutational channels (e.g. CTG>CCG), referred to as the "causal channel" of the mutation. I hypothesised that mutational signatures in which that channel was higher than average would be over-represented in cancers with these mutations. I tested this hypothesis by comparing the levels of signatures in cancers harbouring the mutations to those in cancers that did not harbour the mutations. B) In the second part of the study, I investigated the effects of mutational processes on the relative frequencies of specific pathogenic mutations in cancer driver genes. The causal channels of the different driver mutations (different amino acid changes) within a gene were identified on a tumour type by tumour type basis. I then tested whether observed frequencies of each driver mutation differed significantly from those expected based on mutational process activity alone, thus indicating differential selection between mutations in the same gene. Using a simple mathematical model, I transformed normalised measurements of mutation frequency into estimates of relative risk between mutations. This analysis was then extended to comparisons between mutations in different driver genes with apparently equivalent functional effects in a cancer type.

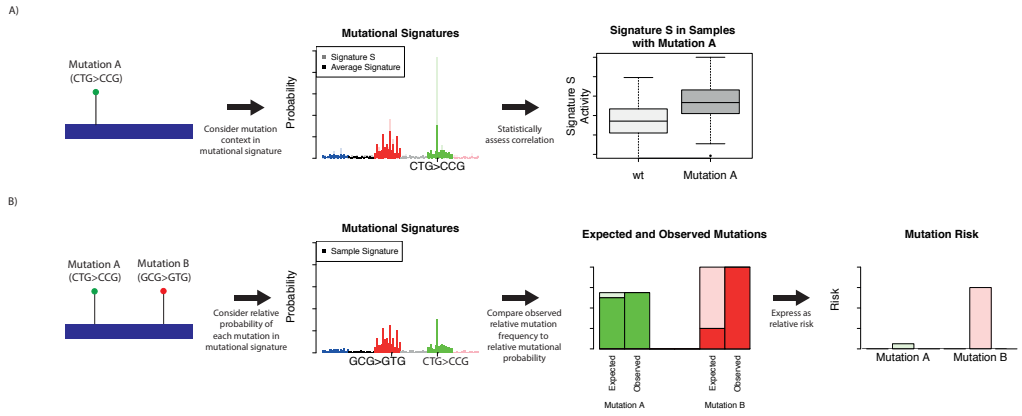

5.5 Methods

5.5.1 Testing for evidence of differential selection between mutations in a cancer type

Here, I present an approach to test mutation frequencies against the null hypothesis of equivalent selection, by developing the model introduced in Chapter 4

Consider mutations M_1 and M_2, assumed to be equivalent in the sense defined in Chapter 4. Let c_i be the causal channel of M_i and let u_i be the underlying rate of occurrence of mutation M_i per year. Let $S = (p_1, ..., p_{96})$ represent the active

mutational signature based on equal trinucleotide frequencies.

Then by 4.1 we have that

$$P(M_1|M_1 \cup M_2) = \frac{u_1}{u_1 + u_2}$$

Or equivalently

$$P(M_1|M_1 \cup M_2) = \frac{p_{c_1}}{p_{c_1} + p_{c_2}}$$

Let $I = \{A_1, ..., A_n\}$ be the set of samples in cancer type C in which exactly one of M_1 or M_2 occurs and no other mutation in the set of mutations under consideration for differential selection occurs. Let $S_i = (p_{i,1}, ..., p_{i,96})$ be the mutational signature of sample A_i.

Therefore, under the null hypothesis of equivalent selection, we can model the number of samples in which M_1 occurs by a Poisson binomially distributed random variable X

$$X \sim \text{Poibin}(q_1, ..., q_n)$$

Where q_i is the probability that M_1 occurs in sample S_i given that either M_1 or M_2 do

$$q_i = \frac{p_{i,c_1}}{p_{i,c_1} + p_{i,c_2}}$$

5.5.2 Modelled relative risk

Now assume that M_1 and M_2 are similar, but not necessarily equivalent, with M_1 having relative risk $r_{1,2}$ compared to M_2. By the same logic as above, we model the probability q_i, that M_1 is present in sample i given that either M_1 or M_2 is present by the following formula:

$$q_i = \frac{r_{1,2} p_{i,c_1}}{r_{1,2} p_{i,c_1} + p_{i,c_2}}$$

Defining I_1 and I_2 as the sets of sample numbers where M_1 and M_2 occurred,

respectively, then the likelihood of the data, L, is given by:

$$L = \prod_{i \in I_1} q_i \prod_{i \in I_2} (1 - q_i)$$

Likelihood maximisation can be used to infer the a value of $r_{1,2}$ for each pair of mutations in each tumour type, based on this formula. Bootstrapping can be used to find approximate confidence intervals around these estimates.

5.5.3 Data collection

Mutation data (single nucleotide alterations- SNAs) were downloaded from the ICGC and TCGA data portals in May 2016. I excluded data sets aligned to a reference genome other than hg19, and those with non-conforming formatting.

5.5.4 Sample-specific mutation collection

Only mutations on canonical nuclear chromosomes were considered. For ICGC data, mutations labelled as "single base substitution" in the simple somatic mutation files were considered for further analysis. For TCGA data, only mutations labelled as 'SNP' in the mutation annotation files were considered.

From these lists, non-synonymous mutations in driver genes were extracted. Driver genes definitions were as is stated below. After filtering for drivers, these mutations were re-annotated using Annovar [Wang et al., 2010]. I included mutations labelled as 'non-synonymous SNV', 'stopgain', or 'stoploss' in a driver gene in the annotation by Annovar.

5.5.5 Definition of driver genes

Driver genes were defined based on a recent study by Vogelstein et al. [Vogelstein et al., 2013].

5.5.6 Sample-specific mutational signature estimation

The total number of SNAs in each of the 96 channels was calculated for each sample. Non-synonymous mutations in driver genes were excluded. Mutational signatures based on equal trinucleotide frequencies were obtained from the Wellcome Trust Sanger Institute (http://cancer.sanger.ac.uk/cosmic/signatures)

in April 2016 (Cosmic Signatures). Information on the presence/absence of these signatures in individual cancer types was obtained from the same source. Non-negative least squares regression, implemented in the R package 'nnls' [Katharine M. Mullen, 2012], was used to model the counts of mutations across categories in each tumour as a linear combination of the Cosmic Signatures present in the cancer type. For whole exome data, the Cosmic Signatures were rescaled to the trinucleotide frequencies of the exome for the regression. The activity of each process in each cancer sample (based on the trinucleotide frequencies of the sample) was estimated as the regression coefficient for that signature in that sample. The activity of each process in each sample, thus identified by regression, was rescaled to find the activity of the process for a genomic sequence with equal trinucleotide frequencies (see Section 4.4). These activities were then normalised to one to find the mutational signature exposures.

The analysis of differential selection was based on a single mutational signature based on equal trinucleotide frequencies for each sample. These signatures were found as follows. For each sample, for each mutation type j, let $p_j(\Pi_k, E)$ represent the frequency of mutation type j in Cosmic Signature k, rescaled to equal trinucleotide frequencies. Define $e_k(E)$ as the exposure to signature k for the sample found in the paragraph above. The sample-specific signature was estimated as $S = (p_1, p_2, ..., p_{96})$, with p_j given by

$$p_j = \sum_{k=1}^{n} e_k(E) p_j(\Pi_k, E)$$

5.5.7 Required mutations for signature assignment

By treating each of the 30 signatures as a multinomial probability distribution, I simulated data sets from each signature with n total informative mutations ($1 < n < 96$). For each signature, for each value of n, I applied non-linear least squares regression to the simulated data to assign weights to the true generating signature and a set of 14 randomly chosen other signatures. I classified the regression as successful when over 50% of the regression weights were assigned to the true signature. I chose to use 15 possible generating signatures as this was above the maximum number

of signatures identified in any individual cancer type. For each signature, for each number n of informative mutations, I calculated the proportion of simulated data sets where the regression was successful. I found that 20 mutations gave an average classification accuracy of 80% across signatures. As a result, I chose to use a cut-off of 20 mutations to strike a balance between including as many tumour samples as possible while still maintaining reasonable accuracy of signature assignment. I repeated the analysis of associations between driver mutations and mutational signatures using a cut-off of 50 mutations per sample for comparison. This analysis recovered 41 associations, of which 37 were also found using the 20 mutation cut-off.

5.5.8 Power calculations

I sought to test the power to detect an association between mutation M and the signature A in cancer type C, where M occurred m times among the c tumours in C. I considered a simple model of cancer initiation, where M is one of a set of mutations R of size $|R| = n$, one of which is required for cancer initiation. For these purposes I assumed $n = 10$.

I identified the channel among the 96 possibilities that matched the mutation M (the causal channel of the mutation). For each random iteration of the power model I randomly selected causal channels out of 96 possibilities of the 9 other mutations in R. I identified the signature exposures of each sample in C. By treating the signatures as multinomial probability distributions, I then calculated the per-sample probabilities that mutation M occurred rather than any of the 9 mutations in each sample. Based on these probabilities I randomly selected m samples to bear the mutation M. I then applied the Mann-Whitney U test described below to test whether the m mutant samples had significantly higher exposure to signature A than the $c - m$ samples without the mutation.

I analysed the power to detect an association for each of 1,019 tests for an association between a recurrent driver mutation and a mutational signature within a cancer type. Mean power to detect associations was estimated at 13% at alpha = 0.05 (min = 0%, max = 96%), and 30/1,020 tests had a power above 50%. I

found that the power was influenced by the number of times a mutation occurred, as well as the enrichment of the mutation causal channel in the signature compared to average in the cancer type (Multiple Regression, $P < 2 \times 10^{-16}$ both variables).

Out of 1,019 triplets tested, relatively few significant associations (43) were found. The low number of associations can be partly explained by the low average power. Even if associations were genuinely present in every case, the expected number of significant tests was 130 based on the estimated power. Part of the reason for this is the technical challenges inherent in deconvolving mutational signature intensities. Timing mismatches between the activity of a mutational selection and the window of selection for a driver mutation probably also contribute to the low numbers of associations.

5.5.9 Comparison of genomic and exonic mutation distributions

Our study used a combination of whole genome sequencing (WGS) and whole exome sequencing (WXS) data. The 1,441 whole WGS samples were distributed predominantly across 8/22 cancer types. In total five associations between mutational signatures and driver mutations were identified across these eight cancer types (see results below). All five of these associations were in liver cancer, where 27% of samples (305/1110) were WGS samples.

To assess the effect of using both whole genome and whole exome samples on my analysis, I analysed the effect on the results of replacing the WGS data with only the exonic subset of mutations. I recovered 41/43 associations between driver mutations and mutational signatures and found no new associations, suggesting that using WGS data in addition to WXS has a limited effect on the analysis.

5.5.10 Variation explained by mutation probability

For each mutation, the probability of the mutation in each sample of a cancer type was calculated based on sample-specific mutational signature exposures. The mean probability across samples was found, as well as the number of times the mutation occurred. Linear regression was carried out to find the proportion of variance in mutation frequencies across different mutations explained by variation in their

probabilities.

5.5.11 Multiple testing corrections

Multiple testing q values were calculated from test P values using the Benjamini and Hochberg method.

5.6 Results

5.6.1 Testing for mutational process and driver mutation associations

I investigated the correlations between mutational process activity and recurrent driver mutations across cancer types. I reasoned that when a mutational process acts, it makes specific driver mutations, caused by a mutation in a specific channel enriched in the mutational signature of the process, more likely. I therefore tested for a difference in the levels of relative mutational process activity between cancers with and without specific driver mutations (Figure 5.1 A). The use of signature and individual channel activity information was designed to increase the sensitivity and specificity of the approach. Where the activity of a mutational process was significantly higher in cancers with a mutation of interest compared to those without, I considered it supporting evidence for a causative relationship between the mutational process activity and the acquisition of the driver mutation.

Data were obtained and curated from the TCGA and International Cancer Genome Consortium (ICGC) data portals (see Methods). Driver genes were classified according to a recent study [Vogelstein et al., 2013]. The data set for analysis represented 11,336 samples across 22 major cancer types (summarised in Table 5.1). There were 1,447 whole genome samples and 9,889 whole exome samples. Analysis using only exonic mutations from the whole genome samples revealed similar relationships between mutational processes and driver mutations (see Methods). Downstream analysis was based on 14,356,672 SNAs, of which 40,753 were non-synonymous mutations in driver genes. I did not consider other types of genome alteration (such as copy number alteration).

Table 5.1: Samples used for study

	Disease	Prefiltered Samples	Filtered Samples
1	AML	394	180
2	Liver	1153	1110
3	Bladder	515	509
4	Glioblastoma	396	389
5	Glioma Low Grade	516	448
6	Breast	1107	909
7	Cervix	198	189
8	CLL	262	199
9	Colorectum	531	525
10	Prostate	741	699
11	Oesophagus	532	512
12	Stomach	450	441
13	Head and Neck	616	610
14	Thyroid	511	179
15	Kidney Clear Cell	573	560
16	Kidney Papillary	282	274
17	Lung Adeno	230	228
18	Lung Squamous	497	491
19	Ovary	380	373
20	Pancreas	803	718
21	Melanoma	344	337
22	Uterine Carcinoma	305	303

I excluded 1,153 samples with insufficient mutations for the signature assignments (fewer than 20 mutations), leaving 10,183 samples for further analysis. To test for potential signature mis-assignment, I also considered a more stringent cut-off of 50 mutations, which gave similar results (see Methods). In each cancer type, I classed as "recurrent" non-silent DNA mutations in driver genes that occurred at least four times in the cancer type (these recurrent mutations were considered candidate tissue-specific driver mutations). For each mutation, I selected the channel among the 96 possibilities that matched the observed mutation (hereinafter the "causal channel" of the candidate driver mutation). For this channel, I identified the signatures where the frequency of the causal channel was above average, relative to all mutational processes active in the cancer type. For each of these signatures, I tested for a correlation between mutational process activity and presence of the mutation in the cancer type. Specifically, I used a one-sided Mann-Whitney U test

to test whether samples in the cancer type bearing the mutation had significantly higher exposure to the mutational signature.

5.6.2 Mutational processes shape driver mutation landscape

There were 43 significant correlations between signature activity and driver mutations (Mann-Whitney U test, FDR = 0.05; one-sided test), out of 1,019 triplets of specific mutations in individual driver genes, mutational signatures and cancer types tested. Three of the associations involved signatures linked to extrinsic mutational processes (i.e. mutagens), 30 involved signatures linked to intrinsic mutational processes and 10 involved signatures with no known aetiology (Table 5.2 for the full list of associations).

Of the associations involving signatures linked to extrinsic mutational processes, signature 4, linked to smoking, was associated with *KRAS G12C* (CCA>CAA) in lung adenocarcinoma (Figure 5.2 A) and with *CTNNB1 D32Y* (TCC>TAC) in liver cancer. Signature 24, linked to aflatoxin, was associated with *TP53 R249S* (GCC>GAC) mutations in liver cancer.

There were multiple associations involving signatures linked to intrinsic mutational processes. APOBEC activity (Signatures 2 and 13) had 11 associations. Remarkably, *PIK3CA E542K* (TCA>TTA) and *E545K* (TCA>TTA) were associated with these signatures across 5 cancer types, accounting for 82% (9/11) of all APOBEC associations (Figure 5.2 B). Additionally, *PIK3CA E453K* (TCT>TTT) was associated with an APOBEC signature in breast cancer.

DNA mismatch repair (MMR)-linked signatures (signatures 6, 15, 20 and 26) showed 9 positive associations across four cancer types (stomach, colorectum, uterine carcinoma and glioma low grade). Of these associations, *PIK3CA H1047R* (ATG>ACG) occurred twice. *FBXW7 R465C* (GCG>GTG), was associated with MMR signatures in both colorectum and stomach cancer (Figure 5.2 C). *KRAS G12D* (ACC>ATC) and *KRAS G13D* (GCC>GTC) were associated with MMR signatures in uterine carcinoma and stomach cancer respectively (Figure 5.2 D). These results suggest an important role for MMR defects shaping the driver mutation spectrum of common cancers, and illustrate the likely sequence of events (early

Figure 5.2: Selected associations between driver mutations and mutational process activity within cancer types. Q-values shown are for Mann-Whitney U test. A) *KRAS G12C* and signature 4 in lung adenocarcinoma. B) *PIK3CA E545K* and signature 2 in breast cancer C) *FBXW7 R465C* and Signature 15 in stomach cancer D) *KRAS G12D* and signature 26 in uterine carcinoma E) *PTEN R130Q* and signature 10 in uterine carcinoma F) *APC R213X* and signature 1 in colorectal cancer.

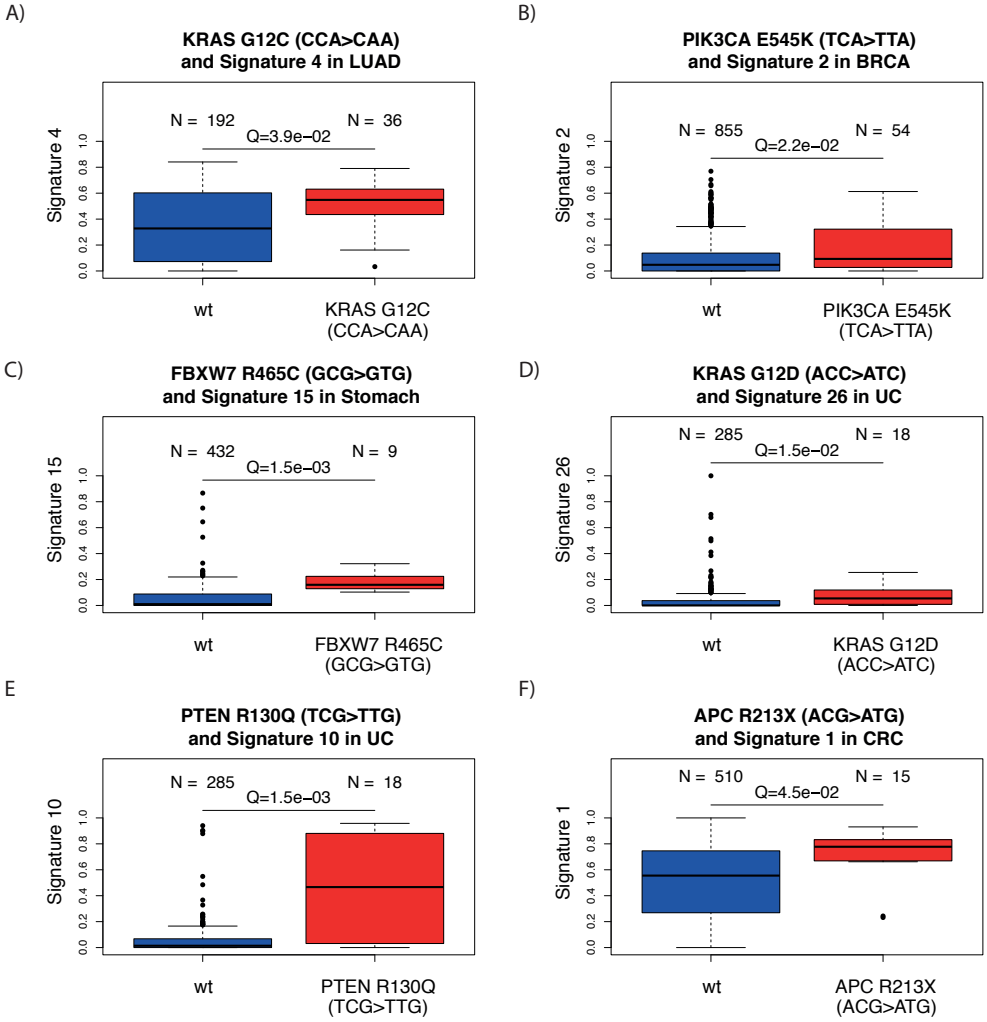

Table 5.2: Associations between mutational signatures and driver mutations within cancer types. 'Frequency': Mutation frequency in the tumour type

	Mutation	Signature	Disease	Frequency	q-value
1	APC R213X (ACG>ATG)	1	Colorectum	0.03	4.50e-02
2	ERBB2 S310F (TCC>TTC)	2	Bladder	0.04	5.35e-03
3	PIK3CA E545K (TCA>TTA)	2	Cervix	0.14	8.98e-03
4	PIK3CA E542K (TCA>TTA)	2	Breast	0.04	1.06e-02
5	PIK3CA E545K (TCA>TTA)	2	Breast	0.06	2.20e-02
6	PIK3CA E545K (TCA>TTA)	2	Bladder	0.05	2.47e-02
7	PIK3CA E542K (TCA>TTA)	2	Lung Squamous	0.03	2.86e-02
8	PIK3CA E545K (TCA>TTA)	2	Head and Neck	0.05	3.69e-02
9	PIK3CA E453K (TCT>TTT)	2	Breast	0.01	3.93e-02
10	CTNNB1 D32Y (TCC>TAC)	4	Liver	0.01	2.76e-02
11	KRAS G12C (CCA>CAA)	4	Lung Adeno	0.16	3.93e-02
12	ALK R259P (GCG>GGG)	5	Glioblastoma	0.01	1.32e-02
13	PTPN11 S189A (TTC>TGC)	5	Glioblastoma	0.01	3.13e-02
14	HRAS Q61R (CTG>CCG)	5	Bladder	0.01	3.93e-02
15	PTPN11 Y197X (ATA>AGA)	5	Glioblastoma	0.01	4.16e-02
16	KIT K642E (TTG>TCG)	5	Melanoma	0.01	4.66e-02
17	FBXW7 R465C (GCG>GTG)	6	Colorectum	0.02	1.34e-02
18	IDH1 R132H (ACG>ATG)	6	Glioma Low Grade	0.72	2.76e-02
19	PTEN R130Q (TCG>TTG)	10	Uterine Carcinoma	0.06	1.48e-03
20	PIK3R1 R348X (TCG>TTG)	10	Uterine Carcinoma	0.03	3.44e-03
21	ARID1A R1989X (TCG>TTG)	10	Uterine Carcinoma	0.03	3.72e-03
22	APC R2204X (TCG>TTG)	10	Uterine Carcinoma	0.02	8.98e-03
23	PTEN R130Q (TCG>TTG)	10	Colorectum	0.01	1.19e-02
24	SF3B1 R957Q (TCG>TTG)	10	Uterine Carcinoma	0.01	1.32e-02
25	FUBP1 R430C (TCG>TTG)	10	Uterine Carcinoma	0.01	1.60e-02
26	PIK3CA R88Q (TCG>TTG)	10	Colorectum	0.02	3.30e-02
27	APC R1114X (TCG>TTG)	10	Colorectum	0.04	3.33e-02
28	PIK3CA E545K (TCA>TTA)	13	Head and Neck	0.05	1.06e-02
29	PIK3CA E542K (TCA>TTA)	13	Lung Squamous	0.03	1.28e-02
30	PIK3CA E545K (TCA>TTA)	13	Bladder	0.05	2.78e-02
31	ATRX R1426X (GCG>GTG)	14	Glioma Low Grade	0.01	4.56e-02
32	FBXW7 R465C (GCG>GTG)	15	Stomach	0.02	1.48e-03
33	KRAS G13D (GCC>GTC)	15	Stomach	0.02	4.56e-02
34	CTNNB1 S37C (TCT>TGT)	16	Liver	0.01	3.93e-02
35	CTNNB1 S45Y (TCT>TAT)	16	Liver	0.01	4.70e-02
36	PIK3CA H1047R (ATG>ACG)	20	Stomach	0.04	7.40e-04
37	KRAS G13D (GCC>GTC)	20	Stomach	0.02	8.98e-03
38	PIK3CA H1047R (ATG>ACG)	21	Stomach	0.04	2.17e-02
39	CTNNB1 S37F (TCT>TTT)	23	Liver	0.01	7.36e-03
40	TP53 R249S (GCC>GAC)	24	Liver	0.01	1.01e-04
41	FBXW7 R465C (GCG>GTG)	26	Stomach	0.02	3.07e-04
42	PIK3CA H1047R (ATG>ACG)	26	Stomach	0.04	7.40e-04
43	KRAS G12D (ACC>ATC)	26	Uterine Carcinoma	0.06	1.46e-02

MMR-linked mutational processes relative to driver mutation acquisition) in some cancers with these defects.

Nine associations with deficiency in DNA-proofreading (signature 10) were

seen in uterine carcinoma and colorectum. *PTEN R130Q* (TCG>TTG) was associated with this signature in both colorectum and uterine carcinoma (Figure 5.2 E). 2/11 positive associations involved stop-gain mutations in the *APC* gene, one in colorectum and one in uterine carcinoma. Therefore it appears that *POLE* defects may cause characteristic driver lesions in these cancer types.

Six of the associations involved signatures that are known to correlate with age at diagnosis [Alexandrov et al., 2015]. Of particular note, signature 1 was associated with *APC R213X* (ACG>ATG) in colorectum (Figure 5.2 F). This result in particular highlights the important role of ageing-related processes in cancer development.

Our test for correlation between mutational processes and driver mutations focussed on processes which exhibit higher activity of the causal channel. This reduces the overall number of tests and increases the power to detect putative associations. However, to probe whether mutational processes and driver mutation acquisition are correlated in general, I repeated the analysis above without restricting the tests to signatures where the frequency of the causal channel was above average in the cancer type. An enrichment for positive associations between driver mutations and signatures where the underlying process has a higher than average activity of the causal channel would be indicative of a mechanistic relationship. Indeed, I found that 24 out of 37 significant associations had higher than average channel activity, compared to only 13 cases where the causal channel was lower than average ($P = 5.5 \times 10^{-5}$; Fisher's Exact Test; Figure 5.3), supporting the notion that the respective mutational processes are responsible for the driver mutation. However, since my analysis is correlative, I cannot entirely rule out the possibility of other explanations for these associations. Despite this, the results above support a model whereby mutational processes play an important role in determining driver mutation spectrum.

5.6.3 Detecting differential selection

Driver mutations are recurrent in cancer because they experience positive selection. Consequently, the frequency that a particular driver is observed across cancers is

Figure 5.3: Causal channels of associations between mutational signatures and driver mutations. Log fold change of the causal channel of the driver mutation in the mutational signature for significantly associated driver mutations and mutational signatures within cancer types (red) and for those with no association (grey). To calculate the log fold change, 1/96 was added to the probability of the causal channel in the mutational signature, and to the average probability of the causal channel across signatures present in the cancer type. The log fold change shown represents the logarithm of the ratio of the two resulting values.

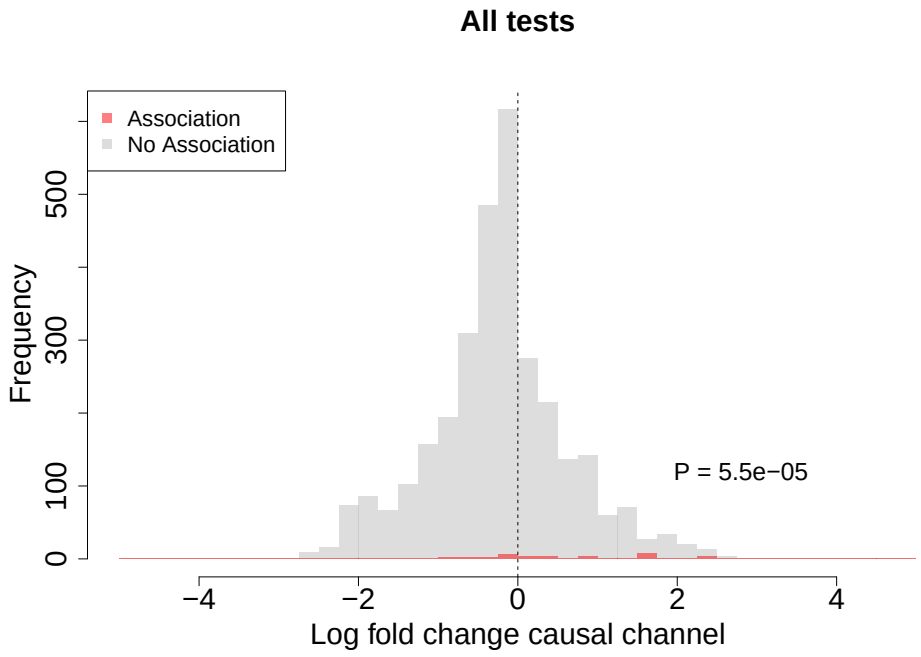

a function both of the mutational likelihood of it occurring in the first place, and also the selective advantage that the mutation confers. Accordingly, the selective difference between the mutations can be inferred by normalising the observed frequency of the mutations across cancers by their underlying mutational likelihood (see Methods for mathematical model). With this logic as my foundation, I therefore aimed to quantify the differences in selective advantage between (typically) mutually exclusive driver mutations by using the results from the first part of this chapter to normalise for mutational likelihood.

To test for differential selection between two related mutations in a cancer type (e.g. mutation of different residues of the same driver gene), I calculated the frequency of each mutation and their relative likelihoods of occurrence, inferred from

the mutational process exposures (as per the analysis above). I then used the Poisson binomial test to examine the null hypothesis that the mutation counts were explained solely by their relative mutational likelihood of occurrence (see Methods). I explored potential differential selection among the most common driver mutations ($> 1\%$ of non-synonymous mutations) in nine genes: *KRAS*, *BRAF*, *NRAS*, *IDH1*, *IDH2*, *TP53*, *PIK3CA*, *SMAD4* and *CTNNB1* in individual cancer types. I conducted pairwise tests among the common mutations from each gene in each cancer type where the common mutations in the gene occurred at least 10 times.

5.6.4 Differential selection between pathogenic amino acid changes within a driver gene

Differential selection between driver genes was common. In total, 19% (655/3,476) of pairwise comparisons between mutational-likelihood corrected frequency of mutations of different residues in the same gene in individual cancer types returned a significant result (Binomial Test, FDR $= 0.05$, Figure A.1-A.11). All 9 genes examined had at least one pair of mutations that occurred at frequencies inconsistent with the underlying mutational likelihood.

Among the most highly significant results, *KRAS G12R* appeared more strongly selected than other *KRAS* mutations, including *KRAS G12C* and *G13D*, in pancreatic cancer (quantified by the relative risk of the mutation occurring relative to a reference mutation; Figure 5.4 A), as did *BRAF V600E* compared to other *BRAF* common mutations, including *BRAF K601E*, in thyroid, melanoma and colorectal cancer. Also highly significant was apparent preferential selection for *PIK3CA H1047R* compared to multiple *PIK3CA* mutations, including *PIK3CA E545K* and *E542K*, in breast cancer (Figure 5.4 B), and for *NRAS Q61K* and *Q61R* above *NRAS G12D* and *G13D* in melanoma. These results suggest that there are strong selective differences among important driver mutations in the same gene in these cancer types.

A number of the results are of potential therapeutic interest. For example, I found evidence that *IDH1 R132H* is selected more strongly than *IDH1 R132C* in low grade glioma (Figure 5.4 C) and glioblastoma. This is of particular interest

Figure 5.4: **A**, Modelled Relative risk (RR) of frequent *KRAS* mutations in pancreatic cancer compared to *KRAS G12R*. For each mutation, the maximum likelihood estimate of relative risk compared to *KRAS G12R* is shown. **B**, **C**, and **D** illustrate modelled relative risk for respectively, *PIK3CA* mutations in breast cancer, IDH1 mutations in glioma low grade, and *KRAS* mutations in lung adenocarcinoma. Grey dashed line indicates relative risk of one. Error bars represent 95% confidence intervals obtained by bootstrapping across 100 iterations.

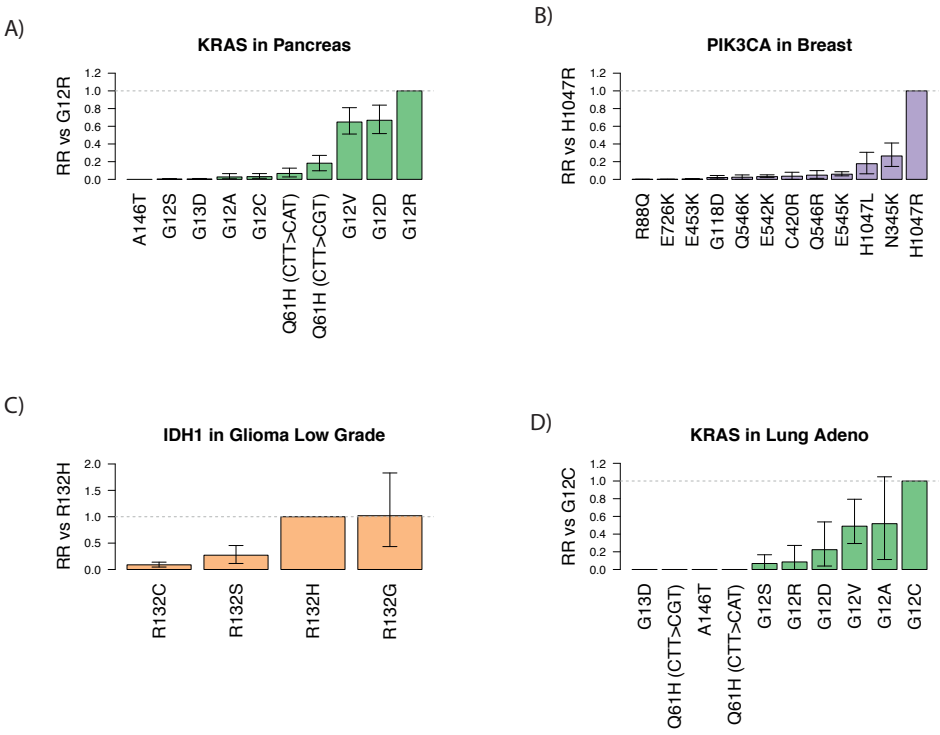

given the potential specificity of therapeutic small molecular inhibitors that target *IDH1* and *IDH2* mutations [Garrett-Bakelman and Melnick, 2016].

KRAS G12C, which was found to be associated with smoking-associated signature 4 in lung adenocarcinoma (see above), also appears more strongly selected than other *KRAS* mutations (including *G12D*, *G12R*, and *G13D*) in this cancer type (Figure 5.4 D). Thus it appears that the high frequency of this *KRAS* mutation compared to others in lung adenocarcinoma is, potentially, due to both smoking-associated mutational processes and the intrinsic selective advantage of the mutation.

Interestingly, the relative selective advantages of particular pathogenic mutations in each gene were broadly consistent across cancer types. Specifically, there were only 7/118 cases of differentially selected mutations where a mutation ap-

peared selected more strongly than another in the same gene in one cancer type, but less strongly in another cancer type. These included 3 pairs of *KRAS* mutations, two pairs of *PIK3CA* mutations and two pairs of *TP53* mutations. Of note, *KRAS* mutations, *KRAS G12C* appeared selected above *KRAS G12D* and *KRAS Q61H* (CTT>CGT) in lung adenocarcinoma, but below these mutations in pancreatic cancer. And *PIK3CA E545K* appeared selected above *PIK3CA H1047R* and *PIK3CA N345K* in colorectum, but below these mutations in breast cancer. Since the method controls for differences in mutational process activity between cancer types, these results provide evidence to support the hypothesis that the mechanisms that underpin the selective advantage caused by a specific driver mutation are broadly uniform across tissue types.

5.6.5 Differential selection between mutationally-exclusive driver genes

I next used the same methodology to investigate differential selection between mutations within and between small sets of genes that typically show mutually exclusive mutation patterns. I considered the common driver mutations in three sets of functionally-related genes: *KRAS*, *BRAF* and *NRAS*; *APC* and *CTNNB1*; and *IDH1* and *IDH2*.

There was evidence of greater selective differences between genes than between different residues within a gene. 12% (306/2,541 pairwise comparisons) of tests were significant for mutations within a gene, whereas 28% (841/2,995) were significant for mutations in different genes (Figures A.12-A.20)). Furthermore, for two of the mutation sets - *KRAS*, *BRAF* and *NRAS* (Figure 5.5); and *APC* and *CTNNB1* (Figure 5.6) - there was significant heterogeneity across cancer types in terms of the number of mutations in each gene with evidence of preferential selection (selection above at least one other mutation in the set) (Fisher test, $Q = 2.2 \times 10^{-3}$, 7.2×10^{-7}, respectively), supporting a model where gene-specific effects on selection vary across cancer types.

Amongst *KRAS*, *BRAF* and *NRAS* mutations, only particular *KRAS* mutations showed evidence of preferential selection over mutations in other genes in pan-

Figure 5.5: The number of mutations from each of *KRAS*, *BRAF* and *NRAS* with a frequency significantly greater than expectation under equivalent selection compared to at least one other mutation in each cancer type. Whereas colorectum and pancreas cancer appeared to be dominated by selection for *KRAS* mutations, melanoma appeared to be dominated by selection for *NRAS* and *BRAF* mutations.

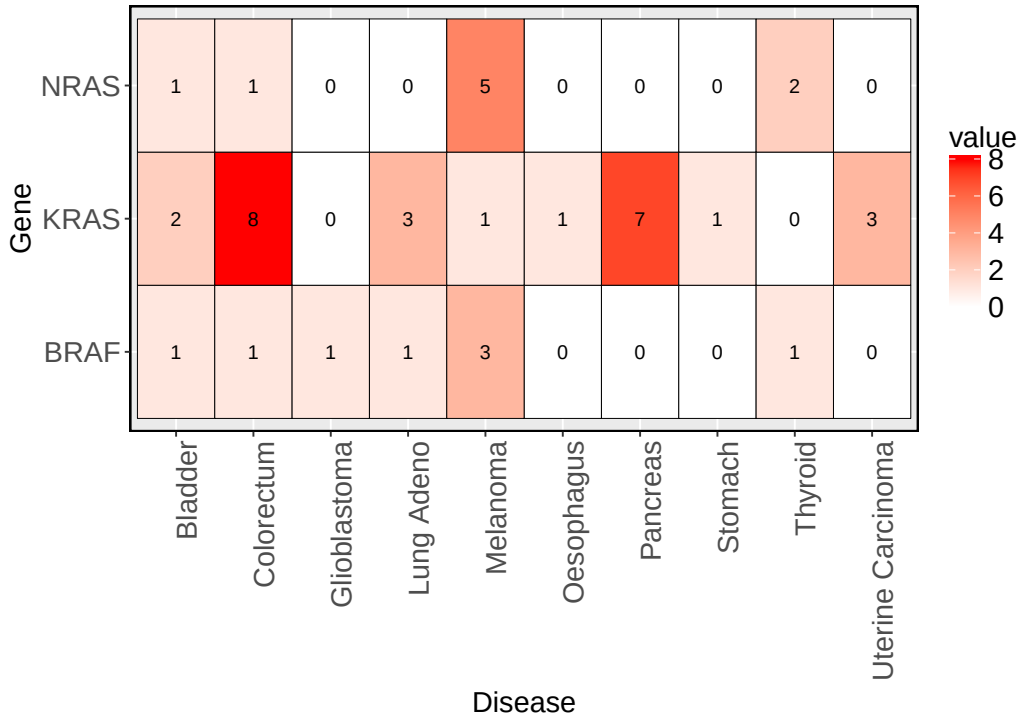

creatic cancer and uterine carcinoma (Figure 5.7 A,B), whereas preferential selection across genes was predominantly in favour of *BRAF* and *NRAS* mutations in melanoma and thyroid cancer (Figure 5.7 C,D). Illustrating this, *BRAF V600E* and *NRAS Q61R* appeared to be selected more strongly than *KRAS G12D* in melanoma and thyroid cancer, but more weakly than this mutation in pancreatic cancer. Other cancer types showed a range of patterns of differential selection for these three genes (Figures 5.7 E,F).

When *APC* and *CTNNB1* mutations were compared, there was evidence for selection of *CTNNB1* mutations over common *APC* mutations in each of liver cancer, uterine carcinoma, prostate cancer and colorectal cancer (Figure 5.8 A,B,C). Interestingly however, evidence for selection of *APC* mutations above *CTNNB1* mutations was found in colorectal cancer only (Figure 5.8 C). I note that this mutation, *APC Q1378X*, falls within the functionally defined mutation cluster region

Figure 5.6: The number of mutations from each of *CTNNB1* and *APC* with a frequency significantly greater than expectation under equivalent selection compared to at least one other mutation in each cancer type. Whereas liver cancer and uterine carcinoma appeared to be dominated by selection for *CTNNB1* mutations, colorectum appeared to be dominated by selection for *APC* mutations.

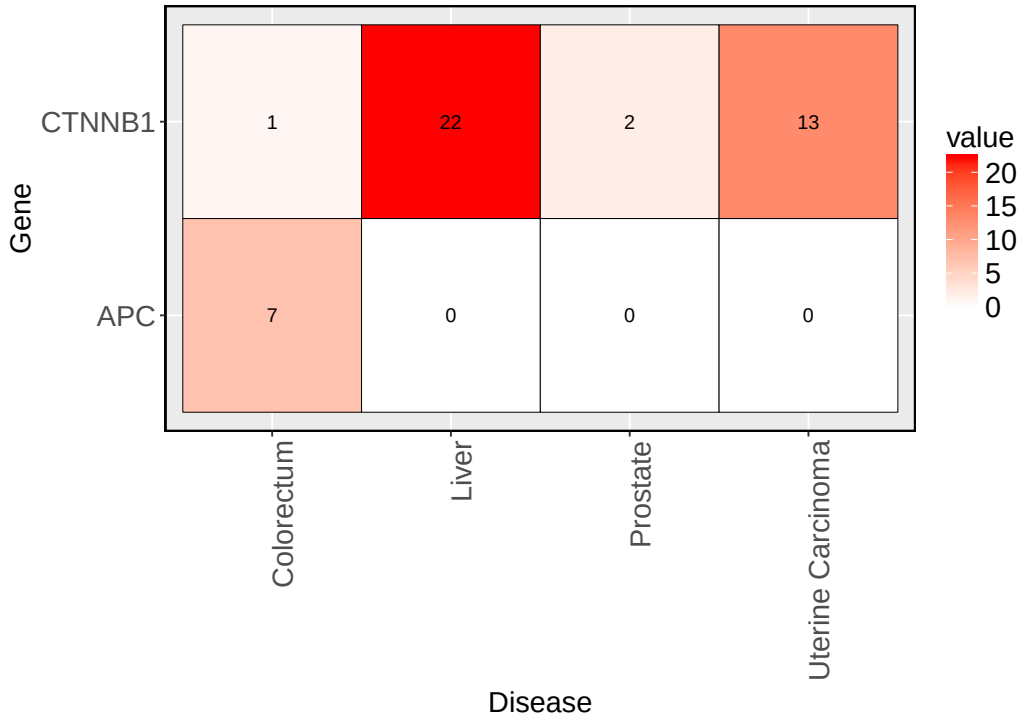

(MCR) of the gene [Rowan et al., 2000].

Among *IDH1* and *IDH2* mutations, I found preferential selection for *IDH1 R132H* (glioma low grade, AML and glioblastoma), *IDH1 R132C* (glioma low grade, *AML*, liver cancer and melanoma), *IDH1 R132G* and *IDH1 R132S* (glioma low grade) above common *IDH2* mutations, as well as preferential selection for *IDH2 R172K* above *IDH1 R132C* in glioma low grade.

Taken together these results inform our understanding of the selective landscape experienced by driver genes, and its similarities and differences between cancer types. Across the cancer types and mutation sets considered there was a positive correlation (correlation coefficient > 0) between mutation frequency and mutation probability in 58/76 cases. Among these cases on average 20% (mean R-squared) of variation in frequency between related mutations within the cancer type is explained by variation in mutation probabilities. This suggests an important role for

Figure 5.7: Evidence for differential selection between mutations in *KRAS*, *BRAF* and *NRAS*. Bar plots show modelled relative risk of *KRAS*, *BRAF*, and *NRAS* mutations (compared to a reference mutation). **A** Modelled relative risk of *KRAS*, *BRAF* and *NRAS*, mutations compared to *KRAS G12R* in pancreatic cancer. **B** As above, with comparison to *KRAS G12A* mutations in uterine carcinoma. **C** As above, with comparison to *BRAF V600E* mutations in melanoma. **D** As above, with comparison to *BRAF V600E* mutations in thyroid cancer. **E** As above, with comparison to *BRAF V600E* in colorectum. **F** As above, with comparison to *KRAS G12C* in lung adenocarcinoma.

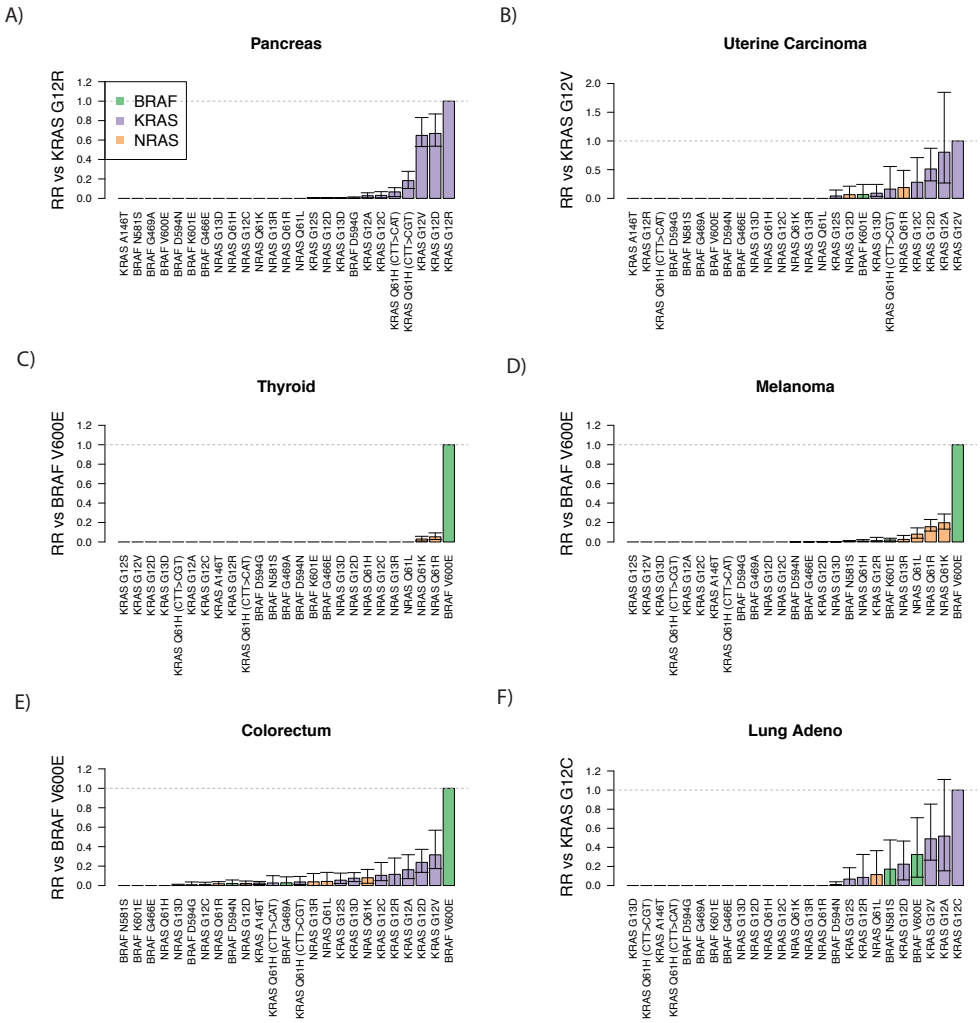

Figure 5.8: Evidence for differential selection between mutations in *APC* and *CTNNB1*. Equivalent to Figure 5.7, for *APC* and *CTNNB1* mutations in **A**, liver cancer, **B**, uterine carcinoma and **C**, colorectum.

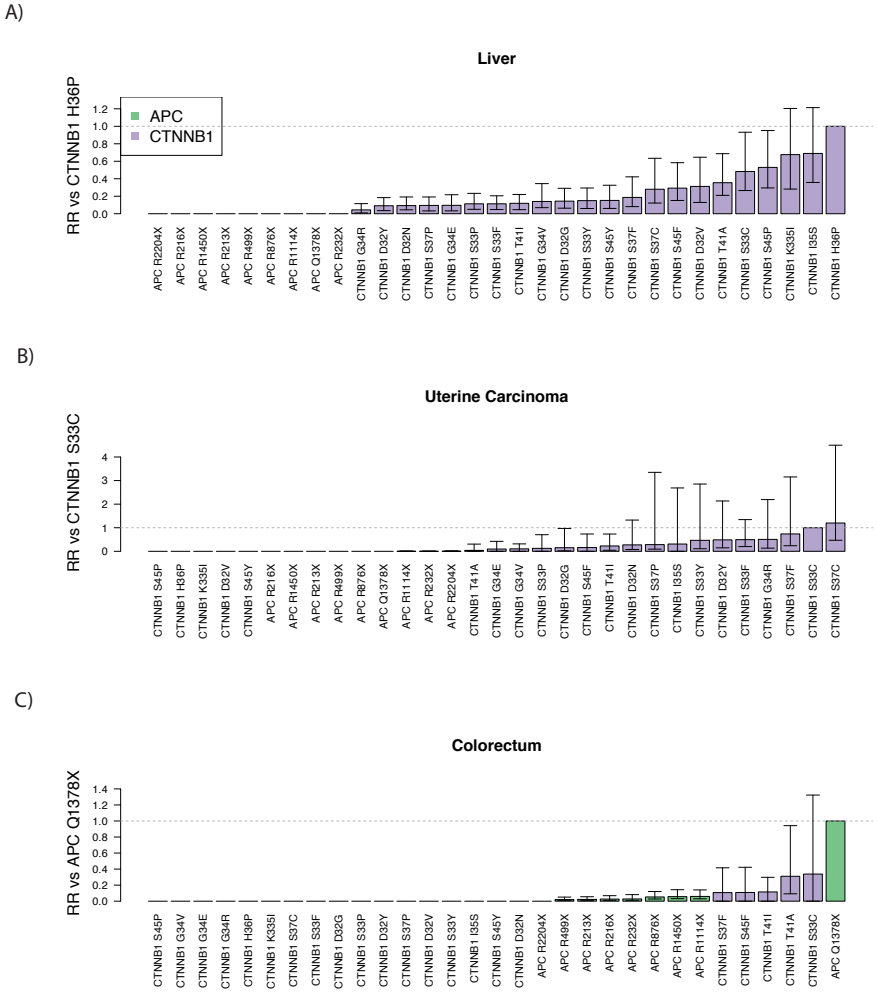

selective differences in explaining this variation. These results suggest that both intra-gene and inter-gene effects contribute to differential selection, with inter-gene but not intra-gene effects varying across cancer types.

5.7 Conclusion

Here, I have demonstrated correlations between mutational processes and key driver mutations across cancer types, and highlighted the possibility that these correlations may actually be the result of the mutational process causing specific driver mutations. Moreover, by normalising for mutational likelihood I have quantified relative selective differences between related key driver mutations across cancer types, which sheds light on the selective landscape constraining cancer evolution.

Many of the associations between mutational processes and driver mutations presented here are novel to the best of our knowledge, and warrant further molecular investigation to explore causality. My analysis suggests that an ageing-associated process (signature 1) may cause initiating events in colorectal cancer because of the implied role of the process in causing *APC R213X* "gatekeeping" mutations in colorectal cancer [Vogelstein et al., 2013, Rowan et al., 2000] suggesting a sometimes critical role for mutations that occur randomly on cell divisions in this cancer type [Tomasetti and Vogelstein, 2015].

Previous work by McGranahan et al. examined the relationship between APOBEC associated mutational processes (signatures 2 and 13) and driver mutations and found that clonal non-synonymous mutations in driver genes occur in an APOBEC context in bladder cancer [McGranahan et al., 2015]. They also described subclonal mutations in driver genes in an APOBEC context in bladder, breast, head and neck, and lung cancers (cervical cancer was not considered). Supporting their findings, I detected associations with APOBEC in bladder cancer and breast cancer, and to a lesser extent in head and neck, lung squamous, and cervical cancer. Notably, I report novel associations between APOBEC activity and *ERBB2 S310F* mutations in bladder cancer. Our findings support the impression of a pervasive effect of APOBEC activity on driver mutation spectra in human cancers. Some as-

sociations I describe have been reported previously, notably the association between pack years of smoking and the *KRAS G12C* mutation in lung adenocarcinoma where the connection between the causal channel of this mutation (C>A in a CCA context) and the general tendency for tobacco carcinogens to cause transversions is well known [Dogan et al., 2012, Riely et al., 2008].

Remarkably, 14/43 associations between mutational signatures and driver mutations involved *PIK3CA* mutations, and most of these associations involved signatures linked to APOBEC, which tends to occur later in carcinogenesis [McGranahan et al., 2015]. Thus, late arising APOBEC linked mutational processes can still have important influences on the driver mutation spectrum. Recent results showing that *PIK3CA* mutations are often subclonal [McGranahan et al., 2015] support this interpretation.

Through normalising for mutational likelihood, I have also been able to quantify the relative contribution of clonal selection, over and above mutational likelihood, in determining driver mutation spectra across cancers. I found evidence for widespread differences in selective effects between mutations in the same gene and related genes, and moreover, that these differences appear to vary across cancer types. These results confirm that not all driver mutations have the same selective effects, and instead exist on a spectrum of selective potency. Both mutational likelihood and selective difference strongly contribute to the occurrence of specific driver mutations in cancers.

The selective differences between mutations identified here relate to a diverse set of genes, including genes encoding proteins involved in intra-cell signalling (*TP53*, *KRAS*, *BRAF*, *NRAS* and *APC*), a protein involved in inter-cell signalling (*CTNNB1*), a transcription factor (*SMAD4*) and proteins involved in metabolism (*IDH1* and *IDH2*). Interestingly the selective differences we have identified also span both traditional oncogenes (*KRAS*) and traditional tumour suppressor genes (*TP53*). As a result of this diversity, it is likely that the selective differences identified here relate to a wide range of differences in biological function. Speculatively, it is possible that selective differences within *SMAD4* could relate to differential

DNA binding affinity of the encoded transcription factor, or that differences among *IDH1* and *IDH2* activity could relate to differences in metabolic enzymatic activity. Although the definitive identification of the biological explanation for these differences is beyond the scope of the current data, this will be important to assess in future work.

On a related point, the differences I have identified could reflect variation in the potential of the mutations in question to initiate disease, or alternately variation in the growth advantages conferred by these cells in established tumours. Interestingly, if there are differences in on-going growth advantages, then our data suggests that the forces of selection acting in tumours are often insufficient (or have insufficient temporal opportunity [Sottoriva et al., 2015]) to displace sub-optimal mutations, as less highly selected mutations remain detectable. For a limited number of driver genes, there is evidence to suggest that specific mutations correlate with disease outcomes [Margonis et al., 2015, Goh et al., 1995]. Further work is needed to clarify whether and to what extent the selective differences indicated here have prognostic and therapeutic implications.

In lung cancer, the *KRAS G12C* mutation provides a striking example of the potential for "alignment" of mutation and selection: the likelihood of the *KRAS G12C* mutation is increased by smoking, but in addition it is also selectively advantageous above other common *KRAS* mutations in the disease. The same is also true for *PIK3CA H1047R* mutations in stomach cancer, wherein MMR-associated processes increase the likelihood of the driver mutation, which is then subsequently strongly selected.

There are caveats to this analysis. First, I have used data from a number of sources, which may vary in terms of quality, depth of coverage and the pipeline used to call mutations. Secondly, I have relied on the assignment of signatures to individual samples and I note that some samples have relatively few mutations, making this assignment less accurate. Relatedly, in some cancer types, there are other active signatures that were not considered in this study. Where other signatures are present, the regression method used here can only approximate the signa-

ture contributions. Thirdly, some mutational signatures are similar to each other in composition, making it difficult to determine whether mutations are generated by one or more independent processes. I rely on assumptions of uniformity of a mutational process across the genomic loci considered, and over time. Finally, causal links between driver mutations and mutational processes are one explanation for the associations presented here, but other explanations cannot be ruled out from these data alone.

In summary, our framework quantifies the combined influence of both mutation and selection on shaping a cancer's driver mutation complement – and importantly emphasises that neither evolutionary force alone provides a sufficient explanation of the observed mutation distribution. In colon cancer for example, *BRAF* mutations (that are relatively uncommon) are mutationally unlikely, but are strongly selected. By contrast, *KRAS* drivers (that are more common), are mutationally much more likely, but are less highly selected. Our data also offer an explanation for the high frequency of driver *APC* mutations and relative paucity of driver *CTNNB1* mutations in the colon: *APC* mutations can be both more strongly selected and more mutationally likely than *CTNNB1* mutations.

Overall, our results begin to quantitatively delineate the distinct contributions of mutation and selection in shaping the spectra of driver mutations in the cancer genome.

Chapter 6

Discussion

Over the course of this thesis, I have presented results on both the timing and causation of mutations during cancer evolution, and have pointed to selective differences between key driver mutations. Here, I discuss the implications of these results for cancer surveillance and prevention, as well as the implications of the results for our wider understanding of the process of cancer evolution.

My findings on mutation timing have potential implications for tumour surveillance. I have argued that *POLE* mutations are early events in colorectal and endometrial cancers in which they occur somatically. CNAs, by contrast, appear to often occur in a cluster of late events (close to the last common ancestor of cancer cells) in colorectal cancer. The early occurrence of *POLE* mutations make them good candidates for surveillance programs, albeit the relatively small proportion of tumours in which these mutations are found must be taken into account. In terms of CNA mutations, our results suggest that there may be limited scope to assess progression towards colorectal cancer in terms of CNA accumulation, since the window of time before the last clonal expansion during which these changes are detectable is relatively narrow.

The results presented here also point to mechanisms of mutation causation that could be of relevance for cancer prevention. The results in Chapters 4 and 5 identify a key role for potentially modifiable alterations to the mutation rate in accumulation of driver mutations. Whereas, the results of Chapter 3 support the hypothesis that WGD events play an important role in the aetiology of colorectal

cancer, and motivate further research into the mechanisms of this type of change.

The differential selection results presented here are of interest for our wider understanding of cancer evolution. These results challenge the prevailing thinking on driver mutations and passenger mutations by demonstrating a spectrum of selective effects between driver mutations. Many previous studies have assumed a fixed selective impact among drivers [Beerenwinkel et al., 2007, Waclaw et al., 2015, McFarland et al., 2014]. Some studies have allowed for a distribution of effects, but have relied on indirect estimates for parameter estimation [Foo et al., 2015]. My results argue in favour of incorporating such distributions in future studies, and also point to possible parameterisations.

These analyses have some limitations. My results on timing and causation can be interpreted as describing the lineage of cells that eventually became the tumour. The population dynamics that describes interactions between cells (including lineages that did not survive to the final tumour) are difficult to access from the tumour-only data I have analysed in this thesis. Similarly, as alluded to in Chapter 5, further experiments are needed to interpret the results on differential selection in terms of cellular dynamics.

Some of the other results here are also informative about these population dynamics, but to a relatively limited extent. My analysis of CNA timing points to historic clonal expansions in copy-number-altered cells. Our analysis of breast cancer risk suggests that the population frequencies of stem and progenitor cells may vary over time in breast tissue. These results begin to reveal complex population dynamics involved in the growth of tumour populations, but, clearly, much remains to be done.

Cellular dynamics can be addressed in two ways. First, by directly sequencing and analysing normal and early-cancer tissue, intermediate lineages that would be lost in later samples can be directly analysed. Recent studies that measure mutation accumulation in normal tissue provide useful data in this regard [Martincorena et al., 2015, Blokzijl et al., 2016]. And it is likely that similar studies focusing on normal tissue dynamics will soon be-

come available (http://www.sanger.ac.uk/science/programmes/cancer-genetics-and-genomics). Secondly, theoretical considerations, and mathematical modelling approaches can be used to impute cellular dynamics in the current data using experimental evidence, similar to the approach in Chapter 2. Both these avenues are of potential interest for future work.

Recently, the longstanding theory of cancer causation by mutation has been challenged from multiple directions, which will also be important to bear in mind in future work. First, mounting evidence suggests that non-genetic factors influence cancer initiation and progression. The role of methylation of the *MLH1* gene in the aetiology of MSI cancers is an obvious example. The role of the immune system has been discussed above. Convincing evidence is emerging that the microbiome plays a role in sustaining tumour growth [Bullman et al., 2017]. These considerations highlight the increasing acceptance that a broad focus is required to understand the spectrum of factors that determine cancer risk, of which mutation processes are only a subset.

In conclusion, I have presented mathematical modelling results on the timing and causation of mutations during cancer evolution. I have analysed the selective differences between putative cancer mutations across cancers by controlling for mutation-causing processes using similar techniques. These results have potential implications for tumour prevention and surveillance. They also begin to shed light on the emerging complexity of the processes that shape tumour genome landscapes and play a role in tumour initiation and progression. In total, the work provides a contribution to the growing body of work on the forces that govern the course of tumour evolution.

Chapter 7

Methods

7.1 Standard Mutation Calling Pipeline

A large part of my work is based on analysis of sequencing data. Except where otherwise specified in the results, I followed the below steps to process DNA sequencing data and identify mutations.

7.1.1 Quality Control

Raw sequencing read data was received in either 'fastq' format. The FastQC software [Simon, 2010] was used to assess the data quality. This software calculates a range of relevant metrics, including the per base sequence quality.

Fastq files for each sample were analysed for quality with the with:

fastqc [sample.read1.fa] [sample.read2.fa]

7.1.2 Alignment and Preprocessing

The Burrows-Wheeler Aligner (BWA) [Heng and Durbin, 2009] was used to align read files against the 'hg19' human genome assembly. I used the BWA-MEM setting, which is based on the Smith-Waterman algorithm.

Read files were aligned using:

bwa mem -M -t 6 -R ucsc.hg19.fasta [sample.reads1.fasta] [sample.reads2.fasta]

to generate an aligned reads file in the 'bam' format.

The aligned reads were prepared for downstream analysis using the Picard software package [Broad, b]. The reads were sorted by coordinate using:

Picard SortSam INPUT = [sample.aligned.reads.bam] SORT_ORDER = coordinate VALIDATION_STRINGENCY = lenient

Duplicate reads were marked:

Picard MarkDuplicates INPUT = [sample.sorted.reads.bam] REMOVE_DUPLICATES = FALSE VALIDATION_STRINGENCY = lenient

A read index was created using:

Picard BuildBamIndex INPUT = [sample.dedup.reads.bam] VALIDATION_STRINGENCY = lenient

Where applicable reads from the same tumour or normal sample but different lanes were merged together.

7.1.3 Somatic Mutations

Somatic mutations were called using Mutect2 [Cibulskis et al., 2013] from the Genome Analysis Toolkit using [Broad, a]. Mutect identifies mutations by assessing the likelihood of mutation at each genomic site and controlling for false discovery rate. The software was run with filtration based on the dbsnp_138.hg19.vcf file:

7.1.4 Mutation context information used to identify mutation channel

The 96-channel context of each SNA was imputed using the R package 'SomaticSignatures' [Gehring et al., 2015].

GenomeAnalysisTK -T MuTect2 -R [ucsc.hg19.fasta] -I:tumor [tumor.sample.dedup.reads.bam] -I:normal [normal.sample.dedup.reads.bam] –dbsnp dbsnp_138.hg19.vcf

7.1.5 Copy Number Alterations

Copy number alterations were called using Sequenza. Sequenza uses a maximum-likelihood approach to infers cellularity and ploidy from paired tumour and normal sequencing data] [Favero et al., 2015]. Bam files were converted to the required 'seqz' format using:

sequenza-utils –fasta ucsc.hg19.fasta -t tumor.sample.dedup.reads.bam -n normal.sample.dedup.reads.bam -gc hg19.gc5Base.txt.gz

The sequenza analysis was run using:

sequenza.extract(window = 1e5, min.reads = 10, min.reads.normal = 10) sequenza.fit(segment.filter = 1e6) sequenza.results()

Appendix A

Supplementary Figures

Figure A.1: Evidence for differential selection between mutations in *KRAS*. Modelled Relative risk (RR) of frequent *KRAS* mutations compared to an informative reference mutation in each cancer type. For each mutation, the maximum likelihood estimate of relative risk compared is shown. Grey dashed line indicates relative risk of one. Error bars represent 95% confidence intervals obtained by bootstrapping across 100 iterations.

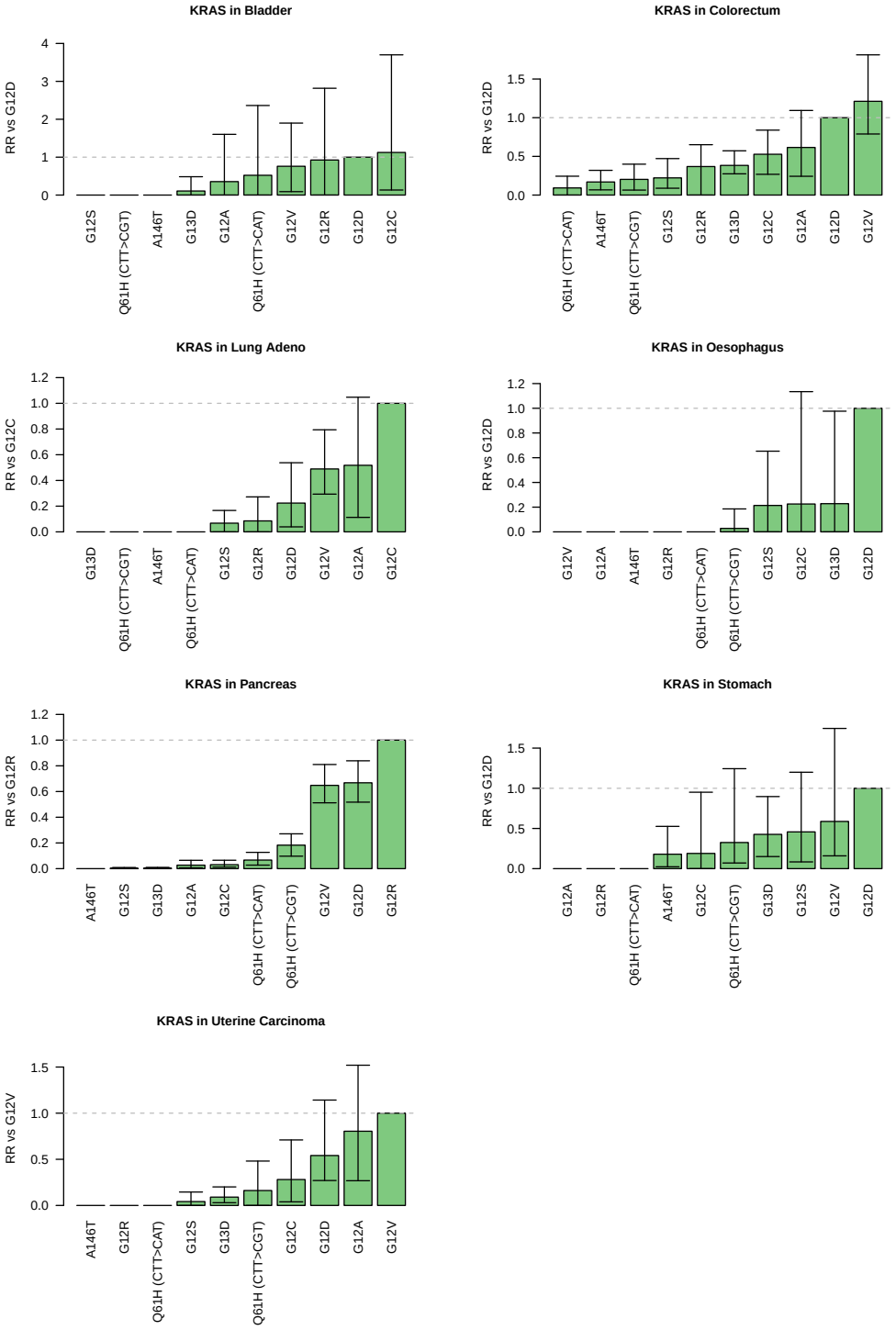

Figure A.2: Same as Figure A.1 for *BRAF* mutations.

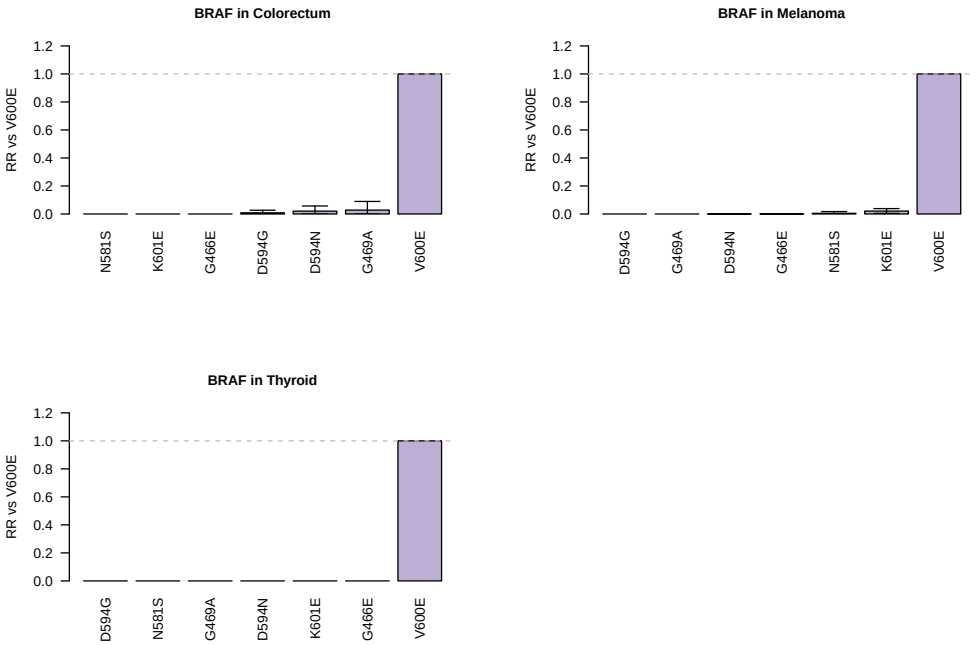

Figure A.3: Same as Figure A.1 for *NRAS* mutations.

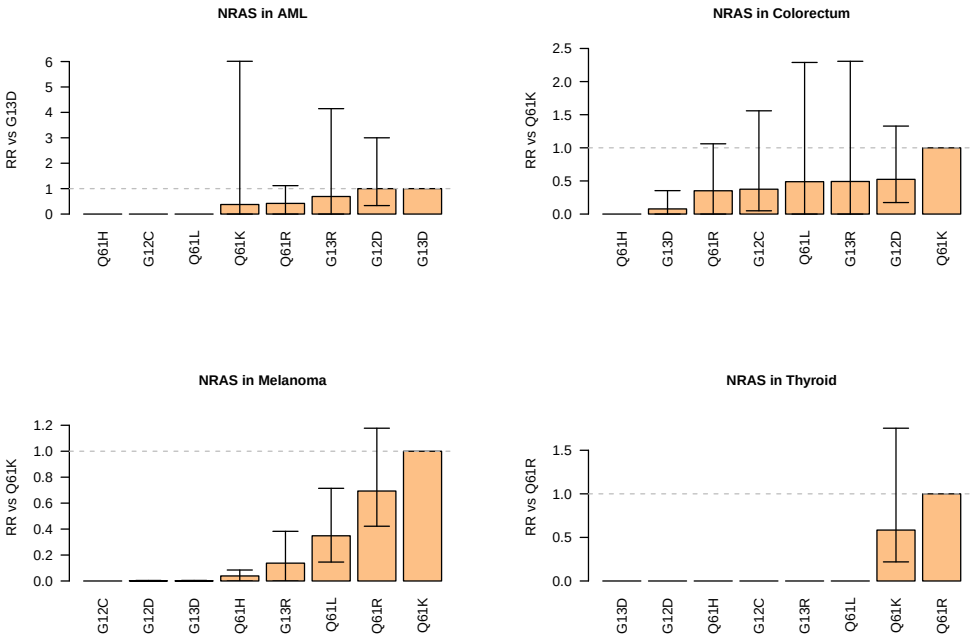

Figure A.4: Same as Figure A.1 for *IDH1* mutations.

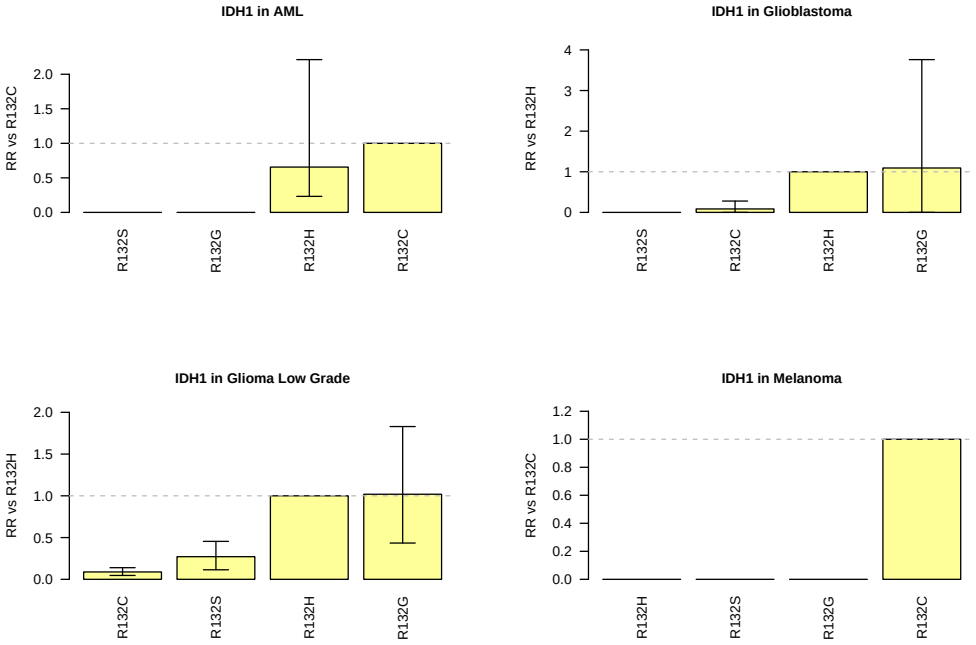

Figure A.5: Same as Figure A.1 for *IDH2* mutations.

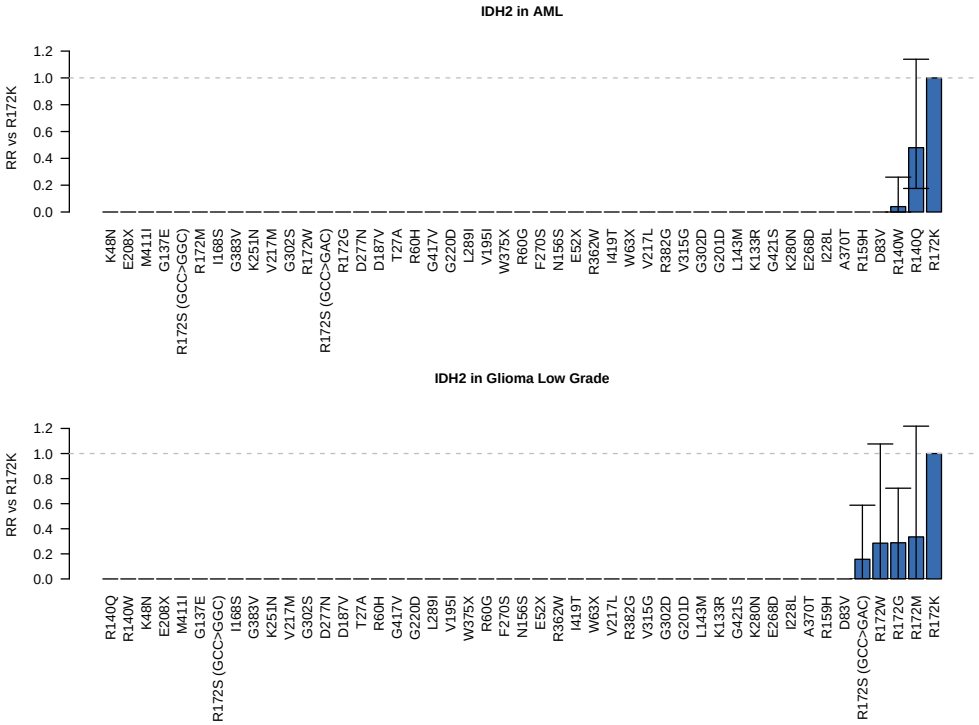

Figure A.6: Same as Figure A.1 for *TP53* mutations.

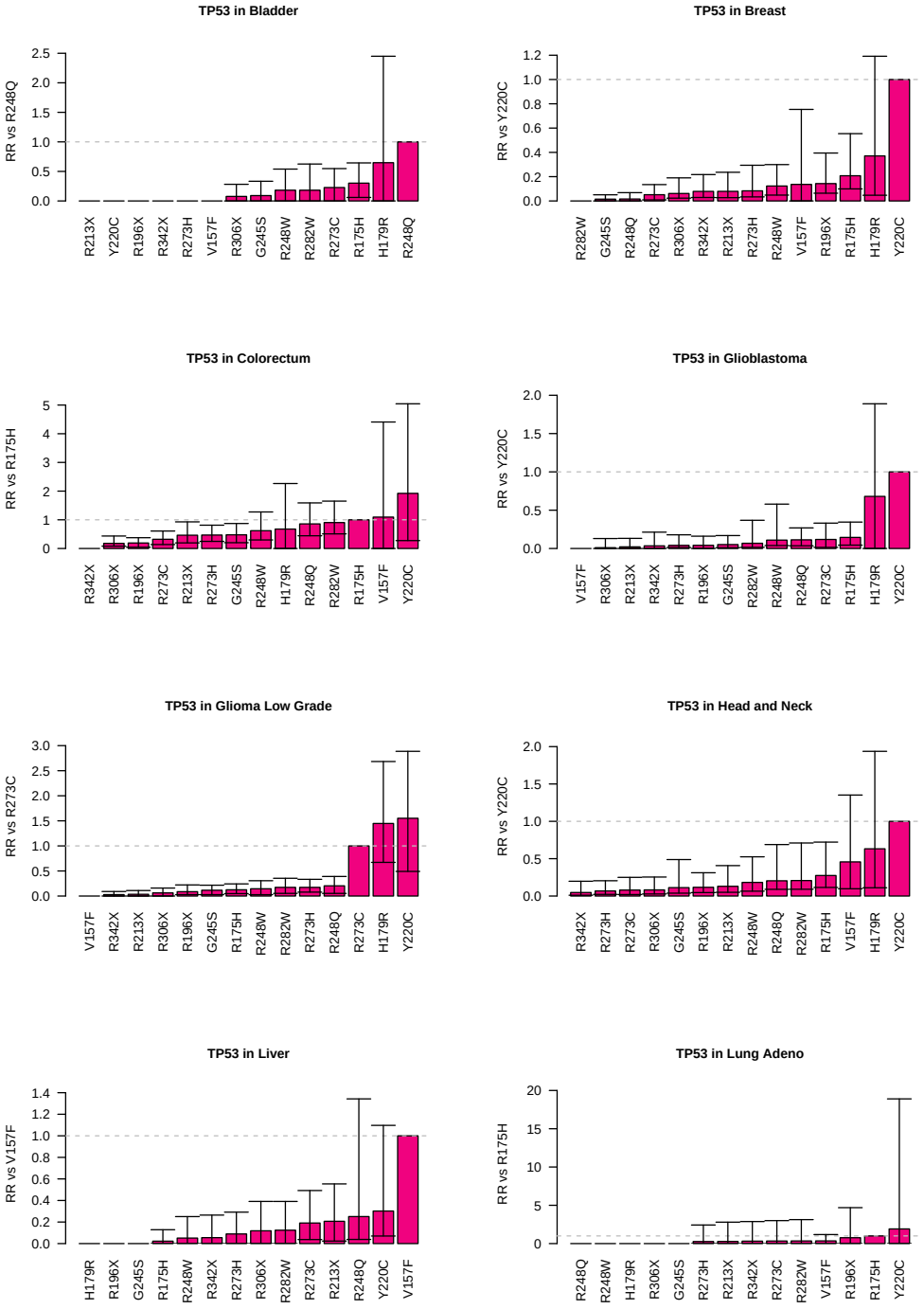

Figure A.7: Same as Figure A.1 for *TP53* mutations (continued).

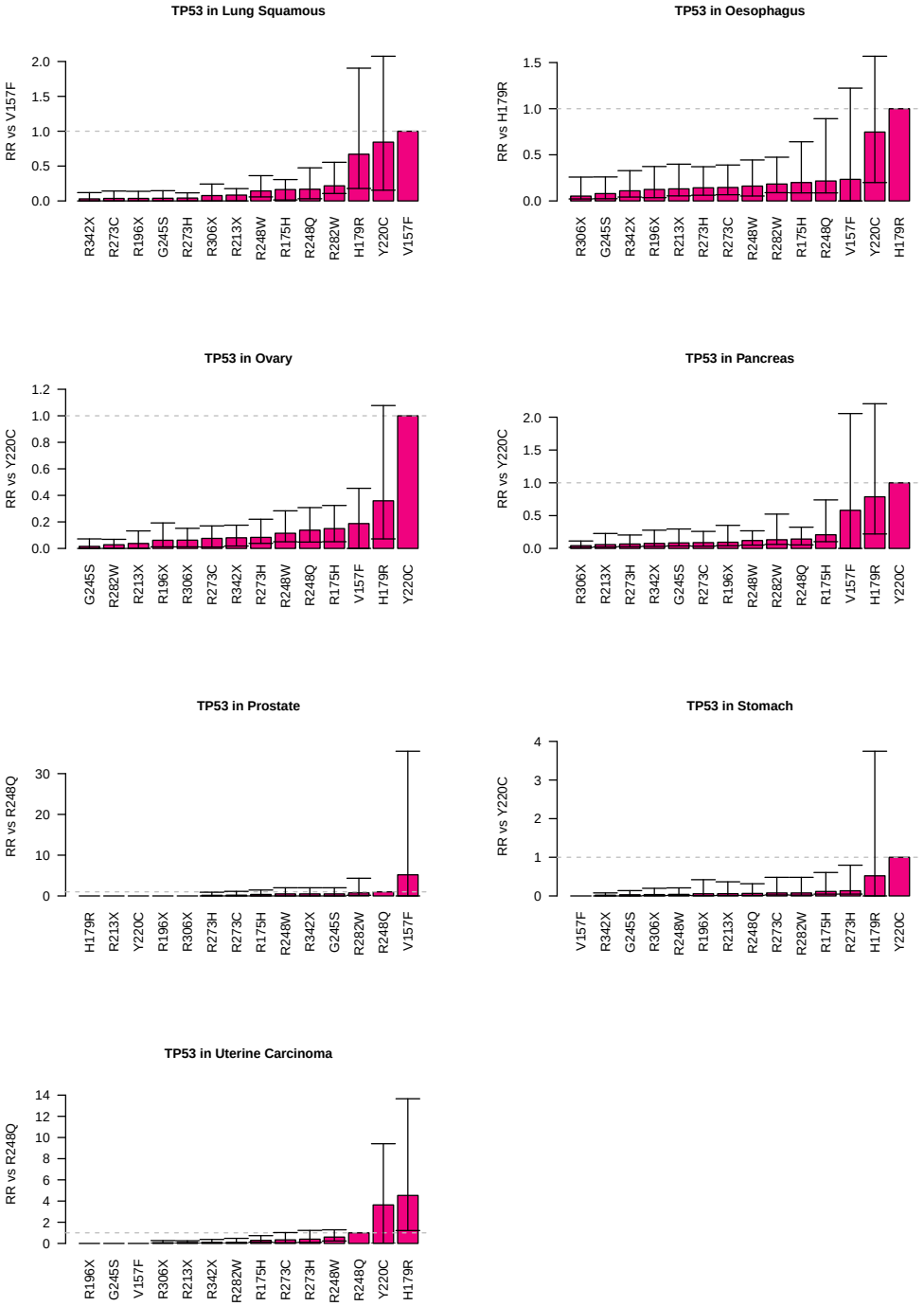

Figure A.8: Same as Figure A.1 for *PIK3CA* mutations.

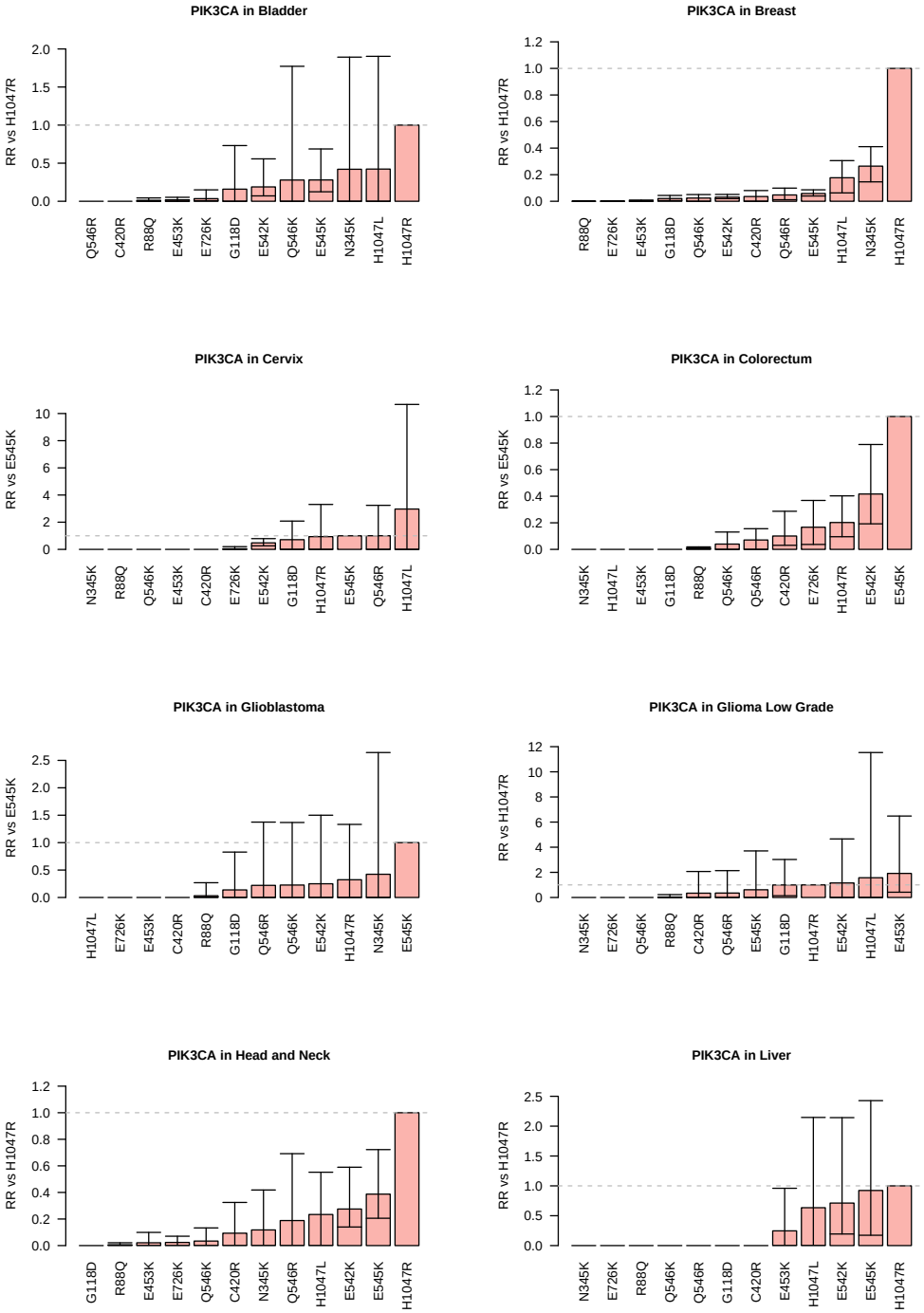

Figure A.9: Same as Figure A.1 for *PIK3CA* mutations (continued).

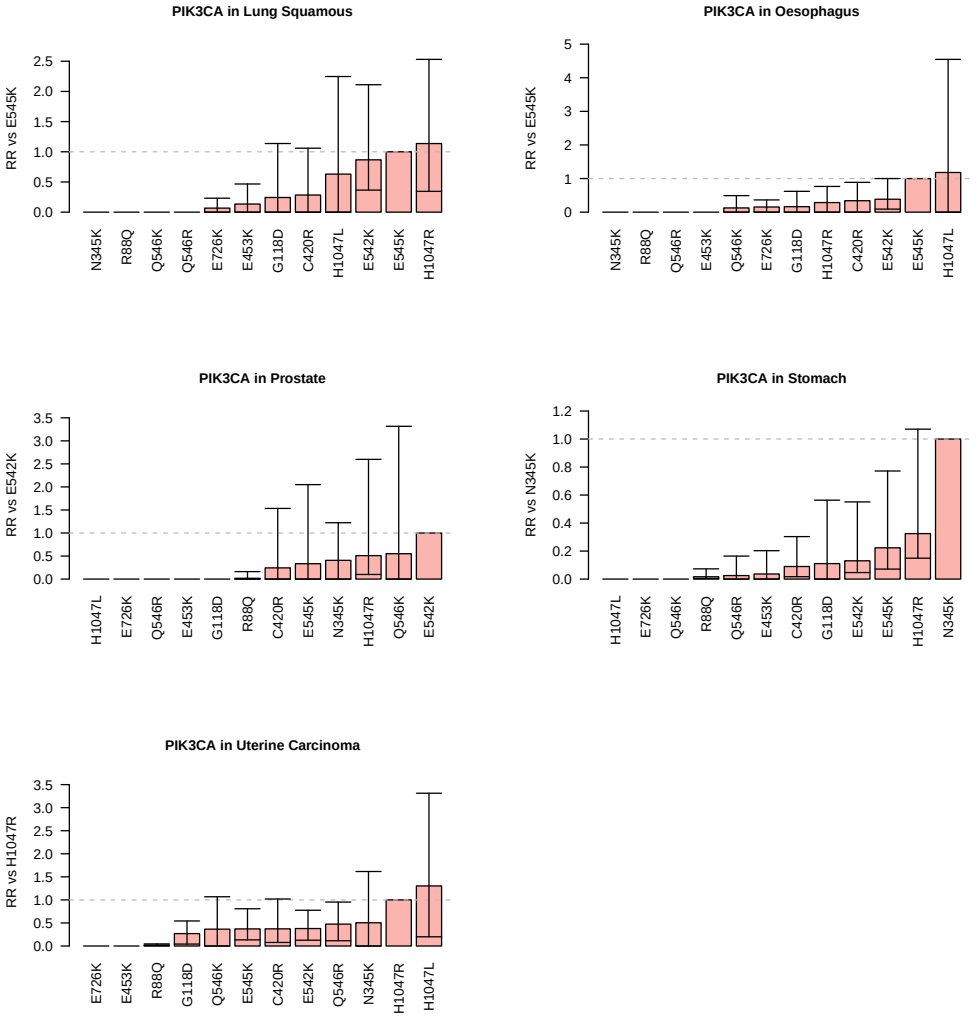

Figure A.10: Same as Figure A.1 for *SMAD4* mutations.

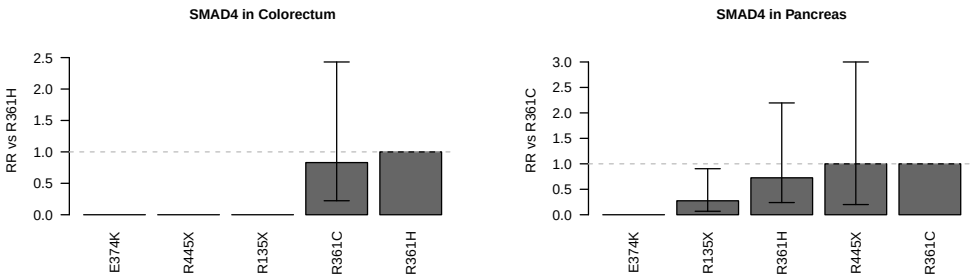

Figure A.11: Same as Figure A.1 for *CTNNB1* mutations.

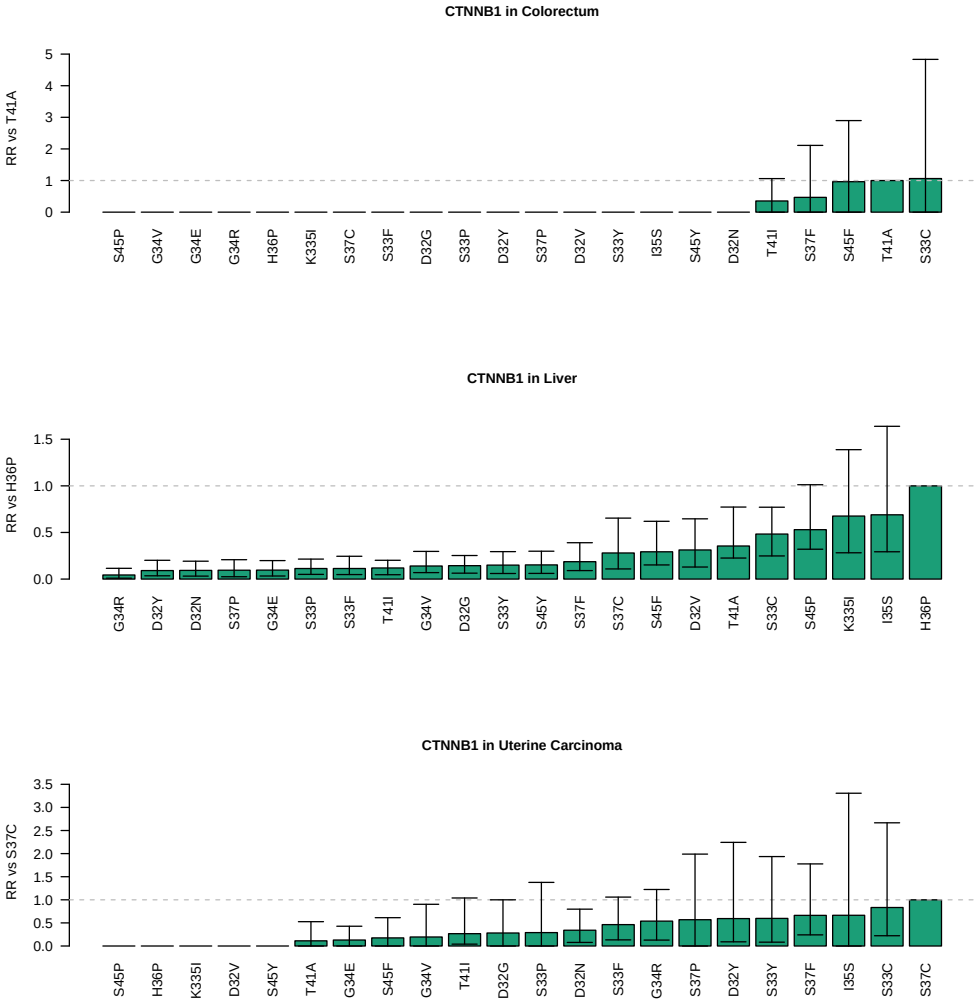

Figure A.12: Evidence for differential selection between mutations in *KRAS*, *BRAF* and *NRAS*. Modelled Relative risk (RR) of frequent *KRAS* mutations compared to an informative reference mutation in each cancer type. For each mutation, the maximum likelihood estimate of relative risk compared is shown. Grey dashed line indicates relative risk of one. Error bars represent 95% confidence intervals obtained by bootstrapping across 100 iterations.

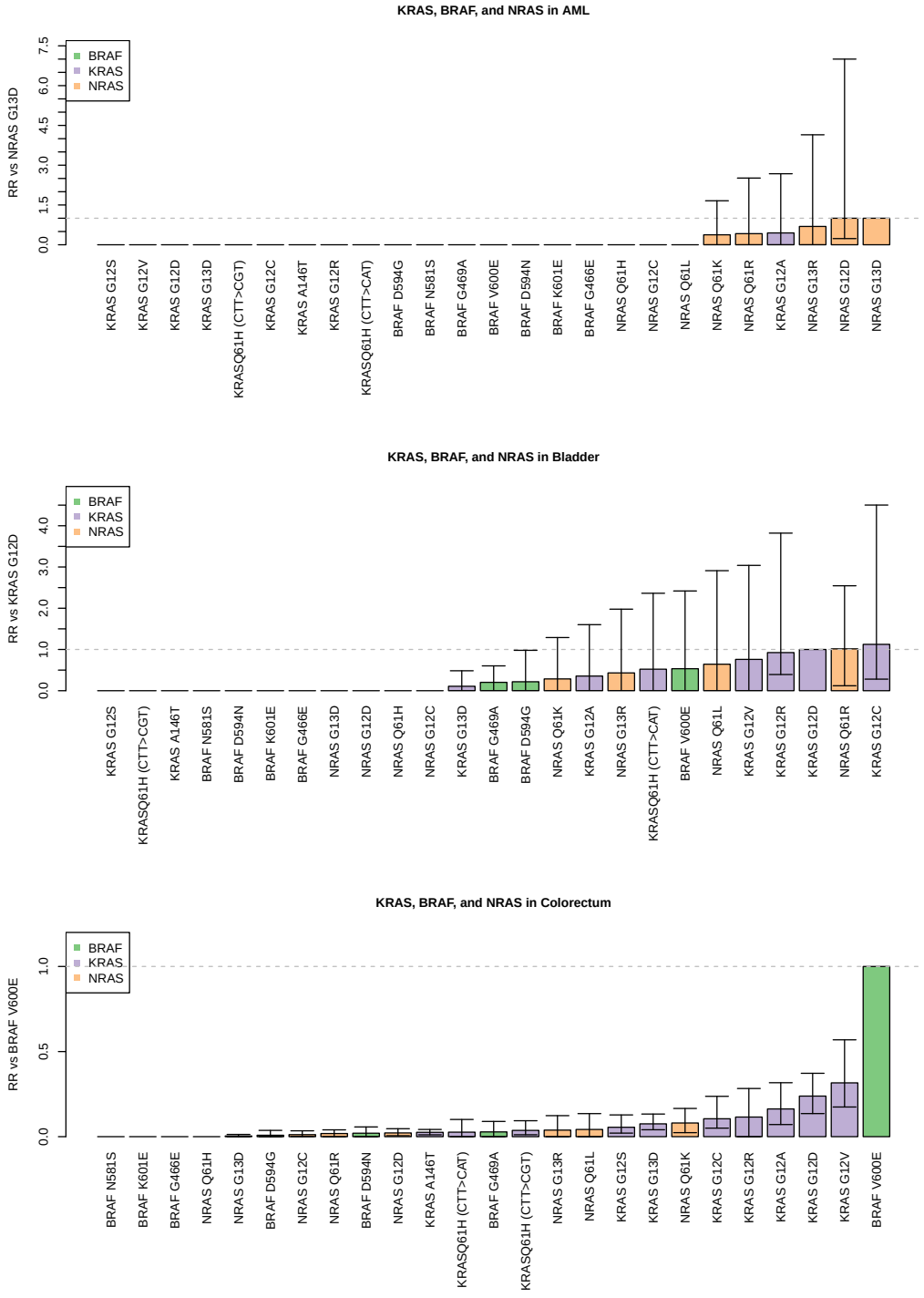

Figure A.13: Evidence for differential selection between mutations in *KRAS*, *BRAF* and *NRAS* (continued). Modelled Relative risk (RR) of frequent *KRAS* mutations compared to an informative reference mutation in each cancer type. For each mutation, the maximum likelihood estimate of relative risk compared is shown. Grey dashed line indicates relative risk of one. Error bars represent 95% confidence intervals obtained by bootstrapping across 100 iterations.

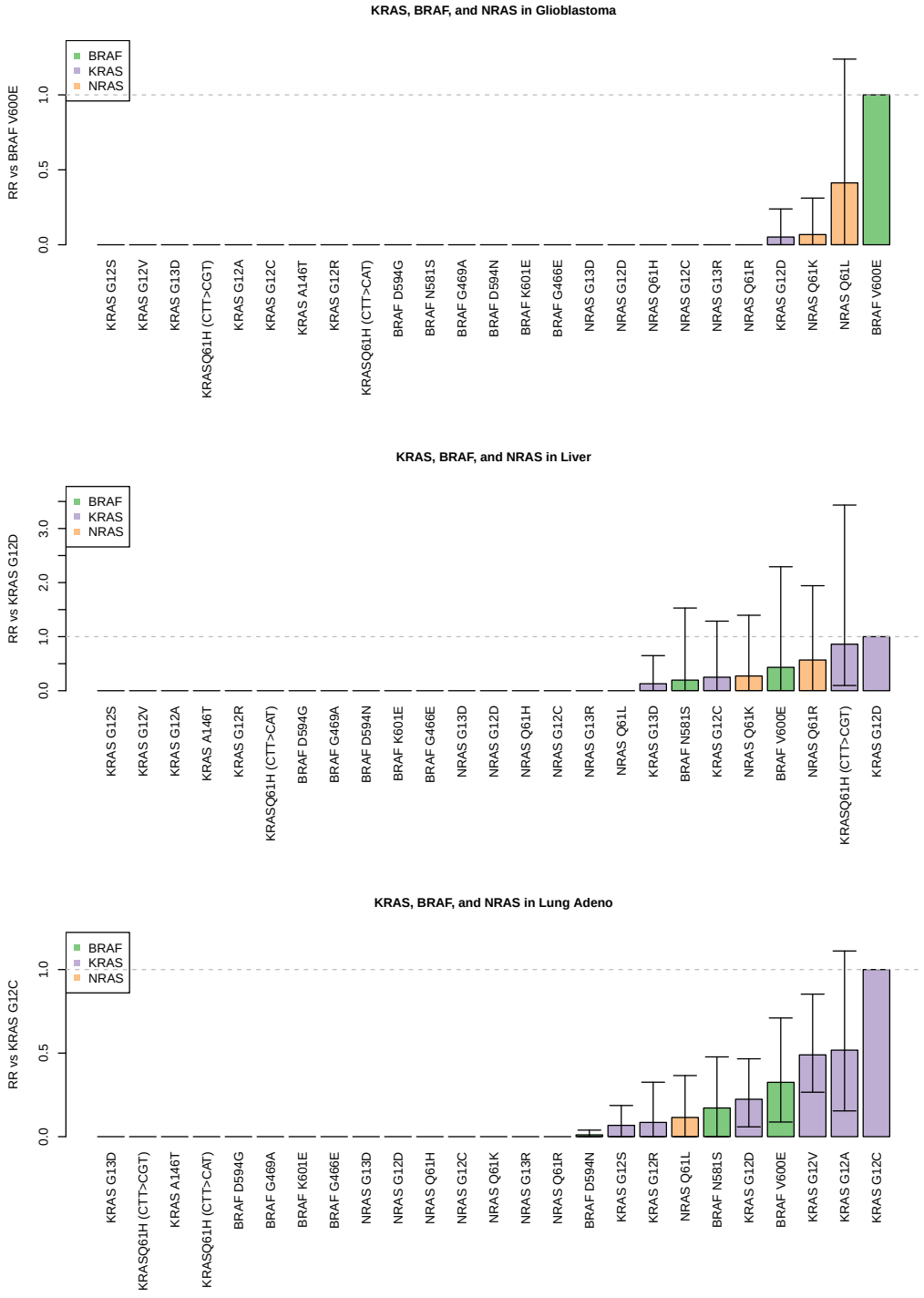

Figure A.14: Evidence for differential selection between mutations in *KRAS*, *BRAF* and *NRAS* (continued). Modelled Relative risk (RR) of frequent *KRAS* mutations compared to an informative reference mutation in each cancer type. For each mutation, the maximum likelihood estimate of relative risk compared is shown. Grey dashed line indicates relative risk of one. Error bars represent 95% confidence intervals obtained by bootstrapping across 100 iterations.

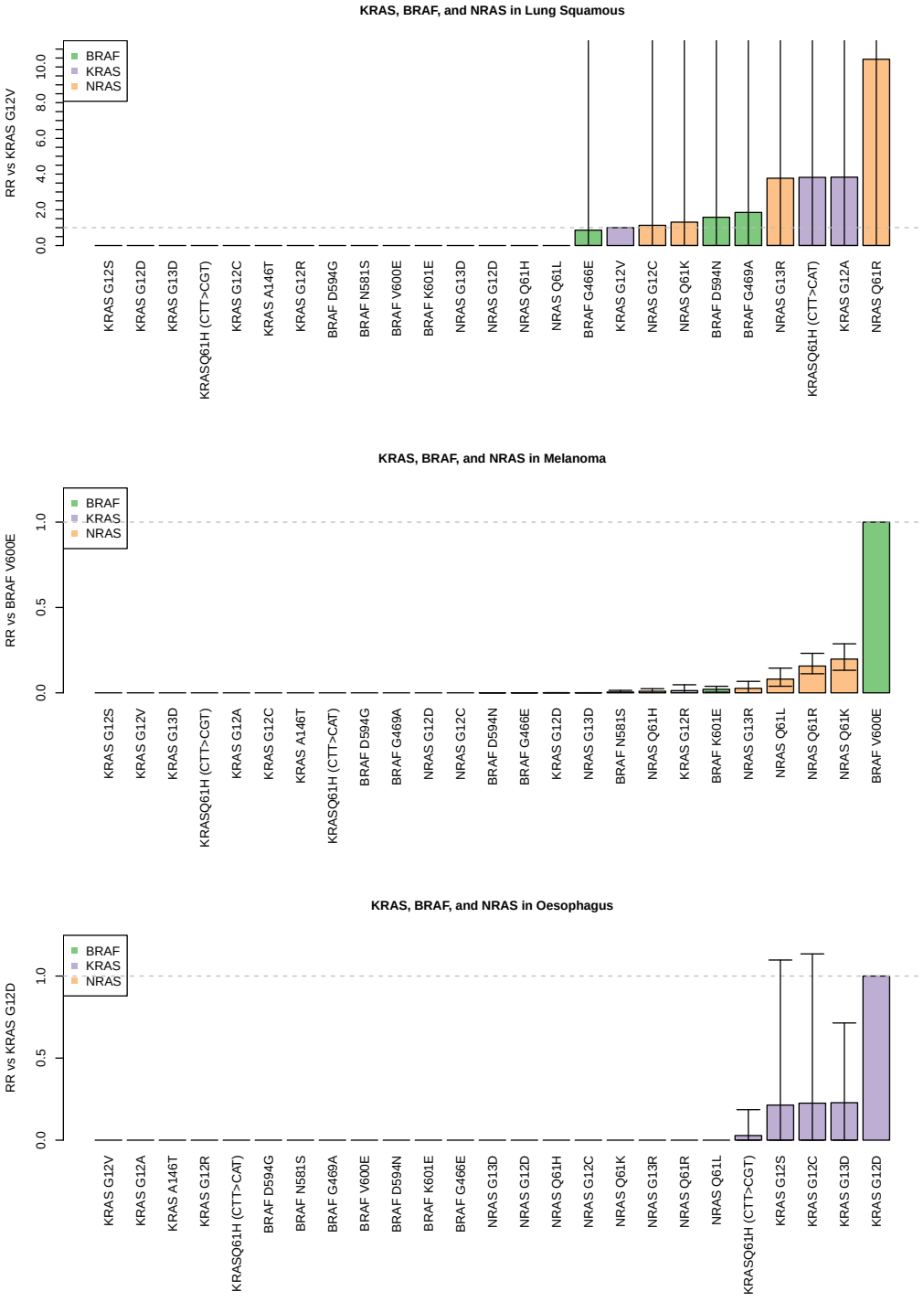

Figure A.15: Evidence for differential selection between mutations in *KRAS*, *BRAF* and *NRAS* (continued). Modelled Relative risk (RR) of frequent *KRAS* mutations compared to an informative reference mutation in each cancer type. For each mutation, the maximum likelihood estimate of relative risk compared is shown. Grey dashed line indicates relative risk of one. Error bars represent 95% confidence intervals obtained by bootstrapping across 100 iterations.

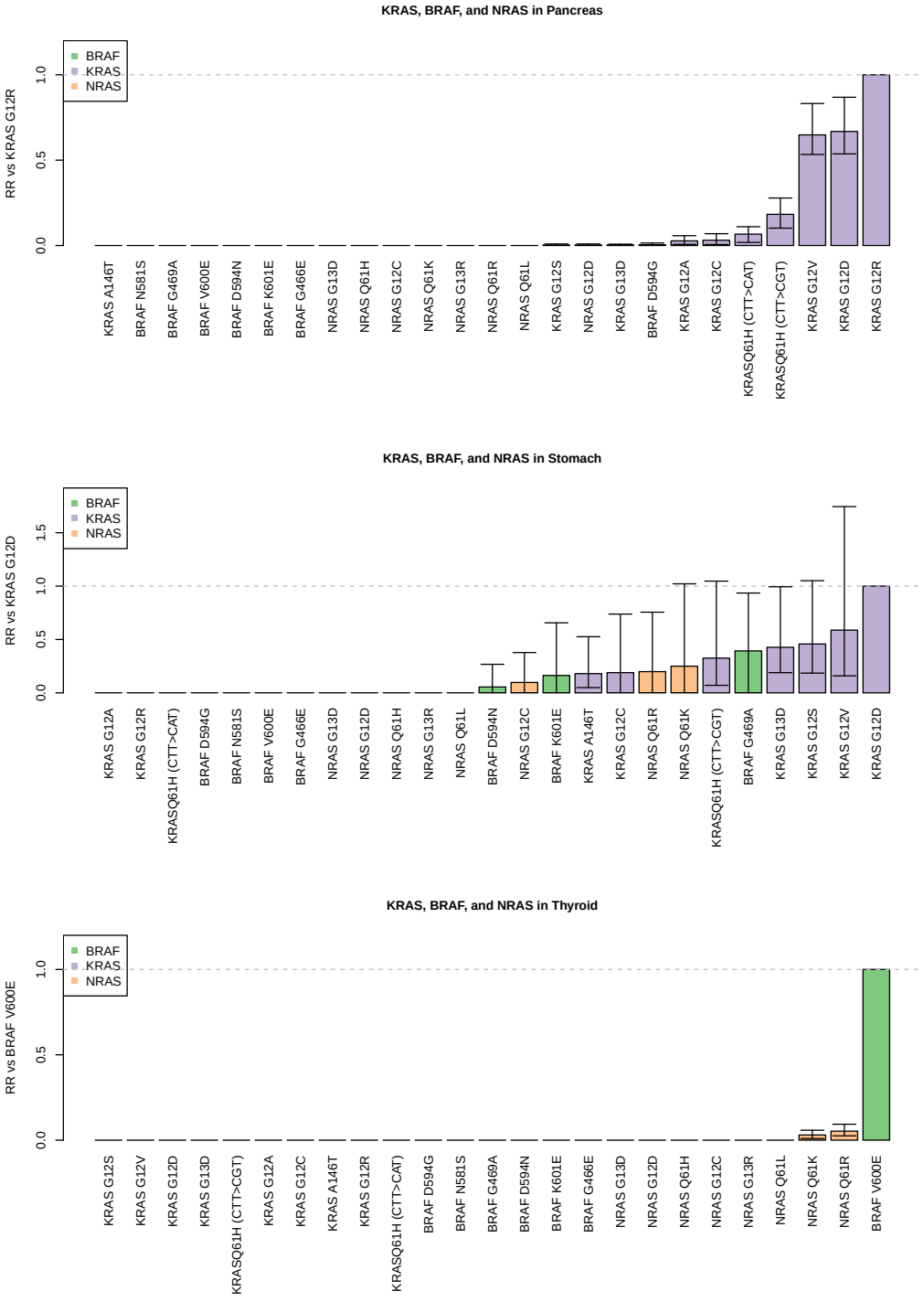

Figure A.16: Evidence for differential selection between mutations in *KRAS*, *BRAF* and *NRAS* (continued). Modelled Relative risk (RR) of frequent *KRAS* mutations compared to an informative reference mutation in each cancer type. For each mutation, the maximum likelihood estimate of relative risk compared is shown. Grey dashed line indicates relative risk of one. Error bars represent 95% confidence intervals obtained by bootstrapping across 100 iterations.

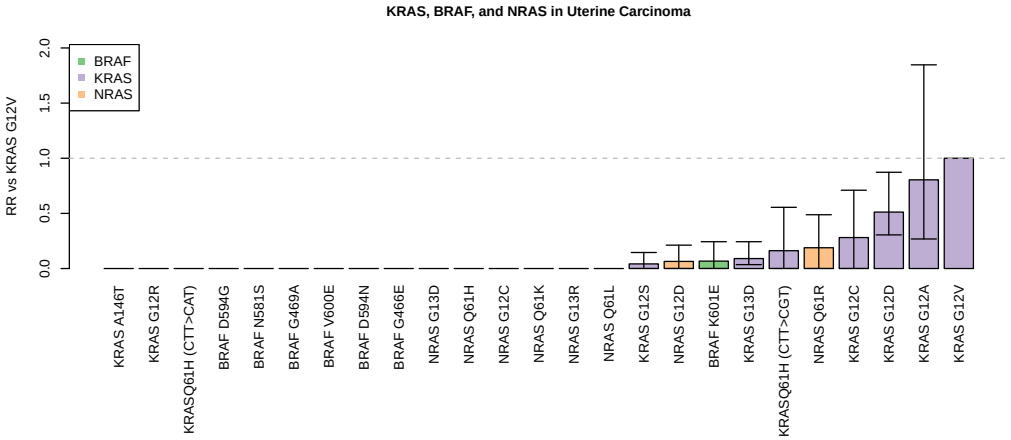

Figure A.17: Same as Figure A.12 for *APC* and *CTNNB1* mutations

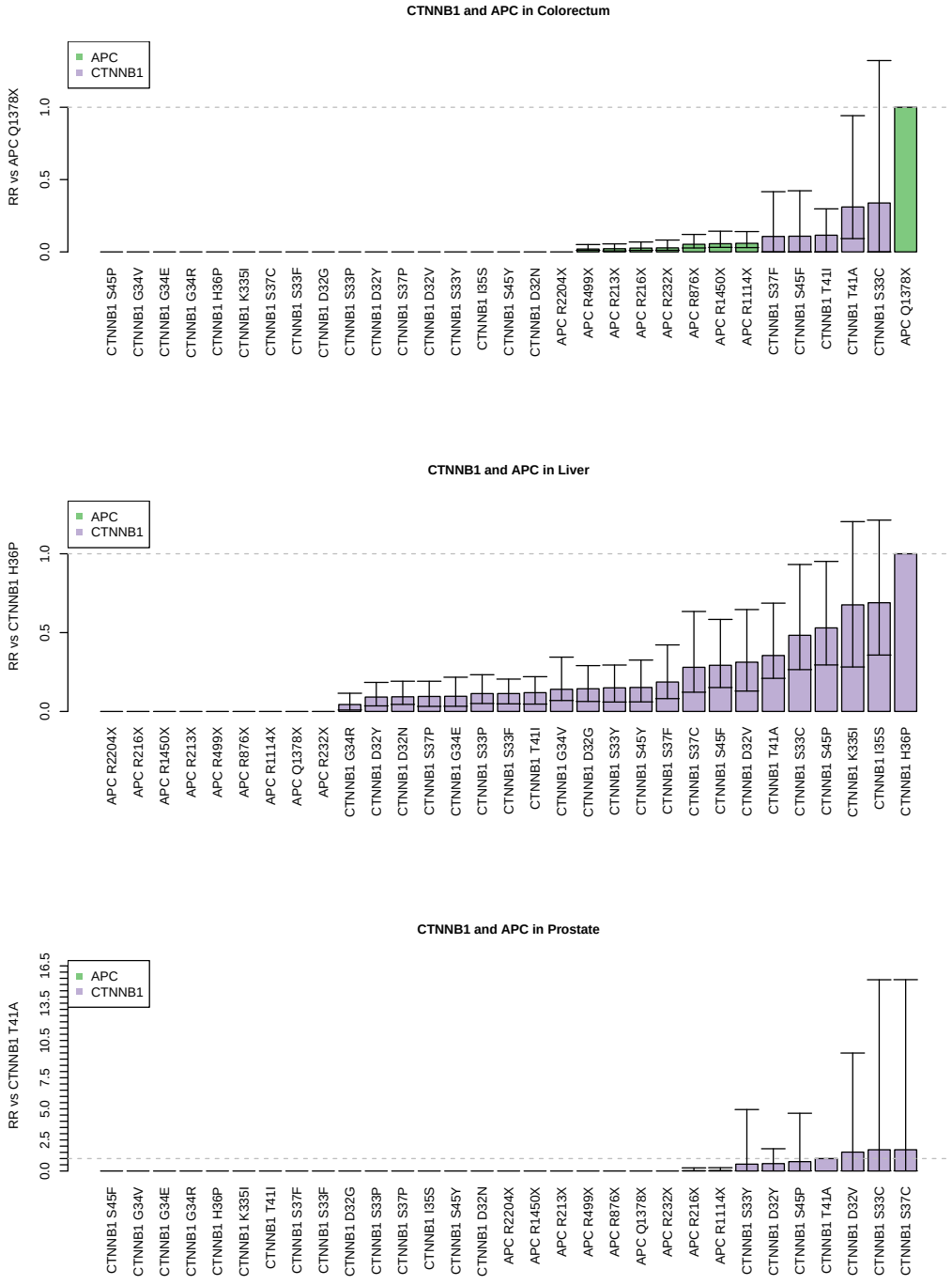

Figure A.18: Same as Figure A.12 for *APC* and *CTNNB1* mutations (continued)

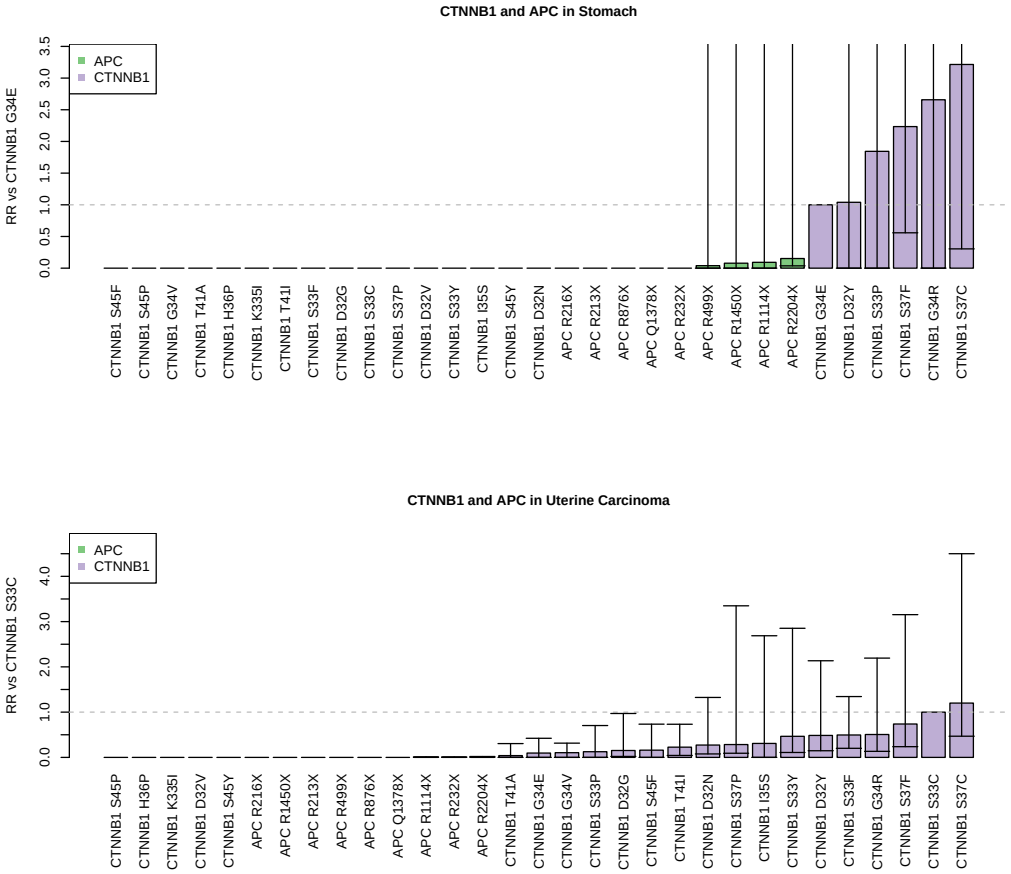

Figure A.19: Same as Figure A.12 for *IDH1* and *IDH2* mutations

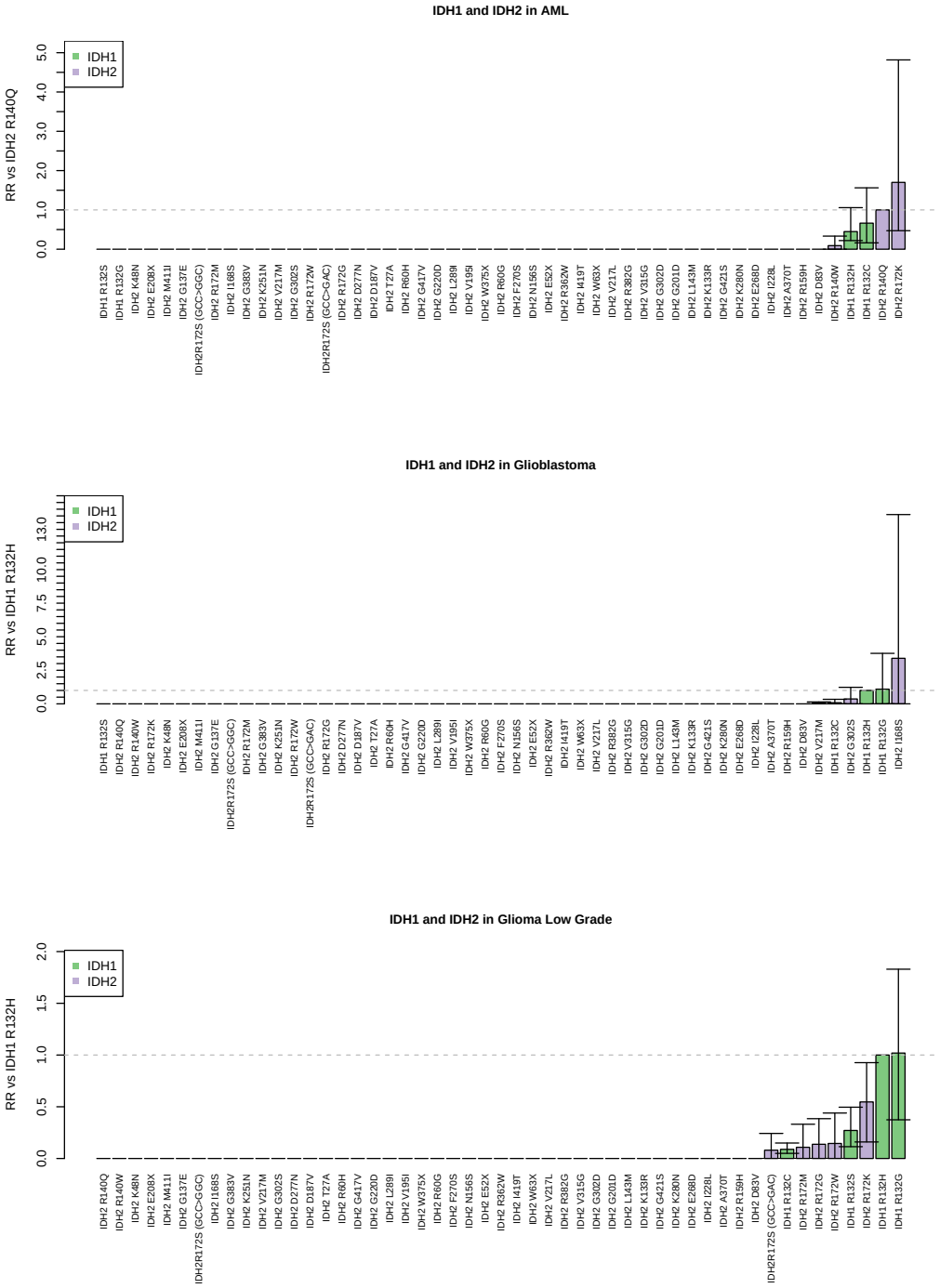

Figure A.20: Same as Figure A.12 for *IDH1* and *IDH2* mutations (continued)

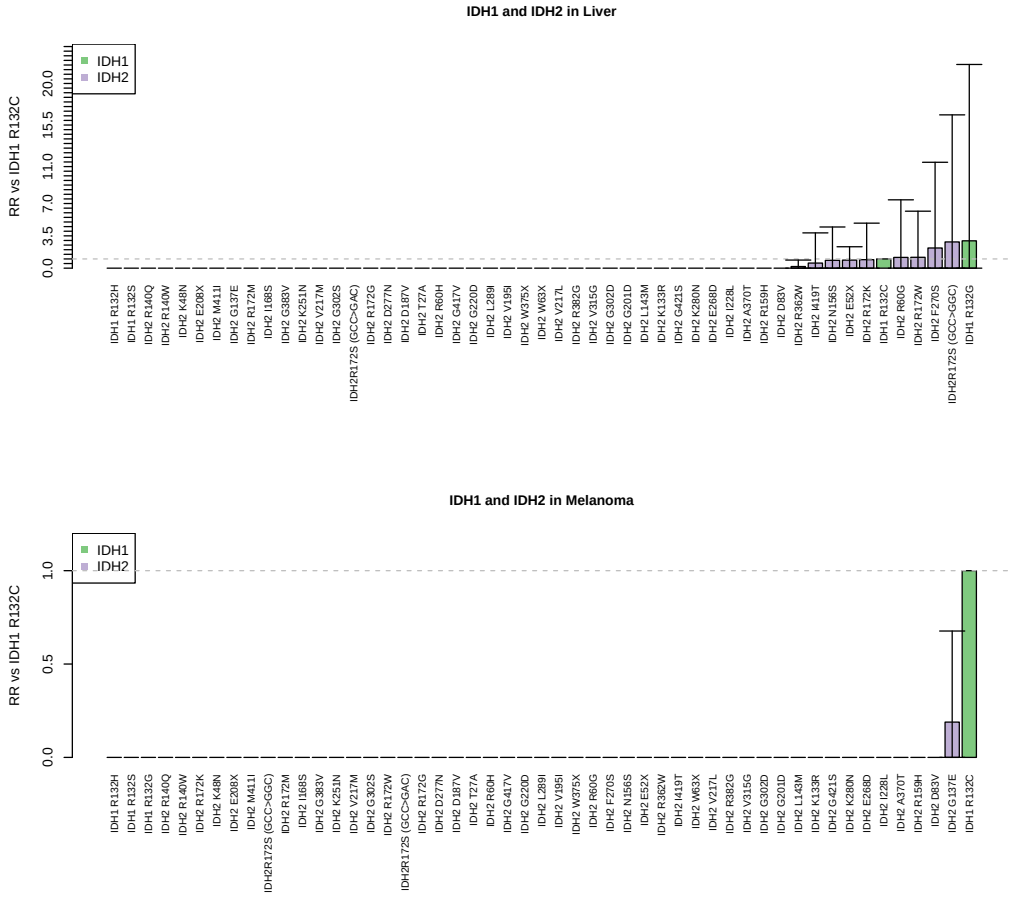

Appendix B

Colophon

This document was set in the Times Roman typeface using LaTeX and BibTeX, composed with a text editor.

Bibliography

[TCG, 2012] (2012). Comprehensive molecular characterization of human colon and rectal cancer. *Nature*, 487(7407):330–7.

[Abbosh et al., 2017] Abbosh, C., Birkbak, N. J., Wilson, G. A., Jamal-Hanjani, M., Constantin, T., Salari, R., Le Quesne, J., Moore, D. A., Veeriah, S., Rosenthal, R., Marafioti, T., Kirkizlar, E., Watkins, T. B. K., McGranahan, N., Ward, S., Martinson, L., Riley, J., Fraioli, F., Al Bakir, M., Gronroos, E., Zambrana, F., Endozo, R., Bi, W. L., Fennessy, F. M., Sponer, N., Johnson, D., Laycock, J., Shafi, S., Czyzewska-Khan, J., Rowan, A., Chambers, T., Matthews, N., Turajlic, S., Hiley, C., Lee, S. M., Forster, M. D., Ahmad, T., Falzon, M., Borg, E., Lawrence, D., Hayward, M., Kolvekar, S., Panagiotopoulos, N., Janes, S. M., Thakrar, R., Ahmed, A., Blackhall, F., Summers, Y., Hafez, D., Naik, A., Ganguly, A., Kareht, S., Shah, R., Joseph, L., Marie Quinn, A., Crosbie, P. A., Naidu, B., Middleton, G., Langman, G., Trotter, S., Nicolson, M., Remmen, H., Kerr, K., Chetty, M., Gomersall, L., Fennell, D. A., Nakas, A., Rathinam, S., Anand, G., Khan, S., Russell, P., Ezhil, V., Ismail, B., Irvin-Sellers, M., Prakash, V., Lester, J. F., Kornaszewska, M., Attanoos, R., Adams, H., Davies, H., Oukrif, D., Akarca, A. U., Hartley, J. A., Lowe, H. L., Lock, S., Iles, N., Bell, H., Ngai, Y., Elgar, G., Szallasi, Z., Schwarz, R. F., Herrero, J., Stewart, A., Quezada, S. A., Peggs, K. S., Van Loo, P., Dive, C., Lin, C. J., Rabinowitz, M., Aerts, H., et al. (2017). Phylogenetic ctdna analysis depicts early-stage lung cancer evolution. *Nature*, 545(7655):446–451.

[Abou-Elhamd and Habib, 2007] Abou-Elhamd, K. E. and Habib, T. N. (2007).

The flow cytometric analysis of premalignant and malignant lesions in head and neck squamous cell carcinoma. *Oral Oncol*, 43(4):366–72.

[Albrektsen et al., 2005] Albrektsen, G., Heuch, I., Hansen, S., and Kvale, G. (2005). Breast cancer risk by age at birth, time since birth and time intervals between births: exploring interaction effects. *Br J Cancer*, 92(1):167–75.

[Alexandrov et al., 2015] Alexandrov, L. B., Jones, P. H., Wedge, D. C., Sale, J. E., Campbell, P. J., Nik-Zainal, S., and Stratton, M. R. (2015). Clock-like mutational processes in human somatic cells. *Nat Genet*, 47(12):1402–7.

[Alexandrov et al., 2013a] Alexandrov, L. B., Nik-Zainal, S., Wedge, D. C., Aparicio, S. A., Behjati, S., Biankin, A. V., Bignell, G. R., Bolli, N., Borg, A., Borresen-Dale, A. L., Boyault, S., Burkhardt, B., Butler, A. P., Caldas, C., Davies, H. R., Desmedt, C., Eils, R., Eyfjord, J. E., Foekens, J. A., Greaves, M., Hosoda, F., Hutter, B., Ilicic, T., Imbeaud, S., Imielinski, M., Jager, N., Jones, D. T., Jones, D., Knappskog, S., Kool, M., Lakhani, S. R., Lopez-Otin, C., Martin, S., Munshi, N. C., Nakamura, H., Northcott, P. A., Pajic, M., Papaemmanuil, E., Paradiso, A., Pearson, J. V., Puente, X. S., Raine, K., Ramakrishna, M., Richardson, A. L., Richter, J., Rosenstiel, P., Schlesner, M., Schumacher, T. N., Span, P. N., Teague, J. W., Totoki, Y., Tutt, A. N., Valdes-Mas, R., van Buuren, M. M., van 't Veer, L., Vincent-Salomon, A., Waddell, N., Yates, L. R., Zucman-Rossi, J., Futreal, P. A., McDermott, U., Lichter, P., Meyerson, M., Grimmond, S. M., Siebert, R., Campo, E., Shibata, T., Pfister, S. M., Campbell, P. J., and Stratton, M. R. (2013a). Signatures of mutational processes in human cancer. *Nature*, 500(7463):415–21.

[Alexandrov et al., 2013b] Alexandrov, L. B., Nik-Zainal, S., Wedge, D. C., Campbell, P. J., and Stratton, M. R. (2013b). Deciphering signatures of mutational processes operative in human cancer. *Cell Rep*, 3(1):246–59.

[Anderson et al., 1989] Anderson, T. J., Battersby, S., King, R. J., McPherson, K., and Going, J. J. (1989). Oral contraceptive use influences resting breast proliferation. *Hum Pathol*, 20(12):1139–44.

[Andor et al., 2016] Andor, N., Graham, T. A., Jansen, M., Xia, L. C., Aktipis, C. A., Petritsch, C., Ji, H. P., and Maley, C. C. (2016). Pan-cancer analysis of the extent and consequences of intratumor heterogeneity. *Nat Med*, 22(1):105–13.

[Armitage and Doll, 1954] Armitage, P. and Doll, R. (1954). The age distribution of cancer and a multi-stage theory of carcinogenesis. *Br J Cancer*, 8(1):1–12.

[Asatryan and Komarova, 2016] Asatryan, A. D. and Komarova, N. L. (2016). Evolution of genetic instability in heterogeneous tumors. *J Theor Biol*, 396:1–12.

[Baca et al., 2013] Baca, S. C., Prandi, D., Lawrence, M. S., Mosquera, J. M., Romanel, A., Drier, Y., Park, K., Kitabayashi, N., MacDonald, T. Y., Ghandi, M., Van Allen, E., Kryukov, G. V., Sboner, A., Theurillat, J. P., Soong, T. D., Nickerson, E., Auclair, D., Tewari, A., Beltran, H., Onofrio, R. C., Boysen, G., Guiducci, C., Barbieri, C. E., Cibulskis, K., Sivachenko, A., Carter, S. L., Saksena, G., Voet, D., Ramos, A. H., Winckler, W., Cipicchio, M., Ardlie, K., Kantoff, P. W., Berger, M. F., Gabriel, S. B., Golub, T. R., Meyerson, M., Lander, E. S., Elemento, O., Getz, G., Demichelis, F., Rubin, M. A., and Garraway, L. A. (2013). Punctuated evolution of prostate cancer genomes. *Cell*, 153(3):666–77.

[Beckman and Loeb, 2006] Beckman, R. A. and Loeb, L. A. (2006). Efficiency of carcinogenesis with and without a mutator mutation. *Proc Natl Acad Sci U S A*, 103(38):14140–5.

[Beerenwinkel et al., 2007] Beerenwinkel, N., Antal, T., Dingli, D., Traulsen, A., Kinzler, K. W., Velculescu, V. E., Vogelstein, B., and Nowak, M. A. (2007). Genetic progression and the waiting time to cancer. *PLoS Comput Biol*, 3(11):e225.

[Ben-David et al., 2017] Ben-David, U., Ha, G., Tseng, Y. Y., Greenwald, N. F., Oh, C., Shih, J., McFarland, J. M., Wong, B., Boehm, J. S., Beroukhim, R., and

Golub, T. R. (2017). Patient-derived xenografts undergo mouse-specific tumor evolution. *Nat Genet*, 49(11):1567–1575.

[Billingsley et al., 2015] Billingsley, C. C., Cohn, D. E., Mutch, D. G., Stephens, J. A., Suarez, A. A., and Goodfellow, P. J. (2015). Polymerase varepsilon (pole) mutations in endometrial cancer: clinical outcomes and implications for lynch syndrome testing. *Cancer*, 121(3):386–94.

[Birkbak et al., 2011] Birkbak, N. J., Eklund, A. C., Li, Q., McClelland, S. E., Endesfelder, D., Tan, P., Tan, I. B., Richardson, A. L., Szallasi, Z., and Swanton, C. (2011). Paradoxical relationship between chromosomal instability and survival outcome in cancer. *Cancer Res*, 71(10):3447–52.

[Blokzijl et al., 2016] Blokzijl, F., de Ligt, J., Jager, M., Sasselli, V., Roerink, S., Sasaki, N., Huch, M., Boymans, S., Kuijk, E., Prins, P., Nijman, I. J., Martincorena, I., Mokry, M., Wiegerinck, C. L., Middendorp, S., Sato, T., Schwank, G., Nieuwenhuis, E. E., Verstegen, M. M., van der Laan, L. J., de Jonge, J., JN, I. J., Vries, R. G., van de Wetering, M., Stratton, M. R., Clevers, H., Cuppen, E., and van Boxtel, R. (2016). Tissue-specific mutation accumulation in human adult stem cells during life. *Nature*, 538(7624):260–264.

[Bozic et al., 2010] Bozic, I., Antal, T., Ohtsuki, H., Carter, H., Kim, D., Chen, S., Karchin, R., Kinzler, K. W., Vogelstein, B., and Nowak, M. A. (2010). Accumulation of driver and passenger mutations during tumor progression. *Proc Natl Acad Sci U S A*, 107(43):18545–50.

[Bresciani, 1968] Bresciani, F. (1968). Cell proliferation in cancer. *Eur J Cancer*, 4(4):343–66.

[Briggs and Tomlinson, 2013] Briggs, S. and Tomlinson, I. (2013). Germline and somatic polymerase epsilon and delta mutations define a new class of hypermutated colorectal and endometrial cancers. *J Pathol*, 230(2):148–53.

[Broad, a] Broad. Genome analysis toolkit: Variant discovery in high-throughput sequencing data.

[Broad, b] Broad. Picard: A set of command line tools (in java) for manipulating high-throughput sequencing (hts) data and formats such as sam/bam/cram and vcf.

[Brown et al., 2014] Brown, S. D., Warren, R. L., Gibb, E. A., Martin, S. D., Spinelli, J. J., Nelson, B. H., and Holt, R. A. (2014). Neo-antigens predicted by tumor genome meta-analysis correlate with increased patient survival. *Genome Res*, 24(5):743–50.

[Bullman et al., 2017] Bullman, S., Pedamallu, C. S., Sicinska, E., Clancy, T. E., Zhang, X., Cai, D., Neuberg, D., Huang, K., Guevara, F., Nelson, T., Chipashvili, O., Hagan, T., Walker, M., Ramachandran, A., Diosdado, B., Serna, G., Mulet, N., Landolfi, S., Ramon, Y. C. S., Fasani, R., Aguirre, A. J., Ng, K., Elez, E., Ogino, S., Tabernero, J., Fuchs, C. S., Hahn, W. C., Nuciforo, P., and Meyerson, M. (2017). Analysis of fusobacterium persistence and antibiotic response in colorectal cancer. *Science*, 358(6369):1443–1448.

[Cabrera et al., 2014] Cabrera, S. M., Bright, G. M., Frane, J. W., Blethen, S. L., and Lee, P. A. (2014). Age of thelarche and menarche in contemporary us females: a cross-sectional analysis. *J Pediatr Endocrinol Metab*, 27(1-2):47–51.

[Campbell et al., 2017] Campbell, B. B., Light, N., Fabrizio, D., Zatzman, M., Fuligni, F., de Borja, R., Davidson, S., Edwards, M., Elvin, J. A., Hodel, K. P., Zahurancik, W. J., Suo, Z., Lipman, T., Wimmer, K., Kratz, C. P., Bowers, D. C., Laetsch, T. W., Dunn, G. P., Johanns, T. M., Grimmer, M. R., Smirnov, I. V., Larouche, V., Samuel, D., Bronsema, A., Osborn, M., Stearns, D., Raman, P., Cole, K. A., Storm, P. B., Yalon, M., Opocher, E., Mason, G., Thomas, G. A., Sabel, M., George, B., Ziegler, D. S., Lindhorst, S., Issai, V. M., Constantini, S., Toledano, H., Elhasid, R., Farah, R., Dvir, R., Dirks, P., Huang, A., Galati, M. A., Chung, J., Ramaswamy, V., Irwin, M. S., Aronson, M., Durno, C., Taylor, M. D., Rechavi, G., Maris, J. M., Bouffet, E., Hawkins, C., Costello, J. F., Meyn, M. S., Pursell, Z. F., Malkin, D., Tabori, U., and Shlien, A. (2017). Comprehensive analysis of hypermutation in human cancer. *Cell*, 171(5):1042–1056 e10.

[Carter et al., 2012] Carter, S. L., Cibulskis, K., Helman, E., McKenna, A., Shen, H., Zack, T., Laird, P. W., Onofrio, R. C., Winckler, W., Weir, B. A., Beroukhim, R., Pellman, D., Levine, D. A., Lander, E. S., Meyerson, M., and Getz, G. (2012). Absolute quantification of somatic dna alterations in human cancer. *Nat Biotechnol*, 30(5):413–21.

[Casasent et al., 2018] Casasent, A. K., Schalck, A., Gao, R., Sei, E., Long, A., Pangburn, W., Casasent, T., Meric-Bernstam, F., Edgerton, M. E., and Navin, N. E. (2018). Multiclonal invasion in breast tumors identified by topographic single cell sequencing. *Cell*, 172(1-2):205–217 e12.

[Castro-Giner et al., 2015] Castro-Giner, F., Ratcliffe, P., and Tomlinson, I. (2015). The mini-driver model of polygenic cancer evolution. *Nat Rev Cancer*, 15(11):680–5.

[Chong and Janne, 2013] Chong, C. R. and Janne, P. A. (2013). The quest to overcome resistance to egfr-targeted therapies in cancer. *Nat Med*, 19(11):1389–400.

[Choudhury et al., 2013] Choudhury, S., Almendro, V., Merino, V. F., Wu, Z., Maruyama, R., Su, Y., Martins, F. C., Fackler, M. J., Bessarabova, M., Kowalczyk, A., Conway, T., Beresford-Smith, B., Macintyre, G., Cheng, Y. K., Lopez-Bujanda, Z., Kaspi, A., Hu, R., Robens, J., Nikolskaya, T., Haakensen, V. D., Schnitt, S. J., Argani, P., Ethington, G., Panos, L., Grant, M., Clark, J., Herlihy, W., Lin, S. J., Chew, G., Thompson, E. W., Greene-Colozzi, A., Richardson, A. L., Rosson, G. D., Pike, M., Garber, J. E., Nikolsky, Y., Blum, J. L., Au, A., Hwang, E. S., Tamimi, R. M., Michor, F., Haviv, I., Liu, X. S., Sukumar, S., and Polyak, K. (2013). Molecular profiling of human mammary gland links breast cancer risk to a p27(+) cell population with progenitor characteristics. *Cell Stem Cell*, 13(1):117–30.

[Christians et al., 1995] Christians, F. C., Newcomb, T. G., and Loeb, L. A. (1995). Potential sources of multiple mutations in human cancers. *Prev Med*, 24(4):329–32.

[Chung et al., 2012] Chung, K., Hovanessian-Larsen, L. J., Hawes, D., Taylor, D., Downey, S., Spicer, D. V., Stanczyk, F. Z., Patel, S., Anderson, A. R., Pike, M. C., Wu, A. H., and Pearce, C. L. (2012). Breast epithelial cell proliferation is markedly increased with short-term high levels of endogenous estrogen secondary to controlled ovarian hyperstimulation. *Breast Cancer Res Treat*, 132(2):653–60.

[Church et al., 2013] Church, D. N., Briggs, S. E., Palles, C., Domingo, E., Kearsey, S. J., Grimes, J. M., Gorman, M., Martin, L., Howarth, K. M., Hodgson, S. V., Kaur, K., Taylor, J., and Tomlinson, I. P. (2013). Dna polymerase epsilon and delta exonuclease domain mutations in endometrial cancer. *Hum Mol Genet*, 22(14):2820–8.

[Church et al., 2015] Church, D. N., Stelloo, E., Nout, R. A., Valtcheva, N., Depreeuw, J., ter Haar, N., Noske, A., Amant, F., Tomlinson, I. P., Wild, P. J., Lambrechts, D., Jurgenliemk-Schulz, I. M., Jobsen, J. J., Smit, V. T., Creutzberg, C. L., and Bosse, T. (2015). Prognostic significance of pole proofreading mutations in endometrial cancer. *J Natl Cancer Inst*, 107(1):402.

[Cibulskis et al., 2013] Cibulskis, K., Lawrence, M. S., Carter, S. L., Sivachenko, A., Jaffe, D., Sougnez, C., Gabriel, S., Meyerson, M., Lander, E. S., and Getz, G. (2013). Sensitive detection of somatic point mutations in impure and heterogeneous cancer samples. *Nat Biotechnol*, 31(3):213–9.

[Cohen et al., 2018] Cohen, J. D., Li, L., Wang, Y., Thoburn, C., Afsari, B., Danilova, L., Douville, C., Javed, A. A., Wong, F., Mattox, A., Hruban, R. H., Wolfgang, C. L., Goggins, M. G., Dal Molin, M., Wang, T. L., Roden, R., Klein, A. P., Ptak, J., Dobbyn, L., Schaefer, J., Silliman, N., Popoli, M., Vogelstein, J. T., Browne, J. D., Schoen, R. E., Brand, R. E., Tie, J., Gibbs, P., Wong, H. L., Mansfield, A. S., Jen, J., Hanash, S. M., Falconi, M., Allen, P. J., Zhou, S., Bettegowda, C., Diaz, L., Tomasetti, C., Kinzler, K. W., Vogelstein, B., Lennon, A. M., and Papadopoulos, N. (2018). Detection and localization of surgically resectable cancers with a multi-analyte blood test. *Science*.

[Colditz et al., 2004] Colditz, G. A., Rosner, B. A., Chen, W. Y., Holmes, M. D., and Hankinson, S. E. (2004). Risk factors for breast cancer according to estrogen and progesterone receptor status. *JNCI Journal of the National Cancer Institute*, 96(3):218–228.

[Cooper, 1982] Cooper, G. M. (1982). Cellular transforming genes. *Science*, 217(4562):801–6.

[Cooper, 2000] Cooper, G. M. (2000). *The cell a molecular approach*. NCBI bookshelf. Sinauer Associates, Sunderland, Mass., 2nd edition.

[Couzin-Frankel, 2015] Couzin-Frankel, J. (2015). Biomedicine. the bad luck of cancer. *Science*, 347(6217):12.

[Cristea et al., 2017] Cristea, S., Kuipers, J., and Beerenwinkel, N. (2017). pathtimex: Joint inference of mutually exclusive cancer pathways and their progression dynamics. *J Comput Biol*, 24(6):603–615.

[da Silva-Coelho et al., 2017] da Silva-Coelho, P., Kroeze, L. I., Yoshida, K., Koorenhof-Scheele, T. N., Knops, R., van de Locht, L. T., de Graaf, A. O., Massop, M., Sandmann, S., Dugas, M., Stevens-Kroef, M. J., Cermak, J., Shiraishi, Y., Chiba, K., Tanaka, H., Miyano, S., de Witte, T., Blijlevens, N. M. A., Muus, P., Huls, G., van der Reijden, B. A., Ogawa, S., and Jansen, J. H. (2017). Clonal evolution in myelodysplastic syndromes. *Nat Commun*, 8:15099.

[Daniel and Young, 1971] Daniel, C. W. and Young, L. J. (1971). Influence of cell division on an aging process. life span of mouse mammary epithelium during serial propagation in vivo. *Exp Cell Res*, 65(1):27–32.

[Datta et al., 2013] Datta, R., Gutteridge, A., Swanton, C., Maley, C. C., and Graham, T. A. (2013). Modelling the evolution of genetic instability during tumour progression. *Evol Appl*, 6(1):20–33.

[Davoli and de Lange, 2012] Davoli, T. and de Lange, T. (2012). Telomere-driven tetraploidization occurs in human cells undergoing crisis and promotes transformation of mouse cells. *Cancer Cell*, 21(6):765–76.

[de Bruin et al., 2014] de Bruin, E. C., McGranahan, N., Mitter, R., Salm, M., Wedge, D. C., Yates, L., Jamal-Hanjani, M., Shafi, S., Murugaesu, N., Rowan, A. J., Gronroos, E., Muhammad, M. A., Horswell, S., Gerlinger, M., Varela, I., Jones, D., Marshall, J., Voet, T., Van Loo, P., Rassl, D. M., Rintoul, R. C., Janes, S. M., Lee, S. M., Forster, M., Ahmad, T., Lawrence, D., Falzon, M., Capitanio, A., Harkins, T. T., Lee, C. C., Tom, W., Teefe, E., Chen, S. C., Begum, S., Rabinowitz, A., Phillimore, B., Spencer-Dene, B., Stamp, G., Szallasi, Z., Matthews, N., Stewart, A., Campbell, P., and Swanton, C. (2014). Spatial and temporal diversity in genomic instability processes defines lung cancer evolution. *Science*, 346(6206):251–6.

[Dewhurst et al., 2014] Dewhurst, S. M., McGranahan, N., Burrell, R. A., Rowan, A. J., Gronroos, E., Endesfelder, D., Joshi, T., Mouradov, D., Gibbs, P., Ward, R. L., Hawkins, N. J., Szallasi, Z., Sieber, O. M., and Swanton, C. (2014). Tolerance of whole-genome doubling propagates chromosomal instability and accelerates cancer genome evolution. *Cancer Discov*, 4(2):175–85.

[Dogan et al., 2012] Dogan, S., Shen, R., Ang, D. C., Johnson, M. L., D'Angelo, S. P., Paik, P. K., Brzostowski, E. B., Riely, G. J., Kris, M. G., Zakowski, M. F., and Ladanyi, M. (2012). Molecular epidemiology of egfr and kras mutations in 3,026 lung adenocarcinomas: higher susceptibility of women to smoking-related kras-mutant cancers. *Clin Cancer Res*, 18(22):6169–77.

[Dow et al., 2015] Dow, L. E., O'Rourke, K. P., Simon, J., Tschaharganeh, D. F., van Es, J. H., Clevers, H., and Lowe, S. W. (2015). Apc restoration promotes cellular differentiation and reestablishes crypt homeostasis in colorectal cancer. *Cell*, 161(7):1539–1552.

[Dowell and Minna, 2006] Dowell, J. E. and Minna, J. D. (2006). Egfr mutations and molecularly targeted therapy: a new era in the treatment of lung cancer. *Nat Clin Pract Oncol*, 3(4):170–1.

[Duan et al., 2018] Duan, M., Hao, J., Cui, S., Worthley, D. L., Zhang, S., Wang, Z., Shi, J., Liu, L., Wang, X., Ke, A., Cao, Y., Xi, R., Zhang, X., Zhou, J., Fan, J., Li, C., and Gao, Q. (2018). Diverse modes of clonal evolution in hbv-related hepatocellular carcinoma revealed by single-cell genome sequencing. *Cell Res*.

[Durinck et al., 2011] Durinck, S., Ho, C., Wang, N. J., Liao, W., Jakkula, L. R., Collisson, E. A., Pons, J., Chan, S. W., Lam, E. T., Chu, C., Park, K., Hong, S. W., Hur, J. S., Huh, N., Neuhaus, I. M., Yu, S. S., Grekin, R. C., Mauro, T. M., Cleaver, J. E., Kwok, P. Y., LeBoit, P. E., Getz, G., Cibulskis, K., Aster, J. C., Huang, H., Purdom, E., Li, J., Bolund, L., Arron, S. T., Gray, J. W., Spellman, P. T., and Cho, R. J. (2011). Temporal dissection of tumorigenesis in primary cancers. *Cancer Discov*, 1(2):137–43.

[Eirew et al., 2008] Eirew, P., Stingl, J., Raouf, A., Turashvili, G., Aparicio, S., Emerman, J. T., and Eaves, C. J. (2008). A method for quantifying normal human mammary epithelial stem cells with in vivo regenerative ability. *Nat Med*, 14(12):1384–9.

[Erson-Omay et al., 2015] Erson-Omay, E. Z., Caglayan, A. O., Schultz, N., Weinhold, N., Omay, S. B., Ozduman, K., Koksal, Y., Li, J., Serin Harmanci, A., Clark, V., Carrion-Grant, G., Baranoski, J., Caglar, C., Barak, T., Coskun, S., Baran, B., Kose, D., Sun, J., Bakircioglu, M., Moliterno Gunel, J., Pamir, M. N., Mishra-Gorur, K., Bilguvar, K., Yasuno, K., Vortmeyer, A., Huttner, A. J., Sander, C., and Gunel, M. (2015). Somatic pole mutations cause an ultramutated giant cell high-grade glioma subtype with better prognosis. *Neuro Oncol*, 17(10):1356–64.

[Faulkin and Deome, 1960] Faulkin, L. J., J. and Deome, K. B. (1960). Regulation of growth and spacing of gland elements in the mammary fat pad of the c3h mouse. *J Natl Cancer Inst*, 24:953–69.

[Favero et al., 2015] Favero, F., Joshi, T., Marquard, A. M., Birkbak, N. J., Krzystanek, M., Li, Q., Szallasi, Z., and Eklund, A. C. (2015). Sequenza: allele-specific copy number and mutation profiles from tumor sequencing data. *Ann Oncol*, 26(1):64–70.

[Foo et al., 2015] Foo, J., Liu, L. L., Leder, K., Riester, M., Iwasa, Y., Lengauer, C., and Michor, F. (2015). An evolutionary approach for identifying driver mutations in colorectal cancer. *PLoS Comput Biol*, 11(9):e1004350.

[Fraley and Raftery, 2002] Fraley, C. and Raftery, A. E. (2002). Model-based clustering, discriminant analysis and density estimation. *Journal of the American Statistical Association*, 97(1):611–631.

[Fraley et al., 2012] Fraley, C., Raftery, A. E., Murphy, B., and Scrucca, L. (2012). mclust version 4 for r: Normal mixture modeling for model-based clustering, classification, and density estimation technical report no. 597. *N/A*.

[Ganem et al., 2009] Ganem, N. J., Godinho, S. A., and Pellman, D. (2009). A mechanism linking extra centrosomes to chromosomal instability. *Nature*, 460(7252):278–82.

[Gao et al., 2016] Gao, R., Davis, A., McDonald, T. O., Sei, E., Shi, X., Wang, Y., Tsai, P. C., Casasent, A., Waters, J., Zhang, H., Meric-Bernstam, F., Michor, F., and Navin, N. E. (2016). Punctuated copy number evolution and clonal stasis in triple-negative breast cancer. *Nat Genet*, 48(10):1119–30.

[Garrett-Bakelman and Melnick, 2016] Garrett-Bakelman, F. E. and Melnick, A. M. (2016). Mutant idh: a targetable driver of leukemic phenotypes linking metabolism, epigenetics and transcriptional regulation. *Epigenomics*, 8(7):945–57.

[Gehring et al., 2015] Gehring, J. S., Fischer, B., Lawrence, M., and Huber, W. (2015). Somaticsignatures: inferring mutational signatures from single-nucleotide variants. *Bioinformatics*, 31(22):3673–5.

[Gerlinger et al., 2012] Gerlinger, M., Rowan, A. J., Horswell, S., Math, M., Larkin, J., Endesfelder, D., Gronroos, E., Martinez, P., Matthews, N., Stewart, A., Tarpey, P., Varela, I., Phillimore, B., Begum, S., McDonald, N. Q., Butler, A., Jones, D., Raine, K., Latimer, C., Santos, C. R., Nohadani, M., Eklund, A. C., Spencer-Dene, B., Clark, G., Pickering, L., Stamp, G., Gore, M., Szallasi, Z., Downward, J., Futreal, P. A., and Swanton, C. (2012). Intratumor heterogeneity and branched evolution revealed by multiregion sequencing. *N Engl J Med*, 366(10):883–892.

[Goh et al., 1995] Goh, H. S., Yao, J., and Smith, D. R. (1995). p53 point mutation and survival in colorectal cancer patients. *Cancer Res*, 55(22):5217–21.

[Going et al., 1988] Going, J. J., Anderson, T. J., Battersby, S., and MacIntyre, C. C. (1988). Proliferative and secretory activity in human breast during natural and artificial menstrual cycles. *Am J Pathol*, 130(1):193–204.

[Gonzalez-Perez et al., 2013] Gonzalez-Perez, A., Perez-Llamas, C., Deu-Pons, J., Tamborero, D., Schroeder, M. P., Jene-Sanz, A., Santos, A., and Lopez-Bigas, N. (2013). Intogen-mutations identifies cancer drivers across tumor types. *Nat Methods*, 10(11):1081–2.

[Gordon et al., 2012] Gordon, D. J., Resio, B., and Pellman, D. (2012). Causes and consequences of aneuploidy in cancer. *Nat Rev Genet*, 13(3):189–203.

[Graham and Sottoriva, 2017] Graham, T. A. and Sottoriva, A. (2017). Measuring cancer evolution from the genome. *J Pathol*, 241(2):183–191.

[Greenblatt et al., 1994] Greenblatt, M. S., Bennett, W. P., Hollstein, M., and Harris, C. C. (1994). Mutations in the p53 tumor suppressor gene: clues to cancer etiology and molecular pathogenesis. *Cancer Res*, 54(18):4855–78.

[Greenman et al., 2007] Greenman, C., Stephens, P., Smith, R., Dalgliesh, G. L., Hunter, C., Bignell, G., Davies, H., Teague, J., Butler, A., Stevens, C., Edkins, S., O'Meara, S., Vastrik, I., Schmidt, E. E., Avis, T., Barthorpe, S., Bhamra, G., Buck, G., Choudhury, B., Clements, J., Cole, J., Dicks, E., Forbes, S., Gray, K., Halliday, K., Harrison, R., Hills, K., Hinton, J., Jenkinson, A., Jones, D., Menzies, A., Mironenko, T., Perry, J., Raine, K., Richardson, D., Shepherd, R., Small, A., Tofts, C., Varian, J., Webb, T., West, S., Widaa, S., Yates, A., Cahill, D. P., Louis, D. N., Goldstraw, P., Nicholson, A. G., Brasseur, F., Looijenga, L., Weber, B. L., Chiew, Y. E., DeFazio, A., Greaves, M. F., Green, A. R., Campbell, P., Birney, E., Easton, D. F., Chenevix-Trench, G., Tan, M. H., Khoo, S. K., Teh, B. T., Yuen, S. T., Leung, S. Y., Wooster, R., Futreal, P. A., and Stratton, M. R. (2007). Patterns of somatic mutation in human cancer genomes. *Nature*, 446(7132):153–8.

[Greenman et al., 2012] Greenman, C. D., Pleasance, E. D., Newman, S., Yang, F., Fu, B., Nik-Zainal, S., Jones, D., Lau, K. W., Carter, N., Edwards, P. A., Futreal, P. A., Stratton, M. R., and Campbell, P. J. (2012). Estimation of rearrangement phylogeny for cancer genomes. *Genome Res*, 22(2):346–61.

[Hambardzumyan et al., 2011] Hambardzumyan, D., Cheng, Y. K., Haeno, H., Holland, E. C., and Michor, F. (2011). The probable cell of origin of nf1- and pdgf-driven glioblastomas. *PLoS One*, 6(9):e24454.

[Hanahan and Weinberg, 2011] Hanahan, D. and Weinberg, R. A. (2011). Hallmarks of cancer: the next generation. *Cell*, 144(5):646–74.

[Harris, 2008] Harris, H. (2008). Concerning the origin of malignant tumours by theodor boveri. translated and annotated by henry harris. preface. *J Cell Sci*, 121 Suppl 1:v–vi.

[Hause et al., 2016] Hause, R. J., Pritchard, C. C., Shendure, J., and Salipante, S. J. (2016). Classification and characterization of microsatellite instability across 18 cancer types. *Nat Med*.

[Helleday et al., 2014] Helleday, T., Eshtad, S., and Nik-Zainal, S. (2014). Mechanisms underlying mutational signatures in human cancers. *Nat Rev Genet*, 15(9):585–98.

[Heng and Durbin, 2009] Heng, L. and Durbin, R. (2009). Burrows-wheeler aligner.

[Homfray et al., 1998] Homfray, T. F., Cottrell, S. E., Ilyas, M., Rowan, A., Talbot, I. C., Bodmer, W. F., and Tomlinson, I. P. (1998). Defects in mismatch repair occur after apc mutations in the pathogenesis of sporadic colorectal tumours. *Hum Mutat*, 11(2):114–20.

[Hong et al., 2015] Hong, M. K., Macintyre, G., Wedge, D. C., Van Loo, P., Patel, K., Lunke, S., Alexandrov, L. B., Sloggett, C., Cmero, M., Marass, F., Tsui, D., Mangiola, S., Lonie, A., Naeem, H., Sapre, N., Phal, P. M., Kurganovs, N., Chin, X., Kerger, M., Warren, A. Y., Neal, D., Gnanapragasam, V., Rosenfeld, N., Pedersen, J. S., Ryan, A., Haviv, I., Costello, A. J., Corcoran, N. M., and Hovens, C. M. (2015). Tracking the origins and drivers of subclonal metastatic expansion in prostate cancer. *Nat Commun*, 6:6605.

[Huh et al., 2015] Huh, S. J., Clement, K., Jee, D., Merlini, A., Choudhury, S., Maruyama, R., Yoo, R., Chytil, A., Boyle, P., Ran, F. A., Moses, H. L., Barcellos-Hoff, M. H., Jackson-Grusby, L., Meissner, A., and Polyak, K. (2015). Age- and pregnancy-associated dna methylation changes in mammary epithelial cells. *Stem Cell Reports*, 4(2):297–311.

[Huh et al., 2016] Huh, S. J., Oh, H., Peterson, M. A., Almendro, V., Hu, R., Bowden, M., Lis, R. L., Cotter, M. B., Loda, M., Barry, W. T., Polyak, K., and Tamimi, R. M. (2016). The proliferative activity of mammary epithelial cells in normal tissue predicts breast cancer risk in premenopausal women. *Cancer Res*, 76(7):1926–34.

[Hussein et al., 2015] Hussein, Y. R., Weigelt, B., Levine, D. A., Schoolmeester, J. K., Dao, L. N., Balzer, B. L., Liles, G., Karlan, B., Kobel, M., Lee, C. H., and

Soslow, R. A. (2015). Clinicopathological analysis of endometrial carcinomas harboring somatic pole exonuclease domain mutations. *Mod Pathol*, 28(4):505–14.

[Jamal-Hanjani et al., 2017] Jamal-Hanjani, M., Wilson, G. A., McGranahan, N., Birkbak, N. J., Watkins, T. B. K., Veeriah, S., Shafi, S., Johnson, D. H., Mitter, R., Rosenthal, R., Salm, M., Horswell, S., Escudero, M., Matthews, N., Rowan, A., Chambers, T., Moore, D. A., Turajlic, S., Xu, H., Lee, S. M., Forster, M. D., Ahmad, T., Hiley, C. T., Abbosh, C., Falzon, M., Borg, E., Marafioti, T., Lawrence, D., Hayward, M., Kolvekar, S., Panagiotopoulos, N., Janes, S. M., Thakrar, R., Ahmed, A., Blackhall, F., Summers, Y., Shah, R., Joseph, L., Quinn, A. M., Crosbie, P. A., Naidu, B., Middleton, G., Langman, G., Trotter, S., Nicolson, M., Remmen, H., Kerr, K., Chetty, M., Gomersall, L., Fennell, D. A., Nakas, A., Rathinam, S., Anand, G., Khan, S., Russell, P., Ezhil, V., Ismail, B., Irvin-Sellers, M., Prakash, V., Lester, J. F., Kornaszewska, M., Attanoos, R., Adams, H., Davies, H., Dentro, S., Taniere, P., O'Sullivan, B., Lowe, H. L., Hartley, J. A., Iles, N., Bell, H., Ngai, Y., Shaw, J. A., Herrero, J., Szallasi, Z., Schwarz, R. F., Stewart, A., Quezada, S. A., Le Quesne, J., Van Loo, P., Dive, C., Hackshaw, A., and Swanton, C. (2017). Tracking the evolution of non-small-cell lung cancer. *N Engl J Med*, 376(22):2109–2121.

[Jeggo et al., 2016] Jeggo, P. A., Pearl, L. H., and Carr, A. M. (2016). Dna repair, genome stability and cancer: a historical perspective. *Nat Rev Cancer*, 16(1):35–42.

[Jones et al., 2008] Jones, S., Chen, W. D., Parmigiani, G., Diehl, F., Beerenwinkel, N., Antal, T., Traulsen, A., Nowak, M. A., Siegel, C., Velculescu, V. E., Kinzler, K. W., Vogelstein, B., Willis, J., and Markowitz, S. D. (2008). Comparative lesion sequencing provides insights into tumor evolution. *Proc Natl Acad Sci U S A*, 105(11):4283–8.

[Junttila et al., 2010] Junttila, M. R., Karnezis, A. N., Garcia, D., Madriles, F., Kortlever, R. M., Rostker, F., Brown Swigart, L., Pham, D. M., Seo, Y., Evan, G. I.,

and Martins, C. P. (2010). Selective activation of p53-mediated tumour suppression in high-grade tumours. *Nature*, 468(7323):567–71.

[Kan et al., 2010] Kan, Z., Jaiswal, B. S., Stinson, J., Janakiraman, V., Bhatt, D., Stern, H. M., Yue, P., Haverty, P. M., Bourgon, R., Zheng, J., Moorhead, M., Chaudhuri, S., Tomsho, L. P., Peters, B. A., Pujara, K., Cordes, S., Davis, D. P., Carlton, V. E., Yuan, W., Li, L., Wang, W., Eigenbrot, C., Kaminker, J. S., Eberhard, D. A., Waring, P., Schuster, S. C., Modrusan, Z., Zhang, Z., Stokoe, D., de Sauvage, F. J., Faham, M., and Seshagiri, S. (2010). Diverse somatic mutation patterns and pathway alterations in human cancers. *Nature*, 466(7308):869–73.

[Kandoth et al., 2013] Kandoth, C., Schultz, N., Cherniack, A. D., Akbani, R., Liu, Y., Shen, H., Robertson, A. G., Pashtan, I., Shen, R., Benz, C. C., Yau, C., Laird, P. W., Ding, L., Zhang, W., Mills, G. B., Kucherlapati, R., Mardis, E. R., and Levine, D. A. (2013). Integrated genomic characterization of endometrial carcinoma. *Nature*, 497(7447):67–73.

[Katharine M. Mullen, 2012] Katharine M. Mullen, I. H. M. v. S. (2012). nnls: The lawson-hanson algorithm for non-negative least squares (nnls).

[Kato et al., 1998] Kato, I., Toniolo, P., Akhmedkhanov, A., Koenig, K. L., Shore, R., and Zeleniuch-Jacquotte, A. (1998). Prospective study of factors influencing the onset of natural menopause. *J Clin Epidemiol*, 51(12):1271–6.

[Kloosterman et al., 2011] Kloosterman, W. P., Hoogstraat, M., Paling, O., Tavakoli-Yaraki, M., Renkens, I., Vermaat, J. S., van Roosmalen, M. J., van Lieshout, S., Nijman, I. J., Roessingh, W., van 't Slot, R., van de Belt, J., Guryev, V., Koudijs, M., Voest, E., and Cuppen, E. (2011). Chromothripsis is a common mechanism driving genomic rearrangements in primary and metastatic colorectal cancer. *Genome Biol*, 12(10):R103.

[Kordon and Smith, 1998] Kordon, E. C. and Smith, G. H. (1998). An entire functional mammary gland may comprise the progeny from a single cell. *Development*, 125(10):1921–30.

[Kuukasjarvi et al., 1997a] Kuukasjarvi, T., Karhu, R., Tanner, M., Kahkonen, M., Schaffer, A., Nupponen, N., Pennanen, S., Kallioniemi, A., Kallioniemi, O. P., and Isola, J. (1997a). Genetic heterogeneity and clonal evolution underlying development of asynchronous metastasis in human breast cancer. *Cancer Res*, 57(8):1597–604.

[Kuukasjarvi et al., 1997b] Kuukasjarvi, T., Tanner, M., Pennanen, S., Karhu, R., Kallioniemi, O. P., and Isola, J. (1997b). Genetic changes in intraductal breast cancer detected by comparative genomic hybridization. *Am J Pathol*, 150(4):1465–71.

[Lawrence et al., 2014] Lawrence, M. S., Stojanov, P., Mermel, C. H., Robinson, J. T., Garraway, L. A., Golub, T. R., Meyerson, M., Gabriel, S. B., Lander, E. S., and Getz, G. (2014). Discovery and saturation analysis of cancer genes across 21 tumour types. *Nature*, 505(7484):495–501.

[Lawrence et al., 2013] Lawrence, M. S., Stojanov, P., Polak, P., Kryukov, G. V., Cibulskis, K., Sivachenko, A., Carter, S. L., Stewart, C., Mermel, C. H., Roberts, S. A., Kiezun, A., Hammerman, P. S., McKenna, A., Drier, Y., Zou, L., Ramos, A. H., Pugh, T. J., Stransky, N., Helman, E., Kim, J., Sougnez, C., Ambrogio, L., Nickerson, E., Shefler, E., Cortes, M. L., Auclair, D., Saksena, G., Voet, D., Noble, M., DiCara, D., Lin, P., Lichtenstein, L., Heiman, D. I., Fennell, T., Imielinski, M., Hernandez, B., Hodis, E., Baca, S., Dulak, A. M., Lohr, J., Landau, D. A., Wu, C. J., Melendez-Zajgla, J., Hidalgo-Miranda, A., Koren, A., McCarroll, S. A., Mora, J., Crompton, B., Onofrio, R., Parkin, M., Winckler, W., Ardlie, K., Gabriel, S. B., Roberts, C. W. M., Biegel, J. A., Stegmaier, K., Bass, A. J., Garraway, L. A., Meyerson, M., Golub, T. R., Gordenin, D. A., Sunyaev, S., Lander, E. S., and Getz, G. (2013). Mutational heterogeneity in cancer and the search for new cancer-associated genes. *Nature*, 499(7457):214–218.

[Lee et al., 2011] Lee, A. J., Endesfelder, D., Rowan, A. J., Walther, A., Birkbak, N. J., Futreal, P. A., Downward, J., Szallasi, Z., Tomlinson, I. P., Howell, M.,

Kschischo, M., and Swanton, C. (2011). Chromosomal instability confers intrinsic multidrug resistance. *Cancer Res*, 71(5):1858–70.

[Lengauer et al., 1997] Lengauer, C., Kinzler, K. W., and Vogelstein, B. (1997). Genetic instability in colorectal cancers. *Nature*, 386(6625):623–7.

[Li et al., 2014] Li, X., Galipeau, P. C., Paulson, T. G., Sanchez, C. A., Arnaudo, J., Liu, K., Sather, C. L., Kostadinov, R. L., Odze, R. D., Kuhner, M. K., Maley, C. C., Self, S. G., Vaughan, T. L., Blount, P. L., and Reid, B. J. (2014). Temporal and spatial evolution of somatic chromosomal alterations: a case-cohort study of barrett's esophagus. *Cancer Prev Res (Phila)*, 7(1):114–27.

[Llosa et al., 2015] Llosa, N. J., Cruise, M., Tam, A., Wicks, E. C., Hechenbleikner, E. M., Taube, J. M., Blosser, R. L., Fan, H., Wang, H., Luber, B. S., Zhang, M., Papadopoulos, N., Kinzler, K. W., Vogelstein, B., Sears, C. L., Anders, R. A., Pardoll, D. M., and Housseau, F. (2015). The vigorous immune microenvironment of microsatellite instable colon cancer is balanced by multiple counter-inhibitory checkpoints. *Cancer Discov*, 5(1):43–51.

[Loeb, 1991] Loeb, L. A. (1991). Mutator phenotype may be required for multistage carcinogenesis. *Cancer Res*, 51(12):3075–9.

[Loeb, 2001] Loeb, L. A. (2001). A mutator phenotype in cancer. *Cancer Res*, 61(8):3230–9.

[Loeb, 2011] Loeb, L. A. (2011). Human cancers express mutator phenotypes: origin, consequences and targeting. *Nat Rev Cancer*, 11(6):450–7.

[Loeb and Mullins, 2000] Loeb, L. A. and Mullins, J. I. (2000). Lethal mutagenesis of hiv by mutagenic ribonucleoside analogs. *AIDS Res Hum Retroviruses*, 16(1):1–3.

[Luksza et al., 2017] Luksza, M., Riaz, N., Makarov, V., Balachandran, V. P., Hellmann, M. D., Solovyov, A., Rizvi, N. A., Merghoub, T., Levine, A. J., Chan, T. A., Wolchok, J. D., and Greenbaum, B. D. (2017). A neoantigen fitness

model predicts tumour response to checkpoint blockade immunotherapy. *Nature*, 551(7681):517–520.

[Luptacik, 2010] Luptacik, M. (2010). *Mathematical optimization and economic analysis*. Springer optimization and its applications. Springer, New York ; London.

[Maciejowski and de Lange, 2017] Maciejowski, J. and de Lange, T. (2017). Telomeres in cancer: tumour suppression and genome instability. *Nat Rev Mol Cell Biol*, 18(3):175–186.

[Maciejowski et al., 2015] Maciejowski, J., Li, Y., Bosco, N., Campbell, P. J., and de Lange, T. (2015). Chromothripsis and kataegis induced by telomere crisis. *Cell*, 163(7):1641–54.

[MacMahon et al., 1970] MacMahon, B., Cole, P., Lim, T., Lowe, A., Mirra, B., Ravnihar, B., Salber, E., Valaoras, V., and Yuasa, S. (1970). Age at first birth and breast cancer risk. *Bull. Wld Hlth Org.*, 43(1):209–221.

[Makova and Hardison, 2015] Makova, K. D. and Hardison, R. C. (2015). The effects of chromatin organization on variation in mutation rates in the genome. *Nat Rev Genet*, 16(4):213–23.

[Maley et al., 2006] Maley, C. C., Galipeau, P. C., Finley, J. C., Wongsurawat, V. J., Li, X., Sanchez, C. A., Paulson, T. G., Blount, P. L., Risques, R. A., Rabinovitch, P. S., and Reid, B. J. (2006). Genetic clonal diversity predicts progression to esophageal adenocarcinoma. *Nat Genet*, 38(4):468–73.

[Margonis et al., 2015] Margonis, G. A., Kim, Y., Spolverato, G., Ejaz, A., Gupta, R., Cosgrove, D., Anders, R., Karagkounis, G., Choti, M. A., and Pawlik, T. M. (2015). Association between specific mutations in kras codon 12 and colorectal liver metastasis. *JAMA Surg*, 150(8):722–9.

[Martincorena et al., 2017] Martincorena, I., Raine, K. M., Gerstung, M., Dawson, K. J., Haase, K., Van Loo, P., Davies, H., Stratton, M. R., and Campbell, P. J.

(2017). Universal patterns of selection in cancer and somatic tissues. *Cell*, 171(5):1029–1041 e21.

[Martincorena et al., 2015] Martincorena, I., Roshan, A., Gerstung, M., Ellis, P., Van Loo, P., McLaren, S., Wedge, D. C., Fullam, A., Alexandrov, L. B., Tubio, J. M., Stebbings, L., Menzies, A., Widaa, S., Stratton, M. R., Jones, P. H., and Campbell, P. J. (2015). Tumor evolution. high burden and pervasive positive selection of somatic mutations in normal human skin. *Science*, 348(6237):880–6.

[Martinez et al., 2016] Martinez, P., Timmer, M. R., Lau, C. T., Calpe, S., Sancho-Serra Mdel, C., Straub, D., Baker, A. M., Meijer, S. L., Kate, F. J., Mallant-Hent, R. C., Naber, A. H., van Oijen, A. H., Baak, L. C., Scholten, P., Bohmer, C. J., Fockens, P., Bergman, J. J., Maley, C. C., Graham, T. A., and Krishnadath, K. K. (2016). Dynamic clonal equilibrium and predetermined cancer risk in barrett's oesophagus. *Nat Commun*, 7:12158.

[Maruvka et al., 2017] Maruvka, Y. E., Mouw, K. W., Karlic, R., Parasuraman, P., Kamburov, A., Polak, P., Haradhvala, N. J., Hess, J. M., Rheinbay, E., Brody, Y., Koren, A., Braunstein, L. Z., D'Andrea, A., Lawrence, M. S., Bass, A., Bernards, A., Michor, F., and Getz, G. (2017). Analysis of somatic microsatellite indels identifies driver events in human tumors. *Nat Biotechnol*, 35(10):951–959.

[McFarland et al., 2013] McFarland, C. D., Korolev, K. S., Kryukov, G. V., Sunyaev, S. R., and Mirny, L. A. (2013). Impact of deleterious passenger mutations on cancer progression. *Proc Natl Acad Sci U S A*, 110(8):2910–5.

[McFarland et al., 2014] McFarland, C. D., Mirny, L. A., and Korolev, K. S. (2014). Tug-of-war between driver and passenger mutations in cancer and other adaptive processes. *Proc Natl Acad Sci U S A*, 111(42):15138–43.

[McGranahan et al., 2015] McGranahan, N., Favero, F., de Bruin, E. C., Birkbak, N. J., Szallasi, Z., and Swanton, C. (2015). Clonal status of actionable driver

events and the timing of mutational processes in cancer evolution. *Sci Transl Med*, 7(283):283ra54.

[McGranahan et al., 2016] McGranahan, N., Furness, A. J., Rosenthal, R., Ramskov, S., Lyngaa, R., Saini, S. K., Jamal-Hanjani, M., Wilson, G. A., Birkbak, N. J., Hiley, C. T., Watkins, T. B., Shafi, S., Murugaesu, N., Mitter, R., Akarca, A. U., Linares, J., Marafioti, T., Henry, J. Y., Van Allen, E. M., Miao, D., Schilling, B., Schadendorf, D., Garraway, L. A., Makarov, V., Rizvi, N. A., Snyder, A., Hellmann, M. D., Merghoub, T., Wolchok, J. D., Shukla, S. A., Wu, C. J., Peggs, K. S., Chan, T. A., Hadrup, S. R., Quezada, S. A., and Swanton, C. (2016). Clonal neoantigens elicit t cell immunoreactivity and sensitivity to immune checkpoint blockade. *Science*, 351(6280):1463–9.

[Meng et al., 2014] Meng, B., Hoang, L. N., McIntyre, J. B., Duggan, M. A., Nelson, G. S., Lee, C. H., and Kobel, M. (2014). Pole exonuclease domain mutation predicts long progression-free survival in grade 3 endometrioid carcinoma of the endometrium. *Gynecol Oncol*, 134(1):15–9.

[Michor, 2005] Michor, F. (2005). Chromosomal instability and human cancer. *Philos Trans R Soc Lond B Biol Sci*, 360(1455):631–5.

[Mitelman et al., 2007] Mitelman, F., Johansson, B., and Mertens, F. (2007). The impact of translocations and gene fusions on cancer causation. *Nat Rev Cancer*, 7(4):233–45.

[Miyamoto et al., 2018] Miyamoto, T., Ando, H., Asaka, R., Yamada, Y., and Shiozawa, T. (2018). Mutation analysis by whole exome sequencing of endometrial hyperplasia and carcinoma in one patient: Abnormalities of polymerase epsilon and the phosphatidylinositol-3 kinase pathway. *J Obstet Gynaecol Res*, 44(1):179–183.

[Moolgavkar et al., 1980] Moolgavkar, S., Day, N., and Stevens, R. (1980). Two-stage model for carcinogenesis- epidemiology of breast cancer in females. *JNCI Journal of the National Cancer Institute*, 65(1):559–569.

[Moolgavkar, 2004] Moolgavkar, S. H. (2004). Commentary: Fifty years of the multistage model: remarks on a landmark paper. *Int J Epidemiol*, 33(6):1182–3.

[Moolgavkar and Knudson, 1981] Moolgavkar, S. H. and Knudson, A. G., J. (1981). Mutation and cancer: a model for human carcinogenesis. *J Natl Cancer Inst*, 66(6):1037–52.

[Moran, 1962] Moran, P. A. P. (1962). *The statistical processes of evolutionary theory*. Clarendon Press.

[Mouw et al., 2016] Mouw, K., Braunstein, L. Z., Kim, J., Polak, P., Getz, G., and D'Andrea, A. D. (2016). Somatic ercc2 mutations are associated with a distinct mutational signature in muscle-invasive bladder cancer. *Int J Radiat Oncol Biol Phys*, 96(2S):S54.

[NCHS, 2016] NCHS (2016). Health, united states, 2015: With special features on racial and ethnic health disparities.

[Nik-Zainal et al., 2012a] Nik-Zainal, S., Alexandrov, L. B., Wedge, D. C., Van Loo, P., Greenman, C. D., Raine, K., Jones, D., Hinton, J., Marshall, J., Stebbings, L. A., Menzies, A., Martin, S., Leung, K., Chen, L., Leroy, C., Ramakrishna, M., Rance, R., Lau, K. W., Mudie, L. J., Varela, I., McBride, D. J., Bignell, G. R., Cooke, S. L., Shlien, A., Gamble, J., Whitmore, I., Maddison, M., Tarpey, P. S., Davies, H. R., Papaemmanuil, E., Stephens, P. J., McLaren, S., Butler, A. P., Teague, J. W., Jonsson, G., Garber, J. E., Silver, D., Miron, P., Fatima, A., Boyault, S., Langerod, A., Tutt, A., Martens, J. W., Aparicio, S. A., Borg, A., Salomon, A. V., Thomas, G., Borresen-Dale, A. L., Richardson, A. L., Neuberger, M. S., Futreal, P. A., Campbell, P. J., and Stratton, M. R. (2012a). Mutational processes molding the genomes of 21 breast cancers. *Cell*, 149(5):979–93.

[Nik-Zainal et al., 2016] Nik-Zainal, S., Davies, H., Staaf, J., Ramakrishna, M., Glodzik, D., Zou, X., Martincorena, I., Alexandrov, L. B., Martin, S., Wedge, D. C., Van Loo, P., Ju, Y. S., Smid, M., Brinkman, A. B., Morganella, S., Aure,

M. R., Lingjaerde, O. C., Langerod, A., Ringner, M., Ahn, S. M., Boyault, S., Brock, J. E., Broeks, A., Butler, A., Desmedt, C., Dirix, L., Dronov, S., Fatima, A., Foekens, J. A., Gerstung, M., Hooijer, G. K., Jang, S. J., Jones, D. R., Kim, H. Y., King, T. A., Krishnamurthy, S., Lee, H. J., Lee, J. Y., Li, Y., McLaren, S., Menzies, A., Mustonen, V., O'Meara, S., Pauporte, I., Pivot, X., Purdie, C. A., Raine, K., Ramakrishnan, K., Rodriguez-Gonzalez, F. G., Romieu, G., Sieuwerts, A. M., Simpson, P. T., Shepherd, R., Stebbings, L., Stefansson, O. A., Teague, J., Tommasi, S., Treilleux, I., Van den Eynden, G. G., Vermeulen, P., Vincent-Salomon, A., Yates, L., Caldas, C., van't Veer, L., Tutt, A., Knappskog, S., Tan, B. K., Jonkers, J., Borg, A., Ueno, N. T., Sotiriou, C., Viari, A., Futreal, P. A., Campbell, P. J., Span, P. N., Van Laere, S., Lakhani, S. R., Eyfjord, J. E., Thompson, A. M., Birney, E., Stunnenberg, H. G., van de Vijver, M. J., Martens, J. W., Borresen-Dale, A. L., Richardson, A. L., Kong, G., Thomas, G., and Stratton, M. R. (2016). Landscape of somatic mutations in 560 breast cancer whole-genome sequences. *Nature*, 534(7605):47–54.

[Nik-Zainal et al., 2012b] Nik-Zainal, S., Van Loo, P., Wedge, D. C., Alexandrov, L. B., Greenman, C. D., Lau, K. W., Raine, K., Jones, D., Marshall, J., Ramakrishna, M., Shlien, A., Cooke, S. L., Hinton, J., Menzies, A., Stebbings, L. A., Leroy, C., Jia, M., Rance, R., Mudie, L. J., Gamble, S. J., Stephens, P. J., McLaren, S., Tarpey, P. S., Papaemmanuil, E., Davies, H. R., Varela, I., McBride, D. J., Bignell, G. R., Leung, K., Butler, A. P., Teague, J. W., Martin, S., Jonsson, G., Mariani, O., Boyault, S., Miron, P., Fatima, A., Langerod, A., Aparicio, S. A., Tutt, A., Sieuwerts, A. M., Borg, A., Thomas, G., Salomon, A. V., Richardson, A. L., Borresen-Dale, A. L., Futreal, P. A., Stratton, M. R., and Campbell, P. J. (2012b). The life history of 21 breast cancers. *Cell*, 149(5):994–1007.

[Notta et al., 2016] Notta, F., Chan-Seng-Yue, M., Lemire, M., Li, Y., Wilson, G. W., Connor, A. A., Denroche, R. E., Liang, S. B., Brown, A. M., Kim, J. C., Wang, T., Simpson, J. T., Beck, T., Borgida, A., Buchner, N., Chadwick, D., Hafezi-Bakhtiari, S., Dick, J. E., Heisler, L., Hollingsworth, M. A., Ibrahimov, E., Jang, G. H., Johns, J., Jorgensen, L. G., Law, C., Ludkovski, O., Lungu,

I., Ng, K., Pasternack, D., Petersen, G. M., Shlush, L. I., Timms, L., Tsao, M. S., Wilson, J. M., Yung, C. K., Zogopoulos, G., Bartlett, J. M., Alexandrov, L. B., Real, F. X., Cleary, S. P., Roehrl, M. H., McPherson, J. D., Stein, L. D., Hudson, T. J., Campbell, P. J., and Gallinger, S. (2016). A renewed model of pancreatic cancer evolution based on genomic rearrangement patterns. *Nature*, 538(7625):378–382.

[Nowak et al., 2006] Nowak, M. A., Michor, F., and Iwasa, Y. (2006). Genetic instability and clonal expansion. *J Theor Biol*, 241(1):26–32.

[Olsson et al., 1996] Olsson, H., Jernstrom, H., Alm, P., Kreipe, H., Ingvar, C., Jonsson, P. E., and Ryden, S. (1996). Proliferation of the breast epithelium in relation to menstrual cycle phase, hormonal use, and reproductive factors. *Breast Cancer Res Treat*, 40(2):187–96.

[Palles et al., 2013] Palles, C., Cazier, J. B., Howarth, K. M., Domingo, E., Jones, A. M., Broderick, P., Kemp, Z., Spain, S. L., Guarino, E., Salguero, I., Sherborne, A., Chubb, D., Carvajal-Carmona, L. G., Ma, Y., Kaur, K., Dobbins, S., Barclay, E., Gorman, M., Martin, L., Kovac, M. B., Humphray, S., Lucassen, A., Holmes, C. C., Bentley, D., Donnelly, P., Taylor, J., Petridis, C., Roylance, R., Sawyer, E. J., Kerr, D. J., Clark, S., Grimes, J., Kearsey, S. E., Thomas, H. J., McVean, G., Houlston, R. S., and Tomlinson, I. (2013). Germline mutations affecting the proofreading domains of pole and pold1 predispose to colorectal adenomas and carcinomas. *Nat Genet*, 45(2):136–44.

[Parkin et al., 2011] Parkin, D. M., Boyd, L., and Walker, L. C. (2011). 16. the fraction of cancer attributable to lifestyle and environmental factors in the uk in 2010. *Br J Cancer*, 105 Suppl 2:S77–81.

[Petljak and Alexandrov, 2016] Petljak, M. and Alexandrov, L. B. (2016). Understanding mutagenesis through delineation of mutational signatures in human cancer. *Carcinogenesis*, 37(6):531–40.

[Pike et al., 1983] Pike, M., Krailo, M., Henderson, B., Casagrande, J., and Hoel, D. (1983). 'hormonal' risk factors, 'breast tissue age' and the age-incidence of breast cancer. *Nature*, 303(1):769–770.

[Polyak, 2007] Polyak, K. (2007). Breast cancer: origins and evolution. *J Clin Invest*, 117(11):3155–63.

[Popnikolov et al., 2001] Popnikolov, N., Yang, J., Liu, A., Guzman, R., and Nandi, S. (2001). Reconstituted normal human breast in nude mice: effect of host pregnancy environment and human chorionic gonadotropin on proliferation. *J Endocrinol*, 168(3):487–96.

[Potter and Prentice, 2015] Potter, J. D. and Prentice, R. L. (2015). Cancer risk: tumors excluded. *Science*, 347(6223):727.

[Purdom et al., 2013] Purdom, E., Ho, C., Grasso, C. S., Quist, M. J., Cho, R. J., and Spellman, P. (2013). Methods and challenges in timing chromosomal abnormalities within cancer samples. *Bioinformatics*, 29(24):3113–20.

[Quintas-Cardama et al., 2009] Quintas-Cardama, A., Kantarjian, H., and Cortes, J. (2009). Imatinib and beyond–exploring the full potential of targeted therapy for cml. *Nat Rev Clin Oncol*, 6(9):535–43.

[Raczy et al., 2013] Raczy, C., Petrovski, R., Saunders, C. T., Chorny, I., Kruglyak, S., Margulies, E. H., Chuang, H. Y., Kallberg, M., Kumar, S. A., Liao, A., Little, K. M., Stromberg, M. P., and Tanner, S. W. (2013). Isaac: ultra-fast whole-genome secondary analysis on illumina sequencing platforms. *Bioinformatics*, 29(16):2041–3.

[Rayner et al., 2016] Rayner, E., van Gool, I. C., Palles, C., Kearsey, S. E., Bosse, T., Tomlinson, I., and Church, D. N. (2016). A panoply of errors: polymerase proofreading domain mutations in cancer. *Nat Rev Cancer*, 16(2):71–81.

[Riely et al., 2008] Riely, G. J., Kris, M. G., Rosenbaum, D., Marks, J., Li, A., Chitale, D. A., Nafa, K., Riedel, E. R., Hsu, M., Pao, W., Miller, V. A., and

Ladanyi, M. (2008). Frequency and distinctive spectrum of kras mutations in never smokers with lung adenocarcinoma. *Clin Cancer Res*, 14(18):5731–4.

[Rosner and Colditz, 1996] Rosner, B. and Colditz, G. A. (1996). Nurses' health study: log-incidence mathematical model of breast cancer incidence. *J Natl Cancer Inst*, 88(6):359–64.

[Rosner et al., 1994] Rosner, B. A., Colditz, G. A., and Willett, C. (1994). Reproductive risk factors in a prospective study of breast cancer - the nurses' health study. *American Jounral of Epidemiology*, 139(8):819–835.

[Rowan et al., 2000] Rowan, A. J., Lamlum, H., Ilyas, M., Wheeler, J., Straub, J., Papadopoulou, A., Bicknell, D., Bodmer, W. F., and Tomlinson, I. P. (2000). Apc mutations in sporadic colorectal tumors: A mutational "hotspot" and interdependence of the "two hits". *Proc Natl Acad Sci U S A*, 97(7):3352–7.

[Roylance et al., 2011] Roylance, R., Endesfelder, D., Gorman, P., Burrell, R. A., Sander, J., Tomlinson, I., Hanby, A. M., Speirs, V., Richardson, A. L., Birkbak, N. J., Eklund, A. C., Downward, J., Kschischo, M., Szallasi, Z., and Swanton, C. (2011). Relationship of extreme chromosomal instability with long-term survival in a retrospective analysis of primary breast cancer. *Cancer Epidemiol Biomarkers Prev*, 20(10):2183–94.

[Russo et al., 2005] Russo, J., Moral, R., Balogh, G. A., Mailo, D., and Russo, I. H. (2005). The protective role of pregnancy in breast cancer. *Breast Cancer Res*, 7(3):131–42.

[Russo et al., 1992] Russo, J., Rivera, R., and Russo, I. H. (1992). Influence of age and parity on the development of the human breast. *Breast Cancer Res Treat*, 23(3):211–8.

[Salk et al., 2010] Salk, J. J., Fox, E. J., and Loeb, L. A. (2010). Mutational heterogeneity in human cancers: origin and consequences. *Annu Rev Pathol*, 5:51–75.

[Sansregret et al., 2018] Sansregret, L., Vanhaesebroeck, B., and Swanton, C. (2018). Determinants and clinical implications of chromosomal instability in cancer. *Nat Rev Clin Oncol*.

[Santin et al., 2016] Santin, A. D., Bellone, S., Buza, N., Choi, J., Schwartz, P. E., Schlessinger, J., and Lifton, R. P. (2016). Regression of chemotherapy-resistant polymerase epsilon (pole) ultra-mutated and msh6 hyper-mutated endometrial tumors with nivolumab. *Clin Cancer Res*, 22(23):5682–5687.

[Sarebo et al., 2006] Sarebo, M., Skjelbred, C. F., Breistein, R., Lothe, I. M., Hagen, P. C., Bock, G., Hansteen, I. L., and Kure, E. H. (2006). Association between cigarette smoking, apc mutations and the risk of developing sporadic colorectal adenomas and carcinomas. *BMC Cancer*, 6:71.

[Saunders et al., 2012] Saunders, C. T., Wong, W. S., Swamy, S., Becq, J., Murray, L. J., and Cheetham, R. K. (2012). Strelka: accurate somatic small-variant calling from sequenced tumor-normal sample pairs. *Bioinformatics*, 28(14):1811–7.

[Schettino et al., 2008] Schettino, C., Bareschino, M. A., Ricci, V., and Ciardiello, F. (2008). Erlotinib: an egf receptor tyrosine kinase inhibitor in non-small-cell lung cancer treatment. *Expert Rev Respir Med*, 2(2):167–78.

[Schiffer et al., 1979] Schiffer, L. M., Braunschweiger, P. G., Stragand, J. J., and Poulakos, L. (1979). The cell kinetics of human mammary cancers. *Cancer*, 43(5):1707–19.

[Scholzen and Gerdes, 2000] Scholzen, T. and Gerdes, J. (2000). The ki-67 protein: from the known and the unknown. *J Cell Physiol*, 182(3):311–22.

[Schulze et al., 2015] Schulze, K., Imbeaud, S., Letouze, E., Alexandrov, L. B., Calderaro, J., Rebouissou, S., Couchy, G., Meiller, C., Shinde, J., Soysouvanh, F., Calatayud, A. L., Pinyol, R., Pelletier, L., Balabaud, C., Laurent, A., Blanc, J. F., Mazzaferro, V., Calvo, F., Villanueva, A., Nault, J. C., Bioulac-Sage, P., Stratton, M. R., Llovet, J. M., and Zucman-Rossi, J. (2015). Exome sequencing

of hepatocellular carcinomas identifies new mutational signatures and potential therapeutic targets. *Nat Genet*, 47(5):505–11.

[Shinbrot et al., 2014] Shinbrot, E., Henninger, E. E., Weinhold, N., Covington, K. R., Goksenin, A. Y., Schultz, N., Chao, H., Doddapaneni, H., Muzny, D. M., Gibbs, R. A., Sander, C., Pursell, Z. F., and Wheeler, D. A. (2014). Exonuclease mutations in dna polymerase epsilon reveal replication strand specific mutation patterns and human origins of replication. *Genome Res*, 24(11):1740–50.

[Shlien et al., 2015] Shlien, A., Campbell, B. B., de Borja, R., Alexandrov, L. B., Merico, D., Wedge, D., Van Loo, P., Tarpey, P. S., Coupland, P., Behjati, S., Pollett, A., Lipman, T., Heidari, A., Deshmukh, S., Avitzur, N., Meier, B., Gerstung, M., Hong, Y., Merino, D. M., Ramakrishna, M., Remke, M., Arnold, R., Panigrahi, G. B., Thakkar, N. P., Hodel, K. P., Henninger, E. E., Goksenin, A. Y., Bakry, D., Charames, G. S., Druker, H., Lerner-Ellis, J., Mistry, M., Dvir, R., Grant, R., Elhasid, R., Farah, R., Taylor, G. P., Nathan, P. C., Alexander, S., Ben-Shachar, S., Ling, S. C., Gallinger, S., Constantini, S., Dirks, P., Huang, A., Scherer, S. W., Grundy, R. G., Durno, C., Aronson, M., Gartner, A., Meyn, M. S., Taylor, M. D., Pursell, Z. F., Pearson, C. E., Malkin, D., Futreal, P. A., Stratton, M. R., Bouffet, E., Hawkins, C., Campbell, P. J., and Tabori, U. (2015). Combined hereditary and somatic mutations of replication error repair genes result in rapid onset of ultra-hypermutated cancers. *Nat Genet*, 47(3):257–62.

[Sieber et al., 2005] Sieber, O. M., Tomlinson, S. R., and Tomlinson, I. P. (2005). Tissue, cell and stage specificity of (epi)mutations in cancers. *Nat Rev Cancer*, 5(8):649–55.

[Simon, 2010] Simon, A. (2010). Fastqc: A quality control tool for high throughput sequence data.

[Sottoriva et al., 2015] Sottoriva, A., Kang, H., Ma, Z., Graham, T. A., Salomon, M. P., Zhao, J., Marjoram, P., Siegmund, K., Press, M. F., Shibata, D., and Curtis,

C. (2015). A big bang model of human colorectal tumor growth. *Nat Genet*, 47(3):209–16.

[Stachler et al., 2015] Stachler, M. D., Taylor-Weiner, A., Peng, S., McKenna, A., Agoston, A. T., Odze, R. D., Davison, J. M., Nason, K. S., Loda, M., Leshchiner, I., Stewart, C., Stojanov, P., Seepo, S., Lawrence, M. S., Ferrer-Torres, D., Lin, J., Chang, A. C., Gabriel, S. B., Lander, E. S., Beer, D. G., Getz, G., Carter, S. L., and Bass, A. J. (2015). Paired exome analysis of barrett's esophagus and adenocarcinoma. *Nat Genet*, 47(9):1047–55.

[Stephens et al., 2011] Stephens, P. J., Greenman, C. D., Fu, B., Yang, F., Bignell, G. R., Mudie, L. J., Pleasance, E. D., Lau, K. W., Beare, D., Stebbings, L. A., McLaren, S., Lin, M. L., McBride, D. J., Varela, I., Nik-Zainal, S., Leroy, C., Jia, M., Menzies, A., Butler, A. P., Teague, J. W., Quail, M. A., Burton, J., Swerdlow, H., Carter, N. P., Morsberger, L. A., Iacobuzio-Donahue, C., Follows, G. A., Green, A. R., Flanagan, A. M., Stratton, M. R., Futreal, P. A., and Campbell, P. J. (2011). Massive genomic rearrangement acquired in a single catastrophic event during cancer development. *Cell*, 144(1):27–40.

[Storchova and Pellman, 2004] Storchova, Z. and Pellman, D. (2004). From polyploidy to aneuploidy, genome instability and cancer. *Nat Rev Mol Cell Biol*, 5(1):45–54.

[Suzuki et al., 2000] Suzuki, R., Atherton, A. J., O'Hare, M. J., Entwistle, A., Lakhani, S. R., and Clarke, C. (2000). Proliferation and differentiation in the human breast during pregnancy. *Differentiation*, 66(2-3):106–15.

[Talhouk et al., 2015] Talhouk, A., McConechy, M. K., Leung, S., Li-Chang, H. H., Kwon, J. S., Melnyk, N., Yang, W., Senz, J., Boyd, N., Karnezis, A. N., Huntsman, D. G., Gilks, C. B., and McAlpine, J. N. (2015). A clinically applicable molecular-based classification for endometrial cancers. *Br J Cancer*, 113(2):299–310.

[Taylor et al., 2009] Taylor, D., Pearce, C. L., Hovanessian-Larsen, L., Downey, S., Spicer, D. V., Bartow, S., Pike, M. C., Wu, A. H., and Hawes, D. (2009). Progesterone and estrogen receptors in pregnant and premenopausal non-pregnant normal human breast. *Breast Cancer Res Treat*, 118(1):161–8.

[Temko et al., 2017] Temko, D., Cheng, Y. K., Polyak, K., and Michor, F. (2017). Mathematical modeling links pregnancy-associated changes and breast cancer risk. *Cancer Res*, 77(11):2800–2809.

[Temko et al., 2018] Temko, D., Van Gool, I. C., Rayner, E., Glaire, M., Makino, S., Brown, M., Chegwidden, L., Palles, C., Depreeuw, J., Beggs, A., Stathopoulou, C., Mason, J., Baker, A. M., Williams, M., Cerundolo, V., Rei, M., Taylor, J. C., Schuh, A., Ahmed, A., Amant, F., Lambrechts, D., Smit, V. T., Bosse, T., Graham, T. A., Church, D. N., and Tomlinson, I. (2018). Somatic pole exonuclease domain mutations are early events in sporadic endometrial and colorectal carcinogenesis, determining driver mutational landscape, clonal neoantigen burden and immune response. *J Pathol*.

[Thibodeau et al., 1993] Thibodeau, S. N., Bren, G., and Schaid, D. (1993). Microsatellite instability in cancer of the proximal colon. *Science*, 260(5109):816–9.

[Tomasetti et al., 2015] Tomasetti, C., Marchionni, L., Nowak, M. A., Parmigiani, G., and Vogelstein, B. (2015). Only three driver gene mutations are required for the development of lung and colorectal cancers. *Proc Natl Acad Sci U S A*, 112(1):118–23.

[Tomasetti and Vogelstein, 2015] Tomasetti, C. and Vogelstein, B. (2015). Cancer etiology. variation in cancer risk among tissues can be explained by the number of stem cell divisions. *Science*, 347(6217):78–81.

[Tomasetti et al., 2013] Tomasetti, C., Vogelstein, B., and Parmigiani, G. (2013). Half or more of the somatic mutations in cancers of self-renewing tissues originate prior to tumor initiation. *Proc Natl Acad Sci U S A*, 110(6):1999–2004.

[Tomlinson et al., 1996] Tomlinson, I. P., Novelli, M. R., and Bodmer, W. F. (1996). The mutation rate and cancer. *Proc Natl Acad Sci U S A*, 93(25):14800–3.

[Traulsen et al., 2013] Traulsen, A., Lenaerts, T., Pacheco, J. M., and Dingli, D. (2013). On the dynamics of neutral mutations in a mathematical model for a homogeneous stem cell population. *J R Soc Interface*, 10(79):20120810.

[van Gool et al., 2015] van Gool, I. C., Eggink, F. A., Freeman-Mills, L., Stelloo, E., Marchi, E., de Bruyn, M., Palles, C., Nout, R. A., de Kroon, C. D., Osse, E. M., Klenerman, P., Creutzberg, C. L., Tomlinson, I. P., Smit, V. T., Nijman, H. W., Bosse, T., and Church, D. N. (2015). Pole proofreading mutations elicit an antitumor immune response in endometrial cancer. *Clin Cancer Res*, 21(14):3347–3355.

[Venkataram et al., 2016] Venkataram, S., Dunn, B., Li, Y., Agarwala, A., Chang, J., Ebel, E. R., Geiler-Samerotte, K., Herissant, L., Blundell, J. R., Levy, S. F., Fisher, D. S., Sherlock, G., and Petrov, D. A. (2016). Development of a comprehensive genotype-to-fitness map of adaptation-driving mutations in yeast. *Cell*, 166(6):1585–1596 e22.

[Vilar and Gruber, 2010] Vilar, E. and Gruber, S. B. (2010). Microsatellite instability in colorectal cancer-the stable evidence. *Nat Rev Clin Oncol*, 7(3):153–62.

[Villadsen et al., 2007] Villadsen, R., Fridriksdottir, A. J., Ronnov-Jessen, L., Gudjonsson, T., Rank, F., LaBarge, M. A., Bissell, M. J., and Petersen, O. W. (2007). Evidence for a stem cell hierarchy in the adult human breast. *J Cell Biol*, 177(1):87–101.

[Visvader, 2011] Visvader, J. E. (2011). Cells of origin in cancer. *Nature*, 469(7330):314–22.

[Vogelstein et al., 2013] Vogelstein, B., Papadopoulos, N., Velculescu, V. E., Zhou, S., Diaz, L. A., J., and Kinzler, K. W. (2013). Cancer genome landscapes. *Science*, 339(6127):1546–58.

[Waclaw et al., 2015] Waclaw, B., Bozic, I., Pittman, M. E., Hruban, R. H., Vogelstein, B., and Nowak, M. A. (2015). A spatial model predicts that dispersal and cell turnover limit intratumour heterogeneity. *Nature*, 525(7568):261–4.

[Wagener et al., 2015] Wagener, R., Alexandrov, L. B., Montesinos-Rongen, M., Schlesner, M., Haake, A., Drexler, H. G., Richter, J., Bignell, G. R., McDermott, U., and Siebert, R. (2015). Analysis of mutational signatures in exomes from b-cell lymphoma cell lines suggest apobec3 family members to be involved in the pathogenesis of primary effusion lymphoma. *Leukemia*, 29(7):1612–5.

[Wang et al., 2010] Wang, K., Li, M., and Hakonarson, H. (2010). Annovar: functional annotation of genetic variants from high-throughput sequencing data. *Nucleic Acids Res*, 38(16):e164.

[Weghorn and Sunyaev, 2017] Weghorn, D. and Sunyaev, S. (2017). Bayesian inference of negative and positive selection in human cancers. *Nat Genet*, 49(12):1785–1788.

[Weinberg and Zaykin, 2015] Weinberg, C. R. and Zaykin, D. (2015). Is bad luck the main cause of cancer? *J Natl Cancer Inst*, 107(7).

[Weinberg, 2014] Weinberg, R. A. (2014). *The biology of cancer*. Garland Science, Taylor & Francis Group, New York, second edition. edition.

[Weinstein, 2002] Weinstein, I. B. (2002). Cancer. addiction to oncogenes–the achilles heal of cancer. *Science*, 297(5578):63–4.

[Weisberg et al., 2007] Weisberg, E., Manley, P. W., Cowan-Jacob, S. W., Hochhaus, A., and Griffin, J. D. (2007). Second generation inhibitors of bcr-abl for the treatment of imatinib-resistant chronic myeloid leukaemia. *Nat Rev Cancer*, 7(5):345–56.

[Williams et al., 2016] Williams, M. J., Werner, B., Barnes, C. P., Graham, T. A., and Sottoriva, A. (2016). Identification of neutral tumor evolution across cancer types. *Nat Genet*, 48(3):238–44.

[Yates et al., 2017] Yates, L. R., Knappskog, S., Wedge, D., Farmery, J. H. R., Gonzalez, S., Martincorena, I., Alexandrov, L. B., Van Loo, P., Haugland, H. K., Lilleng, P. K., Gundem, G., Gerstung, M., Pappaemmanuil, E., Gazinska, P., Bhosle, S. G., Jones, D., Raine, K., Mudie, L., Latimer, C., Sawyer, E., Desmedt, C., Sotiriou, C., Stratton, M. R., Sieuwerts, A. M., Lynch, A. G., Martens, J. W., Richardson, A. L., Tutt, A., Lonning, P. E., and Campbell, P. J. (2017). Genomic evolution of breast cancer metastasis and relapse. *Cancer Cell*, 32(2):169–184 e7.

[Zack et al., 2013] Zack, T. I., Schumacher, S. E., Carter, S. L., Cherniack, A. D., Saksena, G., Tabak, B., Lawrence, M. S., Zhsng, C. Z., Wala, J., Mermel, C. H., Sougnez, C., Gabriel, S. B., Hernandez, B., Shen, H., Laird, P. W., Getz, G., Meyerson, M., and Beroukhim, R. (2013). Pan-cancer patterns of somatic copy number alteration. *Nat Genet*, 45(10):1134–40.

[Zhang et al., 2015] Zhang, C. Z., Spektor, A., Cornils, H., Francis, J. M., Jackson, E. K., Liu, S., Meyerson, M., and Pellman, D. (2015). Chromothripsis from dna damage in micronuclei. *Nature*, 522(7555):179–84.